British Geological Survey
NATURAL ENVIRONMENT RESEARCH COUNCIL

Slope Dynamics Project Report: Holderness Coast - Aldbrough, Survey & Monitoring, 2001 - 2013

Engineering Geology Programme

Internal Report OR/11/063

BRITISH GEOLOGICAL SURVEY

ENGINEERING Geology PROGRAMME

INTERNAL REPORT OR/11/063

Slope Dynamics Project Report: Holderness Coast - Aldbrough, Survey & Monitoring, 2001 - 2013

PRN Hobbs, LD Jones, MP Kirkham, DJR Morgan, CVL Pennington, GO Jenkins, C Dashwood, EP Haslam, KA Freeborough, & RS Lawley

Contributor/editor

V. Banks

Keywords

Aldbrough, Holderness, coast, erosion, landslides, geotechnics, till, terrestrial LiDAR.

Front cover

Aldbrough test site, looking northward (March 2012)

Bibliographical reference

HOBBS, P.R.N., JONES, L.D., KIRKHAM, M.P., D.J. MORGAN, PENNINGTON, C.V.L., JENKINS, G.O., DASHWOOD, C., Haslam, E.P., Freeborough, K.A. & Lawley, R.S. 2013. Slope Dynamics Project Report: Holderness Coast - Aldbrough, Survey & Monitoring, 2001 - 2013. *British Geological Survey Internal Report*, OR/11/063. 150pp.

Keyworth, Nottingham British Geological Survey 2013

BRITISH GEOLOGICAL SURVEY

The full range of our publications is available from BGS shops at Nottingham, Edinburgh, London and Cardiff (Welsh publications only) see contact details below or shop online at www.geologyshop.com

The London Information Office also maintains a reference collection of BGS publications, including maps, for consultation.

We publish an annual catalogue of our maps and other publications; this catalogue is available online or from any of the BGS shops.

The British Geological Survey carries out the geological survey of Great Britain and Northern Ireland (the latter as an agency service for the government of Northern Ireland), and of the surrounding continental shelf, as well as basic research projects. It also undertakes programmes of technical aid in geology in developing countries.

The British Geological Survey is a component body of the Natural Environment Research Council.

British Geological Survey offices

BGS Central Enquiries Desk

Tel 0115 936 3143 Fax 0115 936 3276

email enquiries@bgs.ac.uk

Kingsley Dunham Centre, Keyworth, Nottingham NG12 5GG

Tel 0115 936 3241 Fax 0115 936 3488

email sales@bgs.ac.uk

Murchison House, West Mains Road, Edinburgh EH9 3LA

Tel 0131 667 1000 Fax 0131 668 2683

email scotsales@bgs.ac.uk

Natural History Museum, Cromwell Road, London SW7 5BD

Tel 020 7589 4090 Fax 020 7584 8270

Tel 020 7942 5344/45 email bgslondon@bgs.ac.uk

Columbus House, Greenmeadow Springs, Tongwynlais, Cardiff CF15 7NE

Tel 029 2052 1962 Fax 029 2052 1963

Maclean Building, Crowmarsh Gifford, Wallingford OX10 8BB

Tel 01491 838800 Fax 01491 692345

Geological Survey of Northern Ireland, Colby House, Stranmillis Court, Belfast BT9 5BF

Tel 028 9038 8462 Fax 028 9038 8461

www.bgs.ac.uk/gsni/

Parent Body

Natural Environment Research Council, Polaris House, North Star Avenue, Swindon SN2 1EU

Tel 01793 411500 Fax 01793 411501

www.nerc.ac.uk

Website www.bgs.ac.uk

Shop online at www.geologyshop.com

Foreword

This report is a published product of an ongoing study by the British Geological Survey (BGS) of the coastal change at Aldbrough on the Holderness coast, East Riding of Yorkshire, UK. The test site at Aldbrough has been selected as one of the BGS Landslide Observatories because it is representative of the high rates of coastal recession along this stretch of the east coast. The Aldbrough Landslide Observatory is operated under the BGS 'Slope Dynamics' task within the BGS's 'Landslide' project of the 'Shallow Geohazards and Risk' team. As well as providing new insights with respect to the volumetric rates of recession and the near surface processes, it is a focus for the trialling of new surface and subsurface monitoring technologies. The establishment of the Aldbrough observatory and the initial research findings are reported in a series of reports in addition to this report. These are:

Hobbs, P.R.N., Jones, L.D., & Kirkham, M.P. (2015) Slope Dynamics project report: Holderness Coast – Aldbrough: Drilling & Instrumentation, 2012-2015. *British Geological Survey, Internal Report* No IR/15/001.

Hobbs, P.R.N., Kirkham, M.P. & Morgan, D.J.R. (2016) Geotechnical laboratory testing of glacial deposits from Aldbrough, Phase 2 boreholes. *British Geological Survey, Open Report* No. OR/15/056.

Whilst this report is focused on the survey and monitoring programme, it should be read in conjunction with the reports listed above, which provide further details on drilling and instrumentation and the geotechnical properties of the underlying geology. A series of reports will follow presenting the updated survey and monitoring reports, and their publication will be announced through the BGS project web page. Readers of these reports will probably also be interested in the context for this research, which can be found in:

Hobbs, P.R.N., Pennington, C.V.L., Pearson, S.G., Jones, L.D., Foster, C., Lee, J.R., Gibson, A. (2008) Slope Dynamics Project Report: the Norfolk Coast (2000-2006). *British Geological Survey, Open Report* No. OR/08/018.

Acknowledgements

A large number of individuals have contributed to the project. In addition to the collection of data, many individuals have freely given their advice, and provided local knowledge. The authors would particularly like to thank the following who have contributed directly to parts of the project:

Paul Turner (ex-BGS),
Anthony Cooper (ex-BGS),
Colm Jordan (BGS),
Douglas Tragheim (ex-BGS),
Chris Wardle (ex-BGS)
Paul Witney (ex-BGS)
Graham Hunter & staff at 3DLaserMapping Ltd.
Travis Mason & Andrew Colenutt (CCO)

Special thanks go to Mr. Paul Allison of Aldbrough Leisure Park (Shorewood Leisure Group) who has supported the project throughout by taking an active interest in it and by allowing field work and installations on the company's property at Aldbrough.

The authors would also like to thank the following BGS & ex-BGS staff who helped initiate the project and have reviewed its outputs:

Dr Helen Reeves (BGS)
Dr Vanessa Banks (BGS)
Professor Martin Culshaw (ex-BGS)
Dr Peter Balson (ex-BGS)
Dr John Rees (BGS)

Contents

FIGURES

TABLES

APPENDICES

Frontispiece:

Orthophoto of cliff below Seaside Road, Aldbrough prepared using UAV photogrammetry (25th June, 2013)

1 Summary

The work described in this report forms part of the 'Slope Dynamics' task of the 'Landslides' project which lies within the Shallow Geohazards and Risk theme of the Engineering Geology programme. It has a matching report (Hobbs et al., 2015a) dealing with the ground investigation and instrumentation aspects of the task. It extends the research reported on the North Norfolk coast (Hobbs *et al*., 2008). The Slope Dynamics task has shown that cliff recession, and the geomorphological processes that result in cliff recession, can be accurately monitored over a sustained period; almost 12 years at time of reporting (September 2001 to June 2013). Work is continuing at the site and will be reported separately in due course.

A methodology has been developed that enables changes to be measured quantitatively and facilitates a better understanding of the geomorphological processes associated with cliff recession. The resulting data can be applied widely to coastal change analyses using models based on algorithms comprising a variety of physical and mechanical properties and derived parameters such as factor of safety, for example. Whilst the overall approach used here is observational and deterministic, the data provided could be used to guide stochastic models where quantitative input data might otherwise be lacking or where the complex interrelationship between geology, geomorphology and landslide cyclicity might be under represented. A precise relationship between environmental factors (e.g. rainfall and storms) and landslide activity and cyclicity remains elusive, due mainly to the infrequency of surveys. However, every effort has been made to obtain environmental data and general trends have been observed and described.

The cliffs of the Holderness coast are cut into Devensian tills laid down between 18,000 and 13,000 years ago (Catt, 1991) and have been described as the UK's largest coastal sediment source (Prandle *et al*., 1996). The coastline is unprotected with the exception of formal defences at Bridlington, Hornsea, Mappleton, Withernsea and Easington totalling 11.4 km in length. These provide 'hard points' and encourage bay development between them. In 1991 a 500 m long rock-revetment was built at Mappleton 5 km to the north of Aldbrough. This has affected long-shore drift and increased the erosion rate to the south of Mappleton, but possibly only up to 4.4 km distance (Brown, 2008). In 2000 the East Riding of Yorkshire Council developed an Integrated Coastal Zone Management (ICZM) Plan. This attempted to take account of all interested parties including environment, fisheries, agriculture and rural issues (Eurosion, 2004).

The cliff at the BGS's Aldbrough test site, recently accorded 'Coastal landslide field laboratory' status, is 16 - 17 m high, compared with an average of 15 m (Pethick, 1996), and amongst the highest on the 'soft' cliffed Holderness coast. It consists of a sequence of glacial deposits, which may be considered typical of significant parts of the 50 km long Holderness coastline. The test site is approximately 300 m in length, though for the calculation of recession the data have been clipped to the central 100 m. Cliff recession figures in historic times have exceeded 2 m annually. The data obtained for this report have shown an average recession rate at the test site of 2.7 m per year over a 12 year monitoring period (2001 to 2013). The report has shown that cliff recession, and the geomorphological processes that result in cliff recession, can be accurately monitored, leading to both quantification of the processes and also a better understanding of them.

The principal method used was terrestrial LiDAR commonly referred to as 'terrestrial laser scanning (TLS)'. This method has been compared with traditional aerial LiDAR and photogrammetry techniques. It has allowed 22 repeat surveys to be carried out for a modest mobilisation cost, when compared with the cost of equivalent aerial surveys. The amount of detail recorded during the surveys generally outstrips that produced from an aerial survey of the type available at the time, particularly where the cliffs are steep. The level of detail can also be customised by using multiple scans to reflect complex morphology or varying the density of scans. The main disadvantage of TLS is its limited coverage, though it is suitable for small test sites such as that described here. The method employed here is intended to go beyond simply recording the amount of linear coastal recession. Rather, an attempt has been made to quantify coastal recession in 3D (and 4D) in order to elucidate the geomorphological processes taking place. This aim

has been partially achieved but subtle geomorphological changes to the cliff on a daily or weekly time scale have not been resolved due to the limited frequency of surveys.

Currently, the standard geology map provides no indication of the 3D geology of the UK's cliffed coast. This presents a key problem in extrapolating any geology-based model of coastal recession from the test site to the cliffed coast as a whole. Research on this topic is underway at BGS.

Analysis has been made of the coastal recession at one test site at Aldbrough. This site is broadly typical of a significant proportion of the Holderness coast, in terms of its geology, landslide type, erosion regime and topography. At the Aldbrough test site the cliff is subject to a rapid rate of recession and almost continuous landslide activity. Landslide debris is rapidly removed by the sea. The beach cover to the platform is transient, and is believed to follow a pattern typified by 'ords'. An ord is a local name for a thin veneer of beach sediment over an area of exposed till shore platform (Pringle, 1985). It is thought that erosion of the coast is focused immediately behind the ords and that as the ords migrate southwards; as sediment is transported along the coast, these zones of focused erosion move with them.

Slope stability modelling tends to be aimed at engineering applications where there is usually a large body of sub-surface data available. The models have, until recently, been solely 2D and of either 'limit equilibrium' or 'finite element' type, or some variation of these. These models are highly site specific and have not as yet been applicable regionally. This report assesses this outcome, and in doing so seeks to parallel other BGS initiatives and products based on the quantitative attribution of geological formations, in particular those applied to geohazards. Slope stability modelling (2D methods) has been applied to the Aldbrough test site.

During the 12-year monitoring period the cliffs at the Aldbrough test site have receded by an average of 3 m per year, seriously affecting properties on Seaside Road and the adjacent Aldbrough Leisure Park for mobile homes. Cliff recession at the test site appears to be influenced mainly by landsliding, direct mechanical abrasion from the sea and by erosion produced by surface water runoff and groundwater seepage. Closely-spaced jointing within the soil mass is also a factor. These factors are intimately related as is demonstrated in this report. The relationship between monthly rainfall data, from the closest station, and landslide activity has been investigated, and a reasonable overall relationship for the monitoring period found.

In March 2012 the first sub-surface investigations were carried out at the Aldbrough test site. Four 20 m deep boreholes were drilled for piezometer and inclinometer instrumentation in order to investigate the role of pore pressures in landslide development and pre-cursors to landslides. These data will contribute to a 3D geological understanding of the site. An automatic weather station was also set up close to the test site.

2 Introduction

This report describes the Slope Dynamics task's first monitoring dataset for a single test site on the Holderness coast of eastern England, spanning the period 2001 to 2013. The task, part of the BGS's 'Landslides' project within the 'Shallow Geohazards and Risk' theme, originally included 12 test sites around the English coast for which an annual or bi-annual monitoring programme was initiated (Figure 1). These sites were originally selected to represent non-engineered and non-protected soft cliffs incorporating a diversity of geology, scale, and landslide type and activity. Financial restraints, and the unsuitability of some sites, curtailed this monitoring regime. Of the original twelve test sites only three, Aldbrough in Holderness in the East Riding of Yorkshire plus Sidestrand and Happisburgh in Norfolk, were continued beyond 2004. The two Norfolk sites were discontinued in 2006 and reported in Hobbs *et al*. (2008). The location of the Aldbrough test site is shown in Figure 2 and Figure 4.

The geology at Aldbrough consists of a relatively simple and persistent succession of glacially emplaced deposits dominated by tills. The cliff recession at the site is presently and historically rapid. Historical recession rates for Aldbrough are reported as being 1.16 m for the period 1852 to 1951 using historical maps (Valentin, 1971) and 2.16 m for the period 1951 to 2004 using cliff surveys (East Riding Council, 2009). The coastal erosion and sediment yield of the Holderness coast have been estimated (Balson *et al*., 1998) using a digital terrain model (DTM) of 50 km of coastline, as up to 2 million m^3/year for the cliff and up to 4 million m^3/year for cliff and shore face combined, using data going back to 1786. This report describes an average annual recession rate for the cliff top of 2.7 m per year for the period September 2001 to June 2013. Calculations from parts of 16 terrestrial laser scans (TLS), selected from a total of 23, over the 12 year period produced a material loss of **36,820 m^3** per 100 m length or 368 m^3 per metre length, or **31 m^3** per metre per year for the 100 m cliff length sub-set examined (centred approximately 60 m south of Seaside Road). The data quality was variable with a trend towards improvement through time due to technological advances in both equipment and data processing capabilities. Considerable effort has been put into validating and correcting positional parameters, particularly for early scans where differential Global Positioning System (dGPS) accuracy was poor compared to dGPS/GNSS available today. This has necessitated the use of several computer programs and processing techniques.

The report describes the methods, processing, observations, images, and desk study information which were gathered as part of the task, and attempts to derive an understanding of the slope processes occurring along this active shoreline. This is principally achieved by making accurate 3D computer models of the cliff surface produced by combining TLS and dGPS/GNSS techniques (Hobbs et al., 2002; Buckley et al., 2002; Miller et al. 2007; Miller et al., 2008; Quinn et al., 2010). The raw data produced by the TLS are in the form of a 'point cloud' of XYZ points with laser reflective intensity and, from 2005 onward, photographic data included to allow 'true colour' point clouds. These data are then processed in various software packages to create 'solid' surface models which are then compared from one monitoring epoch to another over time. These comparisons are referred to here as 'change models'. The amount of change is usually calculated from a horizontal datum plane, for example sea level, and hence indicates changes in height above sea level. However, the datum may also be vertical, for example to better depict recession of a near-vertical cliff. Of course, changes in a non-vertical cliff are often not purely unidirectional. For example, as a result of a rotational landslide, parts of a cliff may fall while others rise relative to a horizontal datum; that is, there may have been little net loss of material from the cliff, but rather a re-arrangement. This is partially the case at Aldbrough though landslide deposits are removed from the cliff and foreshore with relative rapidity. Coastal monitoring has tended in the past to be quantitative and linear; that is, measurements, records and estimates of the cliff top line or the high water line have been used to calculate average values for cliff recession (East Riding Council, 2009; Quinn *et al*., 2010). The geomorphology of the process, or processes, is not measured in this methodology. This tendency has also translated to coastline prediction by means of historical extrapolation or probabilistic analysis (Lee *et al*., 2002; Flory *et al*., 2002), and to coastal modelling in general (Walkden and Hall, 2005; Trenhaile, 2009).

During the first two years of monitoring, the TLS and dGPS surveys and data processing were carried out by 3D Laser Mapping Ltd (Riegl, UK) staff. Subsequently, the same laser-scanner equipment was purchased by BGS and combined with a newly acquired dGPS to complete the remaining surveys up to 2005. In 2005 the laser scanner was upgraded; the new model including a digital camera which allowed coloured models to be produced. Data processing methods have been developed and refined over the period of the study and based on a wide variety of software packages. Inevitably over such a period of technological advance in the field of laser scanning and dGPS, there have been improvements in quality. This is reflected in the images and derived models. In addition to the monitoring surveys, reconnaissance and geological surveys were carried out.

3 Background

3.1 GENERAL

Great Britain's first attempt at a comprehensive assessment of the risks of coastal change and flood, within a wider policy framework, was the Shoreline Management Plan (SMP). This consisted of 22 assessments commencing in the early 1990's and covering the entire English and Welsh coast; each planning zone was sub-divided into 'sediment cells' and 'character units' (Aldbrough falling within Character Unit 5 and Policy Unit E: Rolston to Waxholme; *approximately equivalent to Hornsea to Withernsea*). The plans, which are reviewed every 5 or 10 years, provide descriptions of a variety of factors affecting erosion, and classify the results in terms of the proposed action required to reduce risks in a sustainable manner. The SMP represented the first stage of DEFRA's hierarchy of coastal plans, subsequent ones being 'Coastal Strategy' and 'Scheme'. Work for the SMP was commissioned by Coastal Groups with members mainly from local councils and the Environment Agency (EA). The time scales considered were 'short term' (0 to 20 years), 'medium term' (20 to 50 years) and 'long term' (50 to 100 years) starting in 2005. The defined action options applied to the whole project were: 'hold the line', 'advance the line', 'managed realignment' and 'no active intervention'. The current, and second, SMP covering Holderness is entitled "Flamborough Head to Gibraltar Point" and was prepared by Scott Wilson for the Humber Estuary Coastal Authorities Group (SMP, 2010). This plan covered sediment cells 2a, 2b and 2c and added a fifth action option of 'hold the line on a realigned position' thus allowing a change in action to be applied at review.

The SMP covering Holderness (SMP, 2010) cited the following "uncertainties in coastal processes understanding":

- The future rates of cliff recession under different sea level rise rates;
- The yield of beach building material and fine sediment from the Holderness cliffs, shore platform and seabed;
- Discrepancies between the estimated coarse sediment yield and the modelled longshore sediment transport rates;
- The impact of coast protection works on the supply of sediment from the Holderness coast;
- The long-term and contemporary behaviour of Spurn Head;
- The protection provided by Spurn Head to the low-lying land around the Humber; and
- The transport of coarse sediment across the mouth of the Humber to the Lincolnshire coast.

The coastline in Policy Unit E (Character Unit 5), which includes Aldbrough, is classed as having a 'No Active Intervention' policy for the currently undefended sections, with a 'Hold the Line' policy only for the defended section at Mappleton. This applies up to 2055, but with other options considered, subject to further monitoring, specified after this. The 'No Active Intervention' option allows release of sediment from the cliffs to provide natural coastal protection for areas to the south, including the Lincolnshire coast, in addition to maintenance of the "natural character" and beaches (SMP, 2010). The Shoreline Management Plan (SMP, 2010) states in its summary that: "Monitoring of cliff recession and beach profiles along the Holderness coast should continue".

The sustained development of vulnerable coastlines is an important consideration for European countries. To this end the Eurosion Project (EUROSION, 2004) has recommended that a more strategic and proactive approach is required, promoting coastal resilience and the preservation of dynamic coastlines. This approach would be based on "favourable sediment status" for each coastal sediment cell, achieved through the identification of "strategic sediment reservoirs" and the "quantitative assessment of coastal erosion". Thus detailed knowledge of the potential sediment volumes released through coastal erosion within specific coastal cells would provide the building blocks for such an approach. In this way the BGS's Aldbrough field laboratory could provide a model for wider assessments of sediment availability. At the other end of the spectrum the BGS's work provides valuable information for coastal engineers to design coastal protection. Important factors in this regard are the contribution of landsliding to coastal erosion and sediment release, and the style of drainage and retaining structure, and the design of remedial slopes to best mitigate the effects of prolonged cycles of landsliding. The design of newly or previously defended cliffs is also important as instability may continue driven by rainfall and groundwater induced landsliding.

Figure 1 Location of Slope Dynamics task's original test sites on English coast

3.2 ALDBROUGH TEST SITE

The BGS's 'coastal landslide field laboratory' is located at Aldbrough [centred: NGR 525770, 439605; 17m AOD], approximately midway on the extensive Holderness coast in the East Riding of Yorkshire. Aldbrough is situated about 10 km southeast of Hornsea and 2 km southeast of the Building Research Establishment (BRE) 'lowland clay till' geotechnical research site at Cowden (Marsland and Powell, 1985). The 200 m (latterly 300 m) stretch includes Seaside Road, and up until 2004, the road accessing the Caravan Park (Figure 3). The cliff at the test site faces northeast and is 16 m to 17 m in height throughout. It consists of glacial deposits, mainly till, and is actively receding, both by rotational (primary) and toppling (secondary) mechanisms. *Toppling failures, though relatively small, are sudden and frequent, and present a major hazard. A further notified hazard at the site is unexploded ordnance on the*

foreshore. This derives from an MOD coastal firing range a few kilometres to the north at Cowden. Whilst the beach and cliff are open to the public and unfenced, the hazard is clearly signposted, at least at Aldbrough.

Considerable study, both geological and geotechnical has been carried out on the deposits of the Holderness coast (Valentin, 1971; Balson *et al*., 1998; Lee and Clark, 2002, Bell and Forster, 1991; Joyce, 1969; McGown and Derbyshire, 1977; Sladen and Wrigley, 1983; Paul and Little, 1991; Benn and Evans, 1996; Pethick, 1996; Prandle et al., 1996; Gilroy, 1980; Brown, 2008; Quinn et al., 2009; Evans and Thomson, 2010; Pye and Blott, 2010; Lee, 2011). The East Riding of Yorkshire Council (ERYC) has monitored cliff recession along the Holderness coast since 1951 (Lee, 2011). The method used was to monitor the relative position of the cliff top to 120 marker posts on a 12- or 6-monthly basis. The survey has shown that at Aldbrough (survey post No. 59) the total recession between 1954 and 2004 was 95 m (a rate of 1.9 m per year), and between 1990 and 2004 was 33.9 m (a rate of 2.4 m per year) (Lee, 2011; Quinn *et al*., 2010). Thus, the recession rate appears to have increased since 1990. Pye and Blott (2010) carried out a survey of the geomorphology at Aldbrough in order to assess the impact of proposed cliff protection works on adjoining areas giving, inter alia, a figure of 153 million m^3 (0.153 km^3) material loss from the cliff for the entire Holderness coastline (52.1 km) between 1852 and 2009. This represents an average coastal recession of 196 m for this 157 year period.

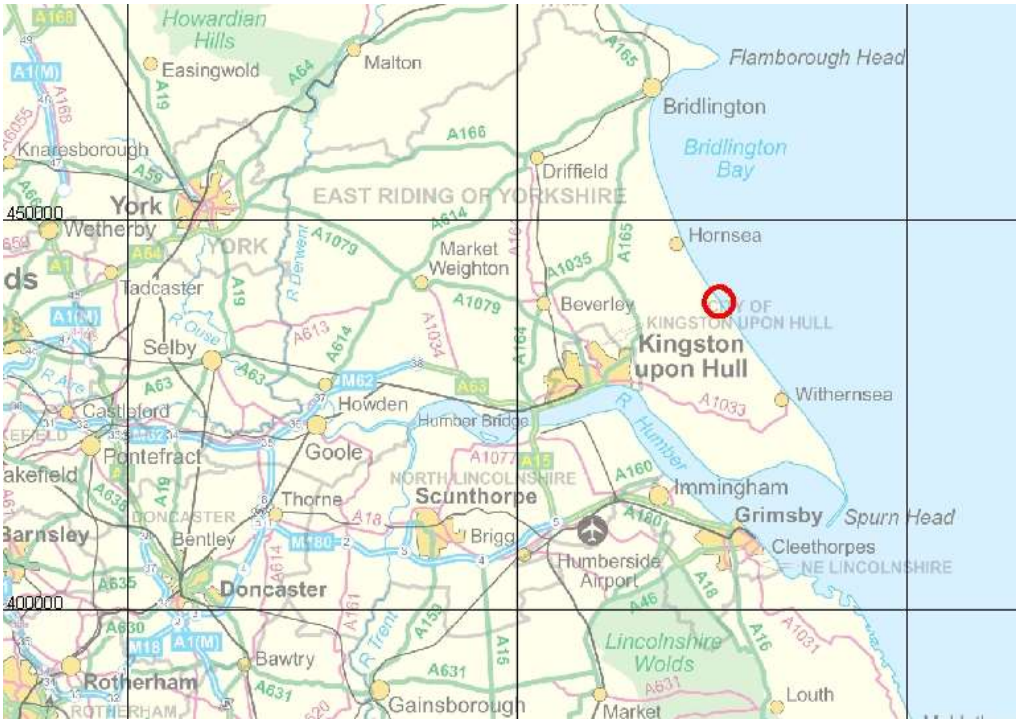

Figure 2 Map showing location of Aldbrough (red) on Holderness coast, East Yorkshire

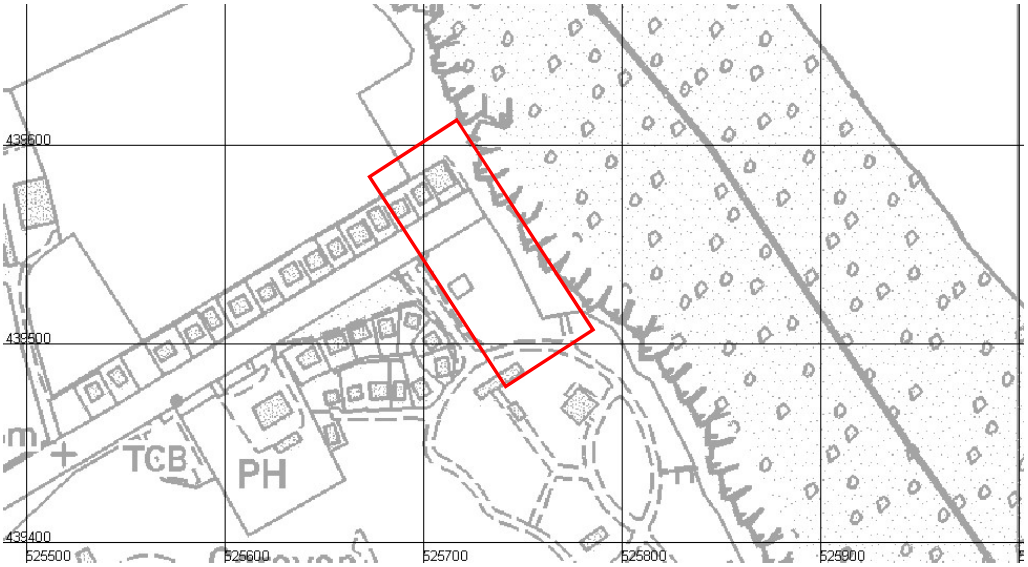

Figure 3 Approximate location of BGS test site
NOTE: cottages either side of Seaside Road (some of which no longer exist) and mobile home park to south

Figure 4 Superficial geology at Aldbrough showing BGS test site (red)
(Blue=Till, Yellow=Alluvium, Pink=Glacio-fluvial)

Figure 5 View towards cliff edge, along Seaside Road (2003)

Figure 6 Cliff and beach, central part of Aldbrough test site (Sep 2003) *(Note: pole adjacent to Seaside Road)*

Historic OS maps from 1855, 1892 and 1929 (Figure 8, Figure 9 & Figure 10) show the parts of the coastal settlement at Aldbrough that have been lost to the sea. These include, at different times, a hotel, guest houses, pub, amusement arcade, lime kilns and a coastguard station. They all show a short coastal road running parallel with the cliff (the southward part of which formerly connected with East Newton) and branching from Seaside Road. The 1929 map also shows a long line of what appear to be beach huts or bungalows along this road; the cliff at this time being very close to the road. It is difficult to draw quantitative conclusions regarding recession rates from these maps as the date of publication of the map does not necessarily match the date of the survey used to produce it. As recently as 1980 there was an

amusement arcade with toilets and car park. Images from the mid-1950's show a wooden stairway down the cliff. The Royal Hotel (pub) was re-built further inland on Seaside Road c.1930 and still stands as the 'Double Dutch' pub (Kent et al., 2002; British History, 2014). Caravan Road, opposite former bungalow No 361 on Seaside Road, has also been recently lost, only a small part of the junction with Seaside Road remaining (July 2013).

Figure 7 Historic OS map dated 1855 showing features now lost to the sea (overlaid on 2000 aerial photo)
Note: registration error at Mount Pleasant farm

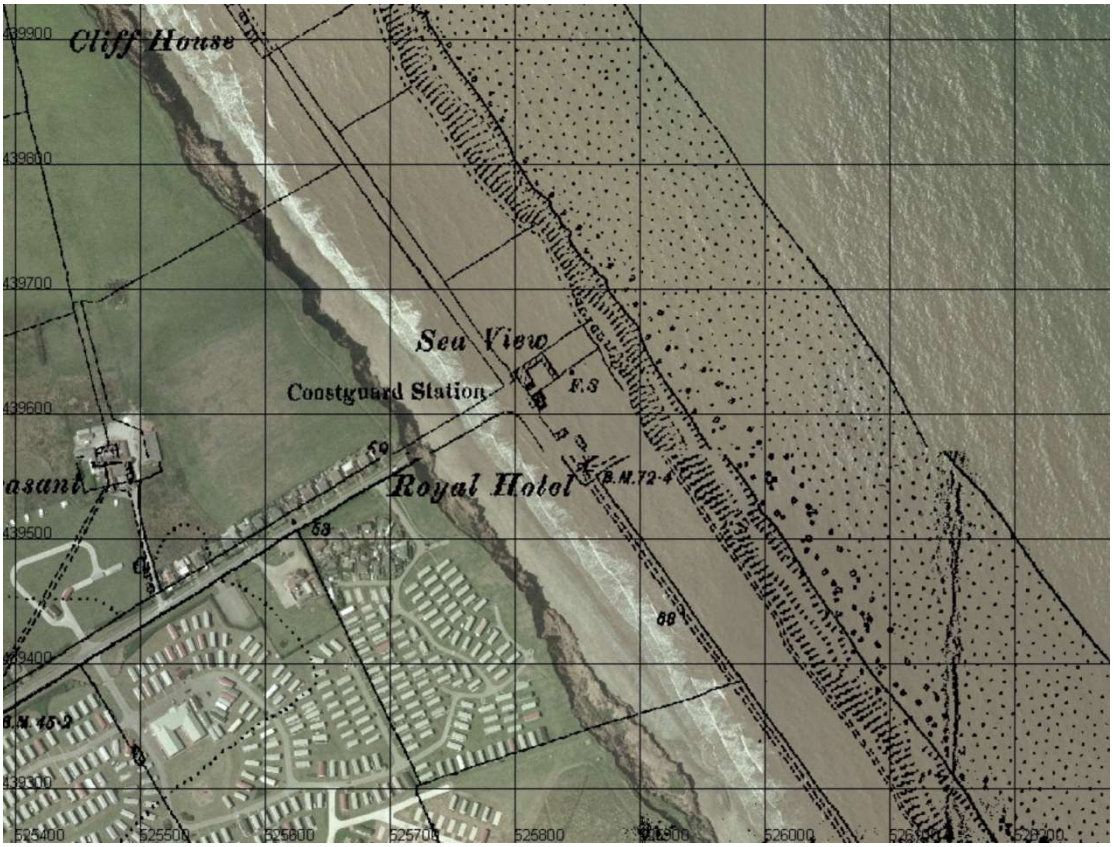

Figure 8 Historic OS map dated 1892 showing features now lost to the sea (overlaid on 2000 aerial photo)

Figure 9 Historic OS map dated 1929 showing features now lost to the sea (overlaid on 2000 aerial photo)

4 Task Methodology

The coastal sections were surveyed using a variety of remote methods, as well as by geological mapping and geotechnical probing, sampling, and testing. The principal methods of surveying the cliffs were long-range terrestrial laser scanning (TLS) combined with dGPS and dGPS/GNSS positioning. Some experimental terrestrial photogrammetry (TP) was also included as part of some surveys. Additionally, and more recently, experimental aerial UAV photogrammetry surveys were undertaken. TLS surveys were carried out either annually or bi-annually using between two and seven scanning locations distributed on both foreshore and cliff top, and the results processed to provide data for models of coastal recession. The TLS and dGPS data were pre-processed using RiProfile (Riegl) and entered into modelling packages including Polyworks™, GoCad™, QT Modeller™, Surfer™, Vertical Mapper™, MapInfo™ and Maptek I-Sight™. The resulting computer models have enabled volume calculations and observations to be made regarding the nature of coastal erosion and 'soft' cliff recession in particular.

4.1 TERRESTRIAL LIDAR (LASER SCANNING), TLS

Terrestrial LiDAR, sometimes referred to as Terrestrial Laser Scanning (TLS) or simply 'laser scanning', is in essence a terrestrial version of the longer-established aerial LiDAR and has been used for a variety of applications such as the monitoring of volcanoes (Hunter *et al.*, 2003), earthquake and mining subsidence, quarrying, buildings, forensics (Paul and Iwan, 2001; Hiatt, 2002) and inland- (Rowlands *et al.*, 2003) and coastal (Hobbs *et al.*, 2002) landslide modelling.

A recurrent problem with TLS, and other remote sensing methods, is that parts of the subject may be obscured from the instrument's view. These are termed 'shadow areas' and are a particular problem in areas where the cliff has a shallow angle, landslide morphologies are complex or where the cliff is wooded. The way to remedy this has been to occupy multiple scan positions, including ones at the cliff-top viewing the cliff obliquely, and to optimise their locations for line-of-sight. These multiple scans, once oriented with respect to national grid co-ordinates using the dGPS / GNSS data, can then be combined to form a single 3D model which can be augmented by roving dGPS data assuming that access to the cliff is possible. This method was used during the early stages of the task to help define the foot and crest of the cliff and remains a useful adjunct to the main survey.

Three laser scanning instruments have been used during this project: the Riegl LPM2K, the Riegl LPM-i800HA and the Riegl VZ1000. The Riegl LPM2K terrestrial laser (Figure 10; left) has a very long-range capability of up to 2500 m, is accurate to ±25 mm, has a measurement rate of up to 4 points per second and is not fitted with a camera. The Riegl LPM-i800HA terrestrial laser (Figure 10; middle) is medium to long-range, can scan up to 1000 m with an accuracy of ±25 mm and is fitted with a camera. The measurement rate is typically 1000 points per second and the calibrated digital camera mounted on the laser enables coloured point-clouds, textured triangulated surfaces or orthophotos with depth information to be captured. The Riegl VZ1000 (Figure 10; right) is long range, can scan up to 1400 m and has an accuracy of ±15mm with a typical scan rate of 42,000 points per second. The VZ1000 also has the capability to provide echo digitisation and full on-line waveform processing, and hence register multiple targets. This can assist with removing vegetation, or any other multiple returns, from the model.

The principle behind the three scanners is the same. The relative distance, elevation angle and azimuthal angle between the instrument and the cliff face are measured semi-automatically in each scan and, once processed, a 3D surface model can be generated. The VZ1000 uses a rotating mirror for the vertical plane and rotates solely in the horizontal plane whereas with both LPM scanners the whole rangefinder unit (with camera in the case of LPM-i800HA scanner) is rotated in the vertical and horizontal planes.

The method developed for the Slope Dynamics task has been to establish 'baselines' running parallel to the cliff, both on the beach platform and on the cliff top at Aldbrough (Figure 11). The laser scanner is set up at each end of the baseline and a 'backsight' or 'tiepoint' reading taken of a target fixed at the other end. This provides horizontal angle data relative to the datum within the scanner. In the case of the VZ

small reflective scanner targets (located with dGPS/GNSS) are placed in the field of view. Both ends of the baseline are located with the dGPS. This establishes the location of the baseline within the British National Grid co-ordinate system. Multiple overlapping scans taken from different locations (for instance from the platform and cliff top) are later combined in the software so that shadow areas are minimised and a more accurate and complete 3D image recorded. Accurate positioning is essential for multiple scanning and for monitoring. At Aldbrough, and indeed at most coastal locations, this usually requires accurate dGPS positioning. The technology of global positioning has improved over the monitoring period and, reflecting the importance of positioning to the overall aims of the task, several upgrades have been implemented throughout the duration of the monitoring period, including a move to full Network Real-Time Kinematic (Network RTK) using the UK-wide Leica SmartNet in 2006 and full Global Navigation Satellite System (GNSS) capability in 2012. The importance of global positioning to this type of monitoring cannot be over-emphasized in order to produce accurate calculations from the models.

Figure 10 Riegl LPM2K (left), LPM-i800HA (middle) and VZ1000 (right) laser scanners

Reflecting the improvements in technology, for recent surveys the method described above has been modified so that a single tiepoint has been positioned in view of all scan positions. This has removed the need for a baseline. The single tiepoint position also lent itself to the use of a dGPS/GNSS base-station, which was set up on the tiepoint, another method recently adopted. This provided a useful alternative to Network RTK which has proved to be intermittent at Aldbrough.

Those shadow areas irresolvable from the baseline are infilled, where accessible, using a roving dGPS unit and the point data are added to the 3D model. Analyses of repeated scans over a regular time interval

can accurately determine the rate of recession, the nature of landslide processes and any other morphological changes in the cliff face and on the platform.

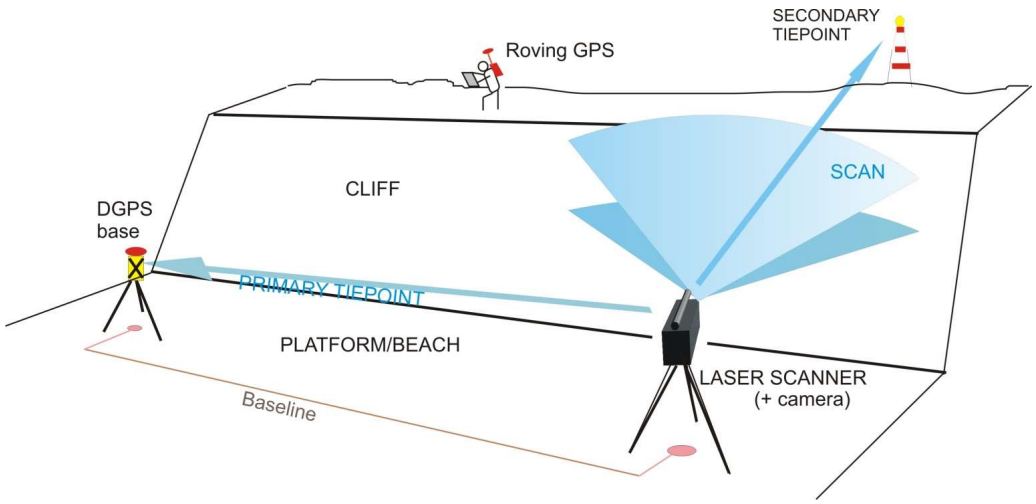

Figure 11 Schematic of 'baseline' method of laser scanning linear features

The key factor in the successful use of long-range TLS is the accurate levelling and horizontal and vertical location of the instrument plus at least one other point (any positional errors are magnified with distance). In most cases, this is achieved with a high quality dGPS / GNSS, which is essential, if the 3D model produced is to be oriented to national grid co-ordinates, and when coastal changes are to be monitored. These types of laser scanner are not effective where the subject is moving (e.g. water, vegetation), or where the laser pulse is reflected by heavy rain, fog, dust or smoke. However, low light level does not present a problem, as it does, for example, with photogrammetry. The addition of colour photography in 2005 has greatly improved the usefulness of the models for geological purposes as it enhances rock type and feature identification.

An attempt has been made to assess the accuracy of the laser scan models as part of the task. However, Buckley *et al.* (2008) highlight the difficulty in quantifying the accuracy of these models. This is because they rely on several unrelated factors, the principal of these being laser range-finding and dGPS accuracy. Manufacturers supply specifications which include factors such as accuracy, repeatability (precision) and resolution. Additional factors that affect accuracy include atmospheric conditions (laser), tripod stability (laser and dGPS), and reflectivity (laser) of subject materials. The estimated influence of these, and other factors, are summarised in Table 1.

Table 1 Summary of TLS surveying factors influencing 3D model accuracy

Method	Source of inaccuracy	Manufacturer's specification: accuracy	Influence on 3D model accuracy
TLS	Range-finding	25mm (50mm*)	Medium
	Reflectivity of subject		Low
	Atmospheric conditions		Low
	Laser beam divergence	0.8 mrad	Medium
	Platform rotation (V and H)	0.009 degrees	High
GPS	Position (x,y)	5mm + 0.5ppm#	

	Height (z)	10mm + 1.0ppm#	
	Satellite configuration		High
	Post-processing		Low
Platform stability/ levelling	Tripod / tribrach level		High
	Height measurement		High

* = rms for Riegl LPM2K. (otherwise Riegl LPMi800HA)
# = rms for Leica SR530 system with rapid static and standard antenna

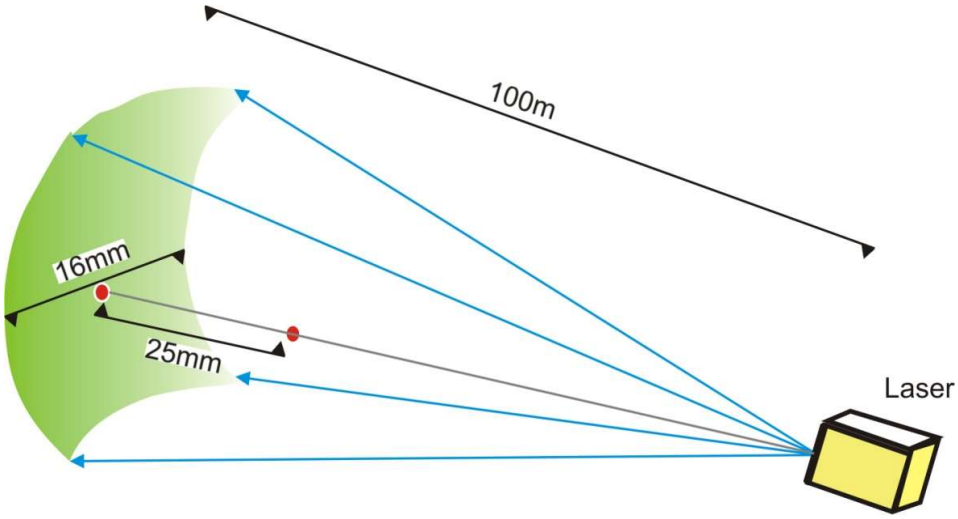

Figure 12 Schematic illustrating accuracy of angular (green) and range (red) components of laser scan (xyz) data

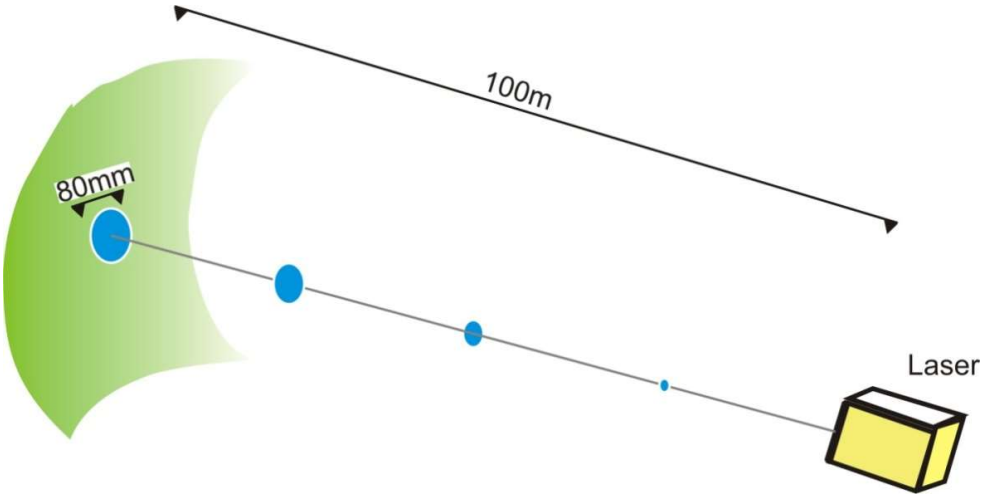

Figure 13 Schematic illustrating laser beam footprint expanding linearly with range

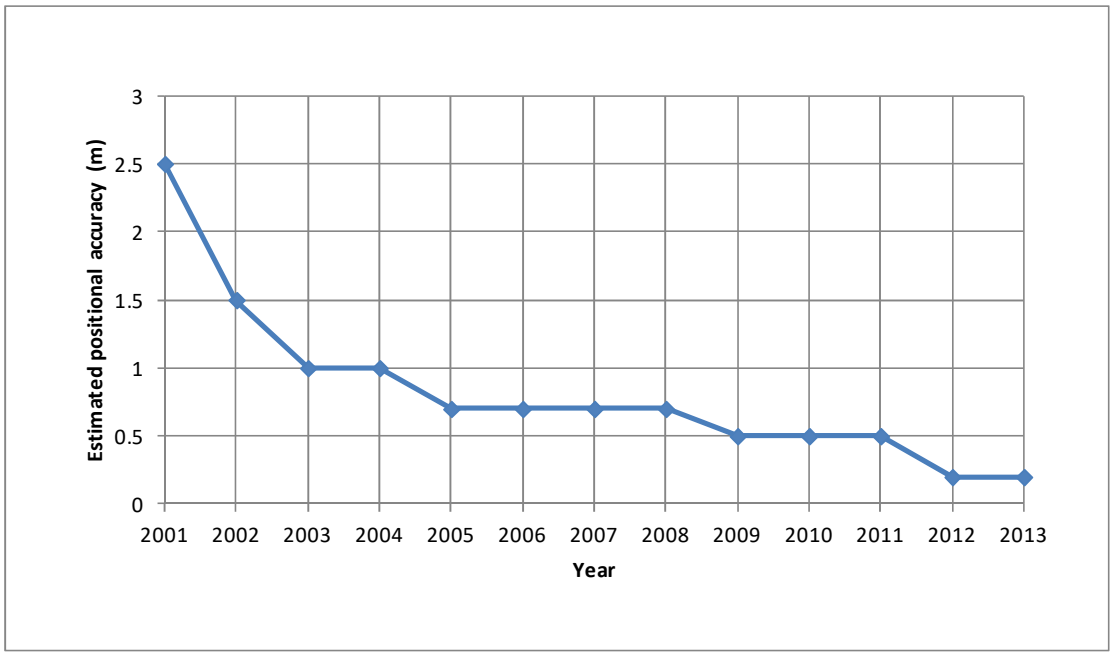

Figure 14 Estimated improvements in positional accuracy of TLS (scanner + dGPS) during task

The range-finding accuracy is quoted as 50 mm for the Riegl LPM2K, 25 mm for the Riegl LPMi800HA and 15 mm for the VZ1000, though repeatability in each case is considerably better; for example, it was found that baseline distances of 100 m were capable of repeat measurement to 1 mm (1 in 250000) under ideal conditions with the LPM scanners. These values are largely unaffected by range if atmospheric conditions are ignored. The pan/tilt mount has a stepper motor resolution of 0.009º. This represents a movement of 16 mm per 100 m range (Figure 12). The laser beam divergence for the LPM2K and LPMi800HA scanners is 0.8 mrad. This is equivalent to an 80 mm increase of beam width per 100 m range (Figure 13). Other ranges are linearly proportional in each case. The significance of this is that where a scan involves large distances, those far objects will be less well defined in terms of position and form than close objects. For example, at a range of 500 m, the laser footprint is about 0.4 m in diameter. This factor particularly affects objects inclined at an acute angle to the direction of the laser beam. An estimate of the improvements in the overall positional accuracy of the combined TLS (scanner + dGPS) during the task is shown in Figure 14 showing how accuracy has improved during the early days of the task from around 2.5 m to <20 cm in the later scans. These improvements have been largely due to equipment upgrades. The general picture, however, is of continuing improvement both in accuracy and ease of use.

The possibility of proliferation of errors in TLS is considered by Buckley *et al.* (2008). They stated that "*although LiDAR data provide a much higher level of accuracy and resolution than traditional field work, an awareness of the sources of error and uncertainty in the workflow, from data collection to modelling, is necessary*". This conclusion has also been borne out by the authors' experience in preparing the data for this report. One of the key problems has been that not all the data over the monitoring period are of equivalent accuracy. Determining where the errors lie in any survey has been a major undertaking, in part due to the fact that, as also stated by Buckley *et al.* (2008), there has been little guidance in these matters in the literature. In practice, scans have been adjusted to match the best scan determined from various reference points (i.e. hinterland features that have remained unchanged throughout the period). This has involved lateral displacement, 2-axis rotations and other ad-hoc manipulations of the data.

4.2 DATA PROCESSING

The TLS data produced by the oriented laser scan and dGPS / GNSS survey were processed to develop a 3D terrain model of the cliff. The raw data produced by the RiPROFILE™ and RiScanPro™ programs

consisted of 'point-clouds' ranging in size from a few thousand points in 2001 to tens of millions in 2013. These data were oriented using the relative dGPS / GNSS positions of both the scanner and the backsights or targets, and output as an ASCII file, made up of *x*, *y*, *z* and intensity values. The data were imported into GoCAD™ 2.1.5 (a digital 3D drawing program) where outlying or extraneous data points and artefacts (e.g. birds 'caught' in the scan, distant 'overshoot' points etc.) were removed and the 'cleaned' data exported. The data were then imported into Surfer™ 8 (a surface mapping program) and triangulated using a geostatistical gridding method to produce a solid surface model. From this model cross-sections and volumes could be extracted, and change models calculated. The data were also imported into QT Modeler™ 5.1 (a 3D model manipulation package), gridded and displayed as a 3D surface model. The resulting model could then be enhanced by overlaying photographs, maps or intensity colouration onto it. A data processing flow chart, typical of the middle period of the task, is shown in Figure 15. This was subsequently simplified with the introduction of more advanced software.

In 2011 the 'IMAlign™' package within Polyworks (InnovMetrics ™) was added to the suite of programs and was used to align individual scans, to check for errors in orientation and to produce the final surface 3D models. As an alternative, a combination of MapInfo™ and Vertical Mapper ™ was used to generate change models and animations, and to calculate volumes. In 2013 the Maptek I-Sight software package was acquired and was used to produce the finalised change models and recession quantities described later in this report.

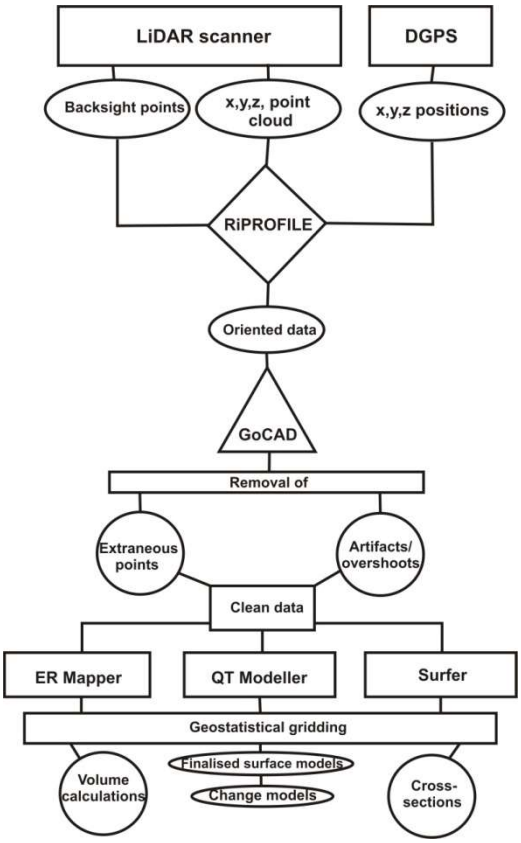

Figure 15 Schematic showing typical data processing software path used mid-task.

A recurring problem with data processing throughout the middle and later periods of this task has been the necessity to degrade or decimate data in order that the 32-bit, or more recently 64-bit, PC's available can cope with it. This process highlights the discrepancies often found between the relative capabilities of 'capture' and 'processing' hardware and software. This issue becomes magnified when considering the new generation of high-speed scanners, e.g. the recently acquired Riegl VZ1000 capable of recording up to 122,000 points per second and devices now on the market capable of 500,000 points per second scanning rate. A pragmatic balance between the density of data that can be handled and the desire for

geomorphological detail has to be struck. The increasing proliferation and expense of software and software licences are also important considerations.

4.3 GEOTECHNICAL SAMPLING AND TESTING

A limited number of disturbed and undisturbed samples were taken of representative lithologies at the Aldbrough site; both from the landslide and unslipped deposits within the cliff. The samples were returned to BGS (Keyworth) for geotechnical testing in the soil mechanics laboratories (section 11.1.1). In addition, a small number of in-situ ultra-lightweight penetrometer tests were carried out on the cliff at the Aldbrough site at an early stage of the task. During Phase 2 of the task six boreholes were drilled between 2012 and 2015 (section 11.1.2) which provided geotechnical samples for laboratory testing; details of which are provided in a separate report (Hobbs et al. 2015b). The testing was carried out in order to provide data for slope stability analysis (section 12.1.1).

4.3.1 Sampling

Disturbed samples for index testing were collected in medium and large plastic bags. Undisturbed samples were collected by an established BGS method utilising 100 mm diameter x 250 mm long plastic tubes with a metal cutter. This required preparation of a 'plinth' of in-situ material approximately 300 x 300 mm in plan, and at least 250 mm in height, into which the tube and cutter were carefully pushed using a combination of gentle downward pressure and trimming around the cutter with a sharp knife. The filled tube was then recovered by breaking the connection with the plinth at the base, removing the metal cutter and its contents using a cheese wire, and finally trimming the ends of the tube with a knife and straight edge. The ends were sealed with plastic caps, taped to prevent moisture loss, and the sample then made ready for transport. The contents of the cutter were removed and saved in a 'medium' plastic bag so that the cutter was ready for the next sampler. The cylindrical shape of the sample maximised its structural integrity and reduced the likelihood of damage in transit. The method minimised the amount of preparation, and hence disturbance, required in the laboratory when compared with a conventional cuboid-shaped block sample. The method also allowed accurate determinations of density to be made, as the dimensions and weight of the specimen were measured in the laboratory. *This tube method is suitable for clays and silts but not for sands or gravels.*

4.3.2 Laboratory Testing

A small laboratory *index* testing programme consisted of determinations of: particle-size analysis, water content, density, and Atterberg Limits (liquid and plastic limits). These were carried out according to BS1377 (1990) in the BGS (Keyworth) soil mechanics laboratories.

The laboratory *mechanical* testing programme consisted of triaxial testing using a GDS 100 mm stress-path system. The test used was the multi-stage 'consolidated isotropic undrained' (CIU) with pore pressure measurements (Head, 1996), allowing 'peak' effective strength parameters to be measured at effective average stresses of 100, 200 and 400 kPa applied to a single specimen. The specimen size was 102 mm diameter with a target length to diameter ratio of 2:1. Top, bottom, and side drains were used to facilitate consolidation. The specimen was saturated, prior to stage 1 isotropic consolidation, by staged ramping-up to an elevated (back) pressure; the final value being determined by the 'B-test' (i.e. pore pressure response to applied load increment). Axial compression was applied in the undrained state following each consolidation stage, with pore pressures measured at either end of the specimen. Stages 1 and 2 of axial compression were discontinued when the stress ratio reached a peak, whereas the stage 3 axial compression was continued beyond shear failure. A post-failure specimen is shown in Figure 16.

Figure 16 Post-failure 100mm diameter triaxial test specimen of Withernsea Till Member (principal shear surface shown by red arrows)

A further geotechnical laboratory test programme carried out on drill core obtained in April 2012 and January 2015 is described in Hobbs et al. (2015b). This work is ongoing at the time of reporting.

4.3.3 Field Testing

Field testing consisted of cone penetrometer tests on the cliffs using the Panda (types 1 and 2) ultra-lightweight penetrometer apparatus (Figure 17). This apparatus is capable of penetrating to depths of 5 m in most types of soil. There are two types of cone available; the larger is disposable and the smaller is fixed (Figure 17).

Figure 17 Panda™ ultra-lightweight penetrometer (Type 1) Note: alternative cones (right)

Four cable percussion boreholes were drilled in March 2012 (Phase 1). Subsequently, two cored boreholes were drilled in Jan 2015 (Phase 2) using the triple tube Geobore-S wireline system. Both are described in Hobbs et al. (2015a). Laboratory testing on samples taken from them are described in Hobbs et al. (2015b),

Both phases included downhole instrumentation: piezometer arrays and inclinometer tubes. The Phase 2 boreholes also included PRIME 3D resistivity arrays. A weather station was installed in Feb 2012.

5 Monitoring surveys

Twenty-three terrestrial LiDAR surveys (TLS) monitoring the Aldbrough test site were carried out between September 2001 and June 2013. Of these years, 2001, 2003, 2005, and 2007 had only one survey and 2008 had no survey. The surveying, monitoring and field testing programme is summarised in Table 2. This shows the equipment used and supplementary data sourced from outside BGS.

Table 2 Monitoring programme for the Aldbrough test site

Date	Survey	LiDAR system	dGPS / GNSS	Geotech.	Weather data	Offshore data
Oct 2000	Rec.		Garmin		Met Office	
Nov 2000	Rec.		Garmin		Met Office	
Apr 2001	Rec.		Garmin		Met Office	
Jun 2001	Rec.		Garmin		Met Office	
Sep 2001	TLS *	Riegl LPM2K	Garmin/Gringo	P	Met Office	
Apr 2002	TLS	Riegl LPM2K	Leica GS50		Met Office	
Sep 2002	TLS	Riegl LPM2K	Leica GS50		Met Office	
Oct 2003	TLS	Riegl LPM2K	Leica SR530	P/B	Met Office	
Apr 2004	TLS	Riegl LPM2K	Leica SR530		Met Office	
Aug 2004	TLS	Riegl LPM2K	Leica SR530	P/U	Met Office	
Sep 2005	TLS	Riegl LPMi800HA	Leica SR530		Met Office	
Sep 2006	TLS	Riegl LPMi800HA	Leica Smart		Met Office	
Oct 2006	TLS	Riegl LPMi800HA	Leica Smart		Met Office	
Aug 2007	TLS	Riegl LPMi800HA	Leica Smart		Met Office	
Apr 2009	TLS	Riegl LPMi800HA	Leica Smart		Met Office	
Oct 2009	TLS	Riegl LPMi800HA	Leica Smart		Met Office	
Mar 2010	TLS	Riegl LPMi800HA	Leica Smart		Met Office	
July 2010	TLS	Riegl LPMi800HA	Leica Viva		Met Office	
Feb 2011	TLS	Riegl LPMi800HA	Leica Viva		Met Office	
Oct 2011	TLS	Riegl LPMi800HA	Leica Viva		Met Office	CCO
Mar 2012	TLS	Riegl LPMi800HA	Leica Viva	Drilling Ph.1	Met Office	CCO
Apr 2012	TLS	Riegl LPMi800HA	Leica Viva	Piezo/Incl.	BGS station	CCO
Jul 2012	TLS	Riegl LPMi800HA	Leica Viva	Piezo/Incl.	BGS station	CCO
Oct 2012	TLS	Riegl LPMi800HA	Leica Viva	Piezo/Incl.	BGS station	CCO
Dec 2012	TLS	Riegl LPMi800HA	Leica Viva	Piezo/Incl.	BGS station	CCO
Mar 2013				Piezo/Incl.	BGS station	CCO
May 2013	TLS	Riegl VZ1000	Leica Viva	Piezo/Incl.	BGS station	CCO
Jun 2013	TLS	Riegl VZ1000	Leica Viva	Piezo/Incl.	BGS station	CCO
Sep 2013	TLS	Riegl VZ1000	Leica Viva	Piezo/Incl.	BGS station	CCO

B = bulk samples
Incl.= Borehole inclinometer monitoring
P = Panda penetrometer,
Piezo = Borehole piezometer array monitoring
Rec.= Reconnaissance survey
TLS =Terrestrial Laser Scan (LiDAR)
U = Undisturbed tube samples
*Survey carried out by 3D Laser Mapping Ltd (Riegl UK).
CCO Channel Coastal Observatory

6 Environmental data

6.1 WEATHER

Local monthly rainfall data were obtained from the Meteorological Office for the period January 2000 to June 2013 for the three weather stations closest to Aldbrough: Leconfield, Great Culvert P. Sta. and Winestead. These are summarised in Figure 18, Figure 19 and Figure 20. As the data from these stations do not provide 100 % continuous coverage their data have been intercalated in some cases (refer to Table 3.

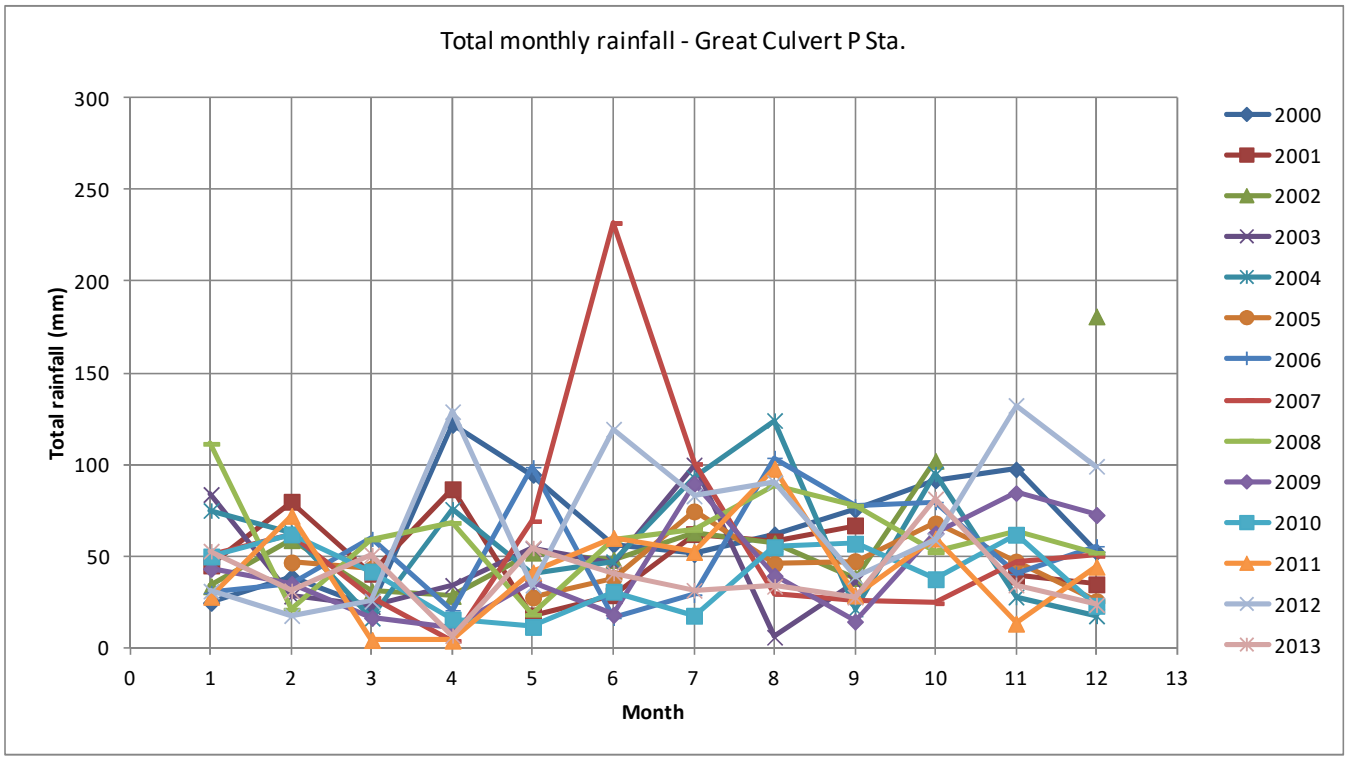

Figure 18 Rainfall: Great Culvert P Sta. (2000 – 2013)
(Source: Met Office)

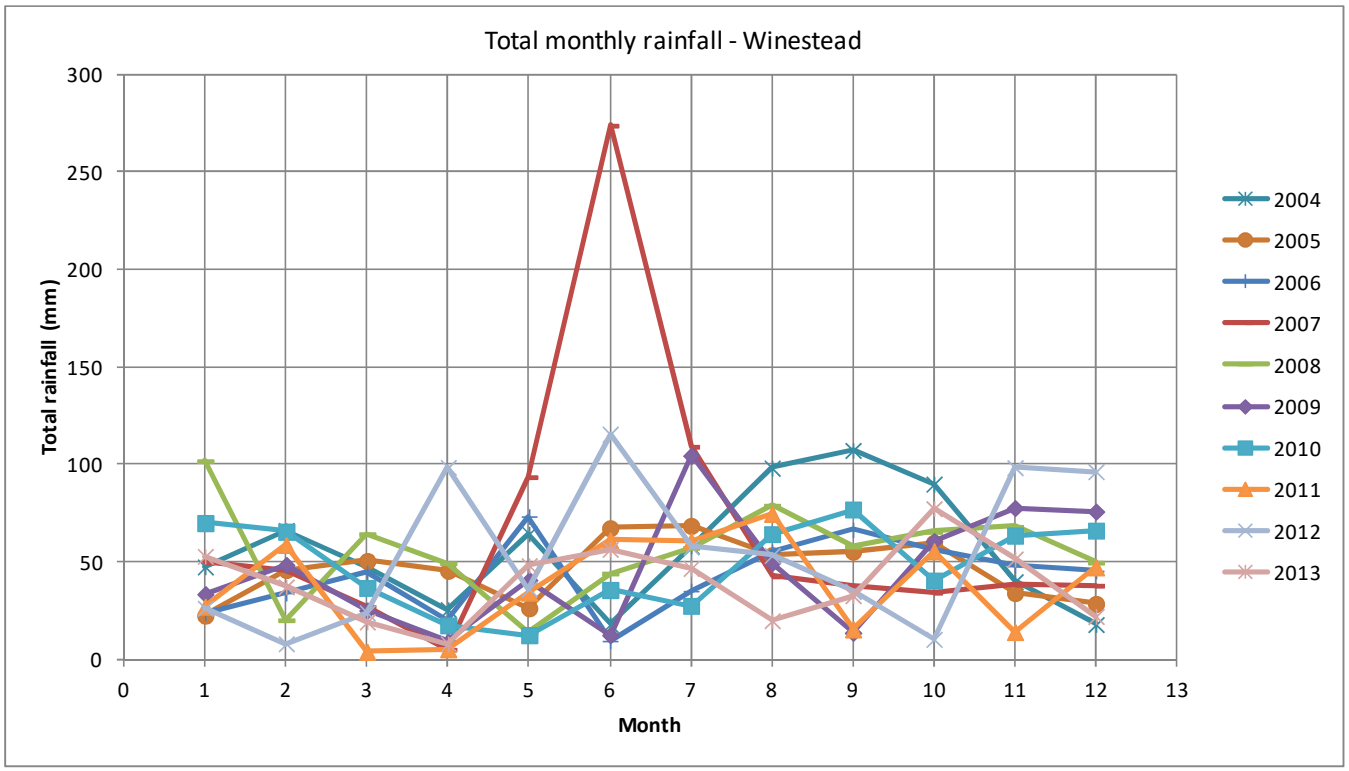

Figure 19 Total rainfall: Winestead (2004 – 2013)
(Source: Met Office)

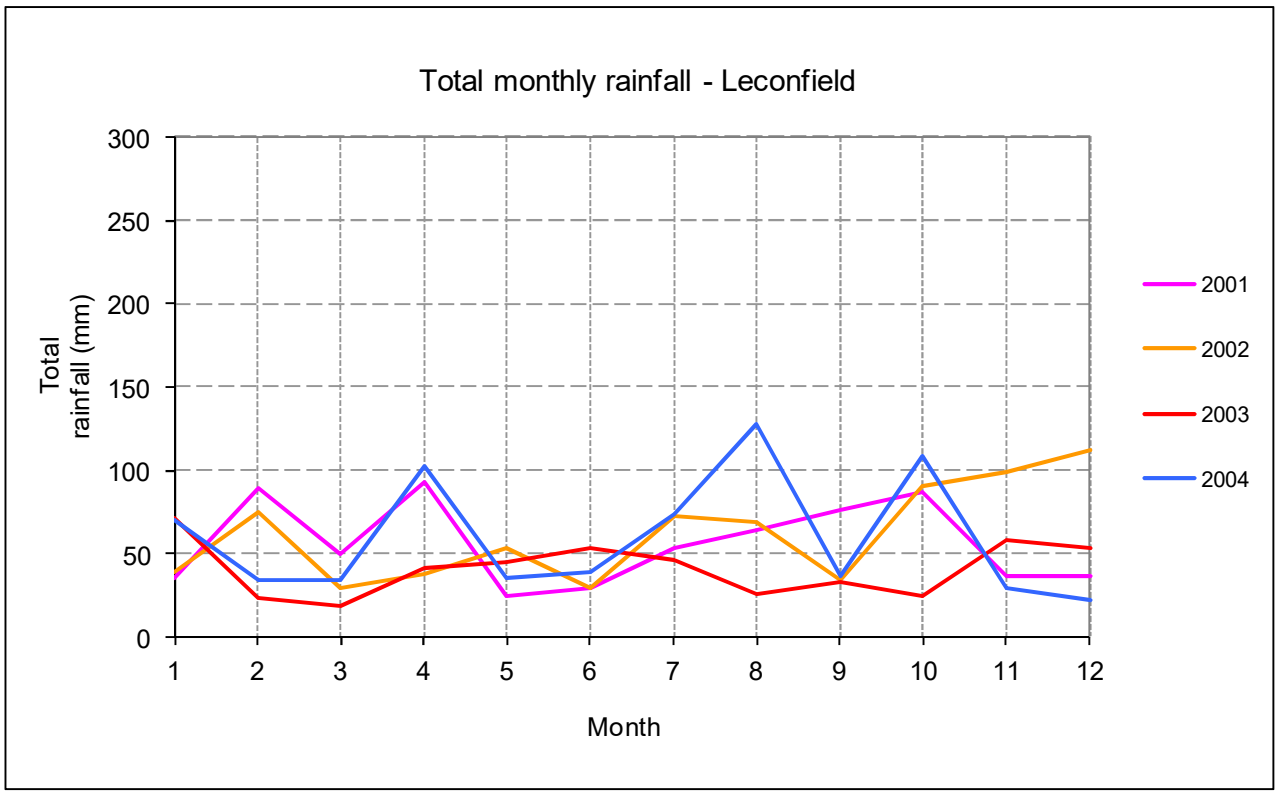

Figure 20 Total rainfall: Leconfield (2001 – 2004)
(Source: Met Office)

The weather station at Leconfield is located at NGR 5032, 4429; 22.8 km from the Aldbrough test site. At such a distance attempts at correlation between rainfall and landslide activity are, at best, tentative.

Other environmental data, such as tidal, wave and storm data have not proved consistent enough for correlating with landslide activity over the extended period of monitoring.

Table 3 Weather stations providing data used in this report

Station	Met Office I.D.	NGR	Elev. (m ASL)	Data used	Distance from test site
Leconfield	370	502545, 443169	7	Apr 01 – Apr 04	22.8 km
Great Culvert P. Sta.	17337	511455, 435559	3	Apr 04 – Aug 04 Sep 06 – Aug 07 Mar 12 – Jun 13	15.1 km
Winestead	55515	530085, 423462	4	Sep 05 – Sep 06 Aug 07 – Jun13	16.8 km
Aldbrough (BGS)		525461, 439627	16	Apr 12 – Jun 13	250 m

On 16th April 2012 a Campbell Scientific CR200X weather station was installed on farm land adjacent to, and owned by, the Aldbrough Leisure Park at Mount Pleasant Farm to the rear of 333, Seaside Road [NGR 525461,439627] (Figure 21). This is currently 250 m WNW from the centre of the test site. The weather station is solar/battery powered and automatically records rainfall, wind speed/direction, temperature, relative humidity, barometric pressure and solar radiation, currently at 10 minute intervals. The purpose of the weather station is to permit continuous monitoring of weather conditions at a location very close to the test area and to determine its effect on cliff stability. Rainfall and wind data in particular will be relevant to landsliding and coastal erosion, respectively. The sensors also allow evapotranspiration (ETo) to be calculated.

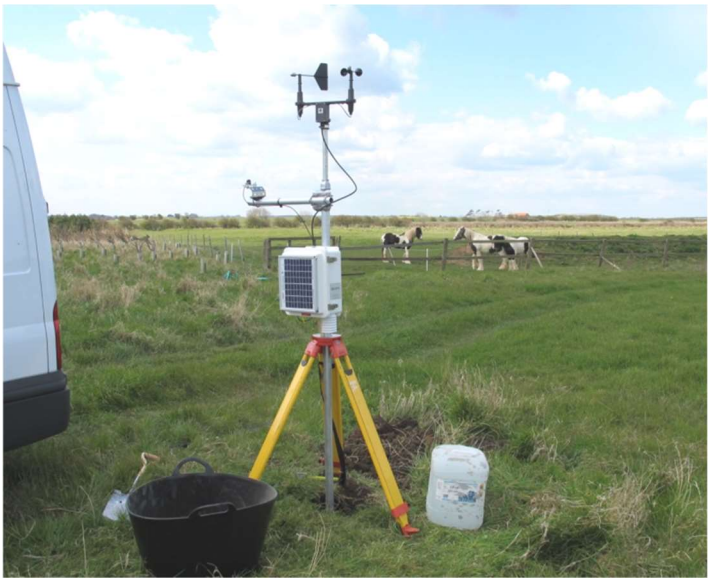

Figure 21 Installation of 'BGS Aldbrough' weather station (16th April, 2012)

Additionally, amateur weather stations linked to the Wundergound network (Wundergound, 2014) are currently as follows:

- Aldbrough, "IEASTYOR21" [NGR 523703, 438494], 2.3km to WSW of BGS test site,
- Burstwick, 12.0 km to SSW of BGS test site,
- Hedon, 13.0 km to SSW of BGS test site,
- Keyingham, 14.1 km to S of BGS test site.

The Aldbrough site (Station name "IEASTYOR21"), only has data available from Jan 2013. These data have not been used in the analyses in this report.

Data from the BGS 'Aldbrough' weather station, available from April 2012, are discussed in Section 11.2.

6.2 OCEANOGRAPHIC

The only published oceanographic data relevant to the Aldbrough test site were from the Channel Coastal Observatory (CCO) Waverider buoy 'Hornsea' from 2008. This buoy is situated 8.8 km north-east of the Aldbrough test site and provides data for wave height and direction. Data up to 2013 (at the time of reporting) have been made available by CCO and are discussed in Section 11.3.

7 Geology

The Glacial Tills forming the cliffs at Holderness are mostly Late Devensian (18,000 to 13,000 years old) and probably represent the products of more than one glacial regime and more than one till-forming process (Clark et al., 2003). Four units were recognised on the Holderness coast (in age-ascending order): the Bridlington Member, the Skipsea Till Member, the Withernsea Till Member and the Hornsea Member; all belonging to the Holderness Formation. Elsewhere the Hessle Till Member is present at the surface. The stratigraphy at Aldbrough is summarised in Table 4. A thin peat was observed in a cliff section between tills by V. Banks (pers. comm.). A peat layer was dated by Evans and Thomson (2010) at 11.6 ka (^{14}C) BP. No peat was observed in borehole core obtained at Aldbrough (Hobbs et al., 2015a). The two major Late Devensian Till members on the Holderness coast are the 'Skipsea Till Member' (Figure 22) and the overlying 'Withernsea Member' (Figure 23). These are believed to be lodgement tills (Lewis, 1999). The Withernsea Member extends from Easington in the south to Mappleton in the north (Quinn *et al.*, 2010). Stratified deposits and shear planes are described as separating the two till members (Catt, 1991), though these have not been observed in borehole core to date (Hobbs et al., 2015a). It is unclear whether the Mill Hill Member is present at Aldbrough (Table 4, Figure 25) though it has been observed in parts of the cliff, and its presence has been assumed in this survey. The Withernsea Member is described as a massive fine-grained diamicton (Lewis, 1999). The Skipsea Till Member is described as a banded stratified and deformed structure with pervasive shears and attenuation structures (Lewis, 1999), though these features have not been observed in borehole core obtained at Aldbrough to date (Hobbs et al., 2015a). These tills are clay matrix dominant and have a clay mineralogy of kaolinite and illite (kaolinite increasing upward), and a clay size content of up to 40 % (Bell and Forster, 1991). The provenance of clasts within the Tills is varied: Norway, North Sea, and Northern England; the main sources being the Lias, the Permo-Trias and the Carboniferous (McMillan et al., 2011). The Dimlington Bed, situated between the Skipsea Till Member and the Bridlington Member, has been observed in borehole core (Hobbs et al., 2015a) and is a thin bed of clayey silt around 2 m thick.

Table 4 Stratigraphy at Aldbrough

Current terminology	*Former terminology*	*Age*	*Stratotype*
Hornsea Member (Holderness Formation)	??	Late Devensian (18,000 – 13,000BP)	Hornsea cliff?
Withernsea Member (Holderness Formation)	Purple Till (Bisat, 1939)	Late Devensian (18,000 – 13,000BP)	Dimlington cliff [TA 376237]
Mill Hill Member (Holderness Formation)	?	Late Devensian (18,000 – 13,000BP)	Dimlington cliff [TA 376237]
Skipsea Till Member (Holderness Formation)	Drab Till (Bisat, 1939)	Late Devensian (18,000 – 13,000BP)	Dimlington cliff [TA 376237]
Dimlington Bed (Holderness Formation)	Laminated Silts	?	
Bridlington Member (Holderness Formation)	*Basement Till* Bridlington Till (Lewis, 1999)	Wolstonian (300,000 – 175,000BP)	Bridlington cliff?

Figure 22 Skipsea Till Member fabric (Holderness Formation)
Note: closely-spaced vertical jointing

The plasticity classification of the tills is 'low' to 'intermediate'; the Bridlington and Withernsea Members being somewhat more plastic than the Skipsea Till Member. All tills plot well above the Casagrande A-line. There is an overall, but slight, coarsening upward of the clay / silt particle size from the Bridlington to the Skipsea Member. Strength tends to decrease upward; the Bridlington and Skipsea Till Member being stronger than the Withernsea and the highly weathered near-surface material. Low strength sensitivity to remoulding was noted throughout. This has implications for the rate of movement of mudflows in till; a 'conveyor belt' type of creep/erosion cycle being favoured, rather than catastrophic flow failure. Deformation till is a common feature of the Holderness coast. This is particularly clearly seen where chalk debris marks the shear surfaces. Such features are found in the Skipsea Till and Bridlington Members, most of the clasts of which are chalk-derived.

Figure 23 Withernsea Member fabric (Holderness Formation)

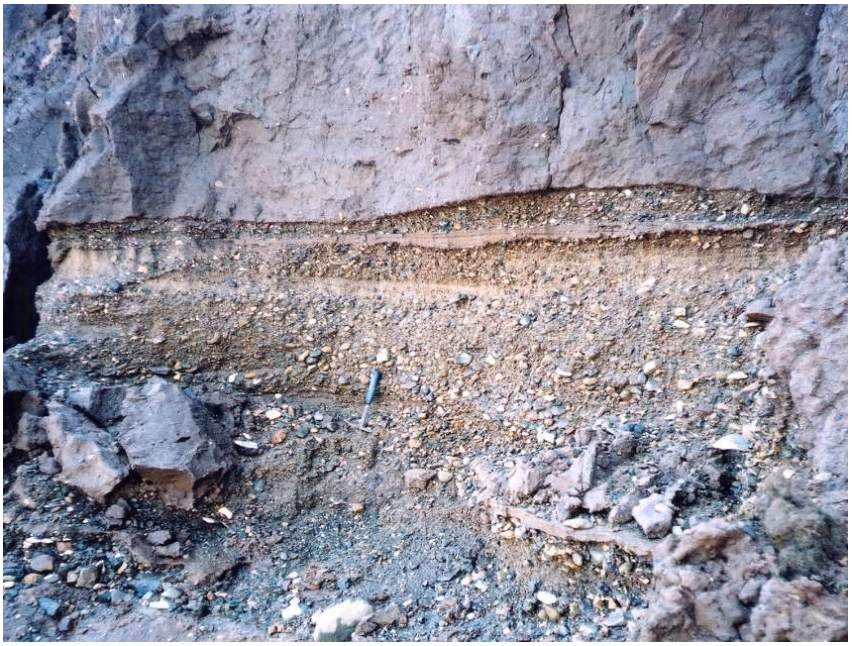

Figure 24 Sand and gravel lenses in the Withernsea Member (Holderness Formation)

Figure 25 Mill Hill Member sands and gravels (Holderness Formation)
Note: active seepage

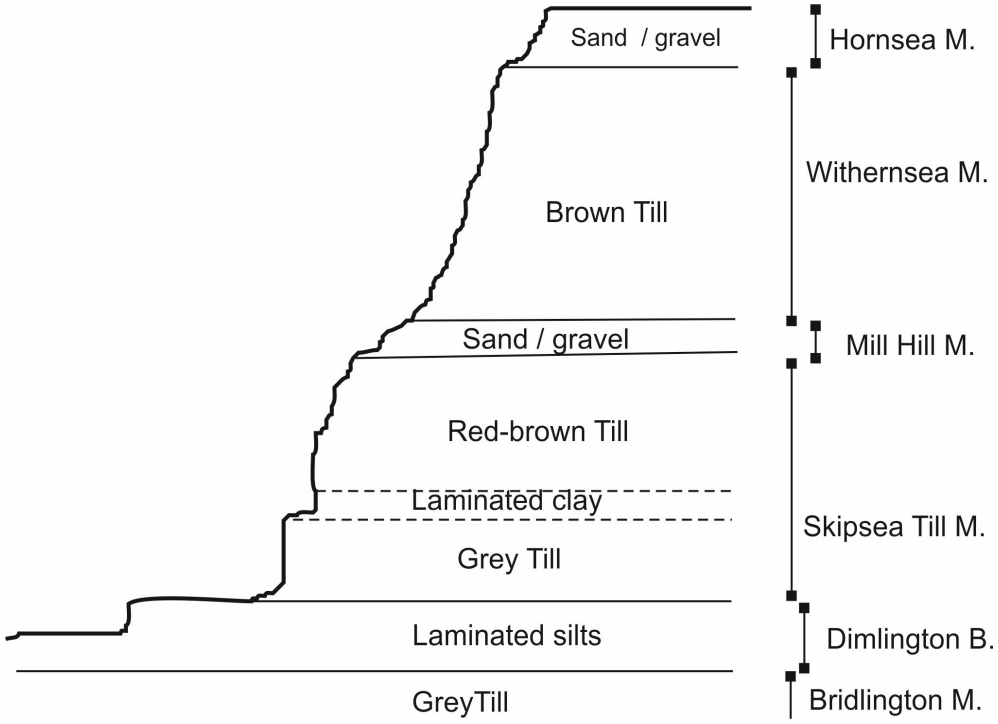

Figure 26 Cliff cross-section showing generalised lithostratigraphy

Referring to Figure 26 the 'Hornsea Member' is described by Evans and Thomson (2010) as *"superficials: rhythmically laminated silts and sands with dropstones (LFA2b)*". This represents a channel infill within the 'Brown till'. Between this and the 'superficials' Evans and Thomson (2010) describe a thin "*Peat dated at 11.6 ka ^{14}C BP*", though this has not observed at the Aldbrough test site to date. However, two very thin bands described as 'coal' or 'shale' have been observed close to the base of the Hornsea Member at a depth of about 1.6 m. The 'Brown till' (Figure 23) is described by Evans and Thomson (2010) as "*massive to laminated brown or red to grey diamicton, LFA4 up to 6 m thick*" and the 'Mill Hill Member' (Figure 25) as "*upward fining sequences of moderately to well-sorted coarse gravels to medium and very fine sands, LFA3*". Contacts between these beds are generally very sharp. The 'red-brown' and the 'grey till' of the Skipsea Till Member (Figure 22) appear to correspond to the "LFA1" unit of Evans and Thomson (2010) which they describe as "clast-poor, massive to laminated, very dark greyish brown chalk-clast-rich diamicton with thin, locally folded, reddish laminated clays ascribed in origin to offshore Liassic and Triassic mudstones. Microfabrics collected from LFA1 showed a NE-SW clast orientation (Evans and Thomson, 2010). Folding is seen in the upper parts of the Mill Hill Member. Fold axial planes were found by Evans and Thomson (2010) to dip towards the N to NE, documenting stress from that direction. The Bridlington Till is not exposed in the cliff at the test site, but to a limited extent in the platform when the beach is absent. Now referred to as the Bridlington Member the Basement Till is Pre-Devensian and comprises a grey clay matrix lodgement till (Catt, 2007; Catt and Digby, 1988; Catt and Penny, 1966). Its relationship to datable deposits at Sewerby places it in the Marine Isotope Stage 6, the penultimate cold stage of the Quaternary (Catt, 2007).

The glacial deposits at Aldbrough and the Holderness coast are underlain generally by a dissected chalk bedrock plateau of the Early Cretaceous (Campanian to Maastrichtian) Rowe Chalk Formation. Formerly known as the Flamborough Formation, this consists of white flint-bearing chalk with marl bands and is believed to lie at depths of 27 m and 29 m bmsl in the vicinity of Aldbrough (BGS borehole nos. TA24SWBJ2 and TA23NEBJ4). It subcrops within only a small area onshore between Barmston and Withernsea and here is about 80 m thick (Sumbler, 1999; Lott and Knox, 1994). The thickness increases to about 380 m offshore.

8 Geomorphology

8.1 CLIFF

The cliff has a NE to ENE aspect, maintains a steep face, and is divided into poorly developed arcuate or elongate embayments. The cliff profile is stepped by virtue of the contrasting resistances to erosion of the tills and the landslide processes affecting the upper and mid parts of the cliff (Figure 27). At high tides the lower, and in the case of storm events the mid, sections of the cliff are subject to considerable mechanical scour from direct wave action. This forms gullies and scour hollows (Figure 27), occasionally in the form of caves (Figure 40).

Figure 27 Marine erosion of cliff toe tills
Note: water-worn unslipped grey till beneath slipped brown tills and scour hollow (right) (Sep 2003)

The cliff height at the Aldbrough test site is between 16 m and 17 m. A dividing line between *shallow* landsliding, controlled by 'structural weaknesses', and *deep* landsliding ('mass failures') was suggested to be at an elevation of 13 m or 15 m OD by Quinn *et al*. (2010) for the Holderness coast; the shallow events having produced up to 2.5 m of cliff-top retreat per event. Quinn *et al*. (2010) also placed a lower bound height of 7 m OD below which mass movement was unlikely to occur, and recession dominated by 'marine erosion and abrasion' more likely. These cliff height classifications apply at Aldbrough, inasmuch as mass movement is predominant and in the form of deep-seated landsliding. Refer also to section 8.3.1.

8.1.1 Sediment yield

The coastal erosion and sediment yield of the Holderness coast have been estimated (Pethick, 1996) using an average recession rate and cliff height and calculated (Pye & Blott, 2010) from the East Riding of Yorkshire Council pin survey dataset. Balson *et al* (1998) quoted a variety of earlier sediment yield estimates which range from 3.2 to 3.9 million m^3/yr (for cliff and shoreface) and 0.5 to 2.0 million m^3/yr. (for cliff only). Sediment yield has normally been calculated by multiplying the length of coastline by the average cliff height by the average recession rate. This has given volumes of up to 2 million m^3 /year for the cliff and up to 4 million m^3 /year for cliff and shore face combined, using data going back to 1786. These data are summarised in Table 5. Cliff height is a problematic factor when considering archive data,

as it varies both parallel and perpendicular to the coast. The method proposed by Balson *et al* (1998) was to quantify the potential yield in terms of both volume and nature of eroded sediment. The influence of lithological variation is thus taken into account. Cliff height has been correlated with geomorphological factors by Quinn *et al* (2010) (section 8.1). Pethick (1996) estimated that 1 million m^3 of sediment was produced per year of which 72% was clay and silt sized and 28% sand sized.

Table 5 Published recession volumes for Holderness

Author	Average volume (m^3/yr)	Average volume (m^3/yr/metre)	Location	Data period
Pethick (1996)	1,000,000	44.6	Holderness	?
Balson et al., (1998)	500,000 – 2,000,000	22.3 – 89.2	Holderness	?
Pye & Blott (2010)	513,488	22.9	Hornsea to Withernsea	1852 - 2009

The published data in Table 5 (average volume in m^3/yr/metre) show a reasonable agreement with the average recession rate from this project (section 10.2.1); though the latter are 35% higher than the lower bounds of Balson et al., (1998) and Pye & Blott (2010). This increase could be construed as significant if the data reported here could be considered comparable with the historic data for the whole Holderness coast. However, the data reported here are 30% lower than those of Pethick (1996). Also the time spans of the published data and the data reported here are very different. As a general comment, if comparisons are to be made of this nature, Holderness could be considered the most favourable environment in which to make them, due to its uniformity over a large distance, when compared with other coastlines in Britain.

8.2 PLATFORM AND BEACH

The till platform at Aldbrough has been exposed only rarely and over a limited area during the study period. It consists of a red or grey till of the Bridlington Member which is found beneath the Skipsea Till Member or the Dimlington Bed (where present). The platform is poorly exposed at low elevation beneath a mobile beach deposit, offshore of which is typically found a large-scale rhythmic sand bar running obliquely to the coast. This is believed to be part of an '*ord*' system of sand features which translate southward with time (Pringle, 1985; Moore *et al*., 2003).

Ord is a local name for a thin veneer of beach sediment over an area of exposed till shore platform allowing waves to reach the cliff toe. It is thought that erosion of the coast is focused immediately behind the ords and that as the ords migrate southwards; as sediment is transported along the coast, these zones of focused erosion move with them (Balson, pers.comm.). Moore *et al* (2003) seem to indicate that an ord is a unit characterised by several geomorphological features including a low beach. In between ords the platform tends to be better exposed. Thus the protection to cliff and platform afforded by the ords is transient at any particular location.

The ability of the beach (if present) to aid resistance to cliff recession is controlled by two factors: firstly the ability to resist mechanical erosion by waves (Hackney *et al*., 2013), and secondly the ability to provide a toe weight against deep-seated landslide movement. The former is reasonably clear as a beach directly protects the toe of the cliff. The latter is less clear as it depends on the geometry of the landslide; for example, whether or not the slip planes daylight at beach level or above (Figure 28). It therefore appears that the presence or otherwise of ords is particularly significant where the cliff is sufficiently high to allow deep-seated rotations of the type illustrated in Section 8.3.

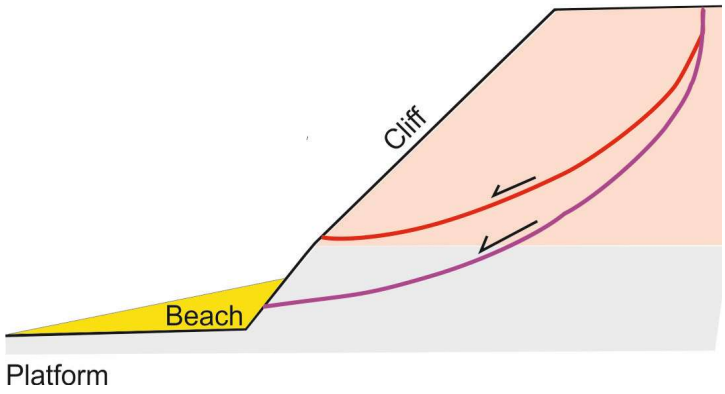

Figure 28 Schematic showing examples of possible slip planes daylighting in cliff face relative to the beach deposit.

Butcher (1991) reported a beach thickness variation of 3 m at Cowden, 2 km north of Aldbrough, over a 5 year observation period.

8.3 LANDSLIDES

Active landsliding has been observed at the Aldbrough site throughout the duration of the project. The principal mode is that of rotation. The secondary modes are toppling and falls, and the tertiary debris flows.

8.3.1 Rotations

The rotations developed from the cliff top, are typically arcuate or elongate in plan (20 to 30 m long), and an estimated 7 to 15 m deep (i.e. almost full cliff height). The rotations observed at Aldbrough tend not to reach below platform level, but are either slightly above platform level (purple line in Figure 28), or are confined to the deposits above the Skipsea Till Member; that is, approximately ⅔ of the cliff height at this location (red line in Figure 28). This compares with a deeper seated landslide described by Butcher (1991) at Cowden which is depicted as having a compound slip surface, rather than a purely rotational one, extending to several metres below sea level; these observations having been made by shear tubes installed in the beach. Butcher (1991) noted that factors of safety increased by up to 19% when the full variation of observed beach levels (3 m) was introduced into his deep-seated (below beach level) slope stability model; thus illustrating a “toe loading” effect.

The pattern of rotation development frequently follows that shown in Figure 29 with examples in Figure 31 to Figure 35 whereby lateral development of rotations results in an elongate embayment, frequently with greatest subsidence within the initiating semi-circular embayment, and decreasing subsidence away from it. Developing pre-subsidence tension cracks may also be found further along the cliff-top. The mechanism is due to the fact that the initial rotation reduces lateral support to the adjacent block which initiates its own rotation, and so on. This is made possible by the very prominent jointing pattern in the tills and stress relief cracking inferred to be running parallel to the cliff. During the later stages of the process the individual embayments tend to amalgamate with further rotation and break-up, the rotated masses adopting a characteristic tilt towards the original movement.

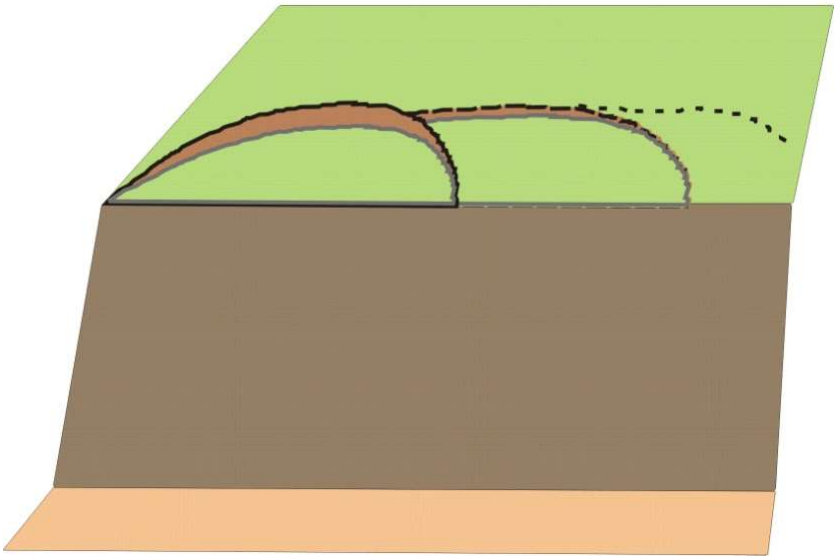

Figure 29 Lateral progression of rotations to form elongate embayment

Figure 30 Early stages of deep-seated rotational landslide development, central embayment (Aug 2004)

Figure 31 Principal mode of landsliding in upper cliff: rotations
(Note: Seaside Road and lateral development of elongate embayment) **(Sep 2004)**

Figure 32 Well-developed deep-seated rotations forming or deepening an embayment, Sep 2002

Figure 33 Early stages of en-echelon rotations showing enhanced deformation northward (towards camera) Refer to Figure 29, **Nov 2005**

Figure 34 Central embayment of test area, looking northward, showing well-developed multiple deep-seated rotations and embayment development (Oct 2011)

Figure 35 Central embayment of test area, looking northward, showing the latter stages of multiple deep-seated rotational landslide degradation and embayment development (Mar 2012)
Note: Cable percussion drilling rig adjacent to Seaside Road
Note: Demolition of bungalow shown in Figure 34

Degradation of the large rotational landslides progresses by means of the individual slipped masses reducing in size and becoming isolated, forming small ridges perpendicular to the cliff (Figure 36). Ultimately, these break up, some of the debris forming armoured mud balls; clay balls surrounded by gravel collected from the beach.

Figure 36 Individual rotational slip masses in latter stages of degradation (Sep 2014)

8.3.2 Toppling and falls

The toppling failures and falls have been observed to emanate from the Skipsea Till Member, and consist of blocks about 2 to 3 m in height. These are produced by virtue of the pre-existing closely spaced, vertical and sub-vertical, orthogonal jointing patterns within the till on the cliff, notch development by extreme wave action at the base of the cliff removing support, development of stress-relief fractures parallel to the cliff and by seepage from the sand and gravel horizon. *These failures are frequent and present a particular hazard to members of the public at the foot of the cliff.* Such a fall was observed (at close hand!) on 20th September 2001 within a particularly active zone (Figure 37). The debris from this topple and fall broke up on impact with the beach. It was estimated to be around 3 m^3 in volume.

Fragments of landslide debris pick up shingle and become 'armoured mud-balls'. These are typically 200 to 400 mm in diameter and are formed by the rolling actions of the sea on blocks of till which have detached from the cliff. These become rounded and subsequently pick up gravel and sand from the beach (where present). This thin coating affords some protection from further erosion though during very active periods of erosion they appear to be absent. These tend to remain on the beach slightly longer than the rest of the till debris which is rapidly removed by the sea, as evidenced by the heavy sediment load colouring the water.

Figure 37 Fall/topple from Skipsea Till Member in cliff depositing debris onto beach (20/09/01) (NOTE: estimated 3 m^3 of material)

Figure 38 Fresh multiple topple within (temporary) backscarp at rear of large, well-developed rotational failure (Oct 2009)

An example of a multiple topple within one flank of a backscarp formed by an earlier large rotational failure is shown in Figure 38. These features appear to have formed as a result of short-term stress relief within a near-vertical backscarp, rather than having developed along pre-existing structural features within the till.

8.3.3 Debris flows

Debris or earth flows are only occasionally observed. These tend to form on mature slopes which have established a relatively shallow slope angle following a cycle of rotations or topples/falls and subsequent degradation, and are in response to heavy or prolonged rainfall events with the possible contribution of seepage. An example of such a debris flow is shown in Figure 39. This is sourced within the Withernsea Member, possibly involving break-up of a multiple topple or rotation, and has a depth of about 1 m.

Figure 39 Debris (or earth) flow within upper and mid-cliff (Dec 2012)
NOTE: Sidescarps

Notch cutting by wave action and falls at the cliff toe within the grey Skipsea Till Member occasionally develop into small caves (Figure 40). These may in turn collapse, creating further cliff instability, though this process has not been observed first hand.

Figure 40 Cave developed at beach level within Skipsea Till Member (Sep 2001)
Note: Active hoop stress fractures

The cliffs at the Aldbrough test site exhibit active instability throughout the year. Several instances of active instability have been observed during the short visits made for the monitoring programme. As described earlier there is more than one failure mechanism. The net result is that a steep overall cliff angle is achieved at certain stages of the cycle and with it a very active landslide regime. This is accompanied

by a very active erosional regime, where considerable quantities of sediment are rapidly removed from the beach and transported seaward and southward along the Holderness coast on an almost continuous basis. Evidence for this is seen in the omnipresent brown suspension in the sea extending to at least 100 m off-shore.

The cycle of landsliding follows the general pattern shown in Figure 29, whereby a single rotational landslide with an arcuate backscarp (Figure 31 and Figure 32), characteristic of a homogeneous medium, is followed by lateral extension due to a new rotational landslide, and so on, to form a laterally stepped sequence where the proximal landslide has developed the most, causing greatest subsidence at the cliff-top, and the distal landslide (or proto-landslide) the least (Figure 33). This process is almost certainly influenced by joint sets oriented sub-parallel, with the cliff line. The result is the development of an elongate embayment with arcuate ends. This part of the cycle was observed to take approximately 2 to 3 years to produce a recognisable feature. Subsequent failure and disruption may be rapid resulting in a more shallow-angled and debris-covered cliff.

Migration south-south-eastward of landslide embayments due to a prevailing angle of wave attack from the north-east has been postulated at Holderness by Pethick (1996) or, in the case of London Clay at Walton-on-the-Naze, due to jointing or groundwater seepage (Flory et al., 2002). Such migrations of embayments have not been observed at the Aldbrough test site over the period of monitoring (refer to Figure 117). For further discussion on this topic refer to Section 13.2).

9 Geotechnics

A limited programme of laboratory testing and in-situ testing was carried out at the Aldbrough test site; the purpose being to characterise the materials involved in landsliding and erosion, and to provide data for slope stability analyses. The results are described below and compared with data derived from the literature for Holderness.

A small number of Panda ultra-lightweight penetrometer tests were carried out at the Aldbrough test site. The locations are shown in Figure 41 and details in Table 6:

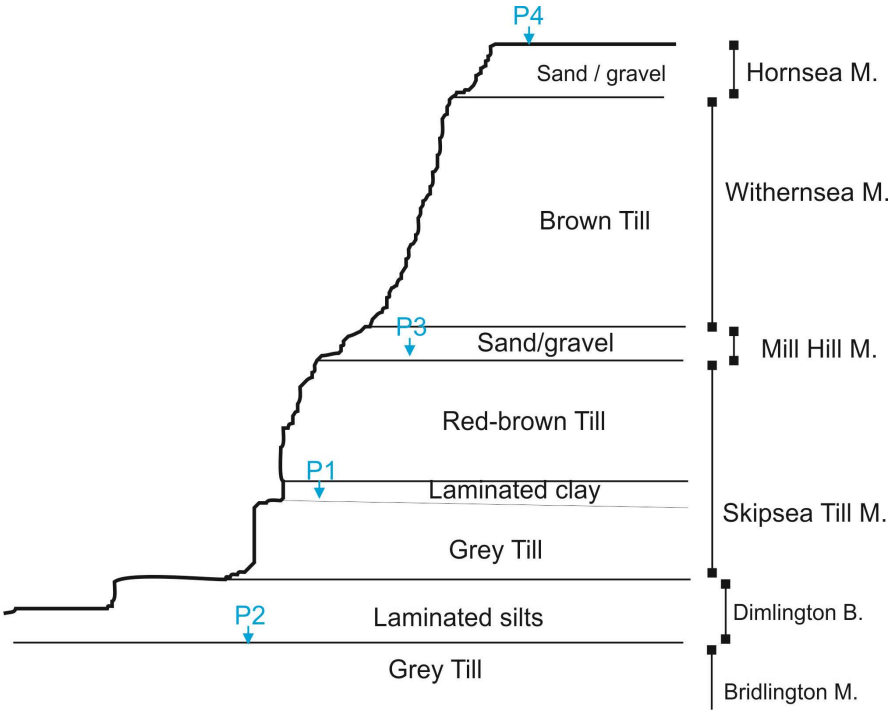

Figure 41 Cliff cross-section showing location of Panda penetrometer tests, P1 to P4 (refer to Table 6)

Table 6 Panda penetrometer tests (refer to Figure 41)

PANDA			
Date	**Formation / member**	**Test depth**	**Location**
20/09/01	Grey till (Skipsea Till M.)	0.51m	1 (0.5 m above beach, fall site)
24/09/03	Grey till (Skipsea Till M.)	1.15m	P1 (lower cliff)
24/09/03	Beach sand + red till (Skipsea Till M.)	1.30m	P2 (platform)
24/09/03	Red-brown till (Withernsea M.)	2.90m	P3 (mid-cliff) 525714.34 439588.45
24/09/03	Hornsea M. + brown till (Withernsea M.)	3.70m	P4 (Cliff top) 525717.65 439550.10
19/08/04	Brown till (Withernsea M.)	1.0 m	ALDU1

The purpose of the penetrometer tests was to determine strength profiles for the major formations, albeit from different locations on the cliff slope. The results are shown in combined form and depths corrected to ordnance datum in Figure 42. Whilst not showing true depth vs. cone resistance behaviour for the cliff overall, the plot shows relative increases in strength from the cliff surface to a depth of up to 5 m. The maximum achievable depth for this equipment was relatively shallow (up to 5 m) and the test was usually terminated by the presence of cobble-size clasts.

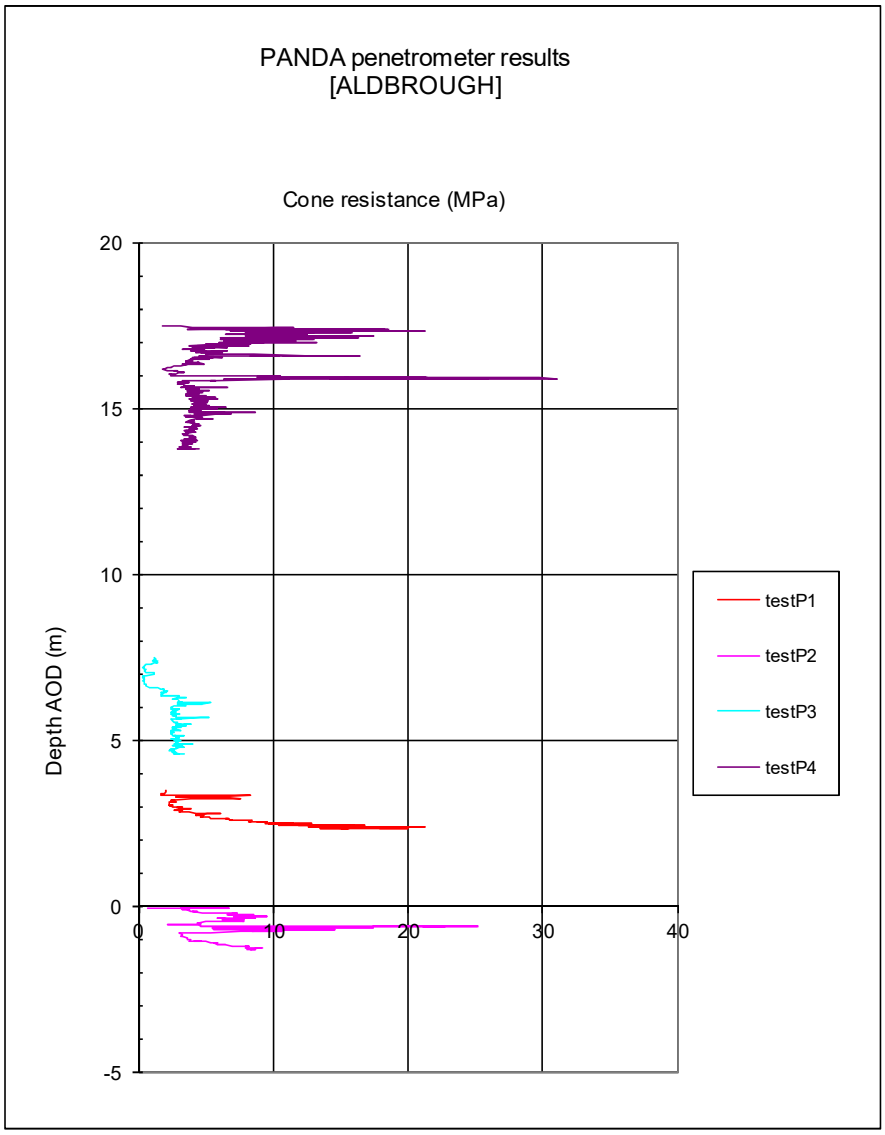

Figure 42 PANDA penetrometer profiles, Aldbrough (tests refer to Figure 41 and Table 6)

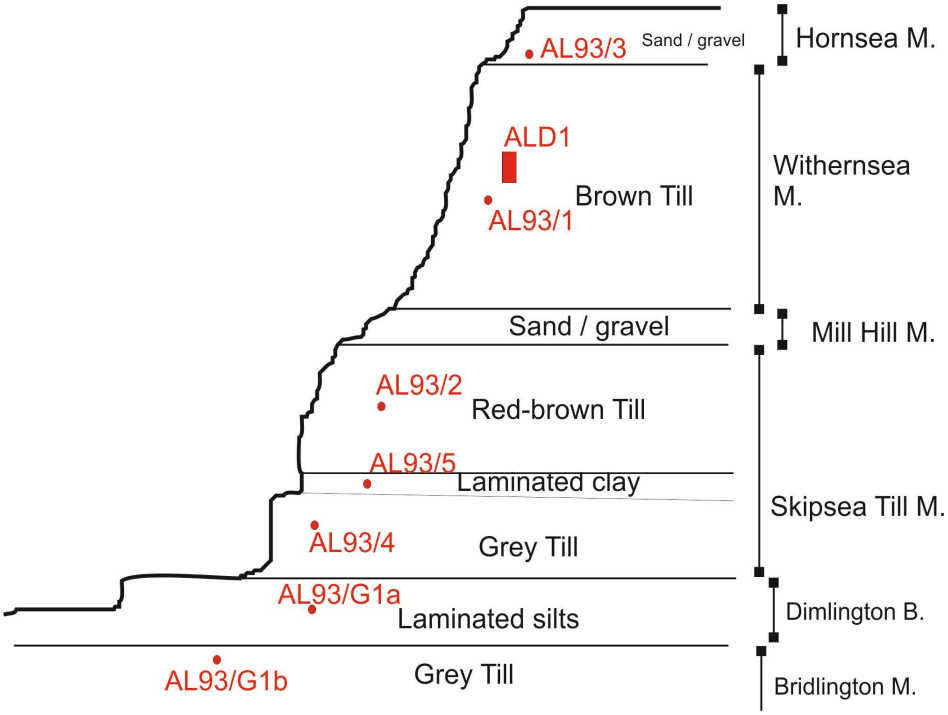

Figure 43 Cliff cross-section showing location of surface geotechnical samples (refer to Table 7)

Table 7 Geotechnical surface samples (refer to Figure **43**)

SAMPLE				
Date	**Lithology / Formation**	*Type*	*Ref. No.*	*Location*
23/09/03	Brown palaeosol (Withernsea M.)	m bag	AL93/3	4m in cliff (adjacent to Panda, P4)
23/09/03	Brown soil (Skipsea Till M.)	m bag	AL93/5	Between red and grey tills (near rockfall site)
24/09/03	Grey till (Skipsea Till M.)	m bag	AL93/4	Fall site, 1.5 m above beach
24/09/03	Brown till (Withernsea M.)	m bag	AL93/1	8 m above dGPS site F14, Adjacent to ALD1.
10/10/03	Grey lamin. Silt (Skipsea Till M.)	s bag	AL93/G1a	From platform at beach level (above sample AL93/G1b)
10/10/03	Red till (Skipsea Till M.)	s bag	AL93/G1b	From platform at beach level
24/09/03	Red till (Skipsea Till M.)	m bag	AL93/2	Location of rockfall, dGPS site F7 (AG/1)
19/08/04	Upper brown till (Withernsea M.)	U100	ALD1	3.8 m below cliff crest (in backscar), adjacent to AL93/1
14/11/12	Bridlington M.	m bag	AL slip plane	Slip zone material from landslide toe (to S of test area)

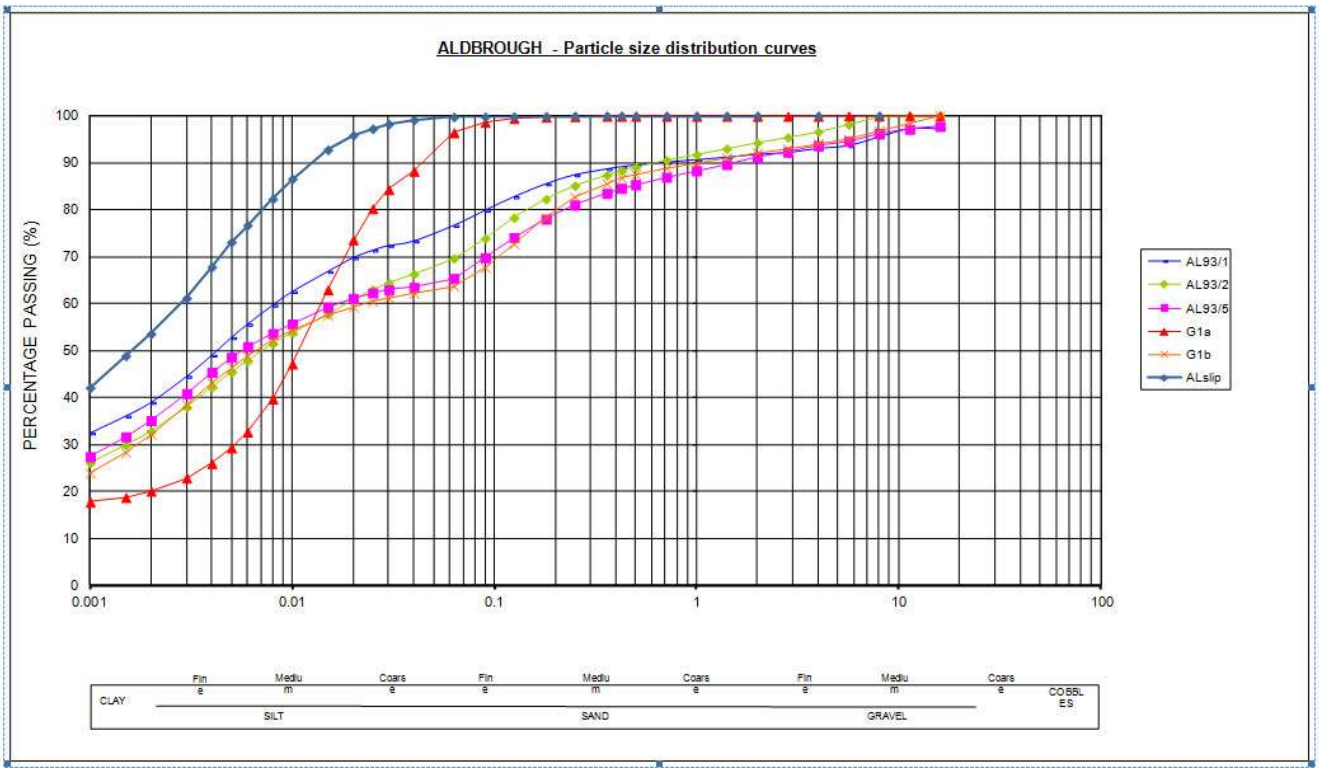

Figure 44 Particle size distribution plot for tills

The particle-size distribution plot (Figure 44) clearly shows the uniformity of the curves obtained and slight gap-grading exhibited by the till samples as distinct from the silt sample (G1a) which is well-graded. The till samples from the Skipsea Till Member display virtually identical particle-size plots. The sole Withernsea Member (till) sample (AL93/1) shows a slightly higher silt and fine sand content. The 'slip-plane' material from the Skipsea Till Member (ALslip) differs from the other tills in that it shows no gap-grading and has higher clay and silt contents with no coarse fraction. This is to be expected as slip plane material tends to be finer grained than the host material.

Table 8 Summary of particle size distribution results

	Strat.	Clay (%)	Silt (%)	Sand (%)	Gravel (%)
AL93/1	Withernsea M.	38.9	37.7	15.1	8.3
AL93/2	Skipsea Till M. (red-brown till)	32.8	36.8	24.6	5.7
AL93/5	Skipsea Till M. (lamin. clay)	35.1	30.3	25.8	8.8
G1a	Skipsea Till M. (lamin. silts)	20.1	76.4	3.5	0
G1b	Skipsea Till M. (red till)	32.2	31.5	28.4	7.9
ALslip	Bridlington M.	53.6	46.2	0.2	0

The results of a single multi-stage isotropically consolidated (multi-CIU) triaxial test on a 103 x 195 mm specimen of undisturbed Withernsea Till Member from a depth (on the cliff slope) of 0.15 m are shown.

Other strength data for Dimlington, Holderness (Bell, 2002) are shown in Table 10. These show an overall strength increase with age/depth from 'Hessle Till' to 'Skipsea Till'. However, the difference between 'Skipsea Till' and 'Bridlington Till' is negligible.

Tests for shrinkage limit were carried out on 'undisturbed' samples from the Phase 1 drilling programme in Borehole 1a at depths of 6.7 m, 15.8 m and 19.7 m, plus a test on a remoulded sample taken from the

cliff. These were carried out using the BGS's in-house 'SHRINKiT' apparatus (NOTE: this is not a BS1377 method, Hobbs et al., 2014). The results are summarised in Table 11 and Figure 45.

Table 9 Results of BGS multi-stage CIU triaxial test on Withernsea Member

Bulk Density γ_b (Mg/m^3)	Dry Density γ_d (Mg/m^3)	Water content, w_0 (%)	Friction angle ϕ (degr.)	Cohesion c (kPa)	Eff. friction angle ϕ' (degr.)	Eff. cohesion c' (kPa)
2.15	1.88	12.6	18.9	0	26.4	3.8

Table 10 Geotechnical test data for Holderness tills (Bell, 2002)
(c = cohesion in kPa; ϕ = angle of friction; L = low strength sensitivity)

	Unconfined compressive strength (kPa)			Direct shear				Triaxial			
	Intact	Remoulded	Sensitivity	c	$\phi°$	c_r	$\phi°_r$	c_u	$\phi°_u$	c'	ϕ'
1. Hessle Till (Dimlington, Hornsea)	138	116	1.31 (L)	30	25	3	23	98	8	80	24
Max	96	74	1.10 (L)	16	16	0	13	22	5	10	13
Min	106	96	1.19 (L)	20	24	1	20	35	7	26	25
Mean											
2. Withernsea Till (Dimlington)											
Max	172	148	1.18 (L)	38	30	2	27	62	19	42	34
Min	140	122	1.15 (L)	21	20	0	18	17	5	17	16
Mean	160	136	1.16 (L)	26	24	1	21	30	9	23	25
3. Skipsea Till (Dimlington)											
Max	194	168	1.15 (L)	45	38	5	35	50	21	25	36
Min	182	154	1.08 (L)	25	20	0	19	17	10	22	24
Mean	186	164	1.13 (L)	27	26	1	25	29	12	28	30
4. Basement Till (Dimlington)											
Max	212	168	1.27 (L)	47	34	2	30	59	17	42	36
Min	163	140	1.19 (L)	23	20	0	18	22	6	19	20
Mean	186	156	1.21 (L)	29	24	1	23	38	9	34	29

Table 11 Shrinkage limit test results for 'undisturbed' Withernsea Member and Skipsea Till Member from Borehole 1a (19/03/12) and remoulded slip plane clay from landslide toe (14/11/12)

Formation /Member	Depth (m)	State	Initial water content, w_0 (%)	Initial bulk density γ_{b0} (Mg/m^3)	Initial dry density γ_{d0} (Mg/m^3)	Liquid Limit, w_L (%)	Plasticity index I_P (%)	Shrinkage limit, w_S (%)	Volume change ΔV_{tot} (%)
Withernsea M	6.7	U	16.6	2.18	1.87	37.0	20.0	10.6	10.7
Skipsea Till M	15.8	U	23.2	2.04	1.65	32.0	13.0	16.2	10.8
Skipsea Till M	19.7	U	13.3	2.25	2.00	30.0	15.0	9.4	6.0
Slip plane 'ALslip' (Bridlington M.)	*16.0*	R	29.8	1.93	1.50	46.3	21.5	15.0	19.6

U = Undisturbed
R = Remoulded

Figure 45 Shrinkage limit test plot for four Aldbrough till samples from BH1a core and from cliff face (slip)
WM = Withernsea M.
STM = Skipsea Till M.
BM = Bridlington M.

10 Terrestrial LiDAR Surveys

10.1 METHOD

Terrestrial LiDAR surveys (TLS) have been carried out at the Aldbrough test site over a thirteen year period from September 2001 to July 2013 (and are ongoing at the time of reporting); comprising 23 surveys (Table 2) of which 16 have been selected in this report for detailed analysis. These have been centred on the same section of cliff and platform (a point approximately 60 m to the south of Seaside Road) but precise survey boundaries have varied throughout the monitoring period. This has been due simply to a lack of reference points but has necessitated clipping to an arbitrarily defined datum in order for 'change' models and volume calculations to be produced from them. This has meant that positioning of the surveys has relied on dGPS throughout. In the early days of the task (2001 to 2002) this had poor resolution which led to inaccurate positioning and scan orientation. These early data have been re-oriented as far as possible by manipulation of point cloud datasets using Polyworks (IMAlign^{TM} and IMSurvey^{TM} modules) and Maptek I-Site software. Until 2004 the scanner used was a Riegl LPM2K which produced low density, monochrome point clouds. From 2005 a higher speed Riegl LPMi800HA scanner was used. This produced denser point clouds and also featured a calibrated digital SLR camera, the results from which were used to attribute the point clouds with 'true' RGB colour. This has had the advantage of making cliff features more recognisable and the results of the surveys more interpretable in terms of geomorphology. Since 2011 a very high-speed Riegl VZ1000 laser scanner has been used, again with a digital SLR camera fitted, and used for subsequent scans.

Weather and tide conditions have meant that not all surveys have been carried out to the same standards of coverage and accuracy. For example, it has not always been possible to eliminate 'shadow' areas by increasing the number of scan locations. This has been due to time and safety constraints for work on the beach platform; for example, due to strong onshore winds or heavy rain. In a few instances access to the

platform was not possible and the survey had to be carried out solely from the cliff-top. The positional accuracy achieved for these surveys was paramount. Problems of tripod stability were frequently encountered due to wet beach sand. Attempts were made, with limited success, to solve this by using oversized tripod feet attachments. GPS satellite 'drop-outs' were also a feature of work on such cliffed coasts, in particular when used in Real-Time Kinetic (RTK) mode requiring a data phone link. After 2003 a non-RTK system was used which utilised a 'base station' which logged its position over the entire duration of the survey (typically 4 hours) and which (after 2005) sent radio updates to the instrument. Typically, the base station was placed on the cliff-top on a tripod or on the vehicle roof in the car park. Since 2006 first Leica's Smart and then Viva dGPS/GNSS systems have been used. These utilise a telephone link to a UK-wide GPS network which has allowed live RTK updates direct to the instrument. This has removed the need for a base station. In some cases, however, the telephone link has failed due to the remote location or due to line usage at the time, and reversion to the base station method was necessary. Since 2011 a Leica 'Viva' system has been used. This is capable of accessing all satellite positioning systems (GPS, GLONASS, Galileo and Compass) where available.

10.2 RESULTS

The results of all TLS surveys are shown in Figures 45 to 65 as 3D point clouds coloured by height scale or by true colour and change models from one survey to the next. Only one survey per year is shown in most cases, though in the case of the survey labelled '2008' the survey was carried out in April 2009. In the figures each survey is represented by two model versions: firstly, the scan itself, and secondly the 'change model' which shows the change from the previous year's scan (12 month period), or in a few cases an earlier scan in the same year (less than 12 month period). For clarity the scale is the same (+1 m to -3 m) for each model. It is possible to show wider scales but these have lower resolution. This scheme does not show the full extent of all losses and gains, as these exceed the chosen scale. However, the key also features a histogram for the change model's pixels, whereby the shape indicates the proportion of points lying beyond the scale. In these plots the models may be partial, only showing areas common to both scans. The change models, unlike those prepared for Norfolk (Hobbs *et al*. 2008), do not show just height change but are based on a 'closest point between models' algorithm.

10.2.1 Cliff recession volumes

Calculations of volume, and derived weight, taken from the cliff component of the models described above, 'clipped' to a common 100 m run and 17.6 m section height, have produced an overall volume loss of **40,500 m^3** for an 11.75 year monitoring period from September 2001 to June 2013.

Table 12 Measured volumes and estimated weights of material lost from cliff (100 m run)

Period start	Period end	Elapsed time (months)	Cumul time (months)	Increm. loss (m^3)	Cumul. loss (m^3)	Cumul. loss/m (m^3)	Increm. loss (tonnes)	Cumul. loss (tonnes)	Cumul. loss / m (tonnes)
Sep-01	Apr-02	7	7	1700	1700	15	3570	3570	32
Apr-02	Sep-02	5	12	800	2500	23	1680	5250	48
Sep-02	Sep-03	12	24	1500	4000	36	3150	8400	76
Sep-03	Apr-04	7	31	3100	7100	65	6510	14910	136
Apr-04	Aug-04	4	35	700	7800	71	1470	16380	149
Aug-04	Sep-05	13	48	6800	14600	133	14280	30660	279
Sep-05	Sep-06	12	60	3100	17700	161	6510	37170	338
Sep-06	Aug-07	11	71	1200	18900	172	2520	39690	361
Aug-07	*Apr-09*	*20*	*91*	*7200*	*26100*	*237*	*15120*	*54810*	*498*
Apr-09	Oct-09	6	97	3200	29300	266	6720	61530	559
Oct-09	Mar-10	5	102	1900	31200	284	3990	65520	596
Mar-10	Jul-10	4	106	1900	33100	301	3990	69510	632
Jul-10	Feb-11	7	113	1100	34200	311	2310	71820	653
Feb-11	Mar-12	13	126	3600	37800	344	7560	79380	722
Mar-12	Jun-13	15	141	2700	40500	368	5670	85050	773
Sep-01	**Jun-13**	**12**	**141**		**40500**	**365**		**85050**	**768**
Loss per year					3450	31		7244	66

Note: No data available for 2008

The breakdown per epoch is shown (to true time scale) in Table 12. These calculations were made using Maptek's I-Site software. The loss rates per year are averaged over the period. A mean bulk density of 2.10 Mg/m^3 has been taken for the material comprising the cliff in the weight calculations, giving a loss of 85,050 tonnes. The plot in Figure 46 shows the cumulative loss (in weight terms) for the common 100 m run clipped from 16 of the 23 scans made.

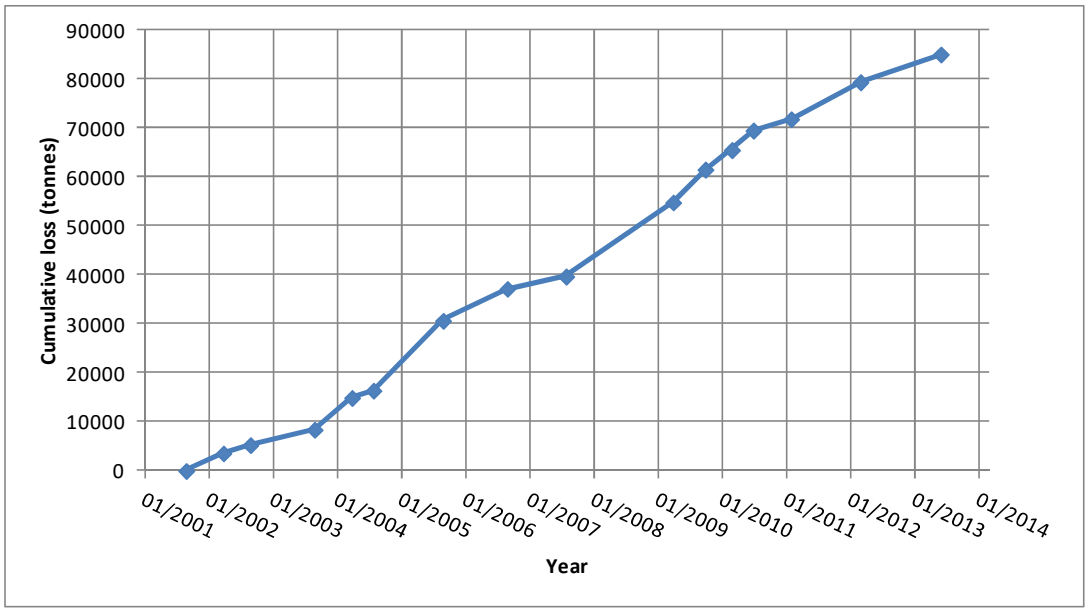

Figure 46 Plot of cumulative weight loss with time from cliff (100m run)

The loss per metre run between September 2001 and June 2013 was 365 m^3 and 768 tonnes. This represents a loss of 31 m^3 and 66 tonnes per metre run per year for a nominal section height of 17.6 m. The largest annual losses were 14,280 tonnes between August 2004 and September 2005. Other high rates

(taken from the steepness of the plot) in Figure 46 are September 2003 to April 2004 and April 2009 to July 2010. The smallest annual loss was 2,520 tonnes between September 2006 and August 2007. Other small losses were from September 2002 to September 2003 and July 2010 to February 2011. Short term (5 to 6 month) epochs from April 2002 to September 2002 and April 2004 to August 2004 produced 1,680 tonnes and 1,470 tonnes, respectively. Autumn and winter losses were approximately double to quadruple the spring and summer losses, though the dataset is not consistent enough in terms of epoch length to merit statistical analysis.

The plot in Figure 46 indicates that between 2001 and 2013 there may have been two cycles of cliff recession taking place each having a 4-year period. However, the data are not of insufficient duration and resolution to make any firm conclusions regarding cyclicity.

Losses due to cliff erosion on the Holderness coast are given by Pye & Blott (2010). For the Hornsea to Withernsea section (22.4 km), which includes Aldbrough, they gave rates of 22.9 m^3 per metre per annum for the period 1852 to 2009, and 41.6 m^3 per metre per annum for the period 2003 to 2009. These compare with 34.5 m^3 per metre per annum for the Aldbrough test site reported here (Table 12).

2001

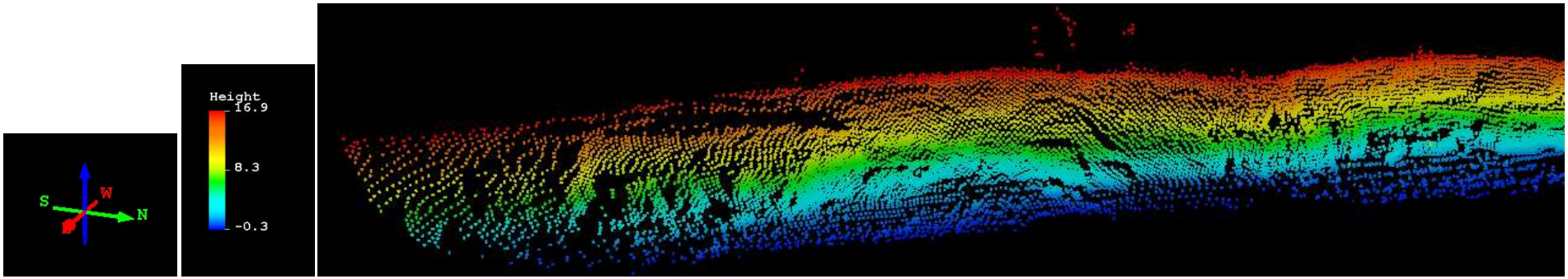

Figure 47 Point cloud for Sep 2001 scaled according to height
NOTE: No true colour point cloud available

2002

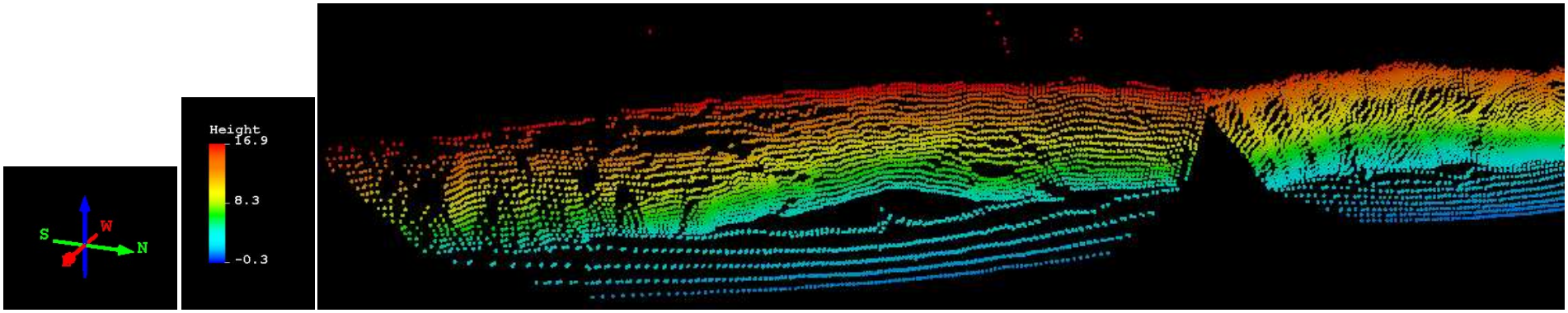

Figure 48 Point cloud for Sep 2002 scaled according to height
NOTE: No true colour point cloud available

ZERO --

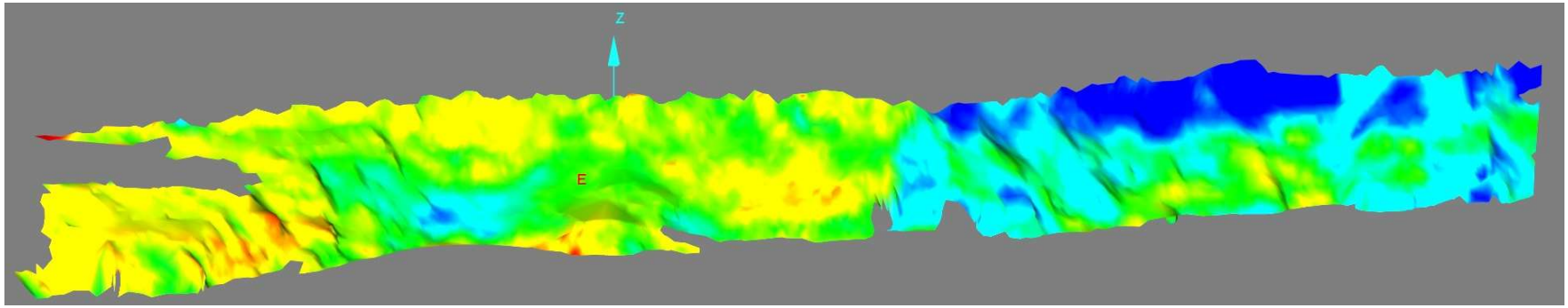

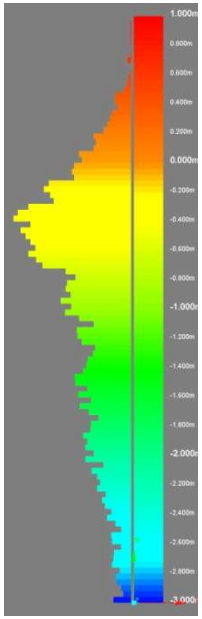

Figure 49 Change model: Sep 2001 to Apr 2002 [I-Site, Maptek] Range: +1.0 m (red) to -3.0 m (blue)

2003

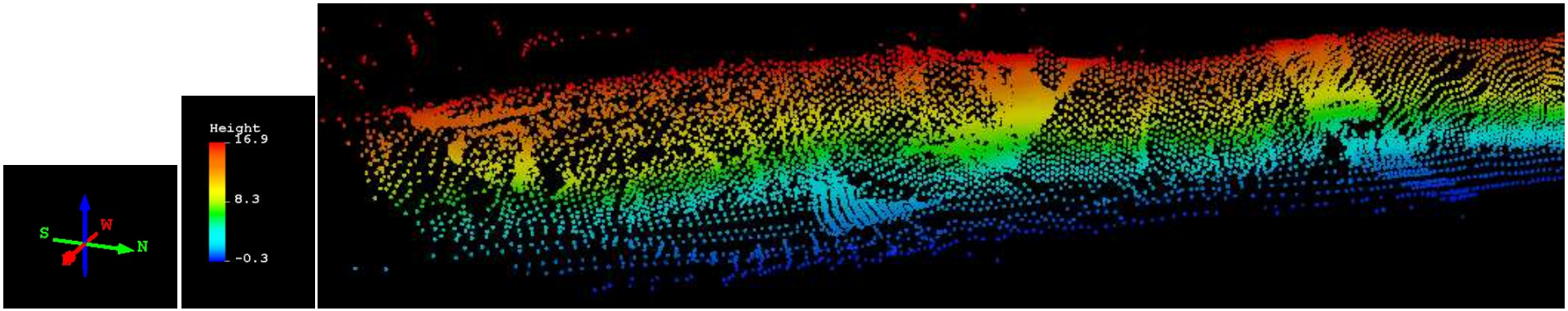

Figure 50 Point cloud for Sep 2003 scaled according to height
NOTE: No true colour point cloud available

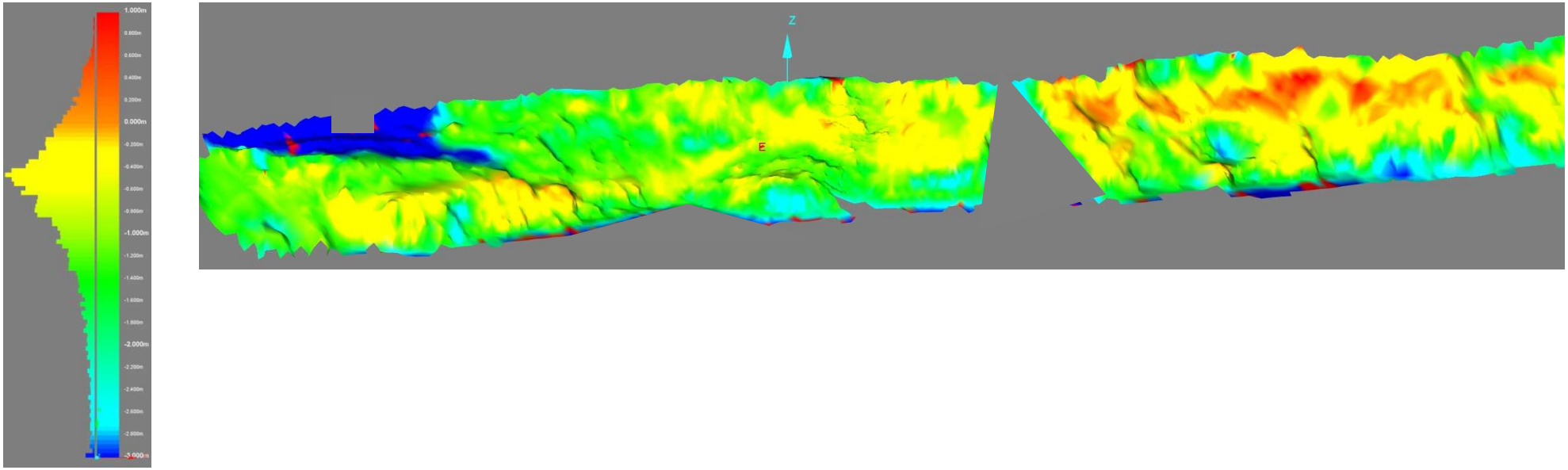

Figure 51 Change model: Sep 2002 to Sep 2003 [I-Site, Maptek] Range: +1.0 m (red) to -3.0 m (blue)

2004

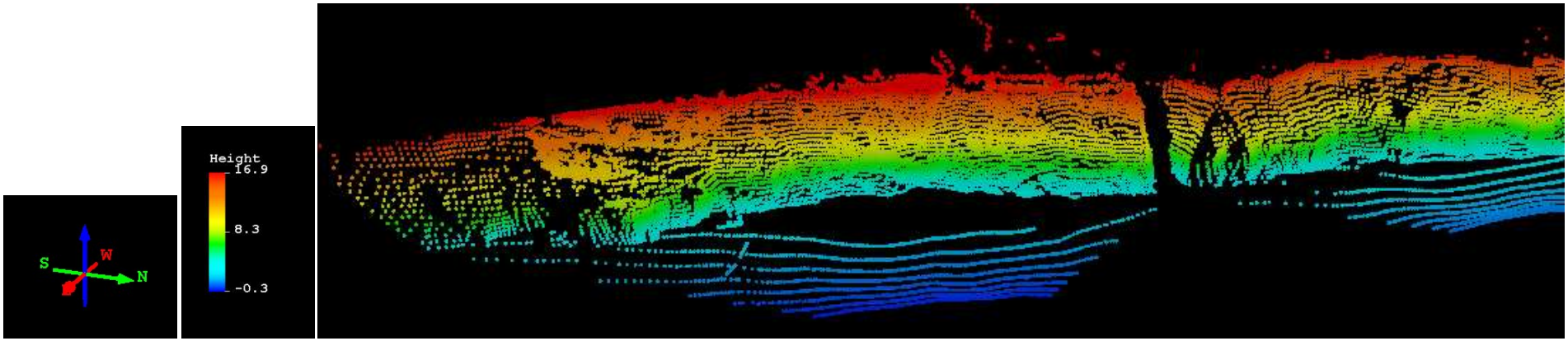

Figure 52 Point cloud for Sep 2004 scaled according to height
NOTE: No true colour point cloud available

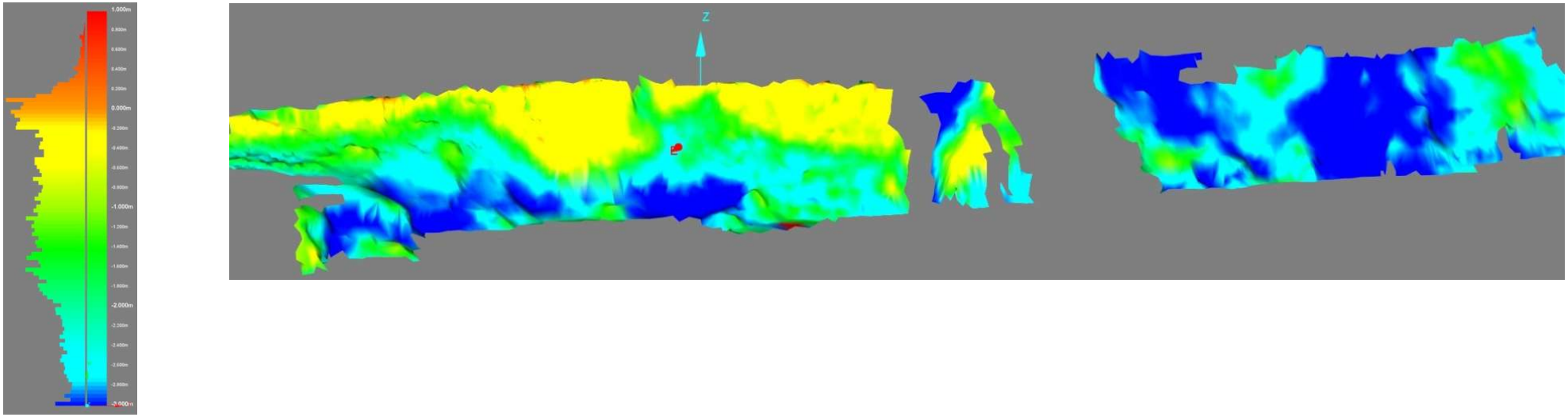

Figure 53 Change model: Sep 2003 to Sep 2004 [I-Site, Maptek] Range: +1.0 m (red) to -3.0 m (blue)

2005

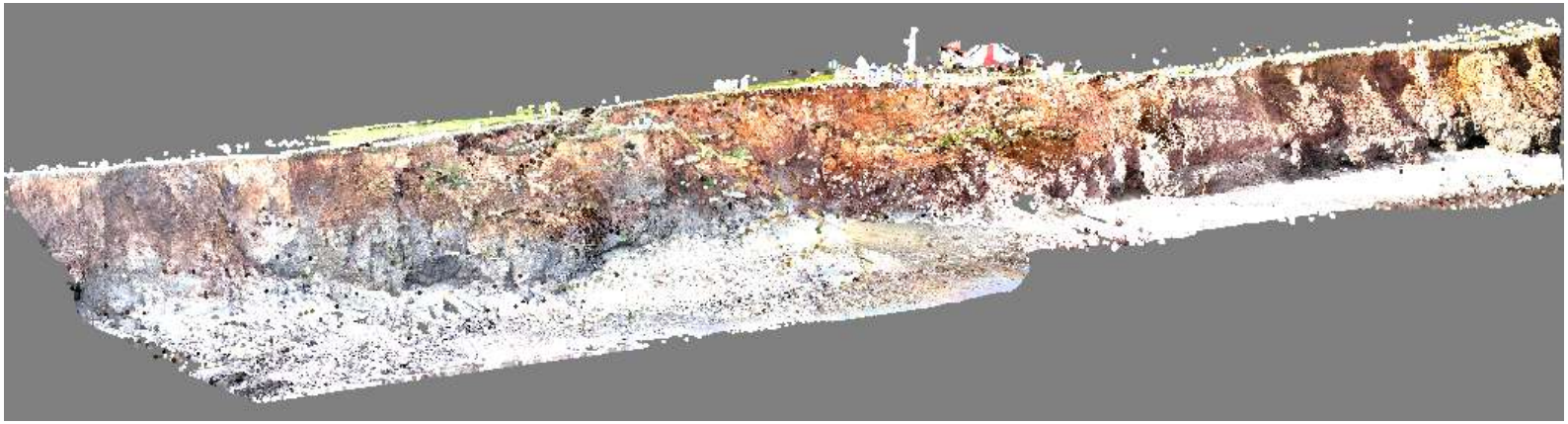

Figure 54 Coloured point cloud for Sep 2005

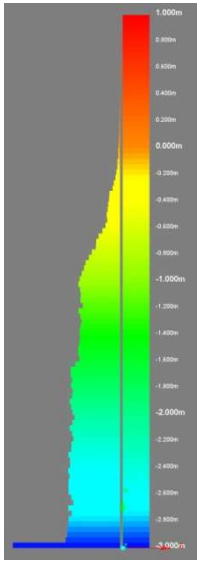

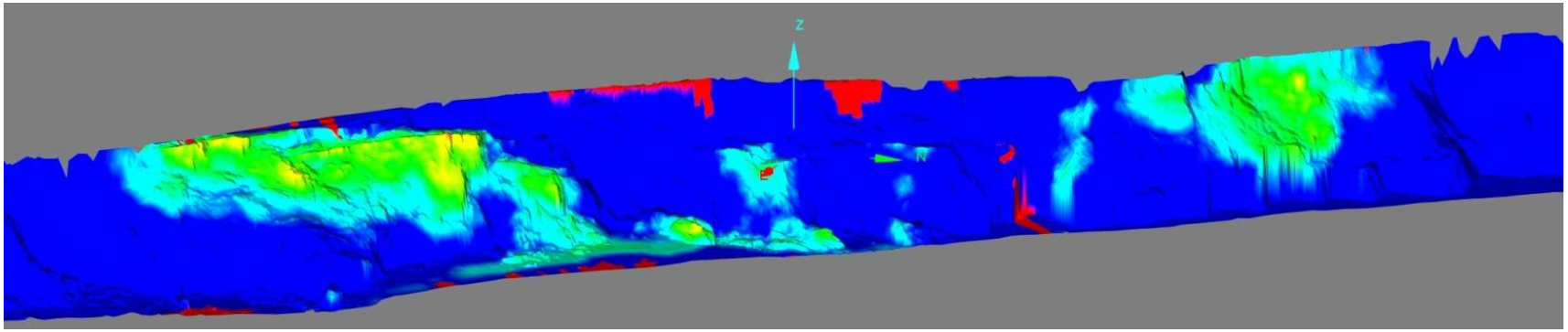

Figure 55 Change model: Sep 2004 to Sep 2005 [I-Site, Maptek] Range: +1.0 m (red) to -3.0 m (blue)

2006

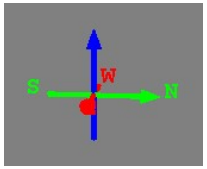

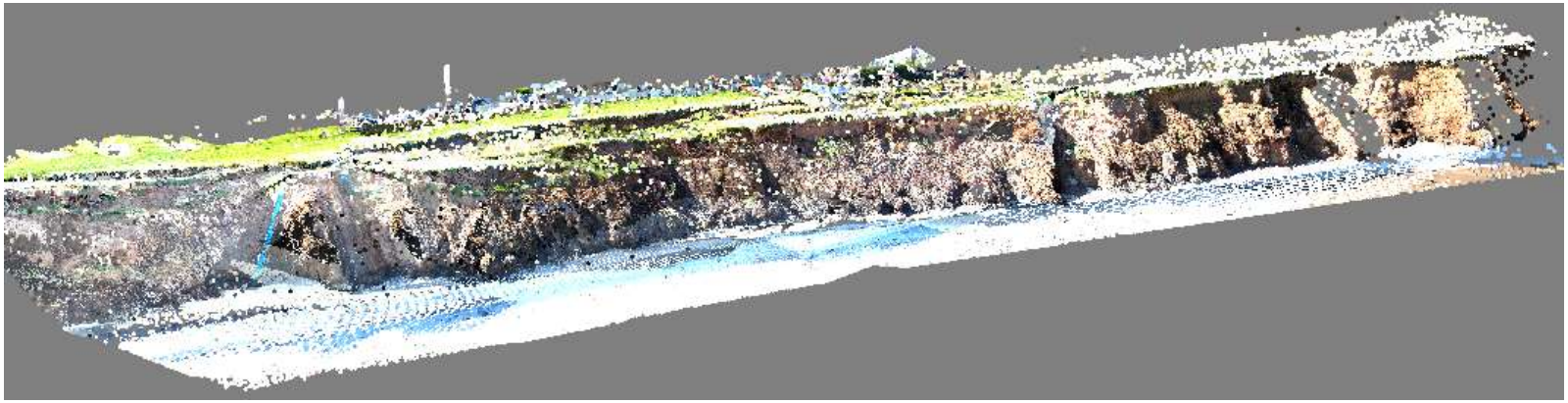

Figure 56 Coloured point cloud for Sep 2006

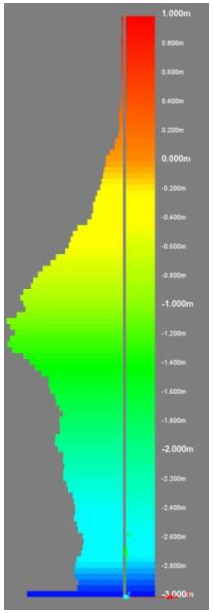

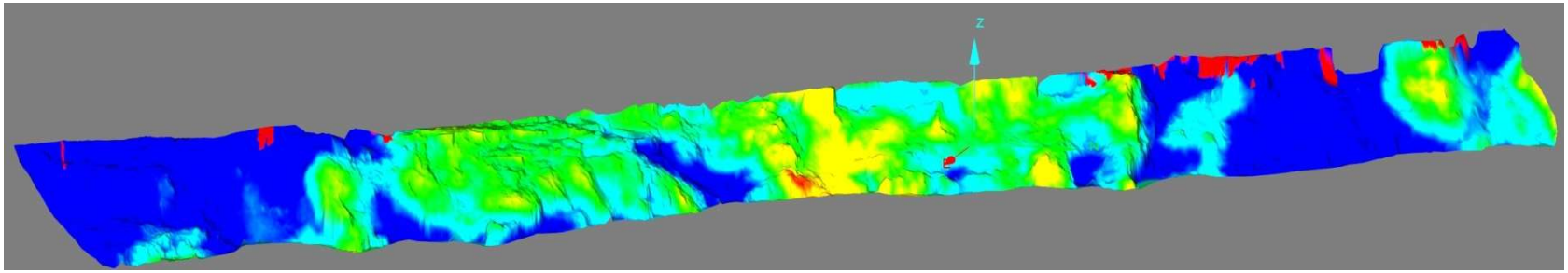

Figure 57 Change model: Sep 2005 to Sep 2006 [I-Site, Maptek] Range: +1.0 m (red) to -3.0 m (blue)

2007

Figure 58 Coloured point cloud for Aug 2007

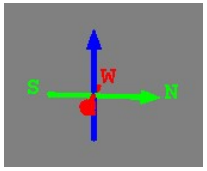

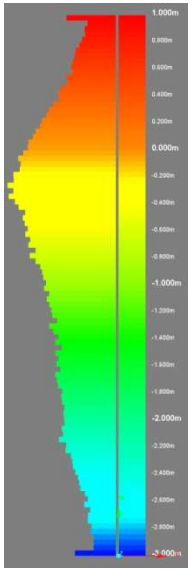

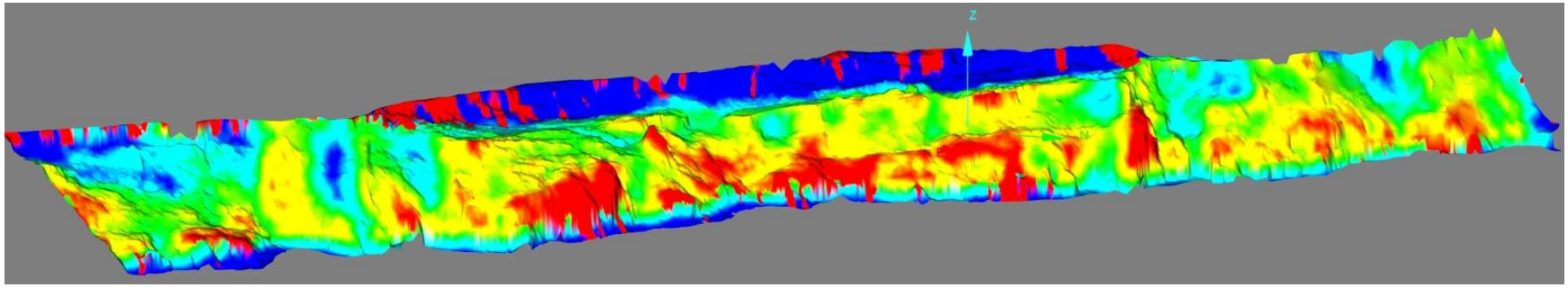

Figure 59 Change model: Sep 2006 to Aug 2007 [I-Site, Maptek] Range: +1.0 m (red) to -3.0 m (blue)

'2008'

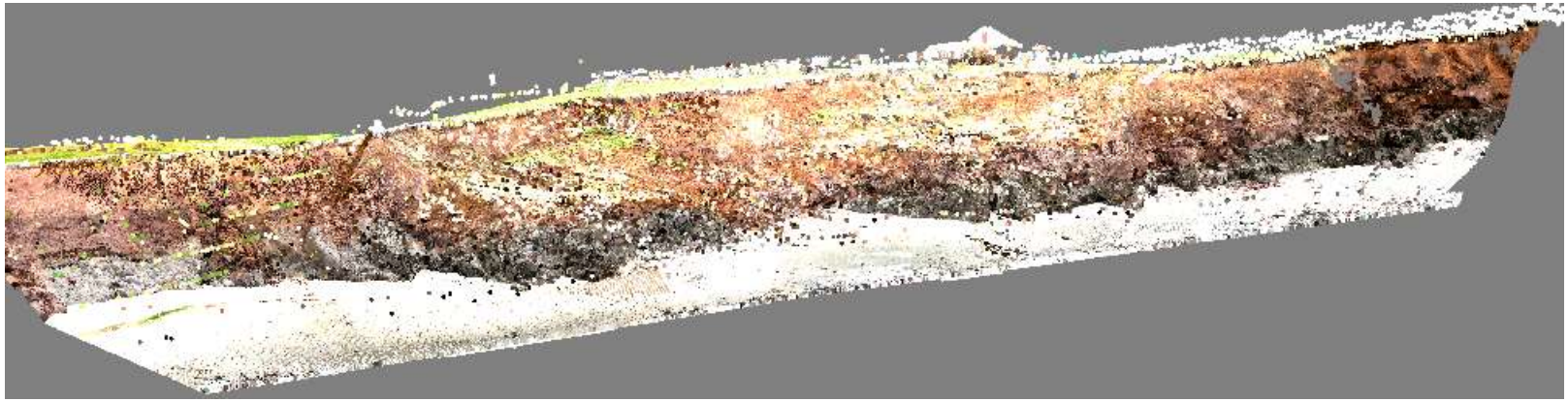

Figure 60 Coloured point cloud for Apr 2009

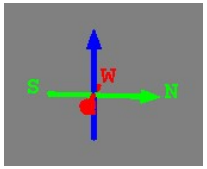

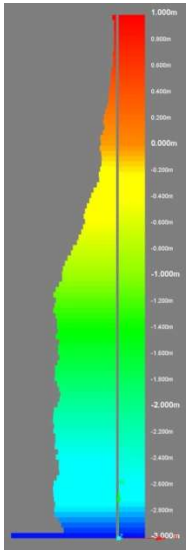

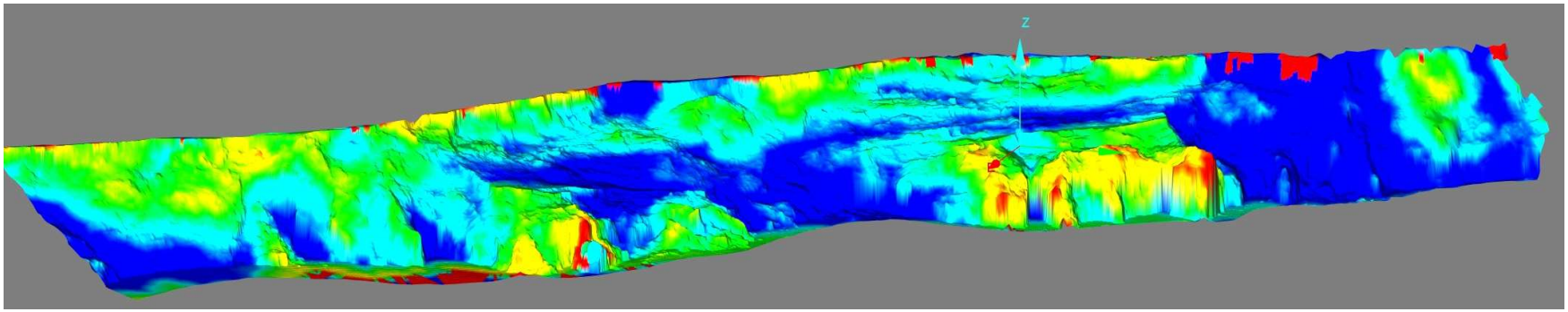

Figure 61 Change model: Aug 2007 to Apr 2009 [I-Site, Maptek] Range: +1.0 m (red) to -3.0 m (blue)

2009

Figure 62 Coloured point cloud for Oct 2009

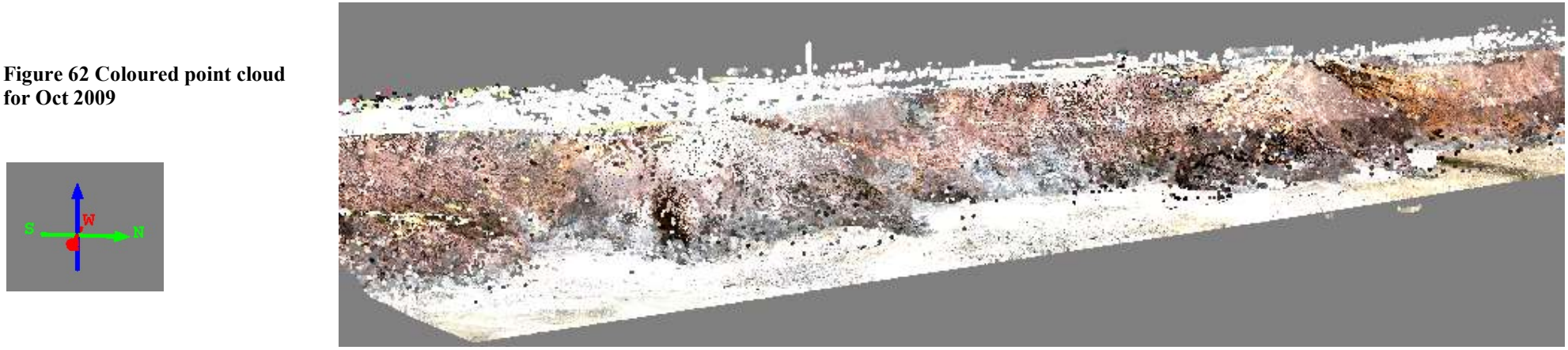

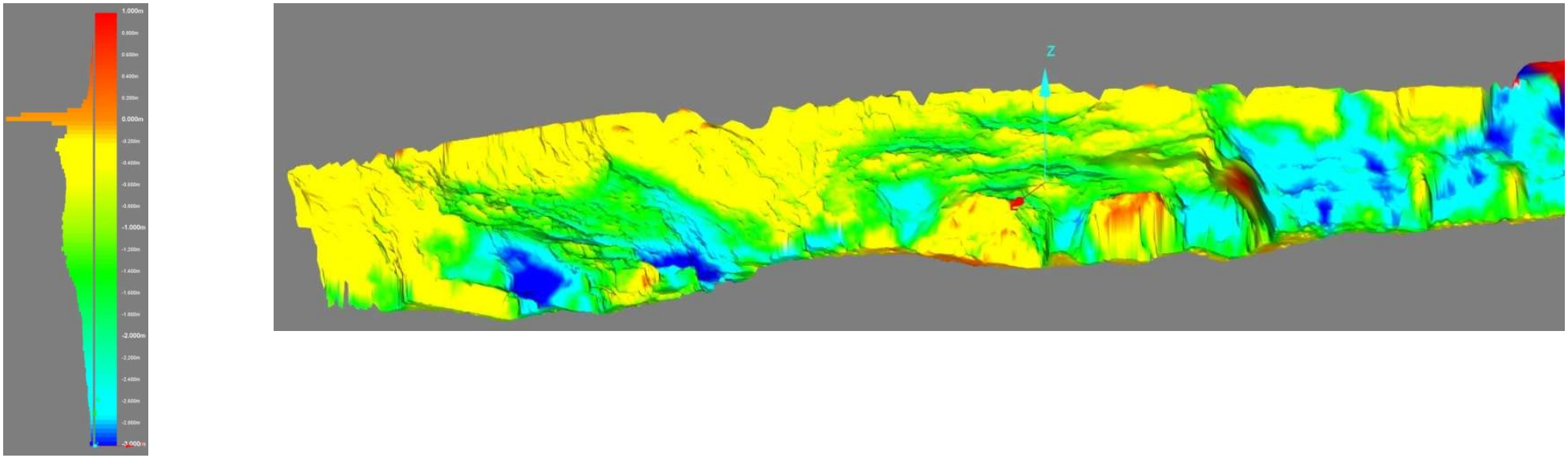

Figure 63 Change model: Apr 2009 to Oct 2009 [I-Site, Maptek] Range: +1.0 m (red) to -3.0 m (blue)

2010

Figure 64 Coloured point cloud for Jul 2010

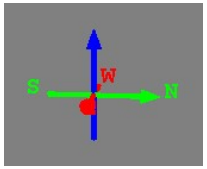

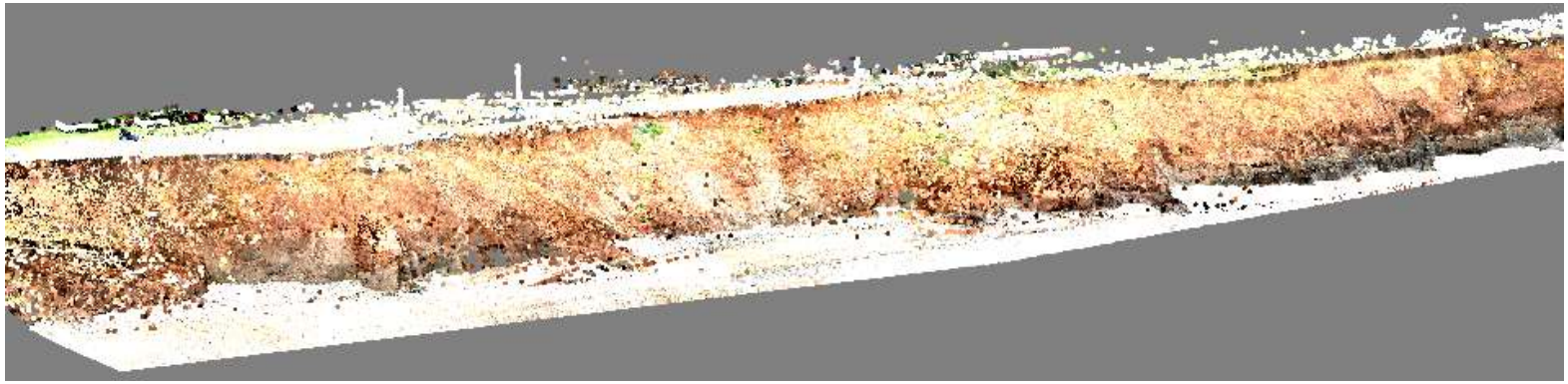

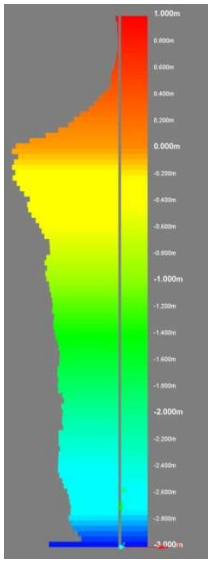

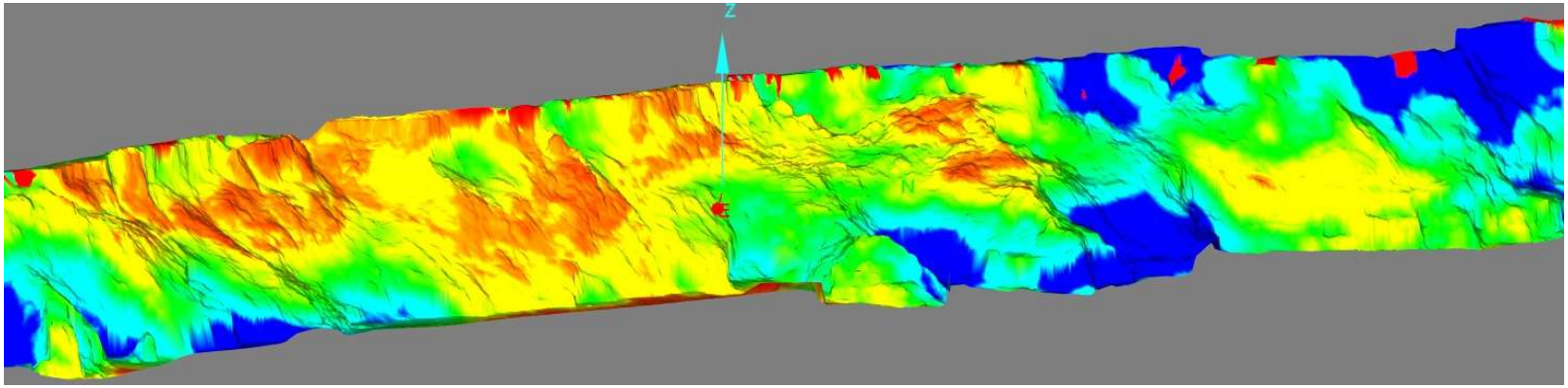

Figure 65 Change model: Oct 2009 to Jul 2010 [I-Site, Maptek] Range: +1.0 m (red) to -3.0 m (blue)

2011

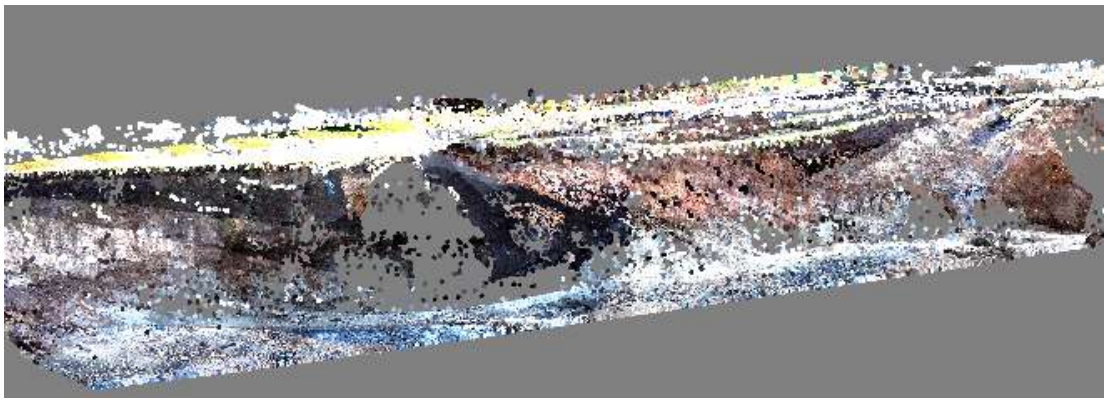

Figure 66 Coloured point cloud for Feb 2011

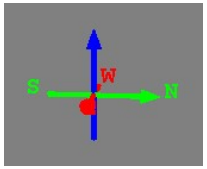

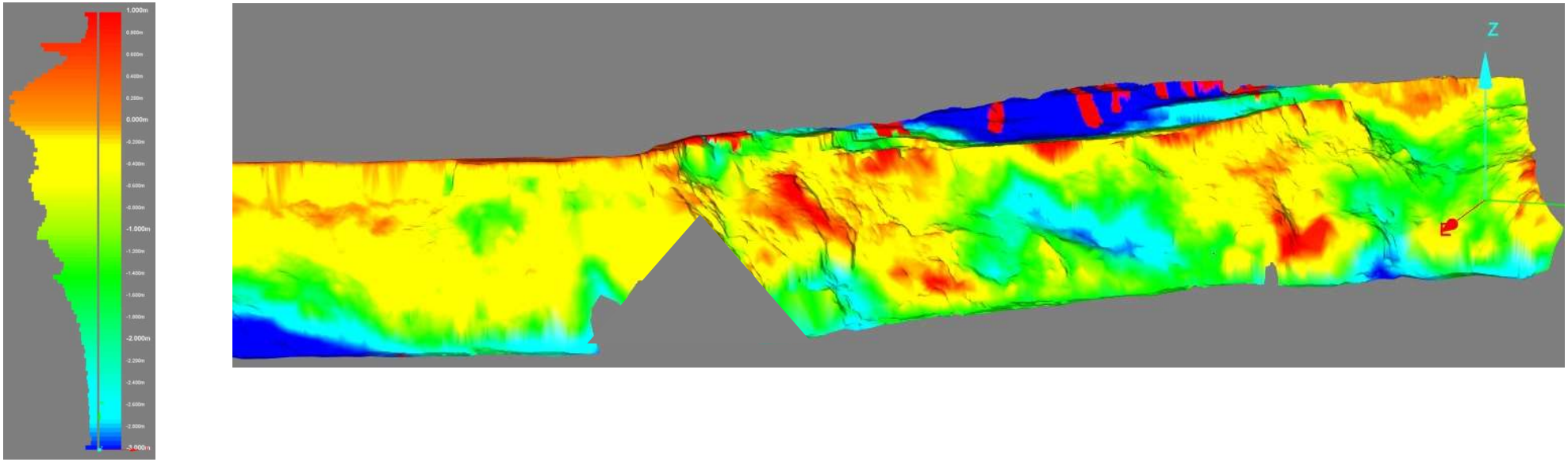

Figure 67 Change model: Jul 2010 to Feb 2011 [I-Site, Maptek] Range: +1.0 m (red) to -3.0 m (blue)

2012

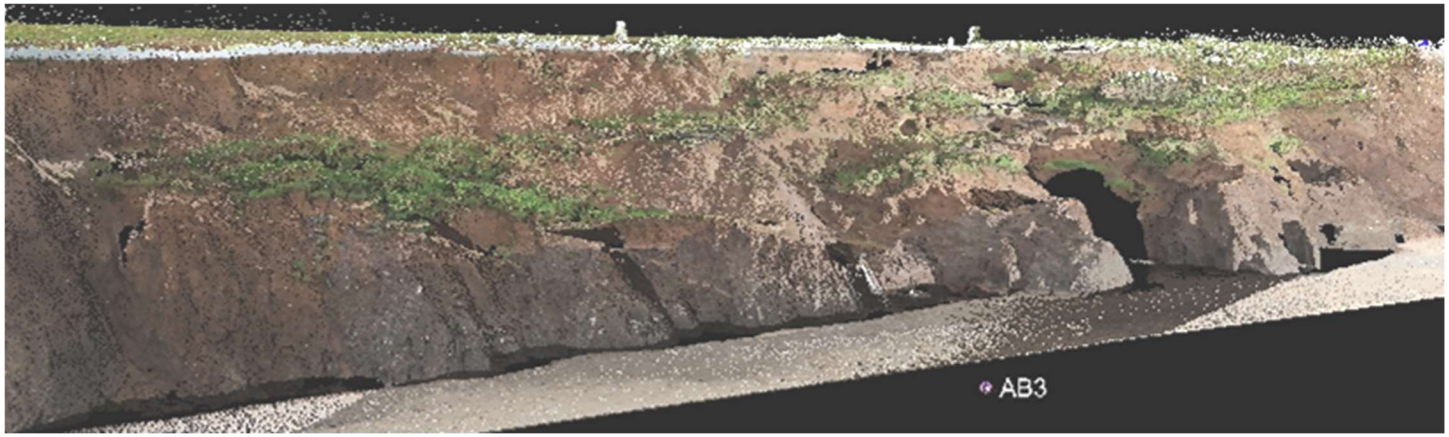

Figure 68 Coloured point cloud for Jul 2012

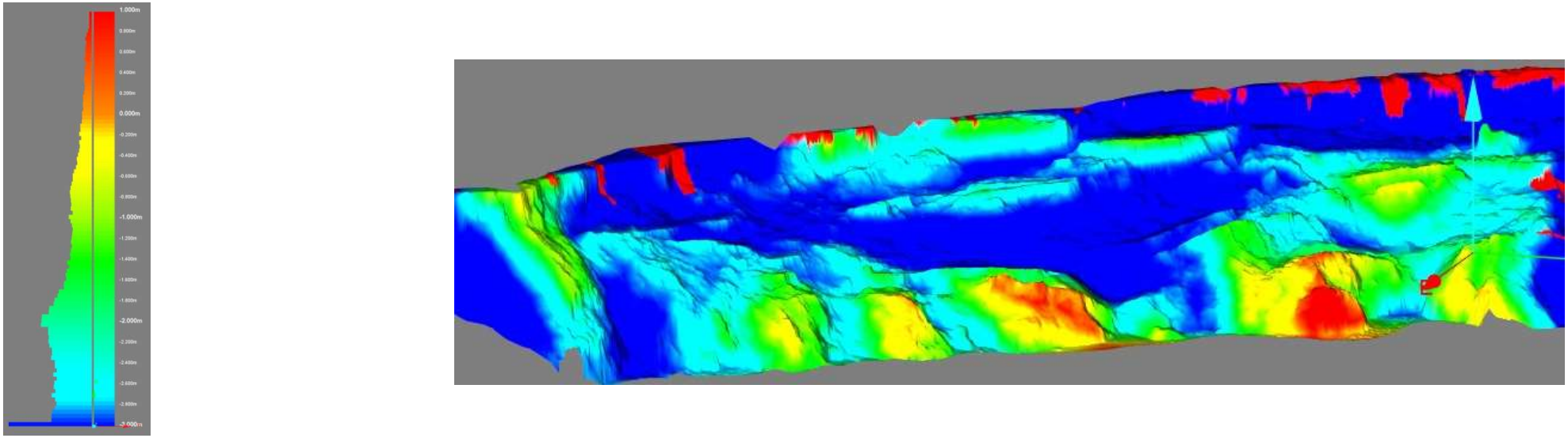

Figure 69 Change model: Feb 2011 to Mar 2012 [I-Site, Maptek] Range: +1.0 m (red) to -3.0 m (blue)

2013

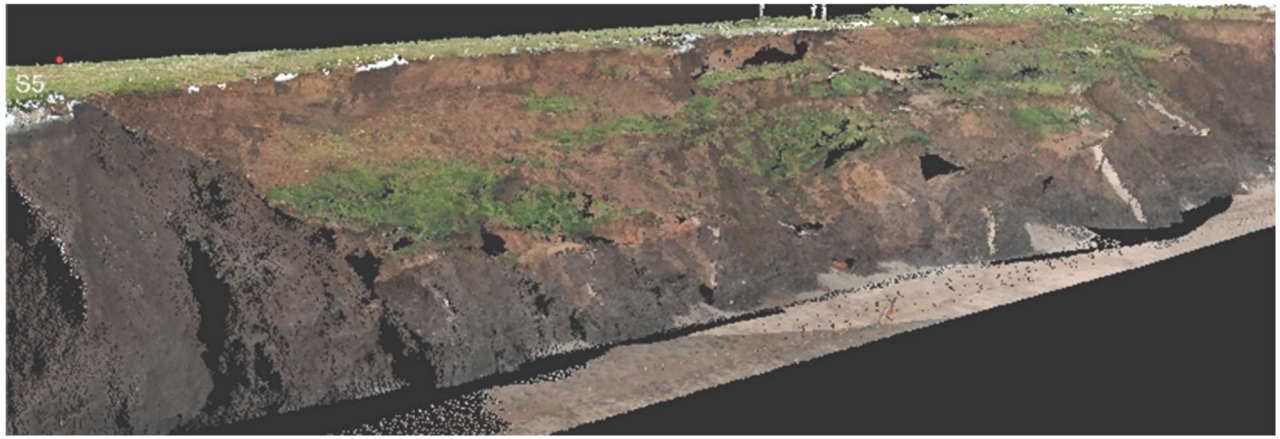

Figure 70 Coloured point cloud for Jun 2013

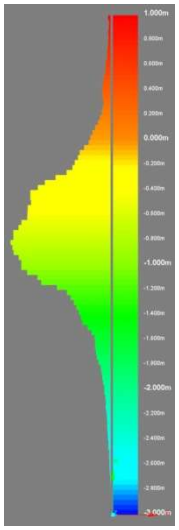

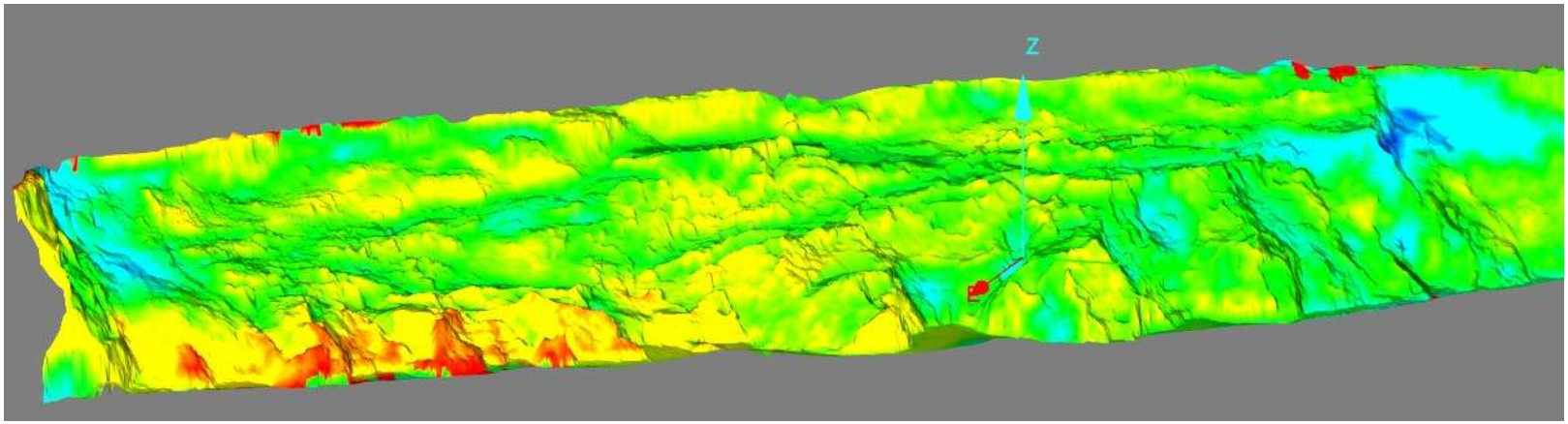

Fi

Figure 71 Change model: Mar 2012 to Jun 2013 [I-Site, Maptek] Range: +1.0 m (red) to -3.0 m (blue)

10.2.2 Change models

Maptek I-Site software was used to produce 3D 'change models' recording changes in the ground surface from one survey to the next. This operates by looking for the closest 'primitive' (point, edge or facet) from one point cloud to the next and calculates the distance from the point to that 'primitive'. In addition to providing values of volumetric change (section 10.2.1), the change models (Figure 47 to Figure 71) provide a visual indication of cliff recession on a scale from +1.0 m (red) to -3.0 m (blue), where the yellow/orange boundary represents zero change. The blue end of the scale thus indicates loss of ground from the cliff (i.e. a movement landwards) whilst the red end of the scale indicates gain of ground on the cliff (i.e. movement seawards). The former usually indicates a landslide depletion zone (mid or upper slope) or direct marine erosion (lower slope), whilst the latter is indicative of the presence on the slope or beach of an accumulated slipped mass or fall. Most change models represent a 12 month period. However, others represent greater or lesser time periods. Some change models have had to be clipped, or sections masked out, because of mismatching of two surveys or poor data density in some areas. The proportion of data falling outside the -3.0 m to +1.0 m scale is indicated by the histogram to the left of each figure.

The first monitoring period (September 2001 to April 2002), shown in Figure 49, indicates a large loss, particularly in the upper part, of the northern embayment and small but uniform change in the southern one. Gain is particularly noted at the southern extremity of the southern embayment representing the toe of some major rotations at this point. Between September 2002 and September 2003 (Figure 51) moderate losses are indicated throughout the cliff section but with high losses in the upper cliff at the southern end. This matches observations of active multiple rotations. The monitoring period September 2003 to September 2004 (Figure 53) indicates large losses at the northern embayment throughout the cliff profile. Large losses are visible in the lower cliff of the southern embayment compared to moderate losses in the upper cliff. These are indicative of progression of steepening of the cliff by removal of landslide debris in the southern part. Widespread large scale losses are observed in both embayments during the monitoring period September 2004 to September 2005 (Figure 55). Two specific areas of moderate loss coinciding with areas of earlier rotational landslide activity in the upper and mid-slope of the southern embayment are visible and, to a lesser extent, in the centre of the northern embayment. This year provided the greatest losses of the whole period of monitoring. The monitoring period September 2005 to September 2006 (Figure 57) indicates major loss in southern and northern ends of test site with more moderate losses in central part. Unusually during the period September 2006 to August 2007 (Figure 59) the areas of loss and gain are intimately mixed throughout. The reason for this is unclear, although the major loss in the upper part of the central area is due to a wide bench produced by combined rotational landslide activity. The monitoring period August 2007 to April 2009, shown in Figure 61 represents 20 months duration rather than the more usual 12 months, due to there being no surveys carried out in 2008. It shows major loss throughout, particularly in the northern part (whole cliff), in the central part (mid and lower cliff) and in the southern part (mid and lower cliff). Minor occurrences of gain occur on the most seaward extremities of two headland features and more or less randomly at the crest of the cliff. Figure 63 represents a six-month period spanning the spring and summer of 2009 (April-October). Here, moderate loss has occurred throughout but with major loss at the northern end and to a lesser extent at the southern end (lower cliff) and in patches elsewhere on the lower cliff. This probably represents minor landslide activity in embayments and gullies, including debris flows. The monitoring period October 2009 to July 2010, shown in Figure 65, reveals considerable seaward movement in the central part, presumably representing winter landslide activity.

Moderate loss throughout the cliff section occurred between July 2010 and February 2011 (Figure 67) with areas of enhanced loss in the central part (mid and lower cliff) of the northern embayment and southern extremity of southern embayment (lower cliff). The former is due to continuing activity on the existing landslide and the latter marked erosion of previously slipped material. The main feature, however, is major loss in the upper cliff spanning much of the northern embayment. This is due to fresh multiple rotations (Figure 72). However, it is unclear why there are small patches of gain within it. They may be due to paved areas and a wall falling forward onto the slope. The monitoring period February 2011 to

March 2012, shown in Figure 69, reveals major loss throughout the upper and mid cliff due to renewed rotations and degradation of previous slipped masses (Figure 73). The lower cliff features several newly established promontories which have not undergone slipping or significant erosion. Between these there has been moderate to major loss, due to mudflow / debris flow. Once again, the reason for the presence of many small patches of apparent gain is not clear, but may be the presence of random building debris on the slope. The final change model between March 2012 and June 2013, shown in Figure 71 reveals moderate loss throughout with a small area of enhanced loss at the northern extremity (upper cliff). This is due to continuing degradation of previously slipped masses. Small promontories within the lower cliff in the southern embayment have remained essentially intact.

Figure 72 Major fresh rotations in central embayment (Feb 2011)

Figure 73 Renewed movement and progressive degradation of pre-existing rotations (upper and mid cliff) in central embayment (April 2012)

10.2.3 Slope profile sections

A set of 2D slope profiles are shown in Figure 75 to Figure 77 labelled A, B and C according to the cross-sections in Figure 74.

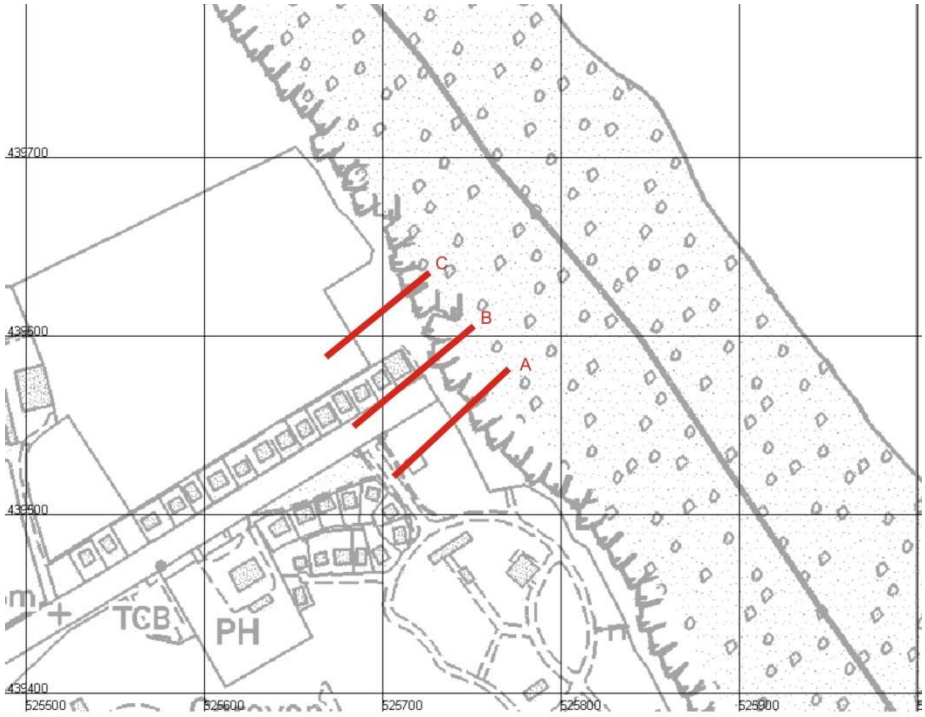

Figure 74 Map of Aldbrough test site showing cross-section lines for derived laser scans (Refer to Figures 75, 76 and 77)

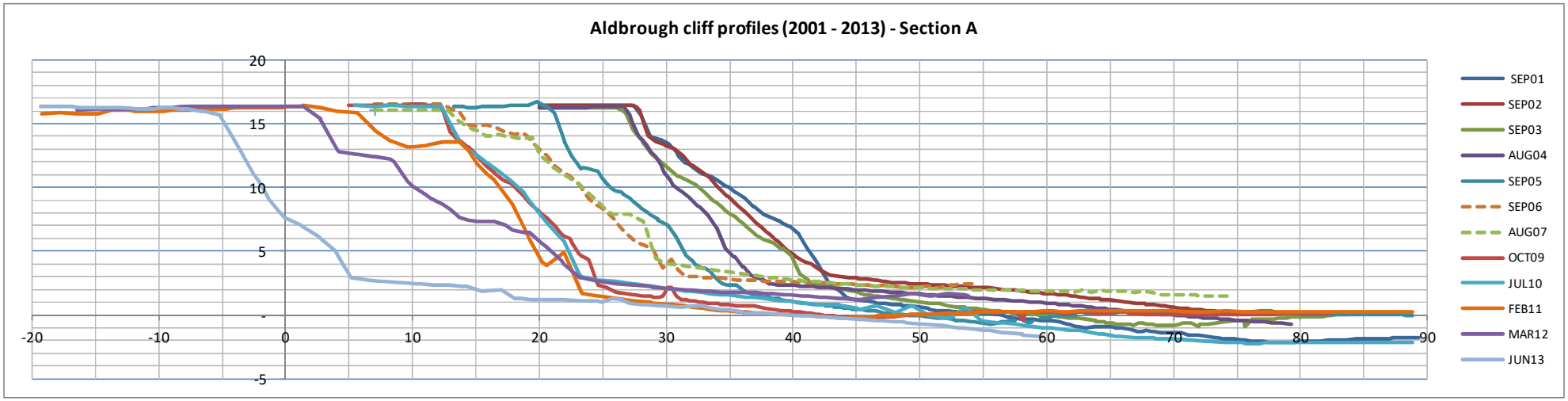

Figure 75 Selected slope profiles by year for cross-section A (refer to Figure 74)
Note: No data collected in 2008

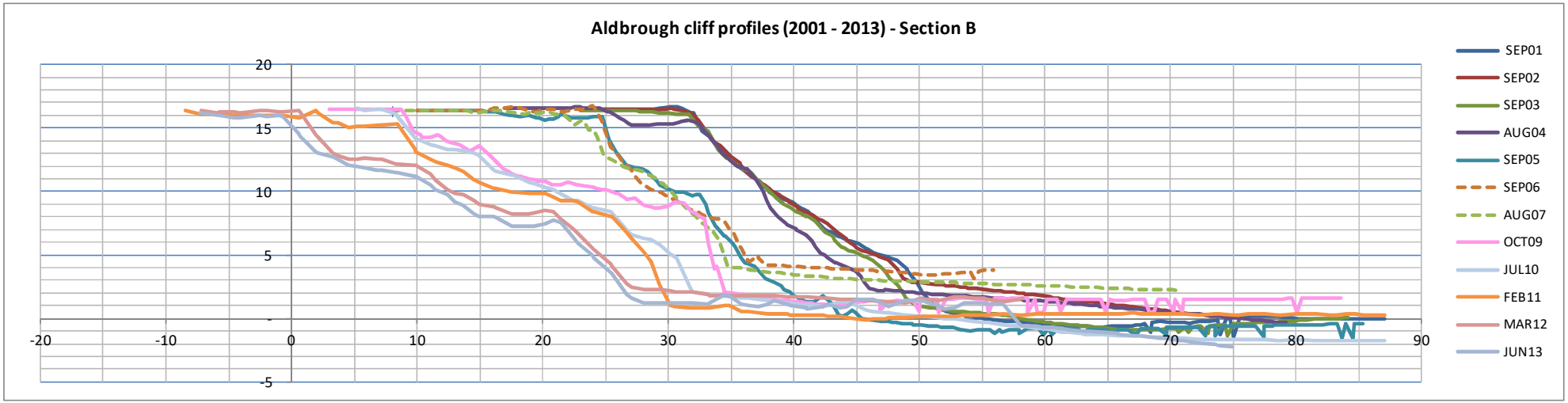

Figure 76 Selected slope profiles by year for cross-section B (refer to Figure 74)
Note: No data collected in 2008

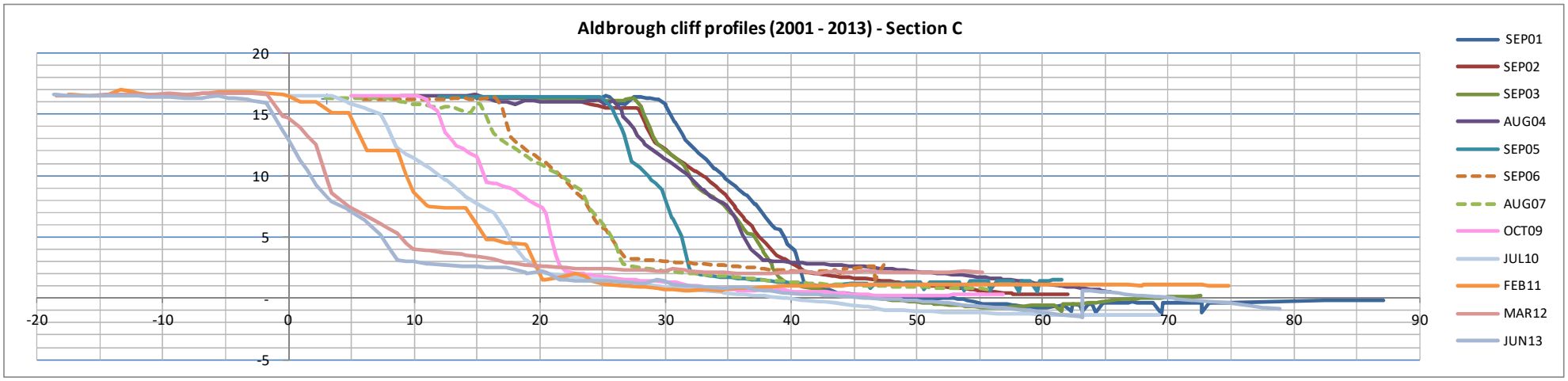

Figure 77 Selected slope profiles by year for cross-section C (refer to Figure 74)
Note: No data collected in 2008.

The profiles show the changing positions and shapes of the cliff and platform with each year between 2001 and 2013 taken from the terrestrial LiDAR data (some surveys having been omitted for clarity). Even after minor adjustments in level, some small errors in position and elevation are visible. These generally relate to errors or poor resolution issues with the dGPS positioning and/or instability of the tripod. Errors of this type have ranged from 0.2 m to 3.0 m depending on conditions and dGPS quality on the day, though most are <1.0 m. However, overall trends in coastal recession are reasonably clear from these data and gross features seen in the profiles are confirmed from observation. We can conclude that: *The methodology, as exemplified by the higher quality scans, is of sufficient resolution & accuracy for the geomorphological purpose to which it is here applied.*

The profiles reveal a pattern of maintenance of the cliff profile but with moderate annual recession, between September 2001 and August 2004, in the case of Section C, whereas Sections A and B show steepening of the cliff between September 2003 and August 2004. The difference between the August 2004 and September 2005 positions show dramatic recession of the cliff and in the case of Section C a steepening. Profiles between September 2005 and September 2006 show a dramatic cliff top recession for Section C, slightly less for Section A, and comparatively little for Section B. Little change in the mid-cliff position was noted in Section B between September 2005 and October 2009. It is interesting to note the steeper profile, throughout the monitoring period, of Section C compared with Sections A and B, with only two exceptions. Section B has overall shallower cliff slopes, to be expected as it is roughly coincident with the centreline of the major embayment at this location. Beach/platform levels apparently varied by up to 5 m over the monitoring period, though the dGPS error is likely to be +/- 1.5 m in the worst cases. Unfortunately, there is no independent confirmation of beach level (see section 10.2.4). The till stratigraphy (and geotechnical properties thereof) are reflected, to a greater or lesser degree, in some of the lower cliff sections of the profiles (e.g. October 2009, section C); that is, the lower cliff, formed by the Skipsea Till Formation, tends to be stronger and hence maintains a steeper angle.

Sections A, B and C show cliff top recessions of 32 m, 33 m and 31 m, respectively over an 11.75 year monitoring period (September 2001 to June 2013). A cyclic pattern of cliff recession can be seen in the profiles. For example, pre-October 2009 the section B profiles are moderately steep whereas after and including October 2009 they become shallower and adopt a similar profile up to and including June 2013. This later period represents multiple rotational landslides throughout the cliff, particularly well shown in the February 2011 profiles. Sections A and C produced steeper profiles the form of which has been maintained throughout (with the exception of Section A, March 2012). Whilst it is likely that there may be cycles of cliff recession which exceed the current monitoring period (11.75 years), the general embayment/promontory regime appears to have been maintained. Volume calculations suggest a four-year cycle of recession (see section 10.2.1). The plot of slope angle (averaged for the three sections) with time (Figure 80) also suggests a four-year cycle in terms of slope angle.

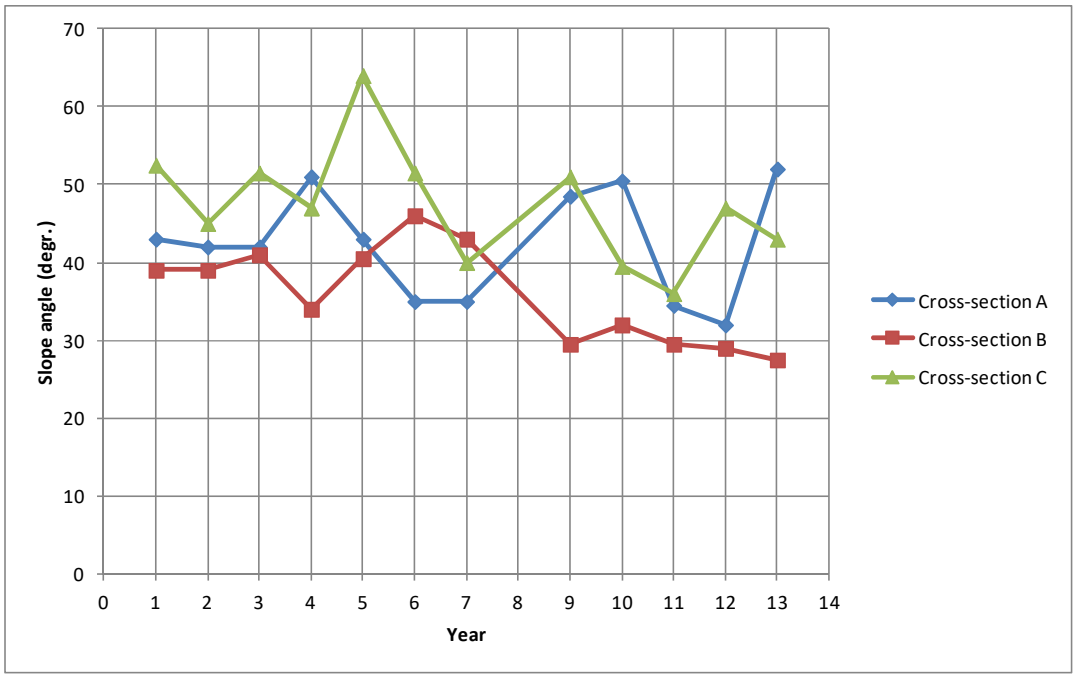

Figure 78 Plot of slope angle vs. time for cross-sections A, B and C

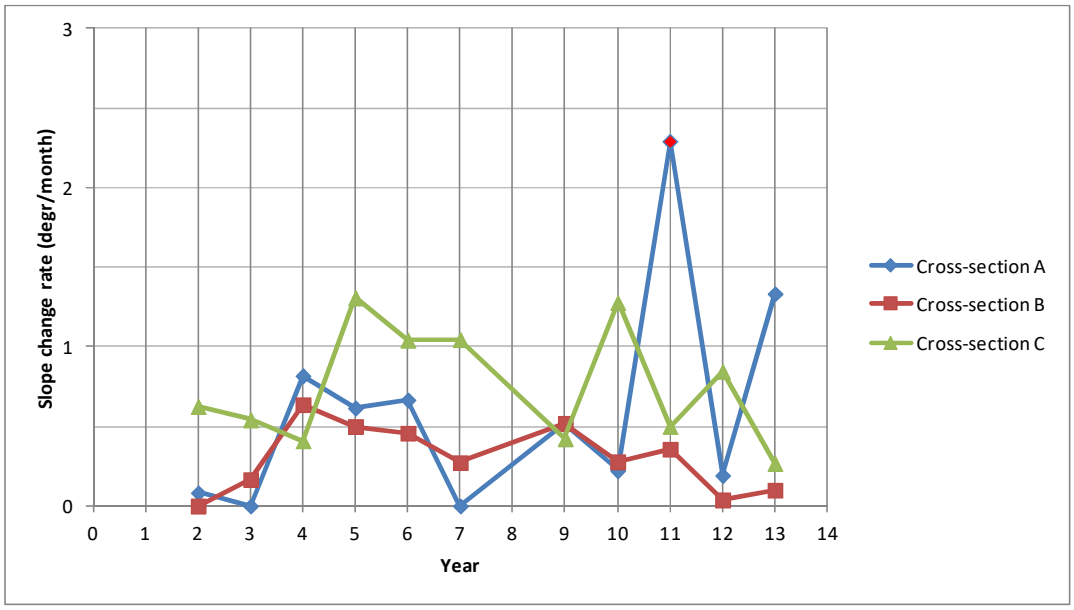

Figure 79 Plot of rate of change of slope angle vs. time for cross-sections A, B and C

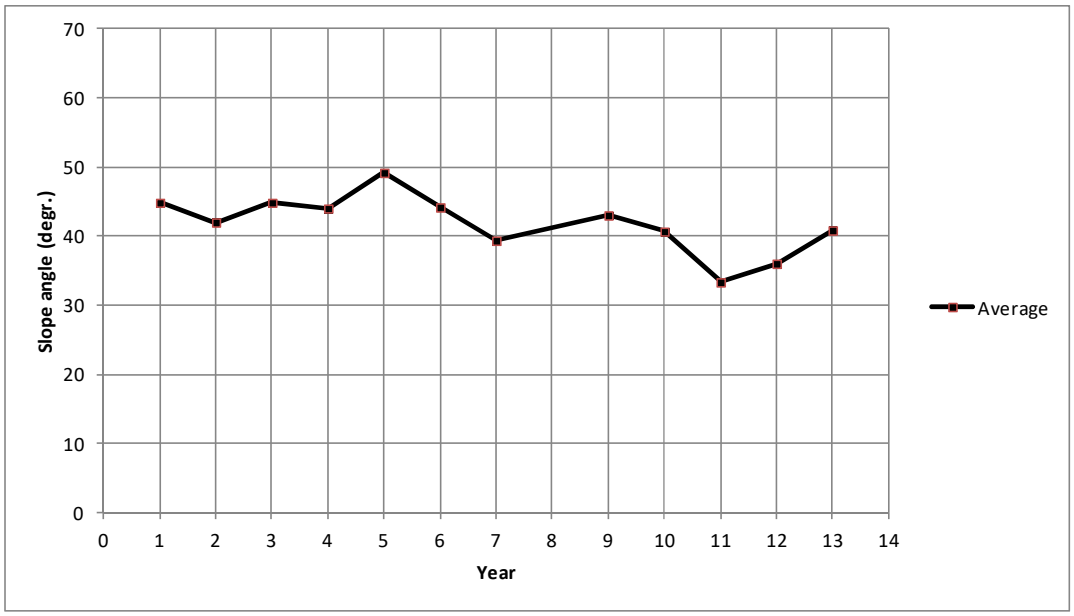

Figure 80 Plot of slope angle vs. time for averaged cross-sections A, B and C

Overall slope angles each year for each cross-section are shown in Figure 78 along with the rate of change (Figure 79). The slope angle refers to the angle (to horizontal) between cliff-top and cliff toe, taken from the TLS data. The data are also shown in Table 13, Table 14 and Table 15. The slope angle of the cliff at the three cross-section locations ranges from 27.5 to 64 degrees.

Table 13 Slope data for cross-section A

Year	Slope angle (degr.)	Slope change	Rate of slope change (degr./month)	Description
2002	43			
2003	42	-	0.08	Minor falls in lower slope
2004	42		0	Minor falls in upper and lower slope
2005	51	+	0.82	Major recession in lower slope, minor mid-slope, *steepest profile*
2006	43	-	0.62	Major recession upper and mid slope
2007	35	-	0.67	Major recession uppermost slope
2008	35		0	Minor fall lower slope
2009	48.5	+	0.52	Major recession throughout except cliff-top
2010	50.5	+	0.22	Minor erosion at toe
2011	34.5	-	2.29	Major rotation in upper slope
2012	32	-	0.19	Major degradation of rotation, *shallowest profile*
2013	52	+	1.33	Massive recession throughout, greatest at toe

Table 14 Slope data for cross-section B

Year	Slope angle	Slope change	Rate of slope change (degr./month)	Description
2002	39			
2003	39		0	Minor recession mid and lower slope
2004	41	+	0.17	Negligible recession
2005	34	-	0.54	Minor recession mid and lower slope
2006	40.5	+	0.5	Major recession throughout
2007	46	+	0.46	Minor recession mid-slope, beach uplift, *steepest profile*
2008	43	-	0.27	Minor rotation mid-slope
2009	29.5	-	0.52	Massive recession in upper half of slope
2010	32	+	0.28	Major recession lower and mid-slope
2011	29.5	-	0.36	Minor recession lower slope, major rotation at cliff-top
2012	29	-	0.04	Major recession throughout
2013	27.5	-	0.1	Minor recession upper and mid-slope, *shallowest profile*

Table 15 Slope data for cross-section C

Year	Slope angle	Slope change	Rate of slope change (degr./month)	Description
2002	52.5			
2003	45	-	0.63	Minor recession upper and mid-slope
2004	51.5	+	0.54	Minor recession throughout
2005	47	-	0.41	Negligible recession upper slope
2006	64	+	1.31	Major recession lower and mid-slope, *steepest profile*
2007	51.5	-	1.04	Major recession upper slope, decreasing downward
2008	40	-	1.05	Minor cliff-top recession
2009	51	+	0.42	Major recession throughout
2010	39.5	-	1.28	Major recession throughout
2011	36	-	0.5	Minor recession mid and upper slope, *shallowest profile*
2012	47	+	0.85	Major recession throughout
2013	43	-	0.27	Minor recession upper and lower slope

10.2.4 Beach levels

Beach levels have been estimated for each survey using the cross-sections from section 10.2.3. These cross-sections are taken from the TLS models which have been tied to a datum coincident with the undisturbed 'correct' hinterland level. This should have removed some, but not all, of the errors emanating from the dGPS / GNSS data (see section 10.2.5). The plots of beach level (Figure 81) show a general

agreement between sections except for section B, Year 5. An overall range of 4 m is indicated with peaks occurring in 2006, 2007 and 2012. An averaged plot of the same data is shown in Figure 82.

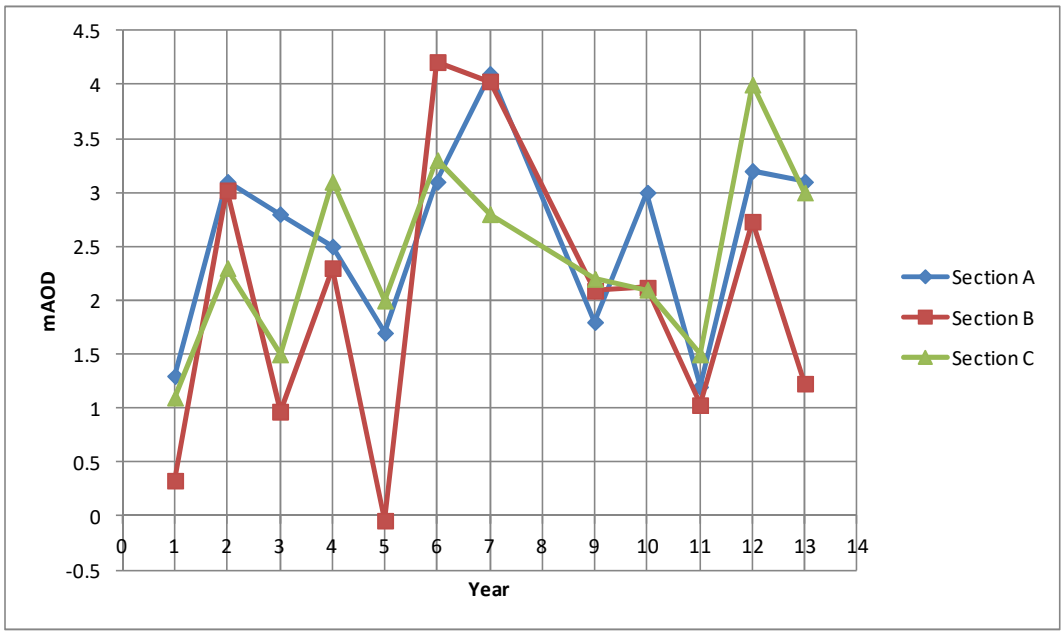

Figure 81 Plot of estimated beach levels, 2001 – 2013, derived from TLS cross-sections.

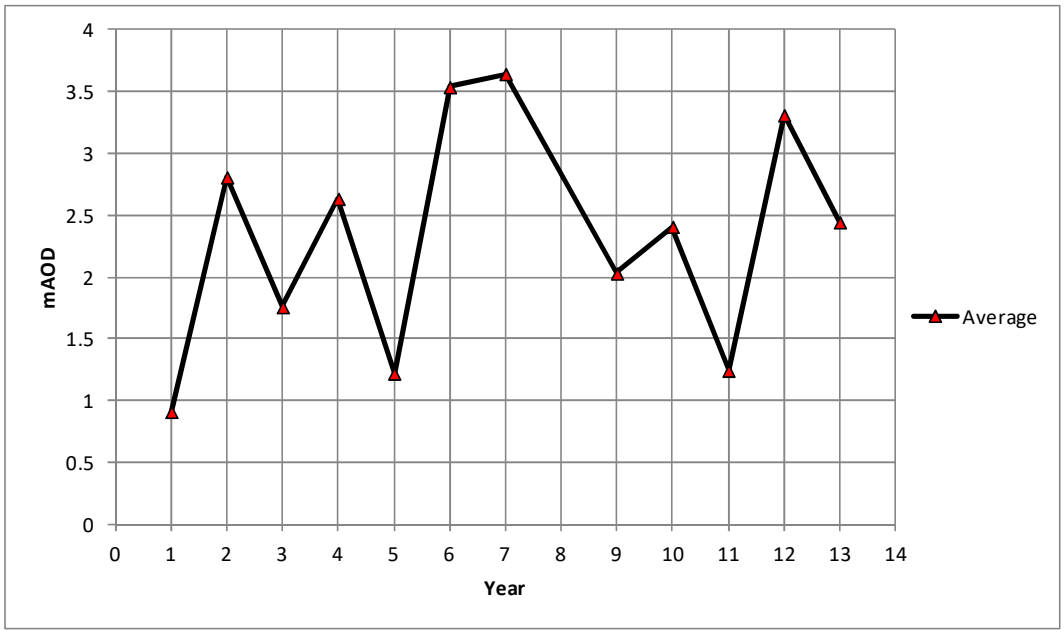

Figure 82 Plot of estimated beach levels, 2001 – 2013, averaged from TLS cross-sections.

10.2.5 Errors

Construction of the survey profiles from the laser scans has revealed various problems associated with TLS carried out in dynamic coastal locations with no fixed points, such as described here at Aldbrough. These are errors in position (x, y and z), particularly in z, of instrument and tiepoints, and errors in level (instrument only). These errors have a major impact on long-range targets and particularly on those having very variable range. Errors in dGPS position tend to be most severe with regard to elevation, though any errors in x, y and z position can cause rotations and displacements of the scans. Errors in level tend to produce rotation of all or parts of the scan. This can result in errors in both elevation and position. Several minor adjustments have been made to the elevations of profiles, in particular to August 2007 and June

2013, by up to 3 m. A major source of error was found to be tilting of the hinterland component of the finished model downwards from north to south by up to 3 m over 300 m run. This is difficult to explain as this section is made up of at least two scans. Corrections applied to errors in the hinterland part of the model have been necessary to ensure that these are coincident; this being the only plausible reference datum available at Aldbrough. In order to do this many dGPS / GNSS datasets, including independent 'cliff-edge' dGPS / GNSS surveys carried out for most monitoring epochs, as well as the NextMap DTM (2001), have been analysed statistically to determine 'true' hinterland elevations. Considerations of scan 'rotation' and 'translation', and indicated errors with dGPS / GNSS surveys, have been taken into account in identifying and correcting problem profiles. These various sources of error are summarised in Table 16.

Table 16 Sources of error in models

Error	*Cause 1*	*Cause 2*	*Cause 3*
Entire model tilted (N-S/E-W)	dGPS / GNSS x, y, z incorrect	LiDAR not level	Unstable tripod
Part of model tilted (N-S/E-W)	LiDAR not level	dGPS x, y, z incorrect	Unstable tripod
Incorrect hinterland elevation	dGPS / GNSS x, y, z incorrect	LiDAR not level	
Incorrect beach elevation	Unstable tripod	LiDAR not level	dGPS x, y, z incorrect

'Unstable tripod' errors are more likely in scans from the beach, whereas 'LiDAR not level' errors are possible throughout the survey, as are dGPS errors, though the latter may vary during a survey. *NOTE: The Riegl VZ1000 scanner has the capability to self-level if the platform is less than 5 degrees from level. This does not apply to the LPM series of scanners.*

Once corrections have been made an estimated accuracy for the model's position for the cliff is around 0.5 m for the central 200 m section. Errors in the northern and southern extremities of the survey and of beach/platform levels and positions are likely to be greater than this. However, these extremities have been clipped out in most cases.

11 Borehole drilling and instrumentation

11.1 DRILLING

The programme of drilling and instrumentation at the Aldbrough test site was instigated in early 2012 (Phase 1) and continued in early 2015 (Phase 2). A detailed account is given in a separate report (Hobbs et al., 2015a). A summary is given below.

11.1.1 Phase 1

In March 2012 two pairs of boreholes were installed (Phase 1) on the cliff top at the Aldbrough test site. These were drilled to a depth of 20 m by Geotechnics Ltd of Coventry using a cable percussion rig and a truck-mounted rotary rig using air/water mist flush. The arrangement of boreholes is shown in Figure 83. Each pair consisted of a cored hole used for piezometer array installation and an open-holed borehole used for inclinometer tubing. The first pair (1a and 1b) were located 10 m from the cliff edge (at the time) and the second pair (2a and 2b) 20 m's from the cliff edge (at the time); the alignment of the pairs being perpendicular to the coastline. Each pair had a separation, parallel with the coastline, of 5 m. The ground between the cliff edge and the borehole locations showed no sign of subsidence or landsliding at the time of drilling. The piezometer arrays contained five sensors in each borehole (boreholes 1a & 2a). At the time of drilling (19th – 22nd March, 2012) the test area had recently undergone significant landsliding (see cover photo). This was centred closely on the borehole alignment. Currently BGS is carrying out three-monthly monitoring of borehole instrumentation (piezometers and inclinometers) and at the same time

continuing with six-monthly TLS. A laser scan ("ALDBH0312") was carried out on 19th/20th March 2012. This included the area containing the borehole operations.

11.1.2 Phase 2

In January 2015 a further pair of boreholes were drilled (Phase 2) to a depth of 20 m (Figure 83) by ESG using a Geobore-S rotary triple-barrel wireline method. These boreholes were situated 8 m landward of Phase 1 boreholes 2a and 2b and in the same alignment; that is, approximately perpendicular to the cliff line. The boreholes were installed with inclinometer casing (borehole 3b) and a 6-element piezometer array (borehole 3a) using the same method and equipment as used in Phase 1. In addition, BGS 'PRIME' resistivity arrays were installed in both boreholes and at the surface parallel with the cliff and aligned with boreholes 3a and 3b. These have electrodes spaced at 1 m intervals throughout each hole. The PRIME system allows data to be uploaded by datalink.

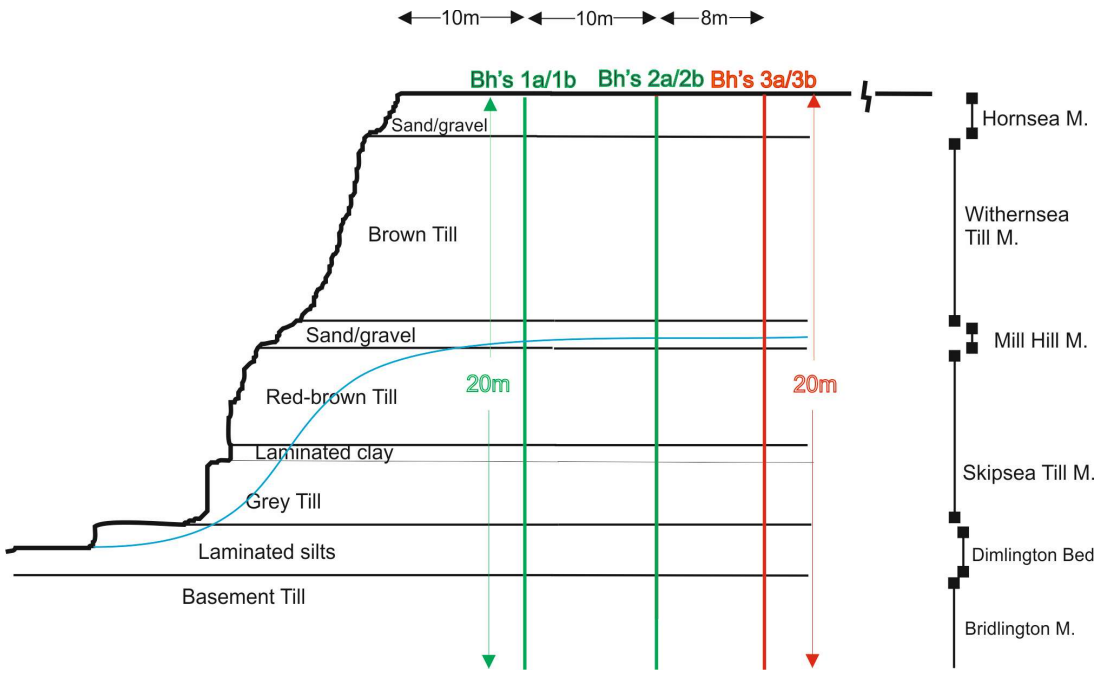

Figure 83 Cross-section at Aldbrough showing boreholes.
NOTE: Water table (blue line) conceptual

Table 17 Summary of boreholes, installations and dGPS survey pins at Aldbrough test site (Hobbs et al., 2015a)

Borehole No.	*BH Depth (m bGL)*	*Location (Easting, Northing), Ht. (aMSL.)*	*Method*	*Instrumentation*	*Instrument depths (m bGL)*
1a	20.5	525684.3, 439529.7, 16.52	Cable percussion (sampled)	VW Piezo array (x5)	4.0, 8.0, 12.0, 16.0, 20.0
1b	20.5	525681.4, 439533.7, 16.56	Rotary (open-holed)	Inclinometer casing (70mm, QJ)	0.0 – 20.0
2a	20.5	525676.5, 439523.6, 16.18	Cable percussion (sampled)	VW Piezo array (x5)	4.0, 8.0, 12.0, 16.0, 20.0
2b	20.5	525673.4, 439527.5, 16.41	Cable percussion	Inclinometer casing (70mm, QJ)	0.0 – 20.0

3a	19.90	525670.1, 439518.8, 16.1	Geobore-S triple barrel wireline	VW Piezo array (x6) PRIME array	1.7, 3.7, 7.7, 11.7, 15.7, 19.7m 1 m intervals 0.9 - 19.9m
3b	19.85	525667.3, 439522.8, 16.3	Geobore-S triple barrel wireline	Inclinometer casing (70mm, QJ) PRIME array	– 19.85m 1 m intervals 0.85 - 19.85m
Survey pin No.		*Location / ht. (aMSL.)*	*Description*		
X1 pin		525690.6, 439537.7, 16.70	Pin with yellow disc on kerb	Caravan Road	
Pin 1		525676.9, 439539.9, 16.40	Pin in road parallel to BH's 1A and 1B	Seaside Road	
Pin 2		525667.7, 439534.7, 16.33	Pin in road parallel to BH's 2A and 2B	Seaside Road	
Pin 3		525659.8, 439529.8, 16.23	Pin in road	Seaside Road	

Figure 84 Location of boreholes at Aldbrough test site
NOTE: Dwellings marked X have been demolished by time of reporting
NOTE: Cliff top shown as red line (March 2012)

11.2 WEATHER STATION

The BGS's 'Slope Dynamics' team installed a Campbell BWS-200 weather station (Figure 85) at Aldbrough on 17th April, 2012. The location is NGR 525459, 439627, that is, 250 m WNW of the centre of the test site (at the time of installation). The weather station measures the following parameters automatically at preset time intervals (currently hourly):

- Air temperature
- Dew point
- Wind speed
- Wind direction
- Precipitation
- Solar radiation
- Air temp
- Relative humidity
- Evapotranspiration
- Barometric pressure
- Battery voltage

Data are logged to a built-in CR200X datalogger and are retrieved manually to a laptop via PC200W software for Windows using an RS232 cable or RS232 - USB converter cable.

Figure 85 BGS's Campbell BWS-200 weather station newly installed at Aldbrough (Apr 2012)

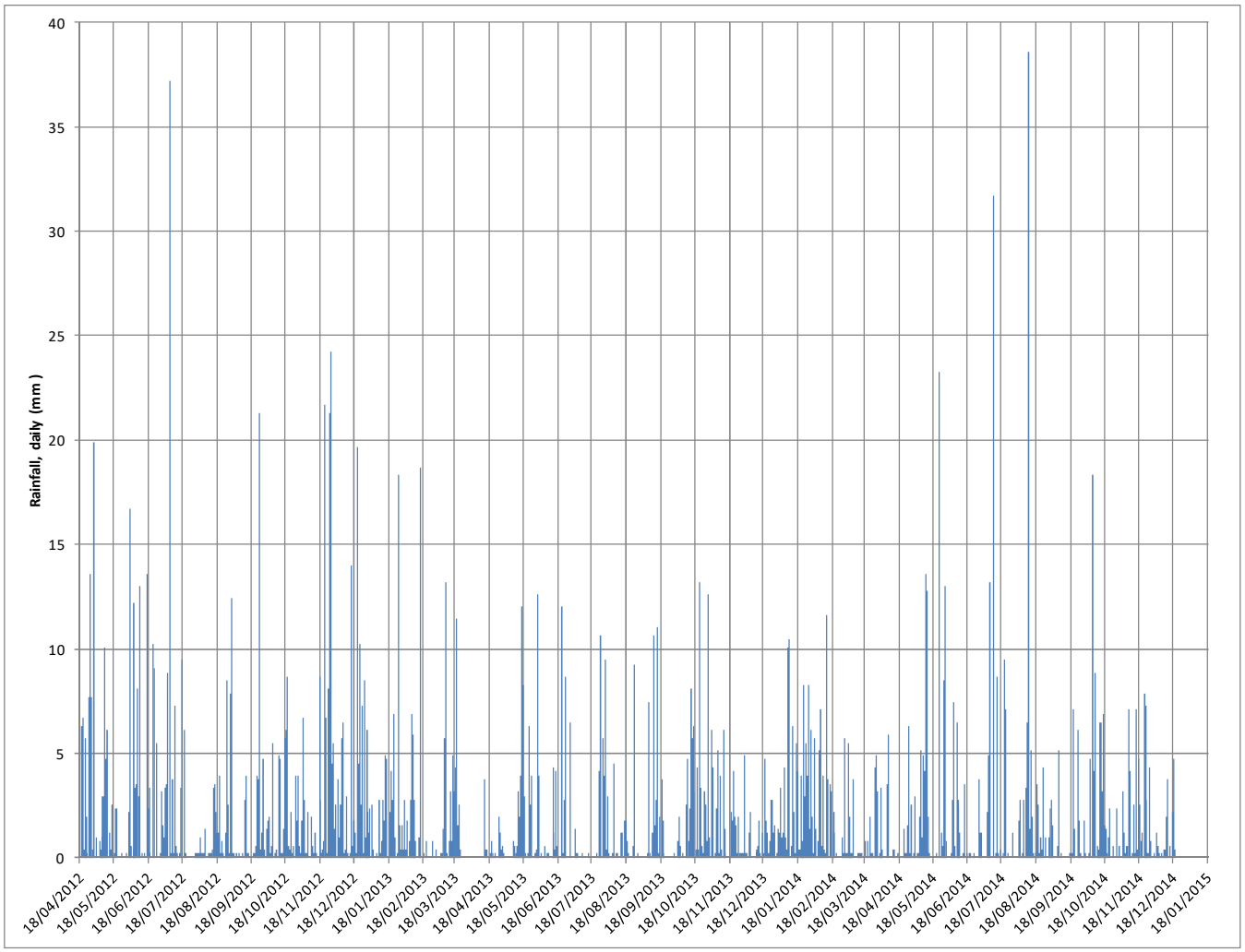

Figure 86 Total daily rainfall 'Aldbrough BGS' weather station, for period 18th April 2012 to 19th Dec 2014 (Total = 1,920 mm in 976 days)

The results for total daily rainfall recorded by the BGS's weather station ('Aldbrough BGS') are shown in Figure 86. Significant rainfall was recorded in 2012 between late-May and mid-July and again in late-November. A similar pattern was observed in 2014. Total monthly rainfall is shown in Figure 87. The total rainfall for the first 12 month period of monitoring (1st May 2012 to 30st April 2013) was **802 mm**. The total rainfall for the second 12 month period of monitoring (1st May 2013 to 30st April 2014) was **579 mm**. The following 6 month period (1st May 2014 to 31st October, 2014) produced **392 mm**.

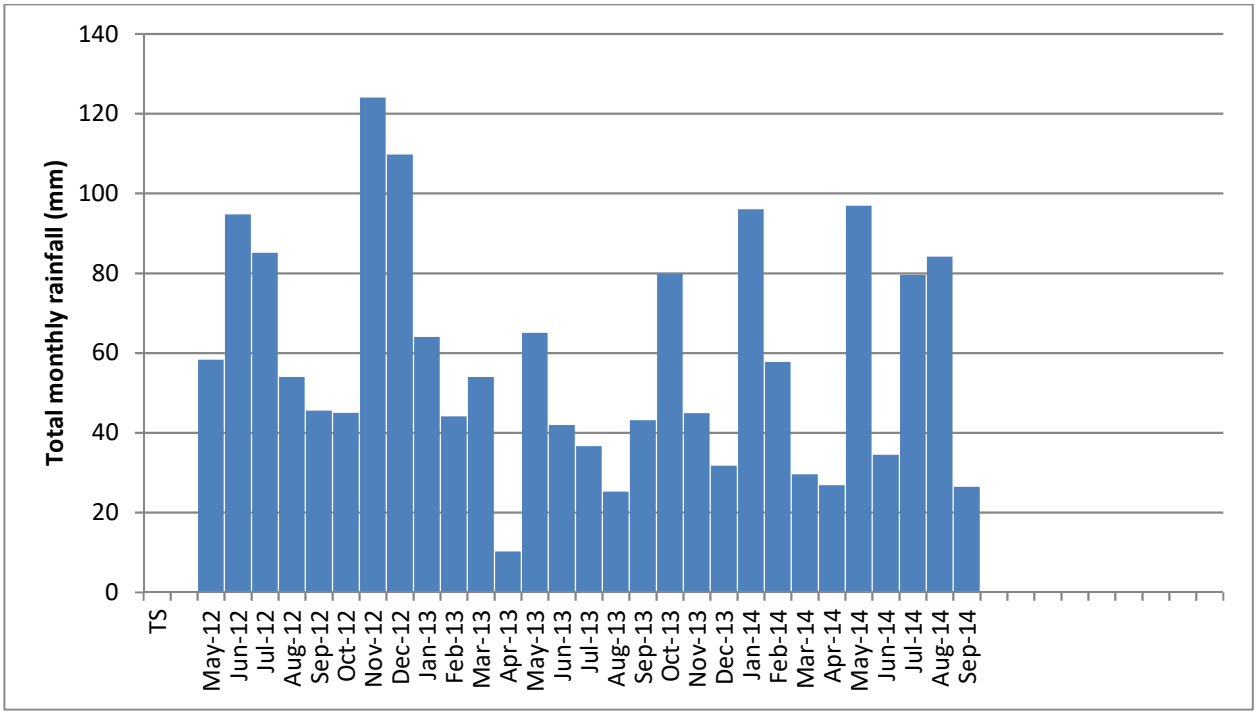

Figure 87 Monthly total rainfall (May 2012 to Nov 2014) for 'Aldbrough BGS' weather station

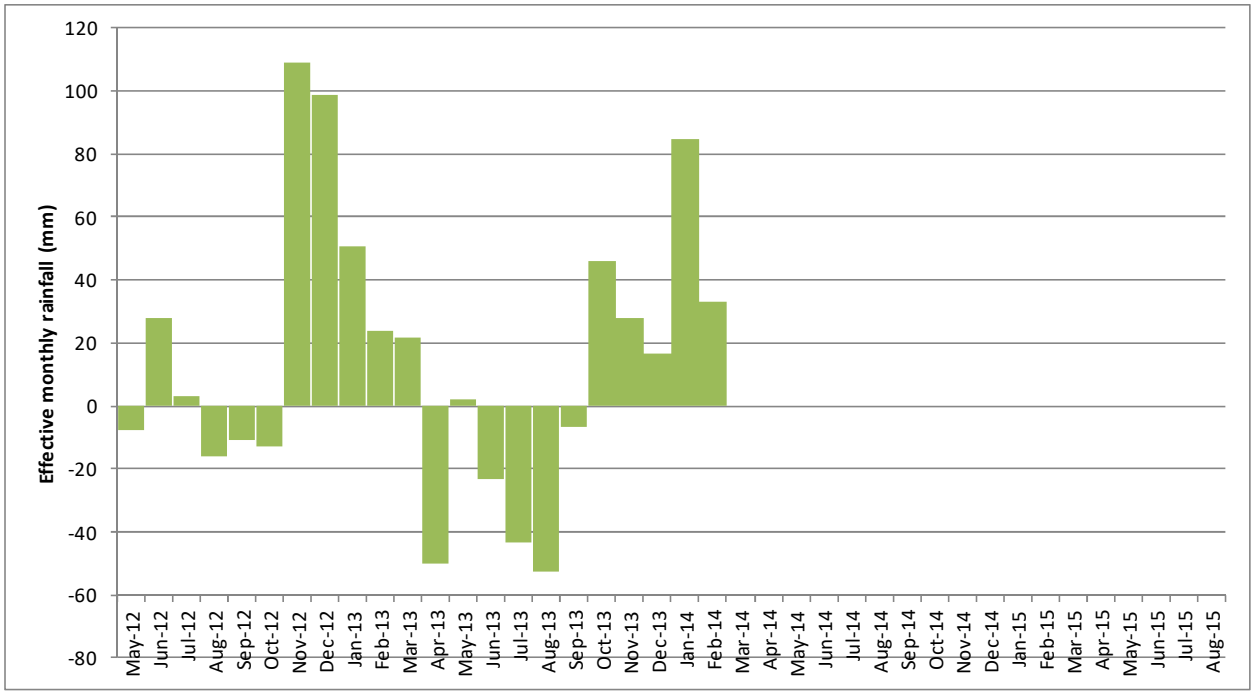

Figure 88 Monthly effective rainfall (May 2012 to Jan 2014) for 'Aldbrough BGS' weather station

NOTE: The effective rainfall plot in Figure 88 is curtailed at Jan 2014 due to damage to the relative humidity/ temperature sensor.

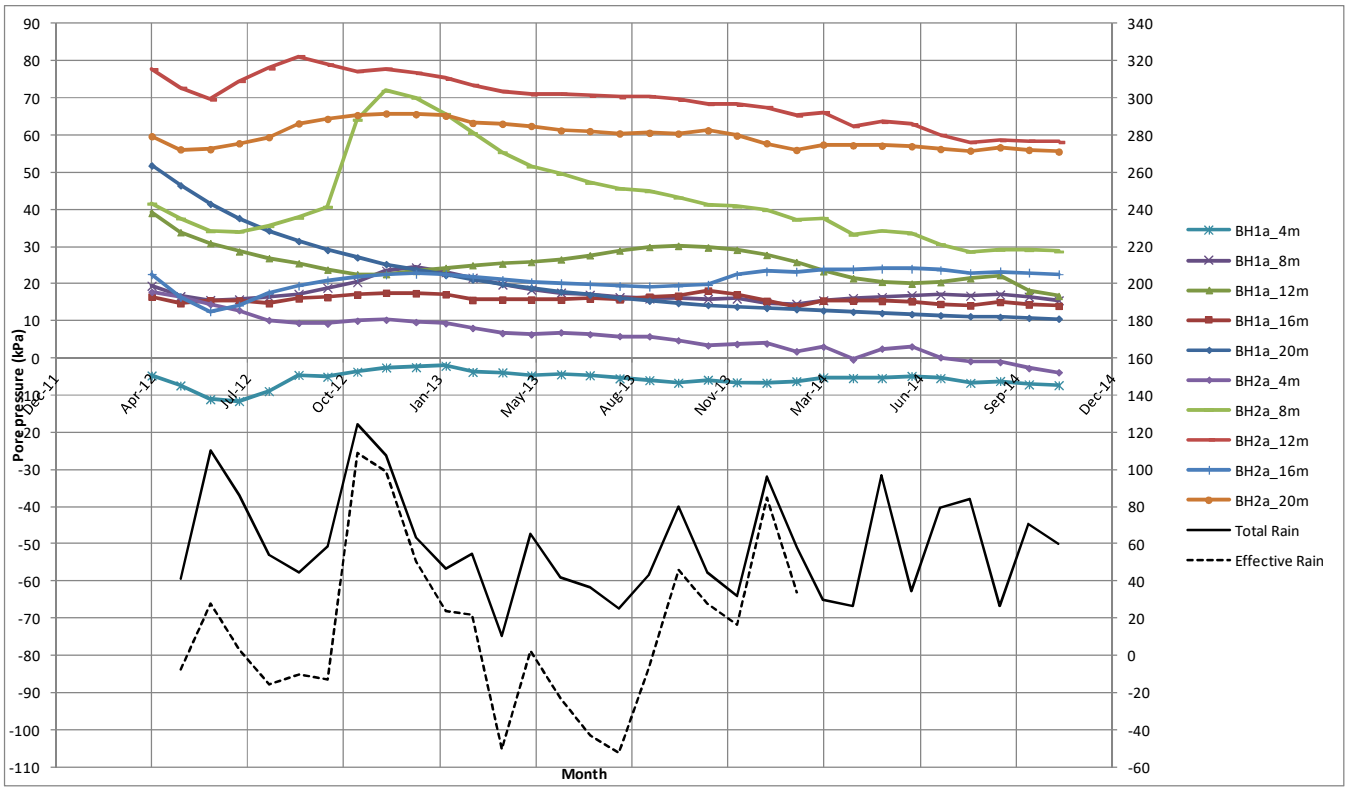

Figure 89 Plot of monthly average piezometer pore pressures and rainfall (effective and total) vs. time from BGS's borehole installations and 'Aldbrough BGS' weather station at Aldbrough (May 2012 to November 2014)

Effective rainfall is calculated by subtracting the potential evapotranspiration (ETo) from the rainfall, where ETo is the amount of water (mm) lost from the soil due to evaporation and plant transpiration. The data required for the 'Penman-Monteith' calculation of ETo are: solar radiation, precipitation, air temperature, relative humidity, wind speed and wind direction. The latitude, longitude and elevation of the weather station are also required. The average ETo based on hourly data for the reported monitoring period was 1.4 mm. A plot of effective rainfall for the recorded monitoring period is shown in Figure 88. November and December 2012 are notable for their high effective rainfall. Effective rainfall data are shown in Figure 88. This plot shows negative values in the summer, particularly in 2013, a strong switch to positive values in November 2012, and to a lesser extent October 2013 and strongly negative values in April 2013. A plot (Figure 89) shows the monthly average piezometric data with monthly average rainfall and effective rainfall from the BGS's Aldbrough weather station plotted on the same time scale. Whilst some sensors had still not equilibrated by late 2012 there may have been a response to the November rainfall by the sensor at 8 m depth in Borehole 2a. This response to rainfall, if indeed it was such, is seen with both rainfall and effective rainfall data. The sensor at 8 m is located in the Skipsea Till Member.

At the time of writing insufficient data exist to make comparisons between rainfall data from BGS's Aldbrough weather station and volume changes derived from the TLS data. However, this should become possible within the next three years (see section 14.1).

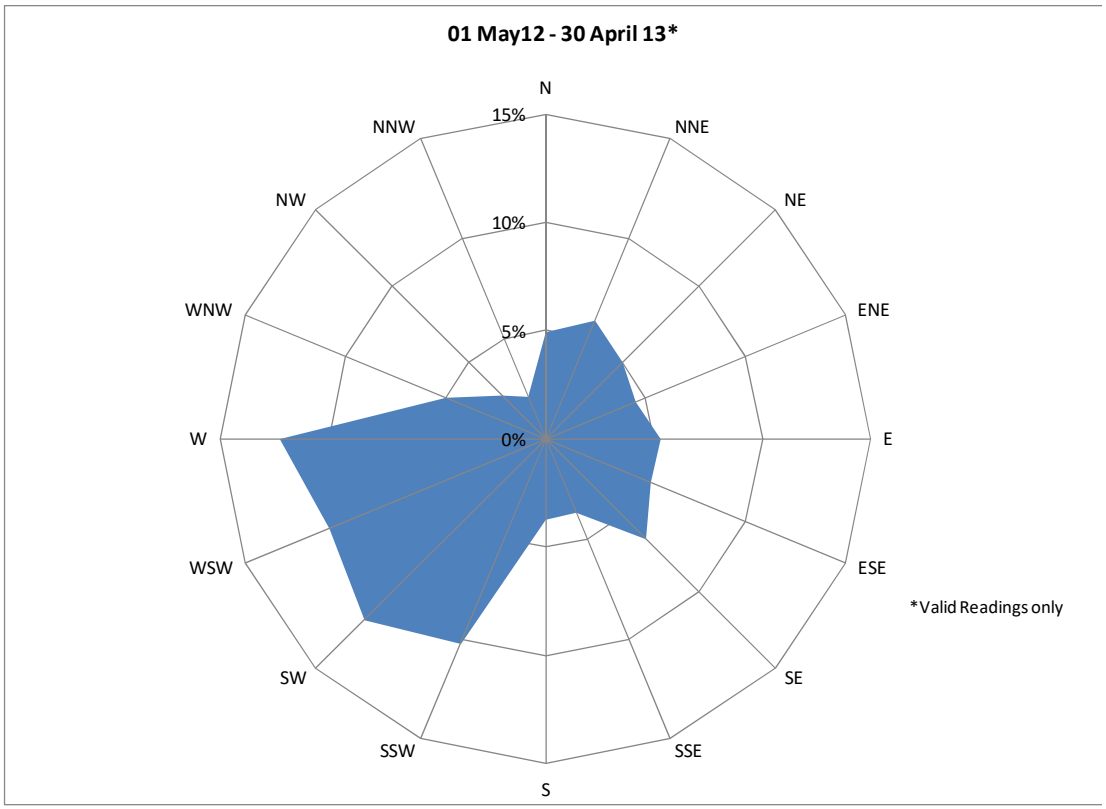

Figure 90 Wind rose diagram illustrating wind direction statistics, for BGS's Aldbrough weather station's first 12 month's data (1st May 2012 to 30th April 2013)

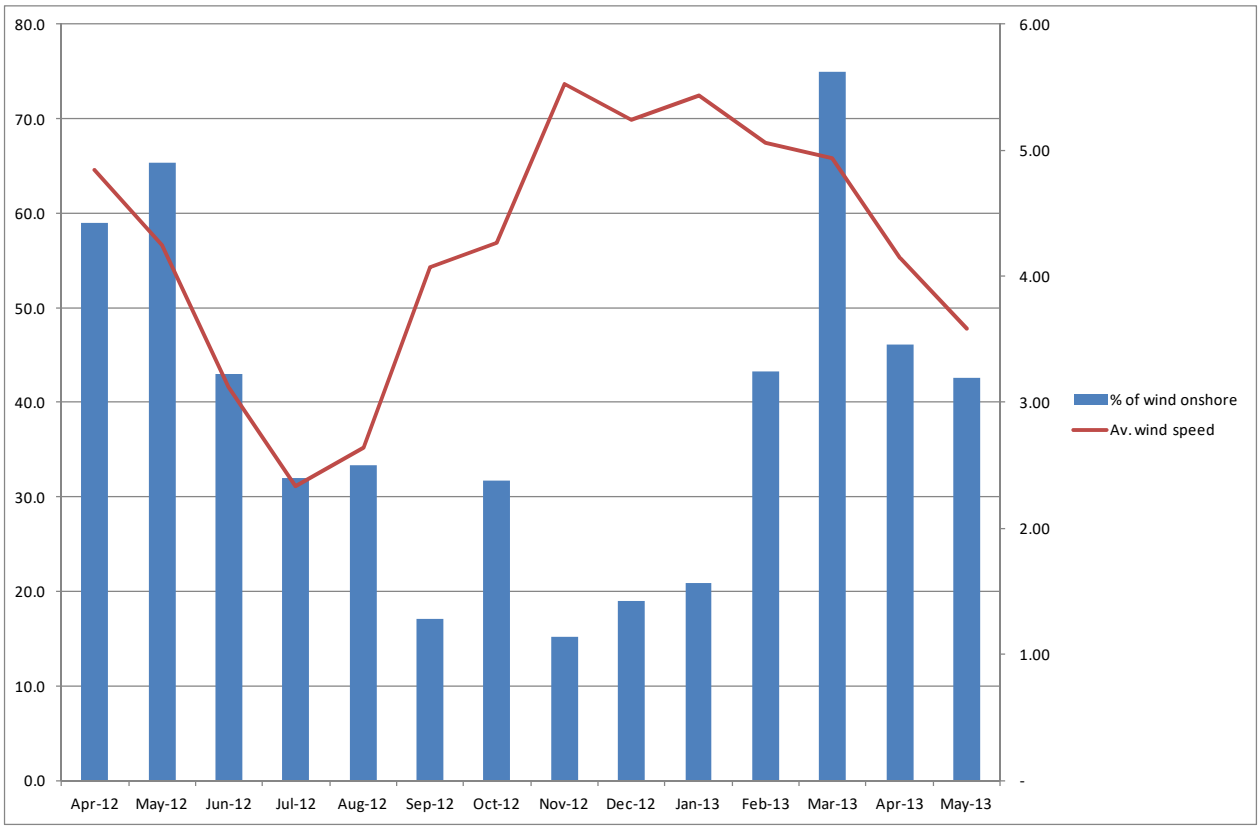

Figure 91 Plot of average monthly wind speed in m/s (Y-axis, right) and percentage onshore (Y-axis, left) (i.e. N340º to N140º), for BGS's Aldbrough weather station, April 2012 to May 2013

.

Results from the wind data recorded by the BGS weather station are shown in Figure 90 and Figure 91 and in Appendix 1. The wind direction diagram (Figure 90) shows a bi-modal disposition with the dominance of wind from the west and south-west and to a lesser extent from the north-north-east, east and south-east. The south-westerlies would be expected to be significant in terms of rainfall, and the north-easterlies less significant. However, this is not borne out by the data which suggest that there is no correlation between rainfall and wind direction, at least for the period monitored. Wave height, and consequently enhanced coastal erosion, would be expected to be associated with wind from onshore, in particular from the north and north-east, i.e. the source direction having the greatest fetch (refer to section 11.3). Monthly wind direction diagrams are shown in Appendix 1. These do not appear to indicate any particular seasonal trends, at least for the period monitored.

The relationship between average wind speed and 'proportion of which onshore' (taken as N340° to N140° at Aldbrough) is shown in Figure 91. Combinations of high wind speed with high percentage of onshore wind were seen in April and May 2012 and March 2013.

11.3 WAVE DATA AND SEDIMENT TRANSPORT

Waves are important in the coastal zone especially in areas of high erosion such as the Holderness coast (Wolf, 1998). Waves in shallow water are subject to many complex and non-linear processes, including bottom friction dissipation and refraction by depth contours and current shear, and other interactions with the ambient current (Wolf, 1998). The tidal range is 5 m in the Holderness area. The nearest wave data to Aldbrough are available from the Channel Coastal Observatory's 'Hornsea' buoy situated at NGR 527071, 448459 where water depth is 12 m (CCO, 2013). The Datawell Directional Waverider Mk III buoy, owned by East Riding of Yorkshire Council, is situated approximately 8.8 km north-east of the Aldbrough test site and was deployed on 5th June 2008. The data for the period 2008 to 2012 are summarised in Table 18 and in Appendix 2. A wave direction rose diagram for this buoy is shown in Figure 92. The lower limit of 'significant wave height', H_S for *storm* designation is 3 m. The exceedance statistics are shown in Figure 93 and the individual instances in Figure 94. Only one storm event was recorded in 2011 (23rd July). This compares with many storms during the previous two years; these mainly occurring in autumn and winter. Principal source direction for storm (and other) waves is from the NNE and NE. *NOTE: the passage of anti-cyclones produces winds from a variety of directions.*

Table 18 Wave height data, Channel Coastal Observatory, Hornsea buoy (CCO, 2013)

Year	Annual exceedance (m)						Annual maximum H_S	
	0.05%	0.5%	1%	2%	5%	10%	Date	A_{max} (m)
2008		3.03	2.78	2.52	1.77	1.44	22nd Nov	3.78
2009	4.34	3.37	2.93	2.34	1.77	1.44	17th Dec	4.87
2010	3.78	3.39	3.12	2.77	2.24	1.80	10th Jan	4.08
2011	2.83	2.41	2.17	1.93	1.65	1.38	23rd Jul	2.99
2012							24th April	4.99
2013							24th Mar	4.50

H_S = Significant wave height (m)
A_{max} = Maximum wave height in each year (m)
Example: 5 % of the H_S values measured in 2008 exceeded 1.77 m

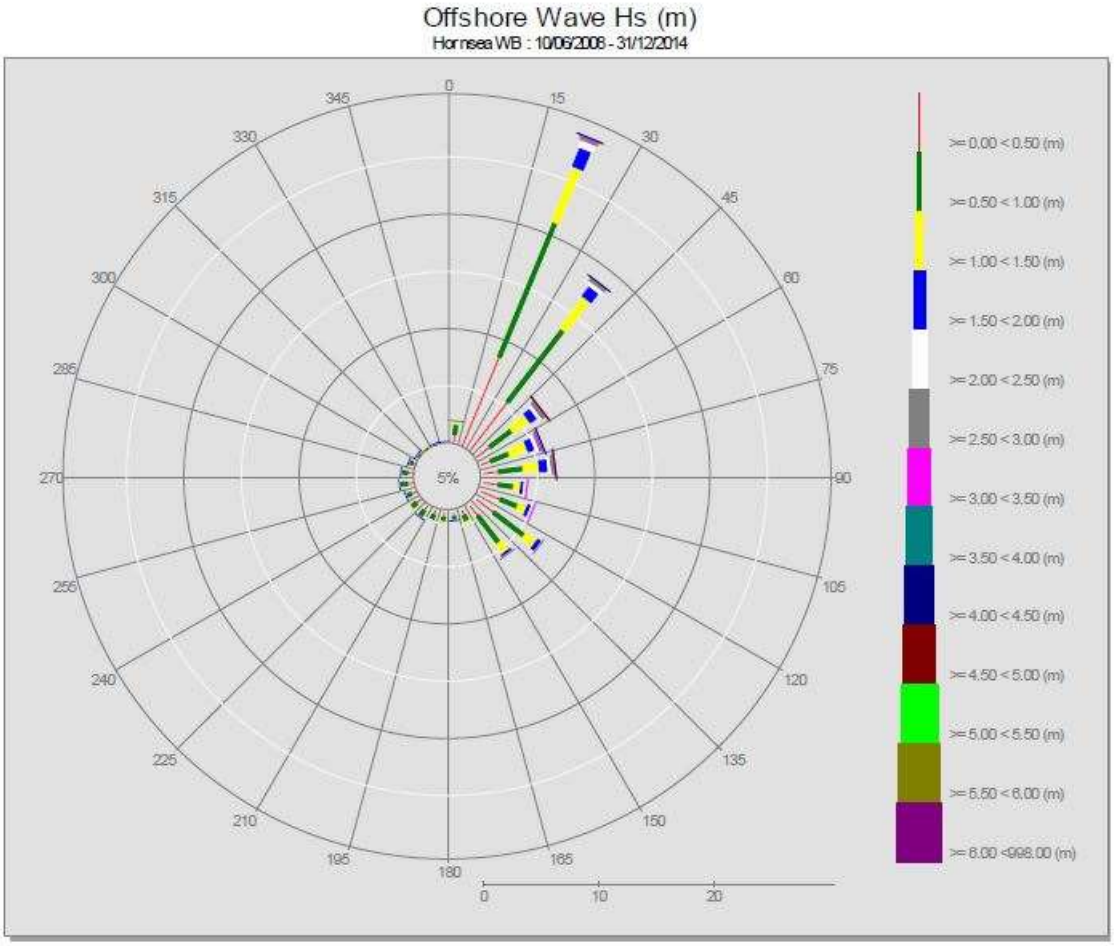

Figure 92 Wave height, H_S, rose diagram for Hornsea buoy for 10th June 2008 to 31st December 2014 (CCO, 2013)

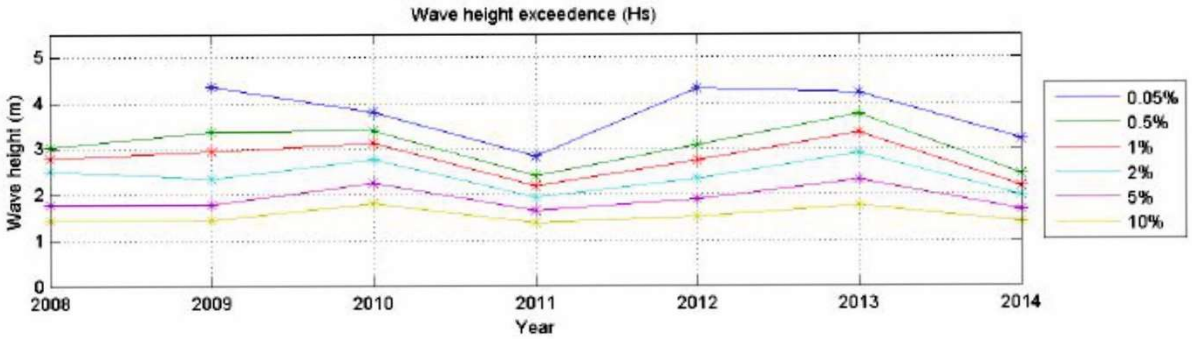

Figure 93 Wave height exceedance for Hornsea WaveRider III buoy (CCO, 2013)

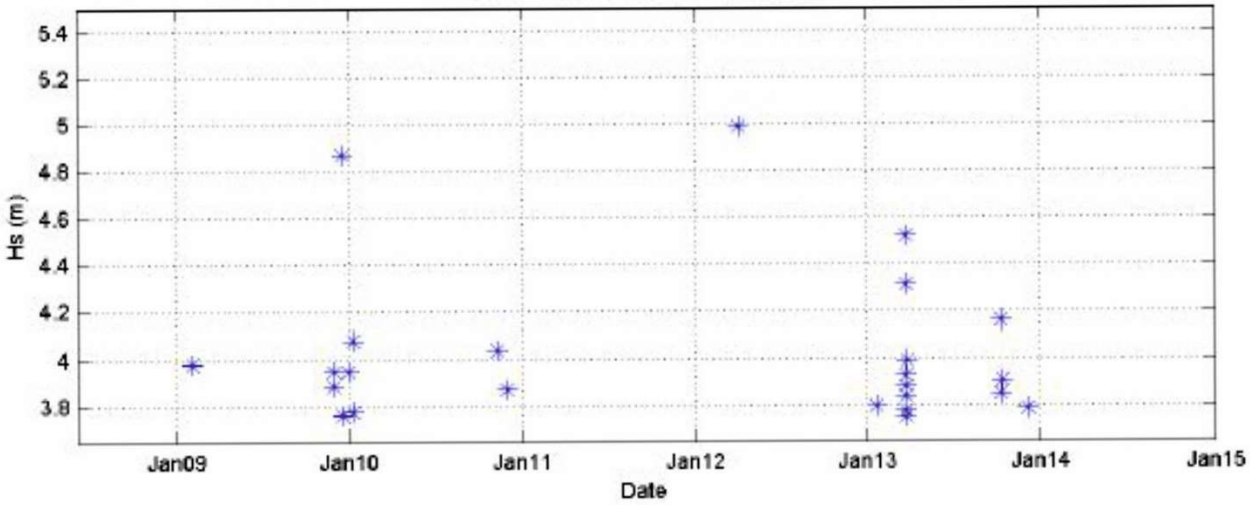

Figure 94 Occurrence of 'storms' at Hornsea WaveRider III buoy (H_S > 3 m) (CCO, 2013)

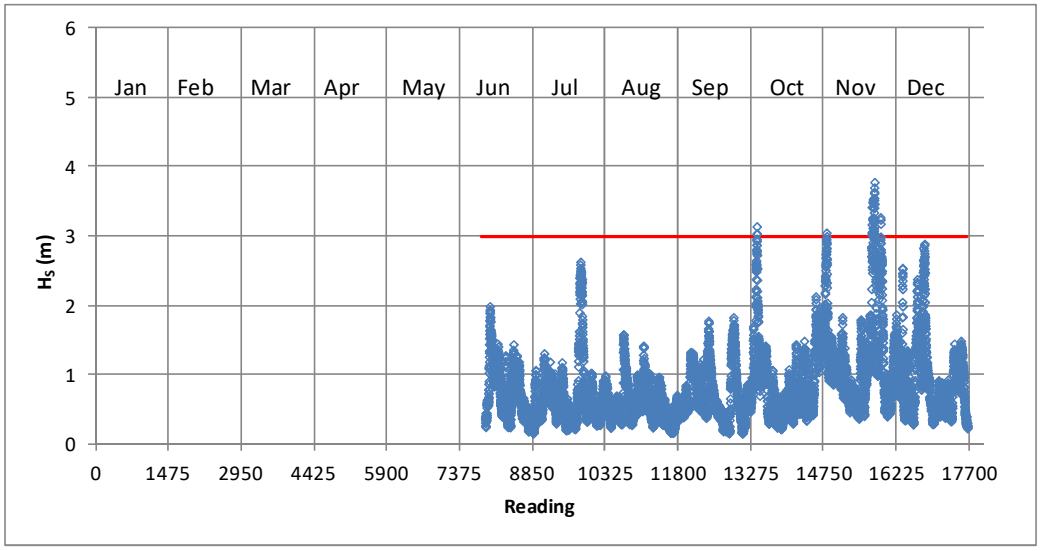

Figure 95 Significant Wave Heights (all data) for 2008, Channel Coastal Observatory, Hornsea buoy (based on data provided by CCO)

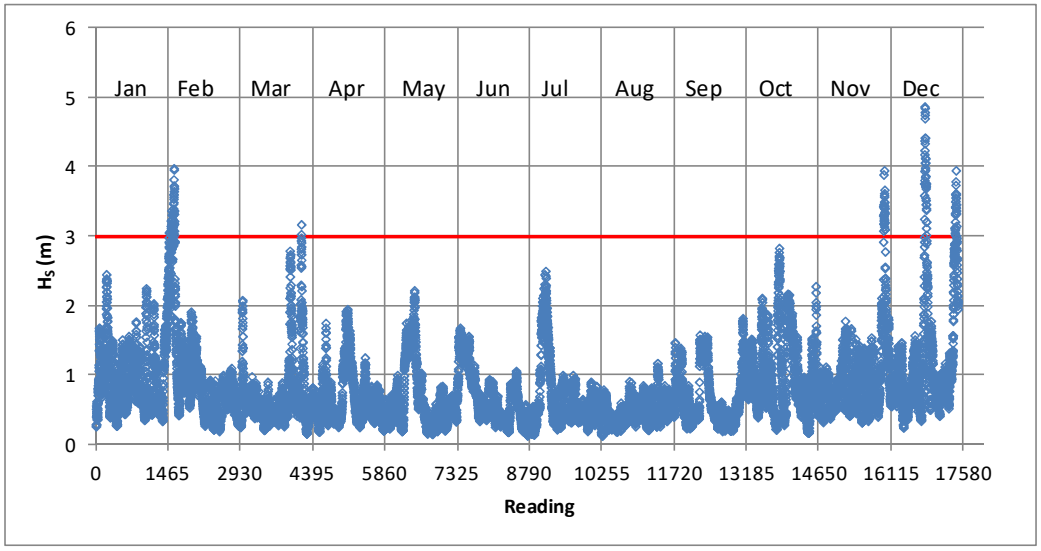

Figure 96 Significant Wave Heights (all data) for 2009, Channel Coastal Observatory, Hornsea buoy (based on data provided by CCO)

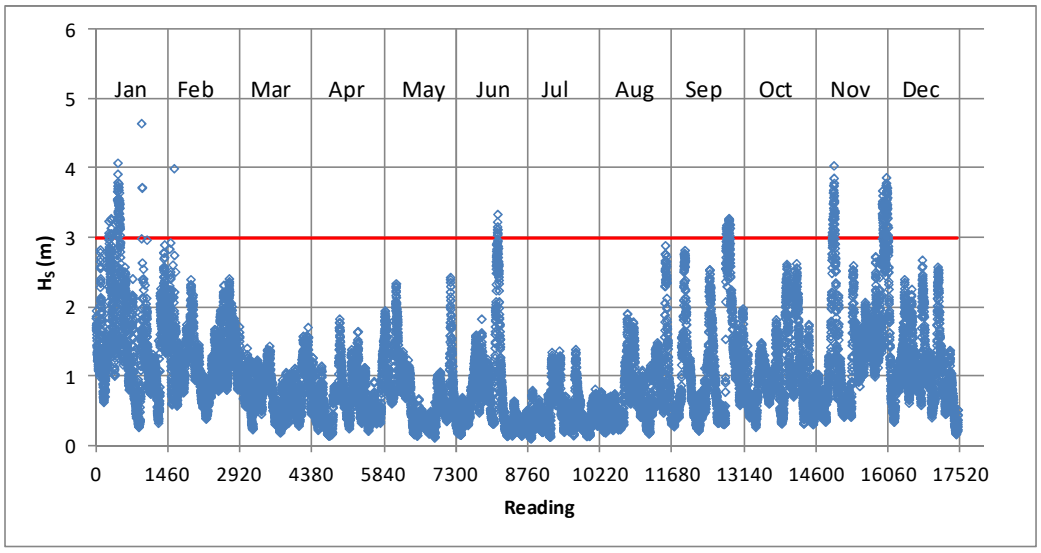

Figure 97 Significant Wave Heights (all data) for 2010, Channel Coastal Observatory, Hornsea buoy (based on data provided by CCO)

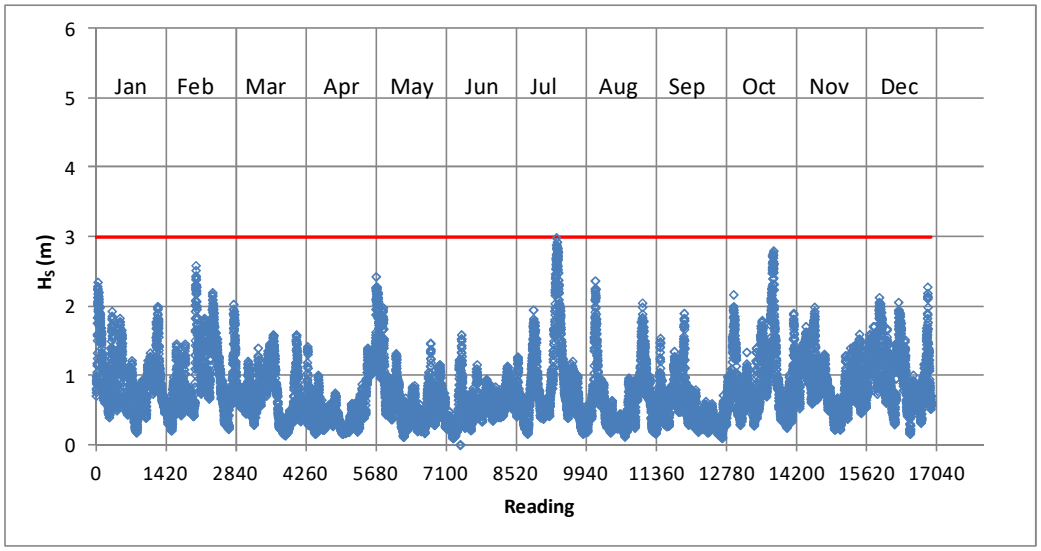

Figure 98 Significant Wave Heights (all data) for 2011, Channel Coastal Observatory, Hornsea buoy (based on data provided by CCO)

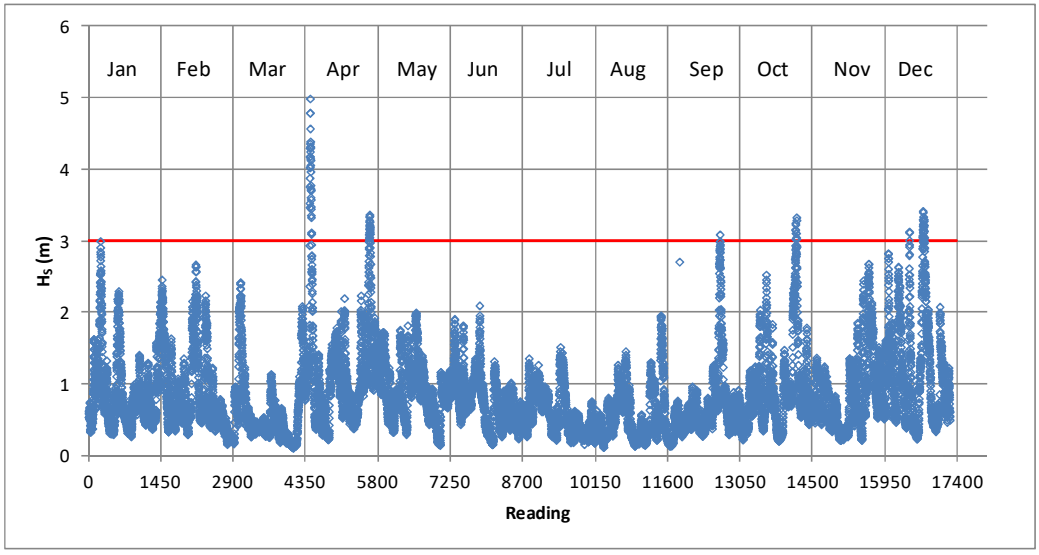

Figure 99 Significant Wave Heights (all data) for 2012, Channel Coastal Observatory, Hornsea buoy (based on data provided by CCO)

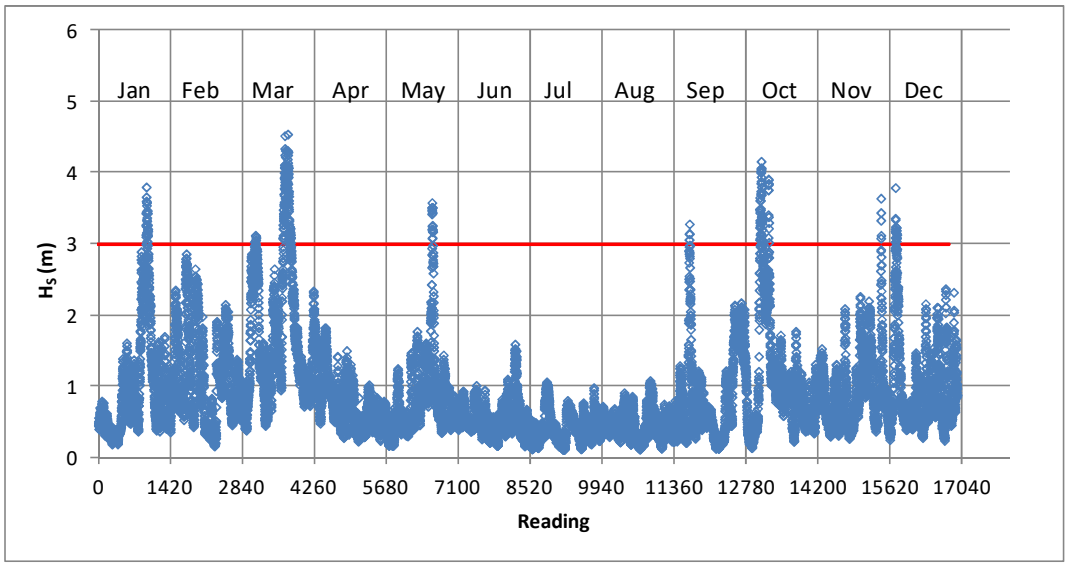

Figure 100 Significant Wave Heights (all data) for 2013, Channel Coastal Observatory, Hornsea buoy (based on data provided by CCO)

Table 19 Storm (H_S > 3m exceedance) dates & energies for 2008 to 2013, Channel Coastal Observatory, Hornsea buoy

2008	2009	2010	2011	2012	2013
	1st-3rd Feb** (61)	6th-7th Jan* (57)	No storms	3–4th Apr** (84)	20th –21st Jan** (61)
	30th Nov** (71)	9th-11th Jan** (65)		29th Apr** (47)	11th Mar (47)
	17th-18th Dec** (91)	20th Jan (235)		27th Oct** (59)	22nd –25th Mar** (76)
	30th-31st Dec** (58)	19th-20th Jun* (67)		14th Dec (46)	24th May* (75)
		24th-26th Sep** (63)		20th–21st Dec** (52)	10th Sep (59)
		8th-9th Nov** (62)			10th–11th Oct** (82)
3rd Oct (64)		29thNov-2ndDec** (62)			13th–14th Oct* (67)
21st-22nd Nov** (73)					30th Nov (75)
25th Nov (64)					6th Dec* (70)

*Short storm
** Prolonged storm
Figure in brackets indicates average wave-climate energy, P in kW/m

Table 20 Wave directions for 2008 to 2013 (all data), Channel Coastal Observatory, Hornsea buoy

Year	2008*	2009	2010	2011	2012	2013
Percentage of all waves onshore (N340 – 140°)	84	84	92	84	88	85
Dominant wave direction, Dirp (percentage)	NNE (45)	NNE (35)	NNE (45)	NNE (38)	NNE (46)	NNE (36)
Percentage of waves height, H_S >3m (storm)	0.6	1.0	1.3	0	0.6	1.7
No. half-hourly height, H_S >3m (storm) readings	54	164	227	0	102	290

*July to December only
Dirp: Compass sector from whence wave comes
H_S: Significant wave height

Wave height data ('Hornsea' WaveRider III buoy) are shown for 2008 to 2013 in Figure 96, Figure 97, Figure 98, Figure 99, and Figure 100. These show similar patterns of seasonal behaviour except that the instances of high waves in 2013 were more frequent and prolonged than in 2012. The number of (half-

hourly) readings where H_S>3 m ranged from zero (2011) to 290 (2013); the latter representing 6 days of storm height waves.

Wave height and derived 'storm' data, including dates and source directions, for the 'Hornsea' WaveRider III buoy are shown in Table 19 and Table 20. 'Onshore' waves (defined here as derived from compass points N340º to N140º) consistently represent 84 %, or over, of the total. This highlights the vulnerability of the Holderness coast to the erosive wave energy which predominantly emanates from an angle of incidence 42.5º to the current average coastline at the Aldbrough test site. There is a remarkable consistency in the source direction of waves (all data); the dominant direction of which is NNE for all years with proportions ranging from 35 to 46%. The percentages of significant wave heights considered as storm related ranges from 0 to 1.7. Rose diagrams showing the full wave direction results for 2008 to 2013 are given in Appendix 2A. *NOTE: These represent data grouped into the 22.5º wide sectors which separate the cardinal, ordinal and inter-ordinal points of the compass, as applied to the data in Table 20.* Averaged monthly wave data for 2008 to 2013 are given in Appendix 2B.

Data from other wave buoys, which are part of the WaveNet network, are available from the 'Cleeton' and 'Ravenspurn' buoys (Oil and Gas UK). These are situated at approximately 40 to 50 km to the ENE of Aldbrough and data from them have not been considered in this report.

The 'Holderness Experiment' carried out between 1993 and 1996 was designed to monitor the processes of sediment transport along the rapidly retreating Holderness coastline and provides the largest single coastal source of sediments to the North Sea (Prandle *et al*., 1996). Various processes have an impact on sediment transport including tides, storm surges and waves. Breaking waves in particular have an important impact on the beach and the near-shore zone (Wolf, 1998). Pethick and Leggett (1993) indicated that high energy waves with long return periods (e.g. 8-15 months) are responsible for (almost) all the net southerly sediment transport and that these are also responsible for offshore bar development.

Most waves were reported to have approached from the north-east and to a lesser extent from the south-east and the east. Wave height varied during the observation period (1993-1996). Relationships between wind direction and wave direction were identified and resolved into 'wind-sea' events and 'swell' events and into long-shore and cross-shore components (Wolf, 1998). Wave height was strongly correlated with wind speed and longer period waves were associated with longer fetch. Clustering of higher waves was found from directions 060º and 120º, these corresponding with the longest fetches (Wolf, 1998). Maximum wave height during normal storm events was observed to be around 4 m, though a 100 year event would produce 7 m high waves (Eurosion, 2004).

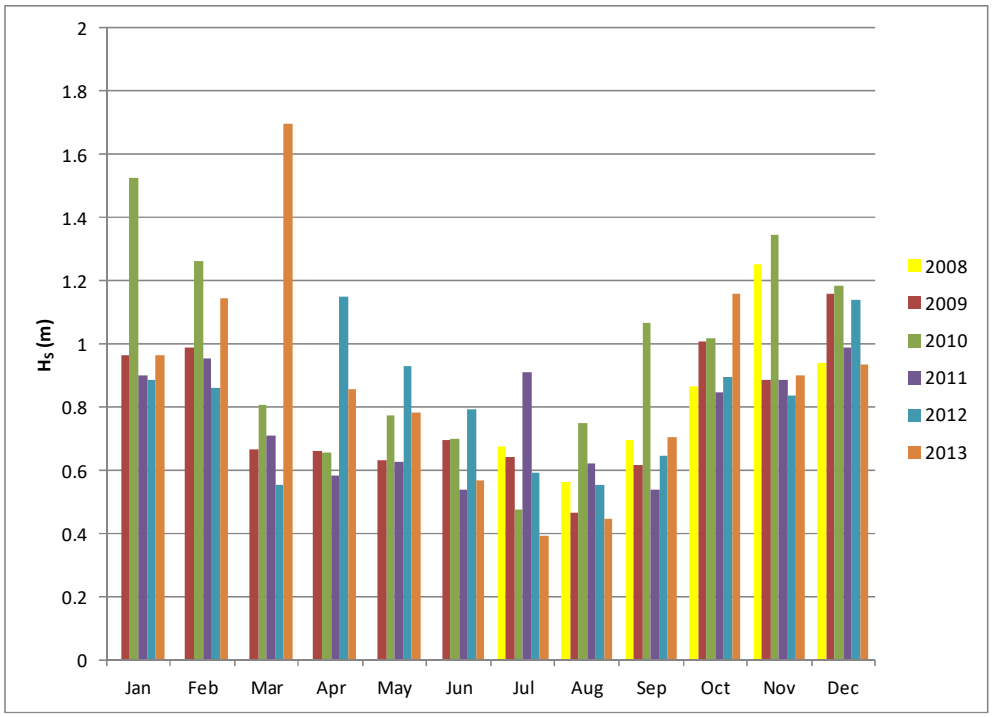

Figure 101 Histogram of average monthly significant wave height, Hs, 2008 to 2013 (CCO data for Hornsea buoy)

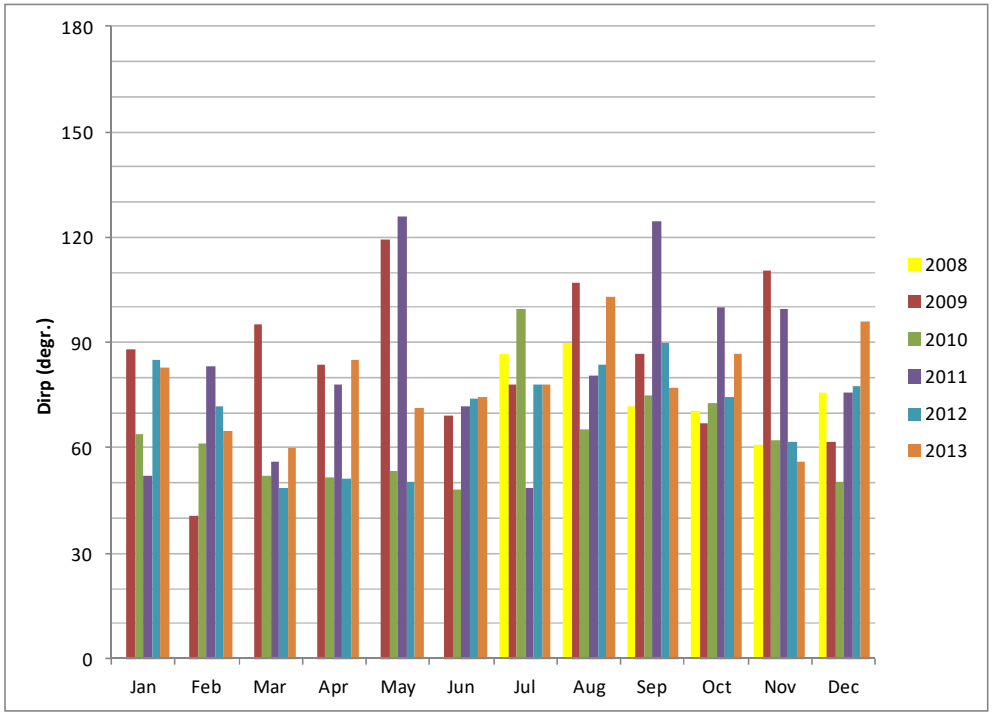

Figure 102 Histogram of average monthly wave direction, Dirp, 2008 to 2013 (CCO data for Hornsea buoy)

A histogram of average monthly significant wave height (HS) for the Hornsea buoy is given in Figure 101. This reveals a seasonal trend of decline in wave height from Jan/Dec to July/August followed by a slightly more rapid increase up to the following December. These trends are consistent across the 6 year period but typically with one anomalous outlier, for example March 2013. A histogram of average monthly wave direction (Dirp) for the Hornsea buoy is given in Figure 102. This shows that there is a subtle seasonal change in wave direction over the six year period from N50° in winter, spring and early summer to N75° in late summer, but with many anomalous results. However, these short-lived anomalies are lost in the annual data shown in the Rose diagrams in Appendix 2A.

12 Cliff Modelling

12.1.1 Slope stability analysis

Initially, two cliff sections were taken representing the steepest (66° overall) and the shallowest (45° overall) cliff profiles measured during the monitoring period; these are Section C and Section A, respectively, from the September 2005 laser scan. The same profiles were applied to both FLACslope and Galena analyses (Table 21). Water levels based on a synthesis of data obtained from the borehole sensors (Hobbs et al., 2015a) and from observations of the cliff were applied to each; 'high' being the worst case scenario and 'low' the best. In addition, a sequence of analyses for each year from 2001 to 2013 were taken on profiles from Section A. In some respects the FLACslope results were used to inform the assembly of the Galena models. The main influence was, however, from direct observation, TLS models and photos.

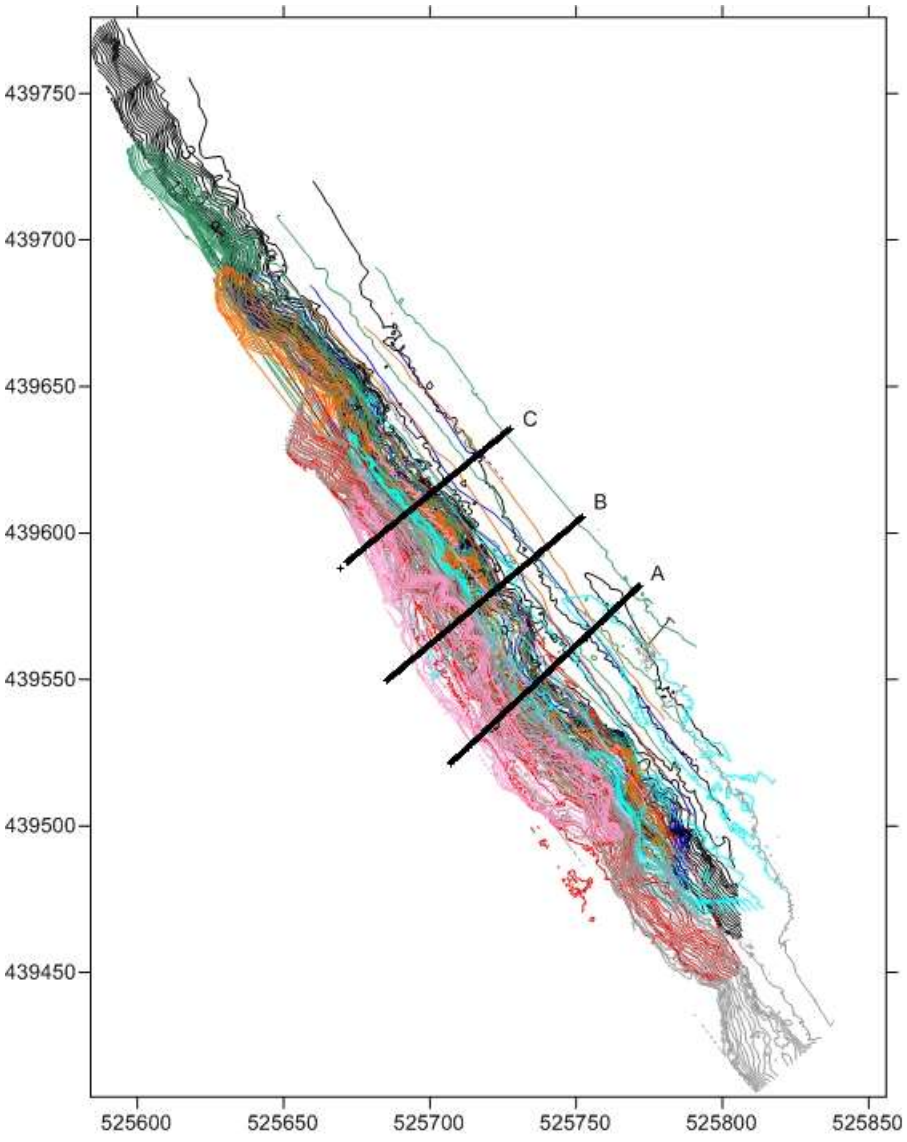

Figure 103 Contour map derived from TLS showing sections A, B and C

Geotechnical data for the slope stability analyses were obtained from laboratory tests as part of this project (Hobbs et al., 2013), and from the literature (Bell & Forster, 1991; Bell, 2002; Powell & Butcher, 2003; Reeves et al., 2006). The values used are shown in Table 22.

Table 21 Slope stability model characteristics

Model	Type	2D	Method	Inputs
FlacSlope v7.0	Finite Element	Yes	Fine mesh, Factor of Safety, F	Geological boundaries, phreatic surface, strength, density
Galena v6.10	Limit Equilibrium	Yes	Sarma non-circular non-vertical slices, Factor of Safety, F	Geological boundaries, phreatic surface, strength, density, slip surface

Table 22 Summary of geotechnical input data for slope stability models NOTE: Cliff top taken as 16.5 mAOD

Stratigraphy (in descending order)	Thickn. (m)	Base (mAOD)	γ_b (kN/m^3)	γ_d (kN/m^3)		c' (kPa)	ϕ' (degr.)	c'$_r$ (kPa)	ϕ'_r (degr.)
						Peak	Peak	Resid.	Resid.
Hornsea M. (Superficial)	3.1	13.4	18	16		10	25.0	5.0	20.0
Withernsea M.	3.9	*9.5*	21	18		28.3	25.8	0.0	24.2
Mill Hill M.	1.0	8.5	18	16		15.0	30.0	0.0	30.0
Skipsea Till M. (upper)	4.2	4.3	22	19		17.0	25.2	0.0	27.0
Laminated Clay	0.6	3.7	19	15		0.0	20.0	0.0	15.0
Skipsea Till M. (lower)	2.7	1.0	21	19		17.0	28.9	0.0	26.6
Dimlington B.	1.3	-0.3	19	15		16.0	25.6	0.0	15.1
Bridlington M.	>		23	19		0.0	31.6	0.0	28.0

12.1.1.1 FLACSLOPE

The FlacSlope (v. 7.0) program provides 2D 'finite element' numerical modelling of continuous media and is a module of the FLAC finite element suite produced by Itasca Corp. The mode of failure is shown as a diagram of displacement with vectors and strain contours. Whilst this does not represent an exact slip surface it does indicate the likely locations and shapes of potential slip surfaces, including multiple surfaces. *NOTE: FlacSlope is not capable of modelling 'flow' or 'rock fall' failure modes.*

The results (see Table 23) show two possible options for the first two analyses of the September 2005 steep section C profile, despite having identical input data. The reason for this is unclear and may represent a 'coming together' of the different failure modes for these particular inputs. The first (ALD1) is a single rotational failure in the upper third of the cliff; that is, within the Withernsea Till Member and superficial geology, giving a recession at the cliff top of about 2 m (Figure 105). This has a downward and outward deformation mode approaching that of toppling. The second (ALD2) is a much larger multiple rotational failure involving the entire cliff with an indicated cliff top recession of 6 to 10 m (Figure 106). This broadly features three concentric slip surfaces, the deepest of which has vectors varying from vertical downward to horizontal outward. Locally, the displacement vectors are horizontal at the Laminated Clay layer. Also, a small zone of major displacement at the cliff toe has an upward and outward direction. A zone of possible tensile stresses and toppling (?) is indicated near the base of the Withernsea Till Member. The third analysis (ALD3) uses the same input parameters as the first two, except for a water table that is lowered in the mid and upper cliff due to the likely drainage effect of the Mill Hill Member. The model shows a large single rotational slip surface (with a dog-leg in the lower third) giving about 8 m of cliff top recession. Locally, the displacement vectors become horizontal within the Laminated Clay and Laminated Silt layers.

All three models give factors of safety (F) in the region of 0.5. The model ALD2 could be construed as giving a close approximation to the multiple rotations observed throughout the monitoring period, but best

illustrated in November 2010 (see title page image). However, field observations indicate that these do not extend to below platform level as indicated by the ALD2 model.

Similar FlacSlope models for TLS at Mappleton and Hornsea during the period 2007 to 2008 were shown in Quinn *et al*. (2010) which accurately recreated 'undrained' failures producing deeper landslides and 'drained' failures producing shallow landslides.

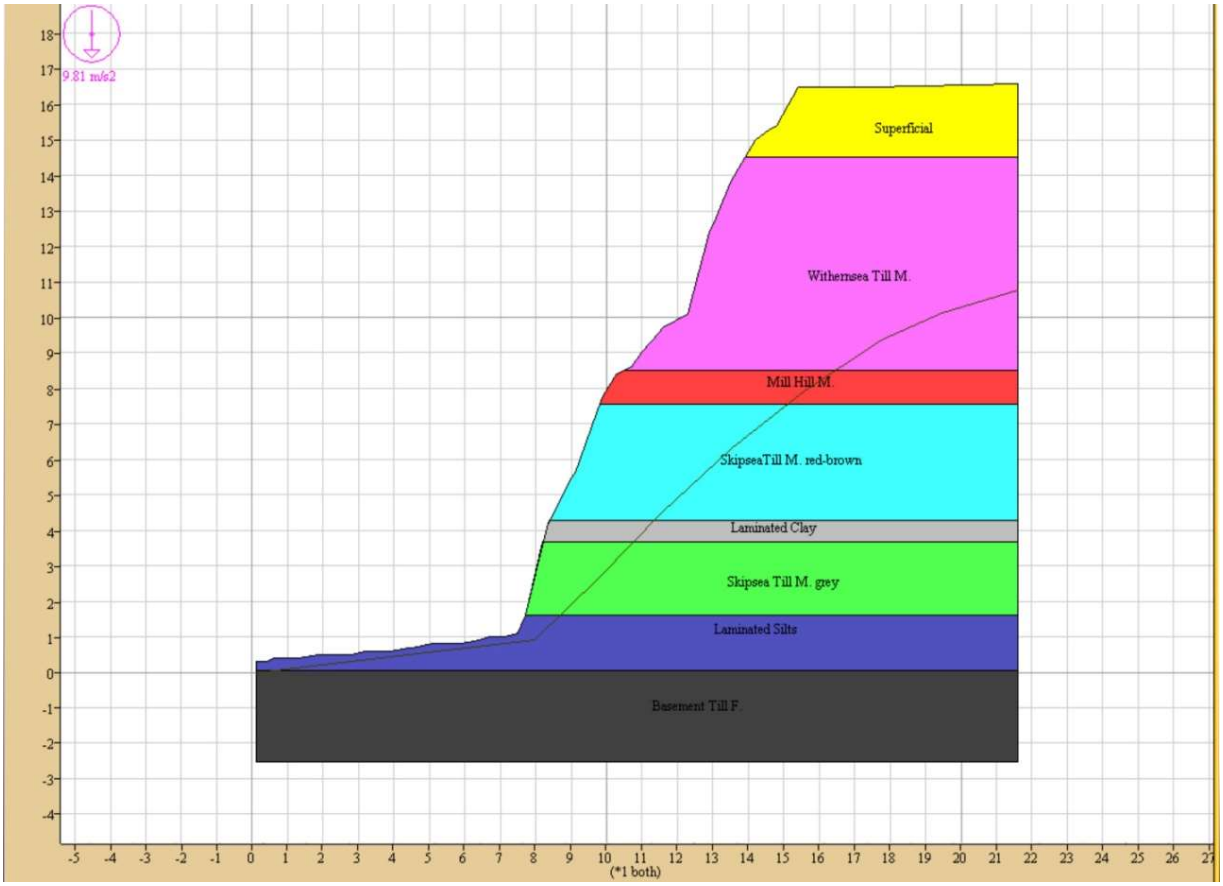

Figure 104 Profile used for models ALD1 and ALD2 (Section C)

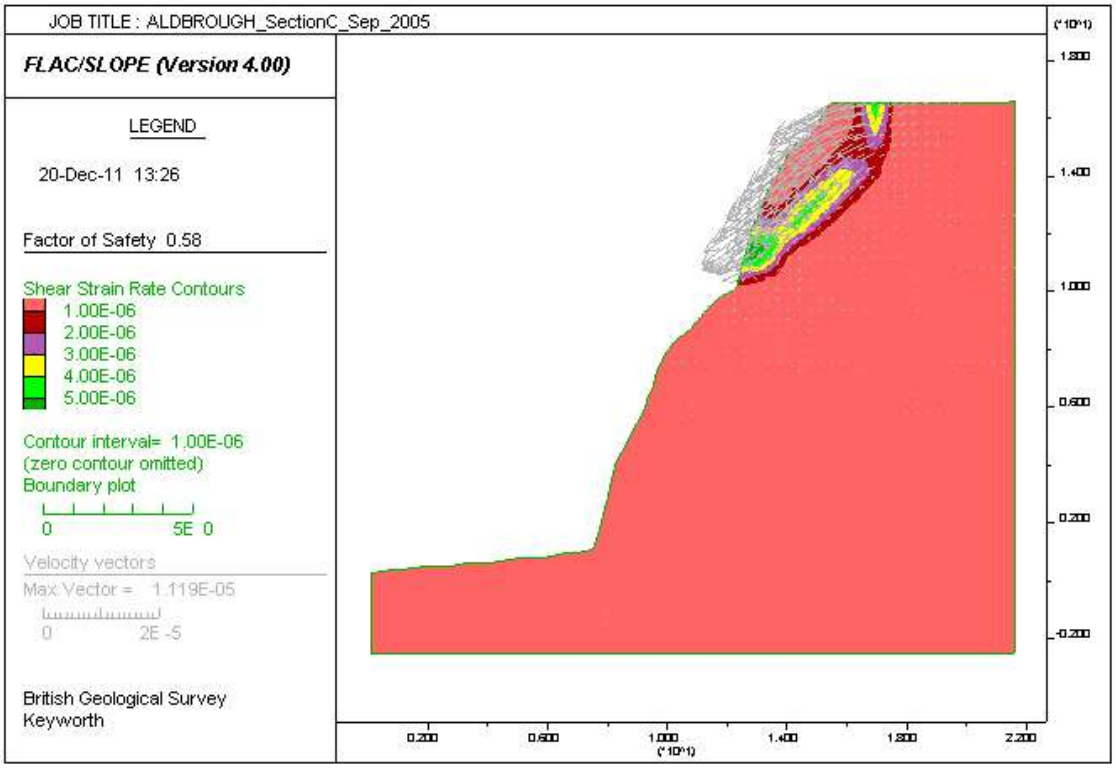

Figure 105 Results of FlacSlope model 'ALD1' for Section C

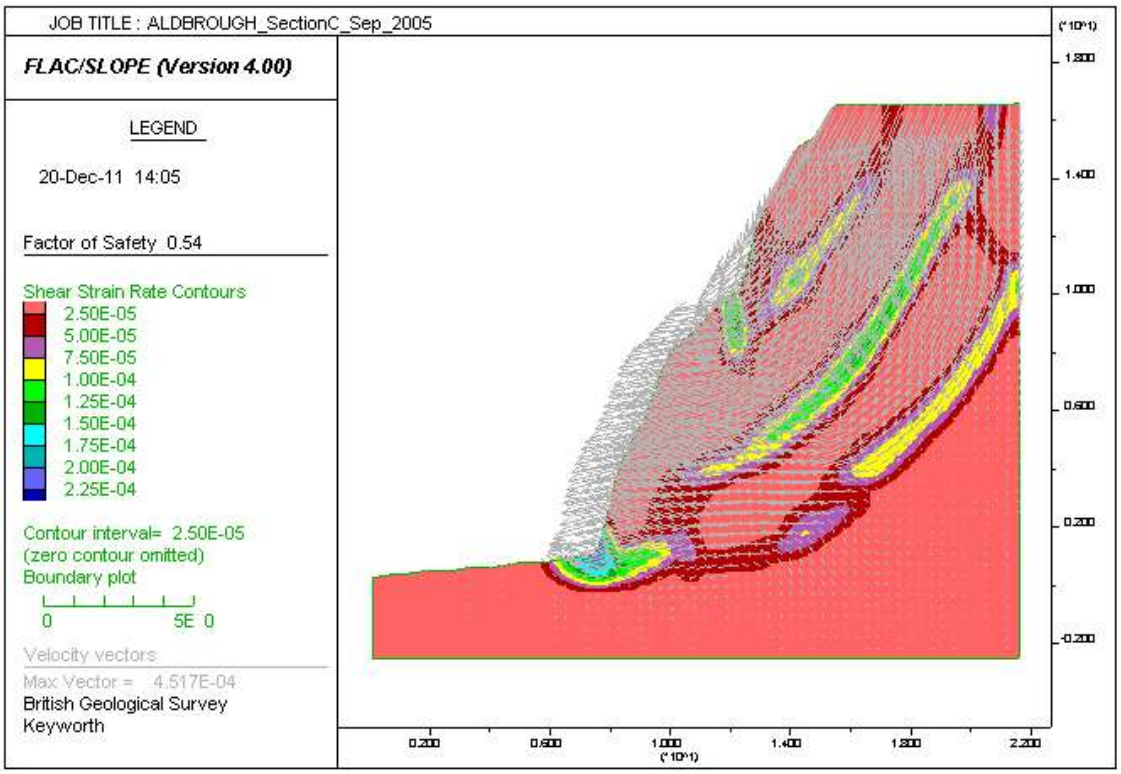

Figure 106 Results of FlacSlope model 'ALD2' for Section C

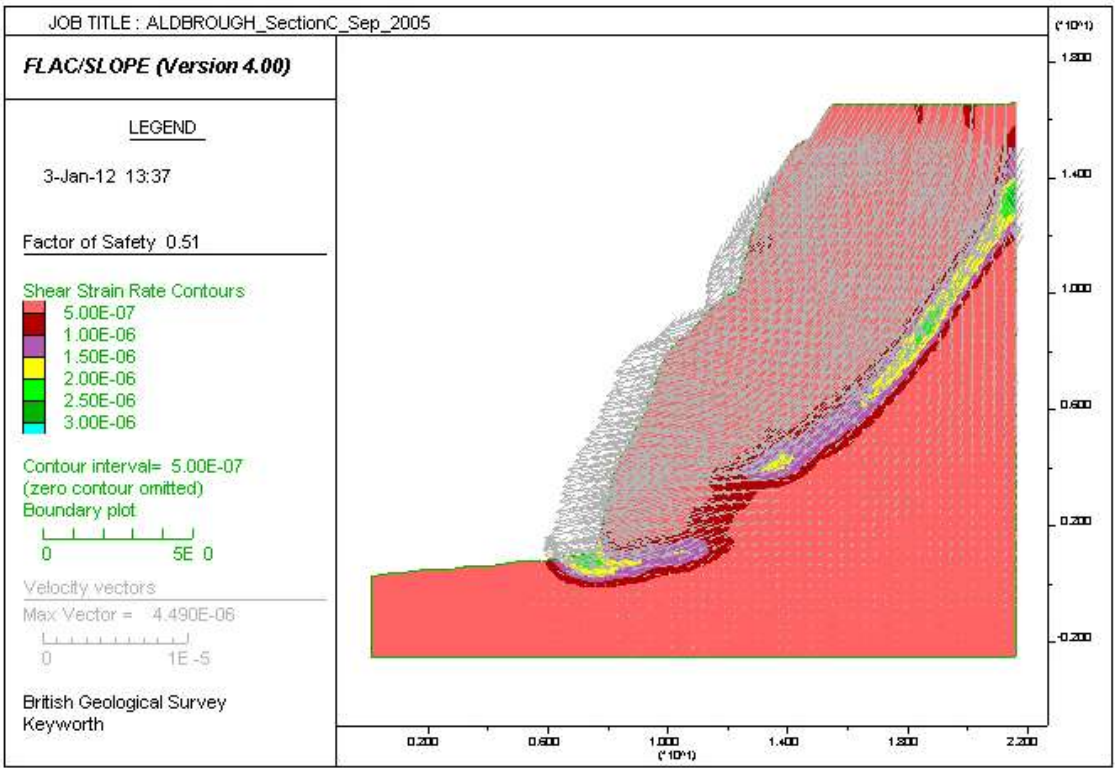

Figure 107 Results of FlacSlope model 'ALD3' for Section C

Table 23 Results of FlacSlope slope stability analyses

Model	Description	Profile	F	Mode of failure interpretation
ALD1	Medium W/T	Sep 2005, C (steep)	0.58	Sarma; Single rotation (upper third)
ALD2	Medium W/T	Sep 2005, C (steep)	0.54	Sarma; Multi rotation (whole cliff)
ALD3	Low W/T	Sep 2005, C (steep)	0.51	Sarma; Single rotation (whole cliff)

The factors of safety all indicate failure (F<1). However as the cliff was stable (F≥1), if only marginally at the time of the survey, it is clear that either the analyses or the input parameters are incorrect. The most likely explanation is that a steady state pore pressure regime has not been established and the effective strength within the till and clay-rich lithologies are enhanced due to suction. If correct, this would follow findings by Butcher (1991), based on stress tests, piezometer data and slope stability analyses, for the cliffs at Cowden 2 km north of Aldbrough and by Quinn et al. (2010) for Holderness generally. More recently, the same hypothesis was proposed for the London Clay Formation cliffs at Sheppey (Dixon and Bromhead, 2002) where it was shown that short-term transient pore pressure reductions, due to undrained unloading of the cliffs by erosion, resulted in enhanced effective strength to considerable depths below cliff top and slope. This process was then further enhanced by dilation of the shearing masses during the early stages of mass movement despite a reduction in strength, with increasing strain, to the residual value (Dixon and Bromhead, 2002). Back analysis from periods during the cycle of landslipping at Warden Point, Isle of Sheppey, and elsewhere (Dixon and Bromhead, 1991) demonstrated an agreement with laboratory ring shear tests, indicating that residual strengths had been mobilised throughout. *NOTE: It is not possible to test the suction hypothesis at Aldbrough at the time of writing (2013), as the cliff is currently too far from the borehole installations to have an unequivocal influence on the piezometers*

12.1.1.2 GALENA

The Galena (v. 6.10) program provides 2D 'limit equilibrium' numerical modelling of continuous media and is produced by Clover Technology. The mode and geometry of (non-circular) failure is pre-determined by the operator (unlike FLACslope). Multiple surfaces may also be investigated with three types of restraining boundary applicable. A Sarma 'non-vertical slices' method was used throughout with

two exceptions for which a Spencer-Wright analysis was used. Simple phreatic surfaces were used throughout rather than changeable piezometric surfaces. It should be noted that piezometric data from the Aldbrough boreholes, whilst informative, were not used directly in the analyses, except in a general sense.
NOTE: Galena is not capable of modelling flow or toppling failure modes.
NOTE: It is not possible to test the suction hypothesis at Aldbrough at the time of writing (2013), as the cliff is currently too far from the borehole installations to have an unequivocal influence on the piezometers.

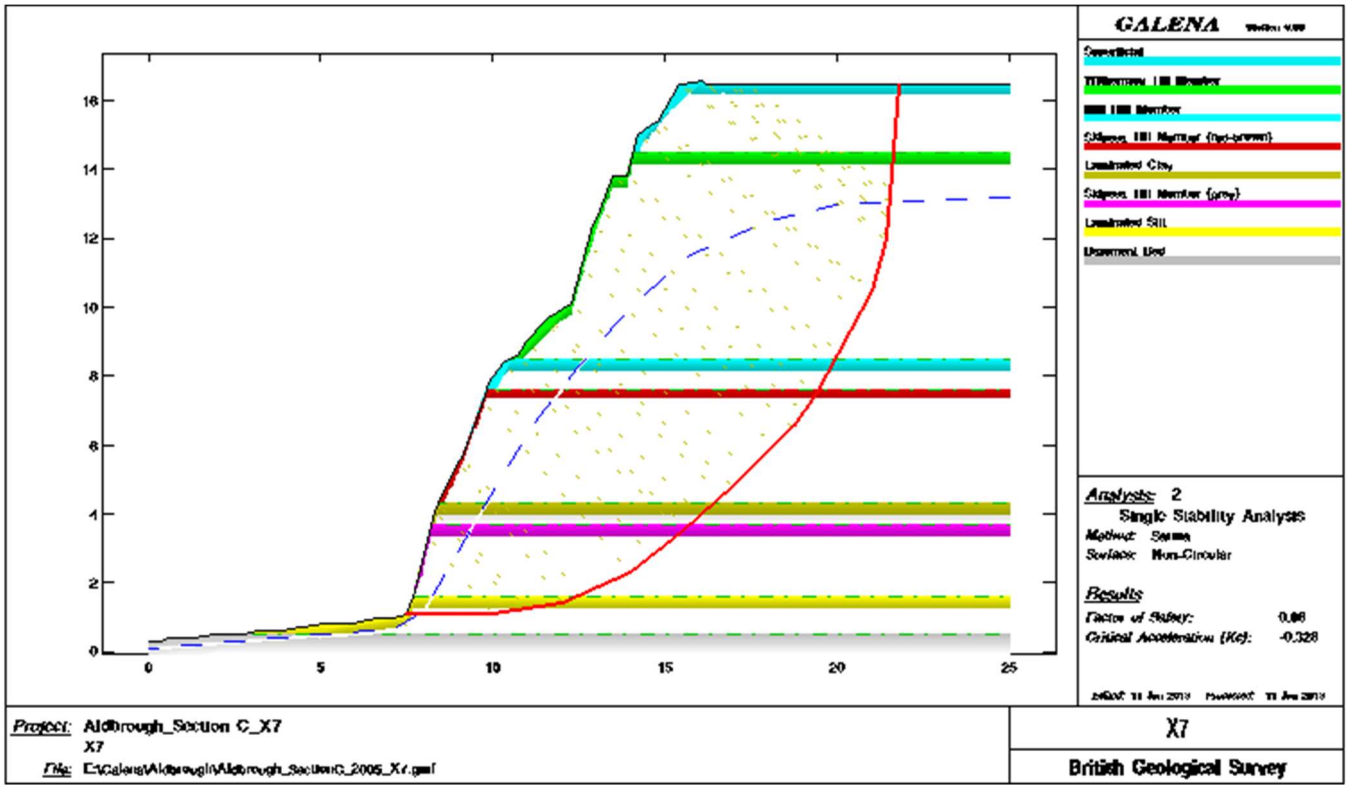

Figure 108 Galena slope stability analysis X7 (F = 0.86) for Section C. Dashed blue line is phreatic surface (assumed), solid red line is slip surface (estimated)

Table 24 Results of Galena slope stability analyses (2005, Sections A & C)

Model	Water table	Profile	Slope angle	FoS	Mode of failure interpretation
X1	High	Sep 2005, C	66°	0.78	Sarma; Single rotation, 13 m deep
X2	Medium	Sep 2005, C	66°	0.85	Sarma; Single rotation, 13 m deep
X3	Low	Sep 2005, C	66°	0.91	Sarma; Single rotation, 13 m deep
X4	High	Sep 2005, A	45°	0.94	Sarma; Single rotation, 13 m deep
X5	Medium	Sep 2005, A	45°	1.06	Sarma; Single rotation, 13 m deep
X6	Low	Sep 2005, A	45°	1.15	Sarma; Single rotation, 13 m deep
X7	High	Sep 2005, C	66°	0.86	Sarma; Single rotation, 16 m deep
X8	Medium	Sep 2005, C	66°	0.87	Sarma; Single rotation, 16 m deep
X9	Low	Sep 2005, C	66°	0.91	Sarma; Single rotation, 16 m deep
X10	High	Sep 2005, A	45°	0.91	Sarma; Single rotation, 15.5 m deep
X11	Medium	Sep 2005, A	45°	1.00	Sarma; Single rotation, 15.5 m deep
X12	Low	Sep 2005, A	45°	1.12	Sarma; Single rotation, 15.5 m deep

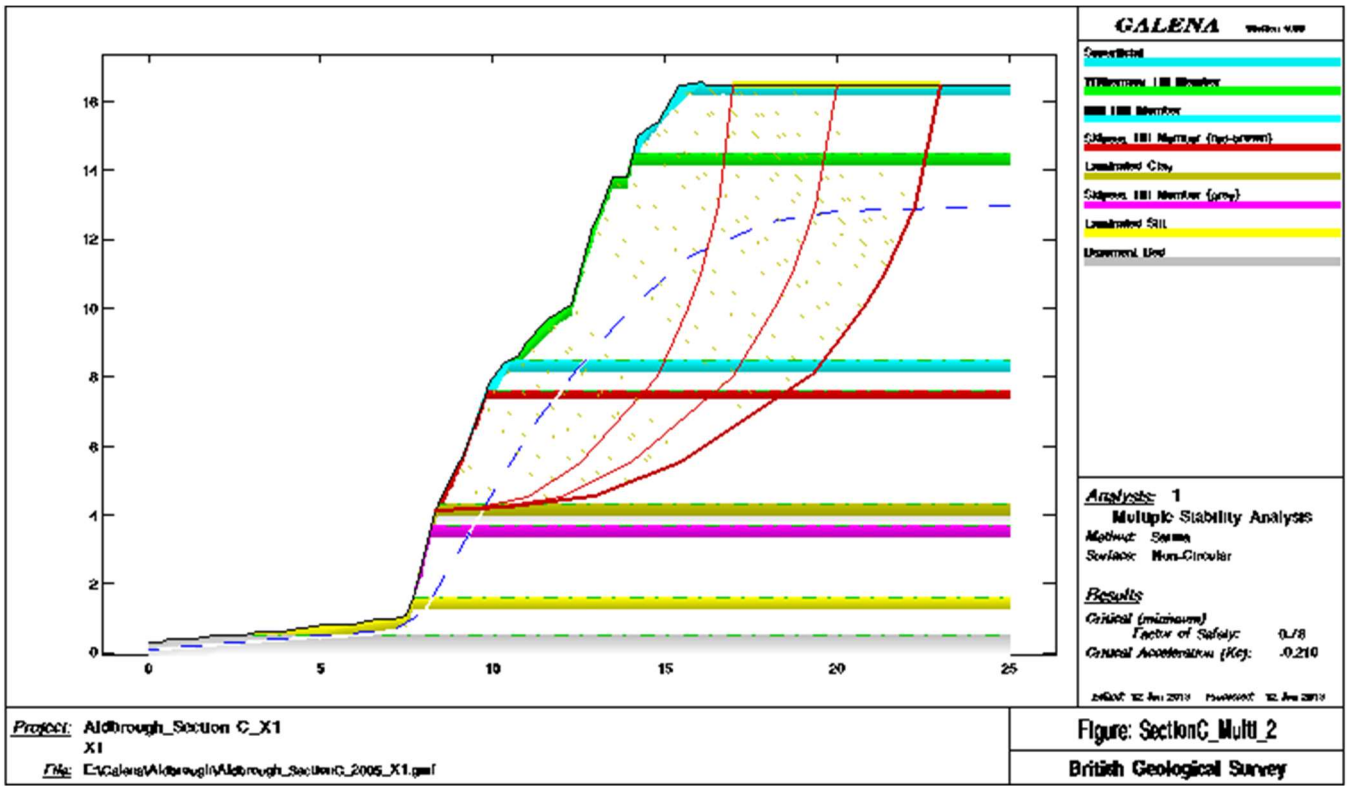

Figure 109 Multiple Sarma non-circular analyses based on Section C, model X1 showing three variations of slip surface giving (from right to left) F= 0.78, 0.78 and 0.81

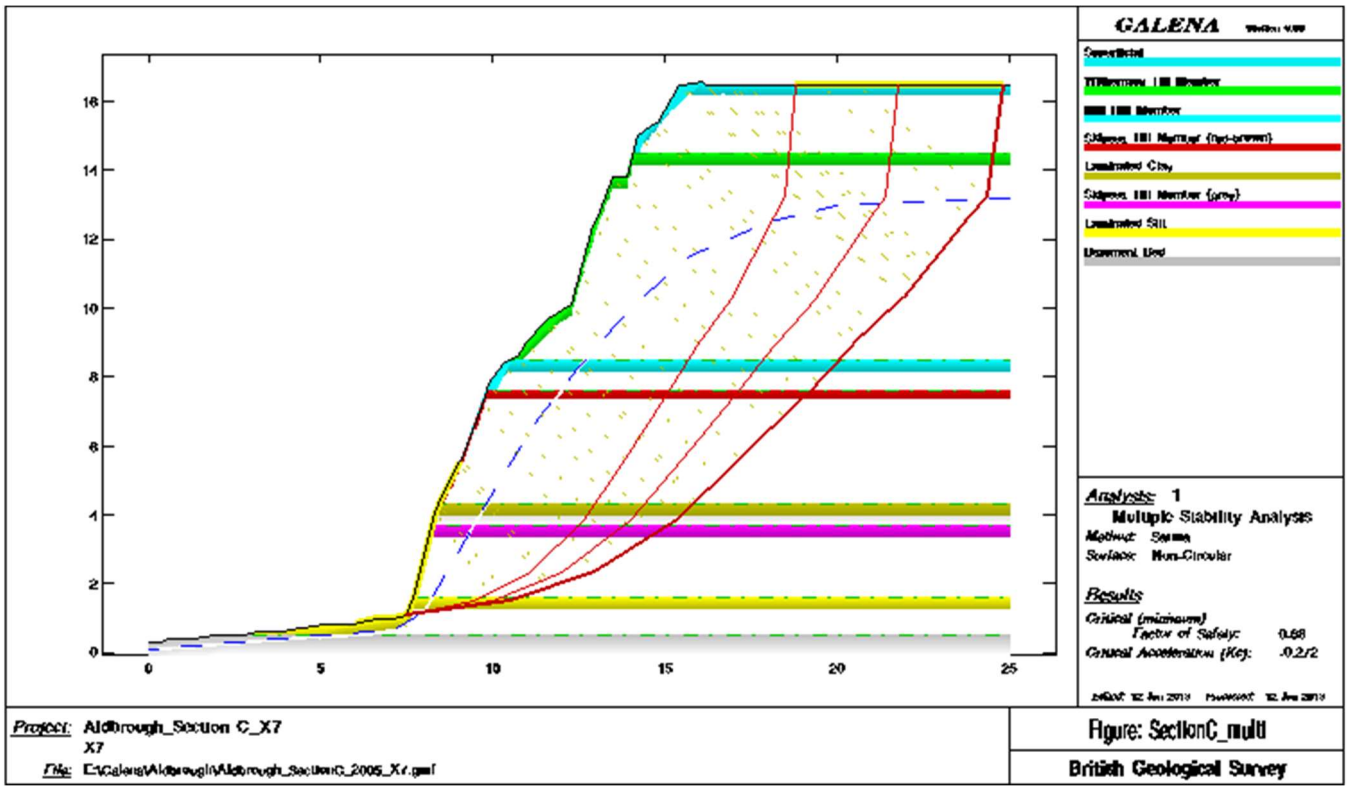

Figure 110 Multiple Sarma non-circular analyses based on Section C, model X7 showing three variations of slip surface giving (from right to left) F= 0.68, 0.69 and 0.85

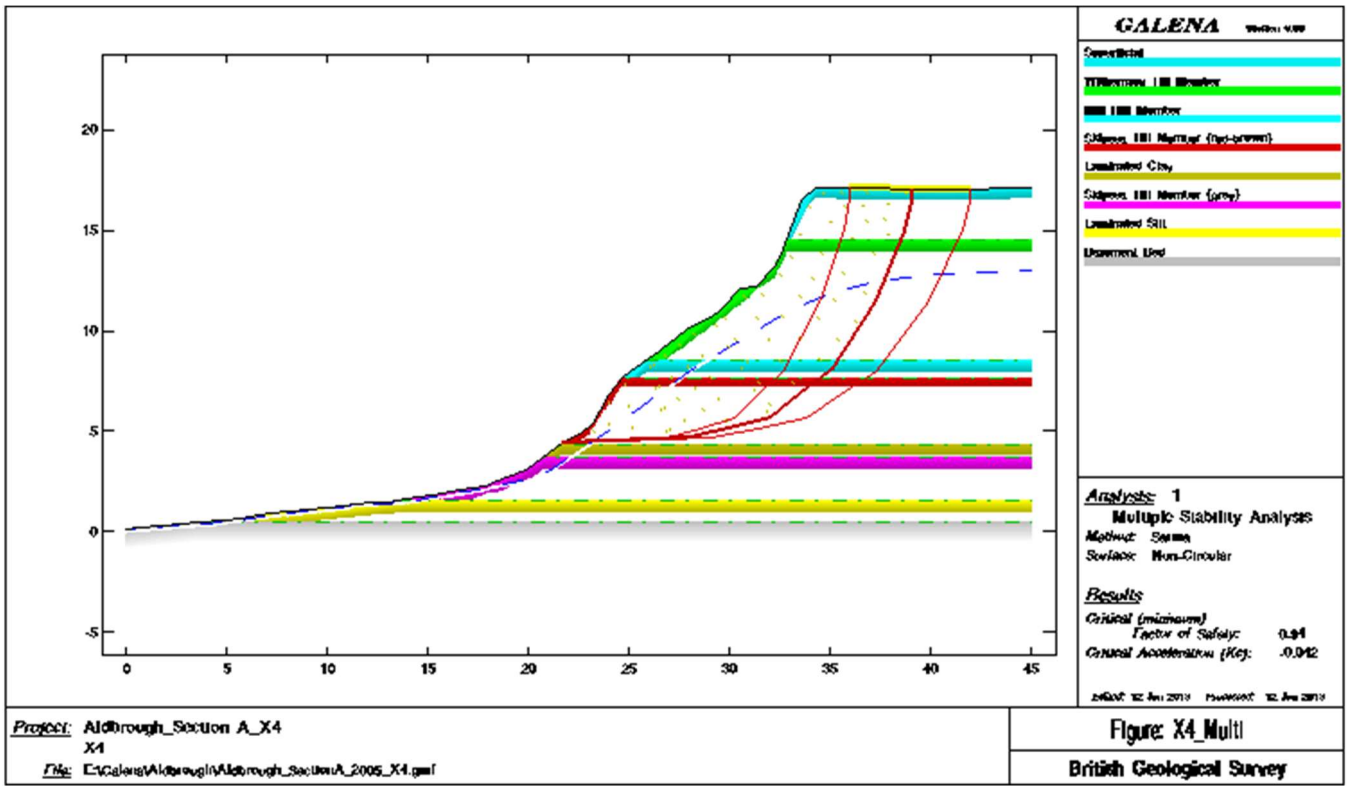

Figure 111 Multiple Sarma non-circular analyses based on model X4 (Section A) showing three variations of slip surface giving (from right to left) F= 0.96, 0.94 and 0.95

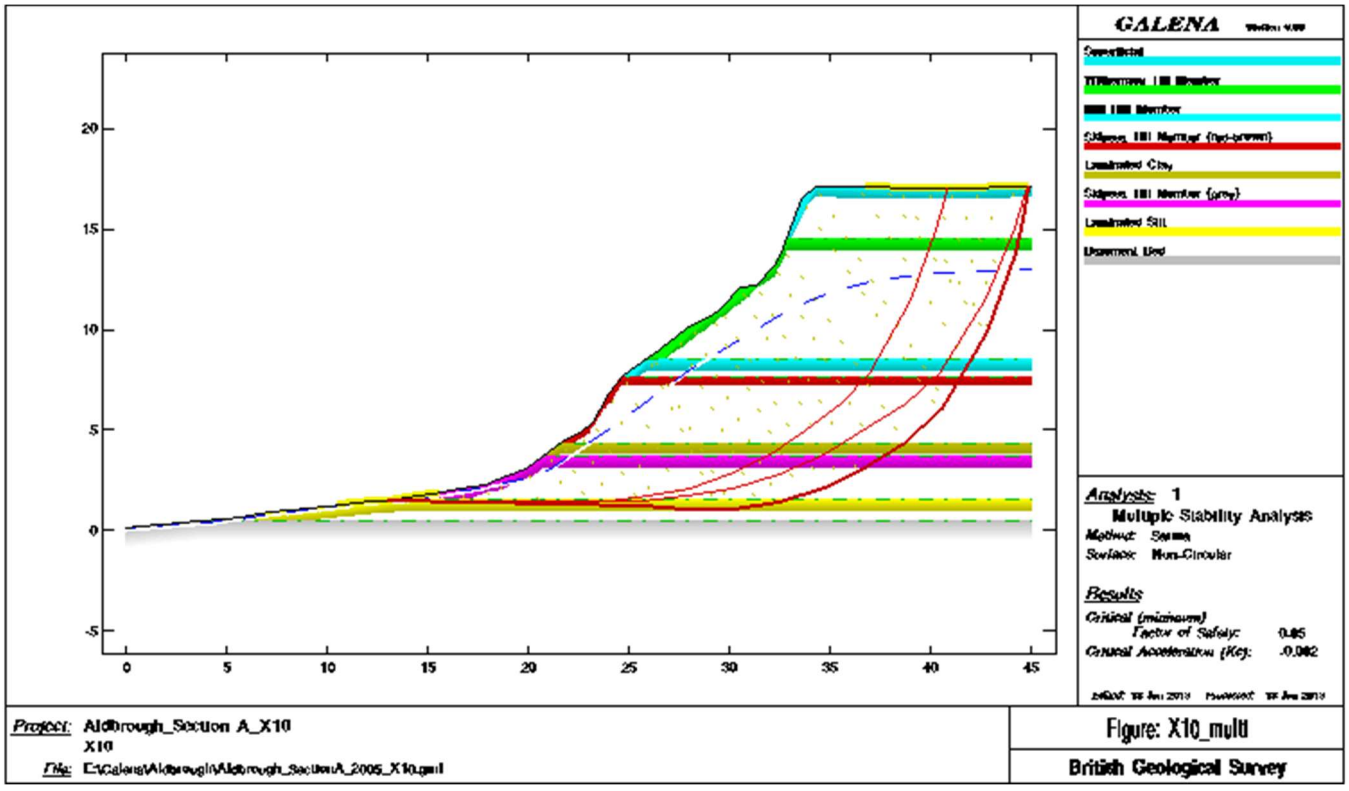

Figure 112 Multiple Sarma non-circular analyses based on model X10 (Section A) showing three variations of slip surface giving (from right to left) F= 0.85, 0.92 and 0.91

Examples of multiple analyses from a single year (2005) are shown in Figure 109, Figure 110, Figure 111 and Figure 112. Here three selected (possible) slip surfaces are shown within certain defined positional restraints, selected to reflect field observations, with the 'critical' surface, or one of several critical

surfaces, (minimum F) shown as a bold red line. The X1 results (Figure 109) show that factor of safety increases from a minimum of 0.78 to 0.81 as the backscarp is moved forward 6 m. In this case the options all have the same exit point at the toe of the cliff. The critical slip surface is that furthest removed from the cliff top (approx. 10 m). However, the difference in factor of safety compared with that 7 m from the cliff top is negligible. The X7 results (Figure 110) show the option with backscarp furthest from the cliff-top (9 m) has the lowest factor of safety (F=0.68) but the difference from that 7 m from the cliff-top is negligible. The X4 results (Figure 111) show the central of the options (5 m back from cliff top) has the lowest F value (0.94) though the variation is negligible. The X10 results (Figure 112) show that the most deep-seated option of the two with backscarp 11 m from the cliff-top has the lowest factor of safety (0.85). This is largely due to this option having a greater proportion of its slip plane lying within either the weak 'Laminated Silts' or the 'Laminated Clays'.

The shapes of the slip surfaces used were guided by field observations, TLS and FLACslope results, and also from other multiple Galena analyses. Surface profiles were taken from laser scans: Section C (2005) and Section A (2005) where the former represents a steep cliff slope (66^{o} overall) and the latter a shallow cliff slope (45^{o} overall).

Some of the models have factors of safety which indicate failure (F<1). However as the cliff was stable (F≥1), if only marginally, at the time of the survey, it is clear that either these analyses or the input parameters are incorrect. The most likely explanation is that of 'undrained unloading' where a steady state pore pressure regime has not been established and the effective stresses within the till and clay formations are enhanced due to suction (refer to discussion in section 11.1.1.1). In general the models respond as expected regarding failure modes and dimensions observed on site. *The piezometric regime on site is likely to be more complex than indicated by the assumed single phreatic surface (water table) used in the models.* Results from long-term monitoring of the piezometer arrays installed in two boreholes in 2012 (refer to section 10.2.1) will be analysed to allow more accurate representation of the situation in future analyses.

Slope stability analyses for a test site at Cowden, 2 km to the north of Aldbrough, were described in Butcher (1986) and Butcher (1991). It is interesting to note that he invoked negative pore pressures (down to -20 kPa) close to the cliff in his compound type landslide model in order to obtain factors of safety commensurate with field observations of a deep-seated (compound) landslide. Modelled slip surfaces bottomed at around 4 m below the cliff toe. The inclusion of a "soft" basal clay layer was an important factor in the analyses.

Models based on a single profile for each year between 2001 and 2013 (except for 2008) were produced. The results are summarised in Table 25 and Figure 113. The analyses are duplicated for 'peak' and 'residual' strength parameters; the former derived from triaxial tests and the latter from ring shear tests (Hobbs et al., 2015b). The results show the effect of reducing the strength values from 'peak' to 'residual'; that is, the factor of safety reduces from above 1.0 (stable condition) to below 1.0 (unstable condition) with only two exceptions (2006 & 2007). In reality the stability probably lies between these values and, of course, fluctuates from stability to instability both with time and location.

Table 25 Results of Galena slope stability analyses (2001 to 2013, Section A)

	Factor of Safety	
Year	Peak	Residual
2001	1.28	0.74
2002	1.54	0.93
2003	1.26	0.77
2004	1.35	1.00
2005	1.14	0.66
2006	1.42	1.07
2007	1.58	1.02
2009	1.24	0.92
2010	1.14	0.86
2011	1.23	0.85
2012	1.29	0.89
2013	1.25	0.89

NOTE: No TLS data available for 2008

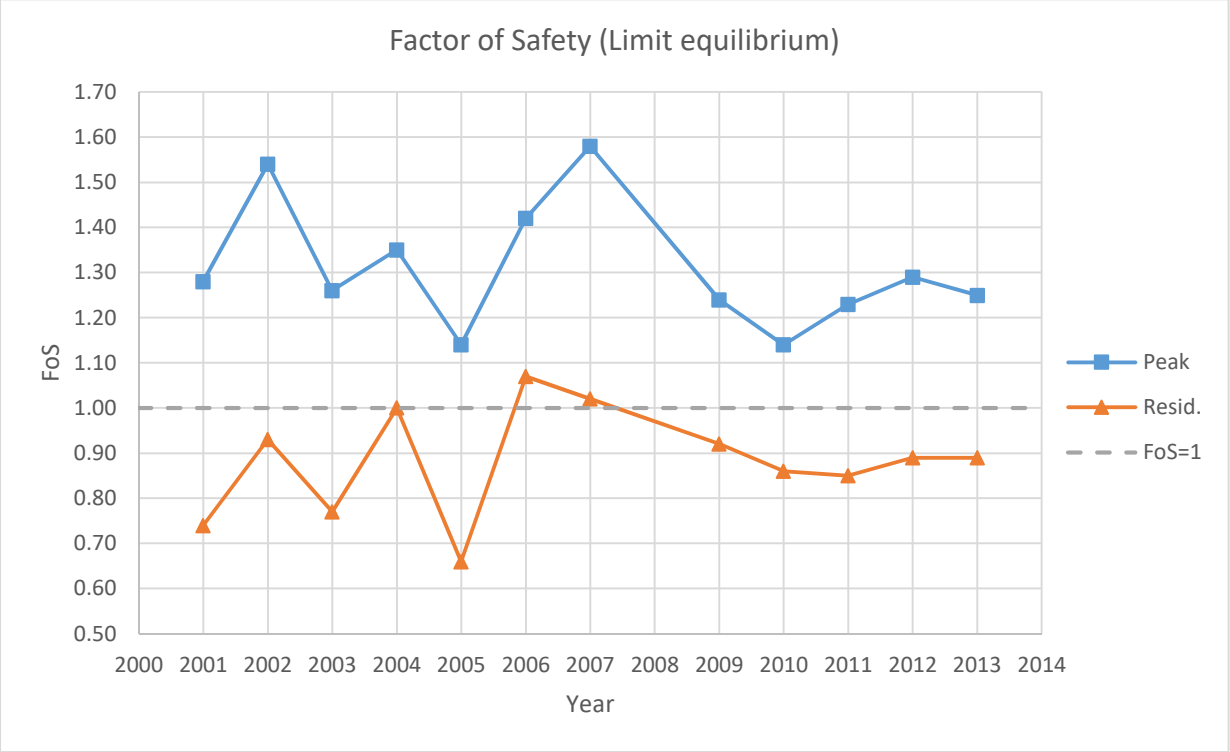

Figure 113 Plot of Factor of Safety over the monitoring period 2001 to 2013 for Section A using 'peak' and 'residual' effective strength data (Hobbs et al., 2015b)

12.2 THE 'SCAPE' MODEL

"*The complexity of cliff, beach and hydraulic processes that interact over variable timescales in producing recession have so far forestalled the development of numerical, process-based models on eroding consolidated coasts*" (Bray and Hooke, 1997). The Soft Cliff and Platform Erosion (SCAPE) model developed in Walkden *et al*. (2002) and Walkden and Hall (2005) is a 2D geomorphic numeric model which caters for episodic, simplified mass movement driven by cliff base erosion, applied to a 'soft rock' shore overlain by a sparse beach (based on the Naze peninsula, Essex). The model system provides predictions of cliff-toe position and represents wave transformation, sediment transport and the development of cliff, talus, shore platform and beach (Dickson *et al*., 2006b). The model is iterative with the starting point of a vertical cliff with no beach. It is capable of being transferred to other locations with the possible exception of the landsliding component. It is ideally suited to the study of the effects of climate change (Section 13). In the model the shore platform is assumed to be the central regulator of coastal retreat (Brooks and Spencer, 2012). Predictions of cliff-toe recession have been added to a simple probabilistic model of landsliding to generate predictions of cliff top recession. The model may be developed into a quasi-3D version using multiple 2D sections. The model has been broadly validated against historical erosion rates derived from maps (Dickson *et al*., 2006b).

The model does not take account of discrete mass movement events and sub-aerial erosion processes (Lee and Clark, 2002; Dickson *et al*., 2006b). In this sense it must be considered a long-term model operating on a much longer time scale than the cycles of landslide development considered in this study. However, the long-term development of a 'soft cliff' coast is ultimately dependent on the sea level and the sea's ability to remove landslide and erosion debris from the foreshore. Storminess must also be a factor. Also, in areas of offshore sediment transport sandbanks affect the wave regime and hence the erosion at the shore (Dickson *et al*., 2006b). A 'rock strength' (constant) factor in the model is calculated using a factor, R, based on a comparison of calculated to observed erosion at specific locations. In their application of the SCAPE model to 50 km of North and North-East Norfolk coastline Dickson *et al*.'s (2006b) best correlation with historic recession rates was achieved for the cliffed sections. Regional rates of erosion were notably well correlated though not necessarily at identical locations on the coast.

13 Climate change, sediment transport and anthropogenic effects

13.1 CLIMATE CHANGE

Currently it is estimated that 3,000 km of UK coastline are subject to erosion (EUROSION, 2004). This problem is likely to be compounded by climate change (Dickson *et al*., 2006b). It is generally expected that future climate change will increase rates of soft-cliff erosion through accelerated rates of sea level rise and changes in wave climate (Walkden *et al*., 2005; Bray and Hooke, 1997). Climate change has recently become intimately linked with change modelling and prediction of geomorphological processes, such that any behaviour-based system must include it and that any such system has a variety of outcomes. It is generally accepted that sea level rise in particular is likely to have a significant impact on 'soft' rock cliffs due to its influence on platform level and cliff-toe erosion (Lee, 2008; Lee, 2011; Walkden *et al*., 2005; Dickson *et al*., 2006a; Dickson *et al*., 2006b; Walkden and Dickson, 2008; Brooks and Spencer, 2012; Quinn *et al*., 2010). It is estimated that the cost of coastal erosion will rise by almost an order of magnitude by the end of this century (Dickson *et al*., 2006b).

The limitations of process-based quantitative geomorphological coastal models, as exemplified by the SCAPE model (section 12.2) of Walkden and Hall (2005), have been outlined by Hanson *et al*. (2010). Alternative methods, such as used for 'FutureCoast' have employed qualitative 'expert' systems which seek to identify trends, rather than to forecast. Methods such as that proposed by Hanson *et al*. (2010) and

Brunsden & Lee (2004) formalise the process of qualitative reasoning, use a wide range of input data and examine the probabilities of a variety of outcomes. This approach, the 'Coastal Simulator', is claimed to be more user-friendly for non-experts and has had climate change scenarios applied to it, including sea-level rise.

Sea-level rise has been predicted to be similar to the global mean value (Hulme and Jenkins, 1998); that is about 300 mm over the next 50 years ('medium' prediction). However, this would be increased to around 390 mm due to ongoing land subsidence. The SCAPE model (Walkden *et al*., 2002 and Walkden and Hall, 2005) showed a positive linear correlation between rates of sea-level rise and average recession rate; approximately 25 mm increase in annual cliff-toe recession rate per 1 mm of sea level rise. Walkden *et al*. (2005) showed that according to the SCAPE model accelerated sea-level rise on the North and North-East Norfolk coastline exerts a more significant impact on erosion rates than changes in offshore wave conditions (Dickson *et al*., 2006b).

However, a key implication from the modified Bruun rule for erosion of sandy coasts (Bray and Hooke, 1997; Bruun, 1962) is that cliffs that release sediment for beach creation will be less sensitive to sea-level rise than other cliff types (Dickson *et al*., 2006b). Nevertheless, there is a popular opinion that the Bruun rule, in original and modified form, are only applicable to specific types of coast and that coastal erosion of 'soft' cliffs is a complex morphodynamic issue (Bray and Hooke, 1997; Stive, 2004). Lee (2011) suggested that historical recession rate extrapolation from the 1951 - 1990 data was a better indicator for 1990 – 2004 than the 'Bruun Rule' which exceeded observed values at Erosion Post 58 (Aldbrough North) by a factor of 1.2 and the 'Historical Projection' of Leatherman (1990) which exceeded it by 4.3. In other words the rate had remained the same (2.16 m/yr) for the two periods according to the East Riding erosion-post data. The value of average erosion rate for 'Aldbrough North' (P062, ERYC post No. 58) has been quoted at 2.23 m/yr (East Riding Yorkshire, 2009).

Sea-level rise, or more strictly relative sea level rise (RSLR), and increased storminess would increase erosion at the toe of the cliff and increase the rate of removal of landslide debris, and hence increase the overall recession rate. Increased desiccation in the summer, if part of the climate change scenario, could also increase the weathering process and the access of rain and seawater to material on the cliff (Quinn *et al*., 2010). It is likely that different coastal regimes from that at Aldbrough, for example low till cliffs where direct wave erosion was dominant over landsliding, would not respond to climate change in the same way.

13.2 COASTAL EROSION AND SEDIMENT TRANSPORT

Historical recession rates for the mobile home park location at Aldbrough are reported as being 1.16 m for the period 1852 to 1951 (*historical maps*, Valentin, 1971) and 2.16 m for the period 1951 to 2004 (*measured*, East Riding Yorkshire Council, 2013). Data from cliff profiles (Figure 114) carried out by East Riding of Yorkshire Council (ERYC) since Autumn 2003 (East Riding Yorkshire Council, 2013), using a combination of 'post' surveys and TLS profiles, in terms of linear cliff-top recession are shown in Figure 115 plotted with the equivalent BGS (TLS) dataset in terms of volumetric recession. The plot shows agreement in broad terms with peaks in 2005-06, 2009 and 2012-13, though the last is subdued in the BGS data. There is some displacement in time between the BGS and ERYC data, but also between the two ERYC profiles (e.g. 2005-06). It is noted that the two ERYC profiles align with the boundaries of BGS's test site.

Historical rates of recession derived from maps are subject to a variety of influences, in particular beach mining during the latter part of the nineteenth century (Brown, 2008).

Figure 114 Map showing locations of East Riding of Yorkshire Council cliff profiles 62 and 63 (East Riding Yorkshire Council, 2013)

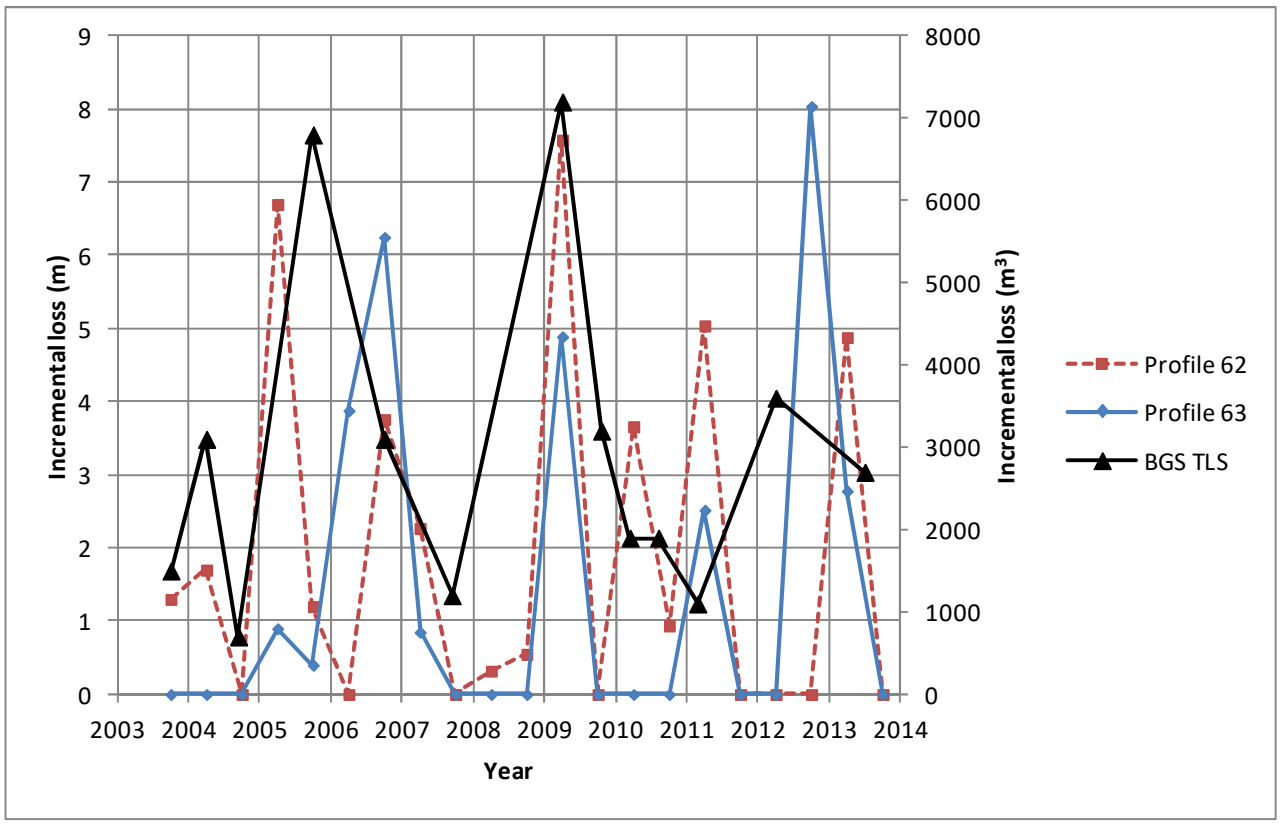

Figure 115 Plot of cliff-top recession (ERYC) vs. time and cliff volume loss (BGS) for period 2003 to 2013 (East Riding Yorkshire Council, 2013) (Refer to Figure 114)

The Land-Ocean Interaction Study (LOIS) established a six-year research project in the early 1990's. As part of this project a study entitled "The Holderness Coastal Experiment, '93-'96" was carried out by the Proudman Oceanographic Laboratory and others (Prandle *et al.*, 1996). The overall objective was to establish rates of material exchange between land and ocean, specifically the transport rate from a rapidly eroding coastline, as exemplified by Holderness which was described as the "*largest UK coastal sediment*

source ... with strong tidal currents, occasional storm surges and broad exposure to wind waves" (Prandle *et al*., 1996). Six experimental installations mounted on the sea floor in two lines of three (adjacent to Aldbrough) measured current profiles, suspended sediment concentrations and pressure (wave height). An additional offshore platform measured 'open-sea' conditions. Other measurements included wave direction, wave type and wave/current interaction.

The removal of landslipped material at Aldbrough, and elsewhere on the Holderness coast, is rapid. An estimated 33% of this material remains on the beach (Brown, 2008). Cambers (1973) gave one to four months as the time interval within which any failed (*landslipped?*) mass was removed. This seems unlikely, however, given that significant proportions of slipped masses and debris from deep-seated rotational landslides have been observed to remain on the cliff slope for over a year. However, if this refers to slipped masses on the foreshore, rather than on the cliff slope, then it would seem a reasonable estimate in most cases, though periods of over a year for landslide debris removal from the foreshore were found on the North Norfolk coast (Hobbs et al. 2008). Quinn *et al* (2010) proposed two mass movement models for Holderness whereby one had the rapid removal of landslide debris resulting in negative pore pressures and shallow drained failures and the other where slow erosion allowed pore pressure equalisation and deep drained or partially drained failures, plus shallow failures in the upper cliff above the main slipped mass.

Assessment of the Holderness coastline as a whole has been made by Pethick (1996) with particular reference to periodicity at different time scales. He stated that the Holderness coastline had maintained its orientation over at least 150 years, and that this was due to maximisation of sediment transport rates resulting from the optimum angle of the coast to principal wave energy incidence angle. He also stated that average recession rates had remained constant during this period. Interestingly, Pethick (1996) also stated that the 'medium term' shoreline was oriented at an average of 152°N and inclined at 24° to the retreat vector. This led to the conclusion that landslide embayments are in effect 'migrating' southward. This also led to the conclusion that measurement of cliff recession by post surveys set 'shore normal' (at right angles to the cliff line), for example the East Riding Council survey (East Riding Yorkshire Council, 2013), must therefore be compromised. This scenario is illustrated in Figure 116 where 'recession' is represented by the shore-normal direction and 'migration' by the shore-parallel direction; the angle between the resultant and the cliffline (152°) being 24°. This means that on a recession measurement profile set up perpendicular to the cliff line, as for East Riding Council, a six-yearly hiatus occurs coinciding, according to Pethick's hypothesis, with the interception of the profile line with either end of an embayment (i.e. promontories) assuming an average embayment width of 26m.

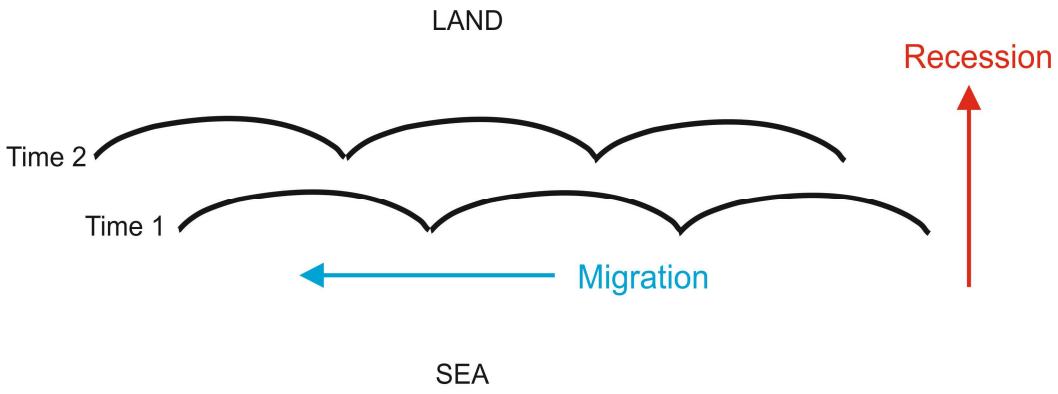

Figure 116 Schematic plan view illustrating hypothesis of migration of cliff embayments (*after* Pethick, 1996)

The loci of promontory positions at the Aldbrough test site and the cliff-top lines at the start and end of monitoring, derived from TLS and dGPS surveys, are shown in Figure 117. It is clear from this map that the promontories have receded from east to west and the embayments have maintained their westerly heading. This makes the measured embayment recession heading approximately 60 degrees (24 + 36) clockwise from that of Pethick (1996).

As part of his overall recession system for Holderness Pethick (1996) also hypothesises that embayments "do not represent individual failure events but rather are composite features in which a temporal sequence of small failures occur". The evidence from our Slope Dynamics study at Aldbrough here reported does not fit with this hypothesis. It is clear that embayments, at least in the case of the Aldbrough test site over the monitoring period, are initiated by large-scale, deep-seated landslides initially occupying the entire embayment or a significant proportion of it in the case of an elongated embayment. Subsequently, the slipped masses fragment and degrade eventually vacating the embayment, thus leaving the possible impression, as stated by Pethick (1996), that "failures are significantly smaller than the embayment and . . tend to take place in the southern extremity of the embayment".

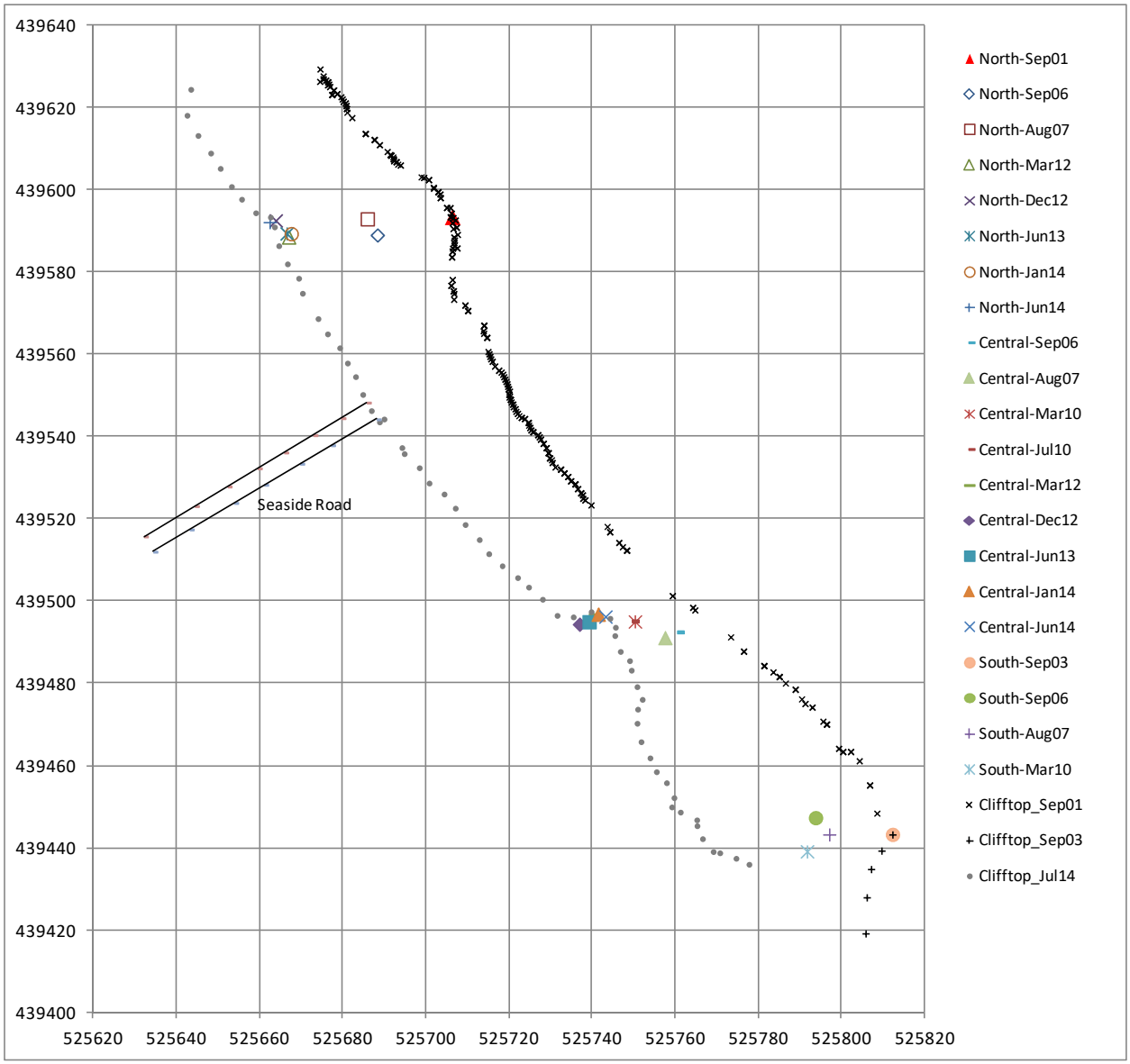

Figure 117 Map showing loci of scan positions on promontories (north, central & south) and selected cliff-top dGPS surveys

13.3 GIS-BASED STABILITY MODELS

A truly universal, generic, process-based coastal model remains elusive despite the inclusion of expert systems approaches (Hanson *et al*., 2010). The extrapolation of site specific cliff recession data to larger coastal environments has been the goal of many investigators. In some ways the Holderness coast represents the best chance in Britain of achieving this, given its relatively uniform topography and geology (Prandle *et al*., 1996). However, certain factors conspire to prevent this desirable outcome. These include a lack of oceanographic data for the North Sea and meteorological data for Holderness, non-steady state

hydrological conditions and the inapplicability of GIS-based stability methods, particularly at the coast. The following section discusses such methods and their likely applicability (or lack of it) to the Holderness coast.

13.3.1 GeoSure

GeoSure has been developed by the BGS to map six geohazard susceptibility themes, including landslides, on a comprehensive national (GB) scale using a deterministic 'approach' that has been 'biased' by expert judgement (the heuristic element). The outcome utilised both available expertise and data for the analyses. Essentially, the methodology is based upon a series of facts which are broadly known and understood, but that the complexity of the problem required the use of intuition (experience, understanding) and experiment to derive an answer (Forster *et al*., 2004; Foster and Diaz-Doce, 2010). To this was added factual data from datasets held by BGS about the geological formations concerned.

The deterministic approach identifies the presence of factors that bring about a hazard at the site being assessed. The causative factors are given a rating according to their relative importance in causing the hazard, and then combined in an algorithm to give a rating of the relative susceptibility of the area being assessed to the hazard occurring at some time. It does not necessarily mean that the hazard has happened in the past or will do so in the future, but if conditions change and a factor intensifies, the hazard may be triggered.
Assessment of hazard is made by:
1. Identifying the factors that are involved in creating the hazard
2. Assessing which are present
3. Assessing how significant they are (usually by numerical ranking)
4. Combining to measure the level of hazard.
5. Reviewing results, adapting algorithm or levels of significance accordingly

Three factors were chosen for inclusion in the Geosure assessment:
• Lithology (strength, permeability and susceptibility to landsliding) LEX-RCS field in DiGMapBG-50
• Discontinuities (BS5930, 2015)
• Slope angle (NEXTMap)

The scoring system has been subjected to a series of trials designed to test the outcome of the slope instability algorithm against actual landslide susceptibility in areas studied by BGS. There is no complete listing of range of information sources used to allocate the scores. Given the 10000+ lexicon codes that have been codified, this is not unexpected. For most lithologies, the rationale behind the given score is apparent after a brief examination (Foster and Diaz Doce, 2010).

The 'slope angle' factor is derived from the NEXTMap terrain model and is classified as: 0-20º, 21-30º, 31-45º and 46-90º as per Hoek (2000). The output is a total GB coverage map showing landslide susceptibility classes A to E where E is the most severe and A the least. The model is readily updated and is currently in its sixth version. Anomalies have been identified, for example where known areas of landsliding have been allocated A or B classes by GeoSure, and corrected. GeoSure has been shown to fail when applied to coastal cliffs (Wildman and Hobbs, 2005). This issue is currently under review as part of the development of a Cliff Instability Susceptibility Tool (CIST) jointly by BGS and the Channel Coastal Observatory (CCO). More recently, this has led to development of the BGS's Coastal Vulnerability Index (CVI).

13.3.2 Stability index mapping

Stability Index Mapping (SINMAP) is a physical, steady state (infinite), GIS-based slope stability model in which relative hazard predictions are primarily governed by local slope gradient, strength parameters

and relative wetness (W) (Pack, 1995; Zaitchik and van Es, 2003; Jeong *et al*., 2007). SINMAP (Stability Index MAPping) is an ArcView extension that implements the computation and mapping of a slope stability index based upon geographic information, primarily digital elevation data. SINMAP has its theoretical basis in the infinite plane slope stability model with wetness (pore pressures) obtained from a topographically based steady state model of hydrology. Digital elevation model (DEM) methods are used to obtain the necessary input information (slope and specific catchment area). Parameters are allowed to be uncertain following uniform distributions between specified limits. These may be adjusted (and calibrated) for geographic "calibration regions" based upon soil, vegetation or geological data. The methodology includes an interactive visual calibration that adjusts parameters while referring to observed landslides. The calibration involves adjustment of parameters so that the stability map "captures" a high proportion of observed landslides in regions with low stability index, while minimizing the extent of low stability regions and consequent alienation of terrain to regions where landslides have not been observed. This calibration is done while simultaneously referring to the stability index map, a specific catchment area and slope plot (of landslide and non-landslide points) where lines distinguish the zones categorized into the different stability classes and a table giving summary statistics (http://hydrology.usu.edu/sinmap/).

The applicability of SINMAP, and similar GIS-based methods, including the BGS's GeoSure, to the Holderness coast is debatable. Firstly, these methods use an 'infinite slope' stability model that does not relate to the observed mode of instability (i.e. rotation, toppling and flow) at Aldbrough and elsewhere on the Holderness coast. Secondly, the steady-state hydrological model and the 'total' (undrained) stress regime employed in the models do not match anticipated suction-affected (negative pore pressures at the cliff face) stress regime of the Holderness cliffs, should such a regime be proven.

13.4 ANTHROPOGENIC EFFECTS

Cliff recession is a complex and uncertain process. Coastal defences can result in significant changes which can disrupt the steady state and lead to the establishment of new processes (Dickson *et al*., 2006b; Lee, 1998). By 2005 coastal defences had been applied to approximately 15% of the UK coastline (Brown, 2008). Anthropogenic influences at the Aldbrough test site are probably confined to small fractured domestic and agricultural drainage conduits which emerge at the cliff face and may discharge onto the cliff slope, though this has only occasionally been observed. Various tarmac and concrete surfaces (including Seaside Road & *former* Caravan Road) have protected the cliff-top, albeit in a minor way, from infiltration. There are no man-made defences in the vicinity. The presence or otherwise of WW2 defences in the area is not known. There are no known pipelines or sewerage outfalls in the vicinity, though a gas installation of unknown type is situated slightly offshore at about 1 km to the south.

The effect, if any, of beach build-up or denudation by coastal defences to the north has not been investigated as part of this study. Hard coastal defences tend to reduce the amount of long-shore drift (southward in the case of Holderness), hence reducing the amount of sediment available for beach replenishment, which in turn can adversely affect cliff stability in the long term. Coastal defences tend to reduce sediment input and modify the sediment budget usually resulting in a sediment deficit down-drift and an accumulation up-drift, often leading to outflanking of defences (Brown, 2008). The 'terminal groyne' effect has been reported (Brown, 2008) whereby set-back of the coastline is accentuated immediately beyond the final down-drift groyne or other component of 'hard' defence. This is particularly a problem where many small intermittent defences occur along a soft-cliff coastline. This effect was graphically illustrated at Happisburgh, North Norfolk (Hobbs *et al*., 2008) where a deep embayment ('crenulate' or 'artificial' bay) developed rapidly, initially at a rate of 9 m per year, as the result of failure of a set of traditional wooden groynes/revetments. A smaller example with multiple crenulate features was recorded at Withernsea (Brown, 2008) situated 15 km south-east of Aldbrough.

The nearest defences to Aldbrough are at Mappleton (6 km) and Hornsea (10 km), the former a small rock bund and the latter traditional groynes. In 1991 a 500 m long rock-revetment was built at Mappleton 5 km to the north of Aldbrough. This has affected long-shore drift and increased the erosion rate to the south of

Mappleton, but possibly only up to a down-drift distance of 4.4 km (Brown, 2008). If correct, the effect of these on the beach and cliffs at Aldbrough is therefore likely to be small or negligible.

14 Relationship between landsliding and environment

Coastal landslides and erosion are influenced, both directly and indirectly, by environmental factors, in particular rainfall and waves. Unfortunately, as has been explained earlier in the report, the record of local rainfall for the monitoring period (2001 to 2012) has only been available from stations some distance from the site and not on a continuous basis (Section 6.1); similarly for the marine records of wave heights and storms (Section 11.3). The rainfall issue has been solved as of April 2012 by the installation on site of a Campbell weather station ("Aldbrough BGS"). Wave heights have been available (2008 to 2013) from a single Coastal Channel Observatory buoy ("Hornsea").

14.1 RAINFALL

The likely effects of rainfall on coastal cliffs at Aldbrough may be summarised as follows:

- Infiltration into sediments and raising of water table or piezometric head(s).
- Direct erosion of cliff face and landslide debris.
- Erosion due to surface runoff on the cliff face and ponding.
- Saturation of near surface deposits on cliff face (cycle of wetting/drying leading to shrink/swell).
- Flushing of salts introduced to near surface deposits on cliff face by sea water spray.

14.1.1 Data availability

Rainfall data were obtained from the Met Office (via the BADC) from 7 weather stations within 23 km of the Aldbrough test site (Section 6.1). Of these, three were selected on the basis of correlation coefficients when compared with the last 2 years' rainfall data for the 'Aldbrough BGS' station (section 11.2). The selected stations were 'Leconfield', 'Great Culvert P. Sta.' and 'Winestead'. In practice, the data from these stations has been intercalated, due to gaps in the Met Office datasets, to form a continuous daily record. *As of April 2012 data from only 'Aldbrough BGS' have been used.*

The total daily rainfall results from the 'Aldbrough BGS' station are shown in Figure 86 (see also section 11.2).

14.1.2 Correlations

Volumetric losses per 100 m cliff width, derived from the TLS surveys plotted with total rainfall summed over the same periods are shown in Figure 118. This plot shows an overall positive response of volume loss to rainfall amount, but with some lags, particularly in 2003/4 and 2007/9 (no TLS data were obtained during 2008). Elsewhere in the plot a more or less contemporaneous response is shown; for example in 2005. It is anticipated that the rainfall peak in 2012/13 will be matched by a volume peak in 2013/14. Future additional data should improve the ability to analyse these broad correlations. The plot also suggests that a greater frequency of TLS surveys would almost certainly have led to improved correlations.

An alternative explanation for the plot in Figure 118 might be that there are cycles of landslide activity which are independent of rainfall. This supposition would suggest a cycle of about 4 years, based on data to date. This cycle length tends also to agree with East Riding's cliff-top GPS & TLS profile data (East Riding Yorkshire Council, 2013); refer to section 13.2. It is possible that major rainfall events interfere with this cycle, for example by bringing it forward. The most likely explanation is that a cycle of landslide-dominated cliff recession is influenced by both rainfall and waves (see section 14.2); rainfall promoting instability and waves, and particularly storm waves, removing the landslide debris, and thus re-establishing the conditions for further instability. The migration of 'ords' also has an effect (section 8.2).

Regarding the last two years' records ('Aldbrough BGS'), significant rainfall was recorded in June/July and November/December, 2012, and between late-May and mid-July and again in late-November, 2013. Total monthly rainfall is shown in Figure 87; 802mm being recorded for the first 12 months of monitoring. A plot (Figure 89) shows the monthly average piezometric data with monthly average rainfall and effective rainfall from the BGS weather station. There appears to have been a response to the November 2012 rainfall at 8m depth in Borehole 2a. This response to rainfall, if indeed it was such, is seen with both rainfall and effective rainfall data (*effective rainfall is calculated by subtracting the potential evapotranspiration (ETo) from the rainfall*). A plot of effective rainfall for the recorded monitoring period is shown in Figure 88. November and December 2012 are notable for their high effective rainfall. *Effective rainfall data are not available for the period 2001 to 2011.*

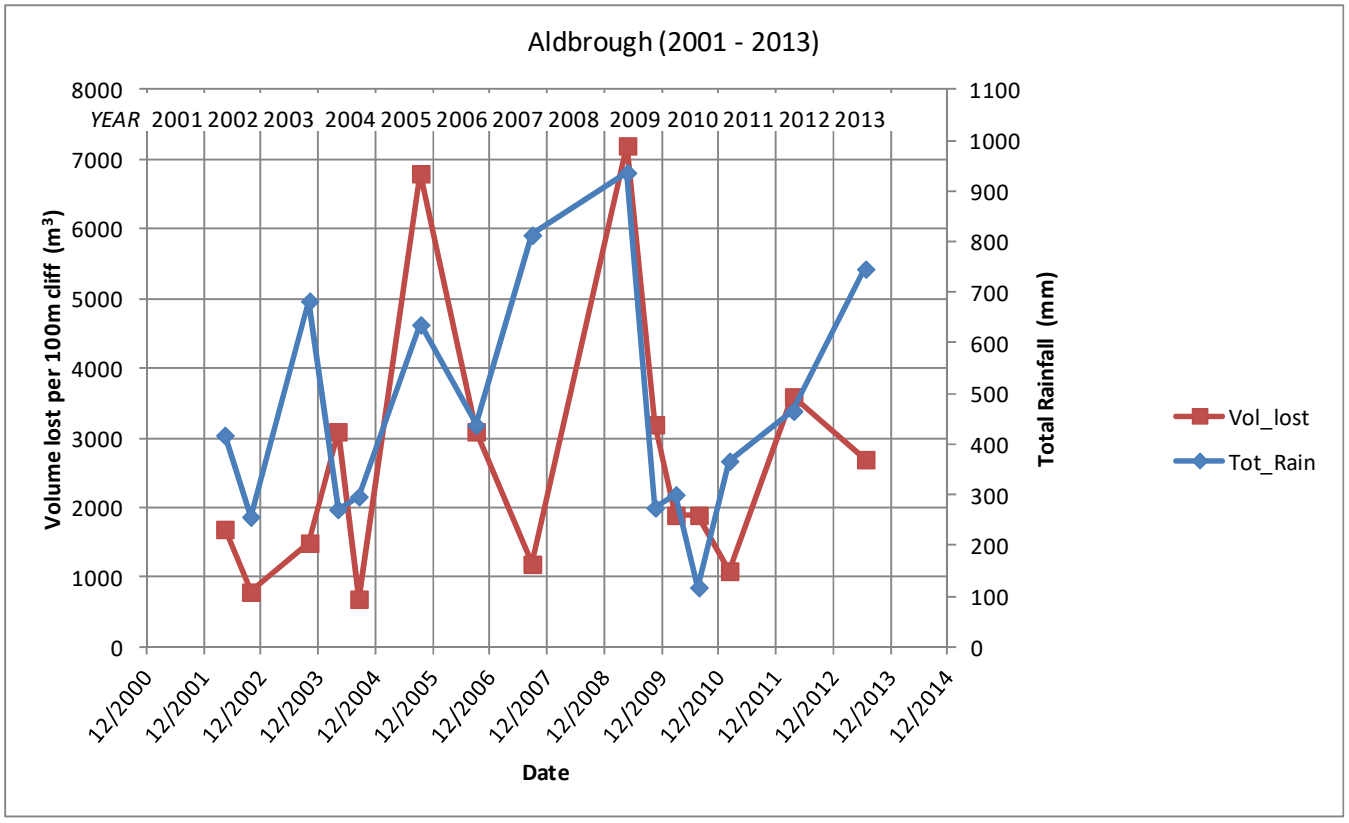

Figure 118 Plot of total rainfall and volume lost from the cliff (100m width) for selected TLS surveys over the whole monitoring period at Aldbrough

14.2 WIND AND WAVES

Wind and wave data for Aldbrough are described in Section 6.1 and section 6.2, respectively. The likely effects of wind and waves on coastal cliffs at Aldbrough may be summarised as follows:

- In the offshore environment wind, particularly from certain azimuthal directions, causes waves which directly erode the beach, platform and cliff. The effect on the cliff is principally a result of hydraulic action, but also mechanical action as waves contain beach and cliff debris which impacts and abrades the cliff. Hydraulic action is directly related to wave energy (Sunamura, 1983). Wave height is strongly correlated with wind speed and longer period waves are associated with longer fetch. *NOTE: 'Significant wave' heights in excess of 3m are considered to indicate 'storm' conditions (CCO, 2013).*
- High energy waves are responsible for most beach depletion, the movement of 'ords' (Pringle, 1985) and the net southerly sediment transport and offshore bar development. Waves also directly erode the base of the cliff and platform and produce notches (Bird, 2008).and even small caves (Figure 40).

- 'Salt crystallisation weathering' has been cited as a mechanism of 'soft' cliff degradation (Hampton & Griggs, 2004). However, this is unlikely to be a significant factor at Holderness as high temperatures are required to approach the full effect. Also tills are probably less susceptible than some other rock or soil types.

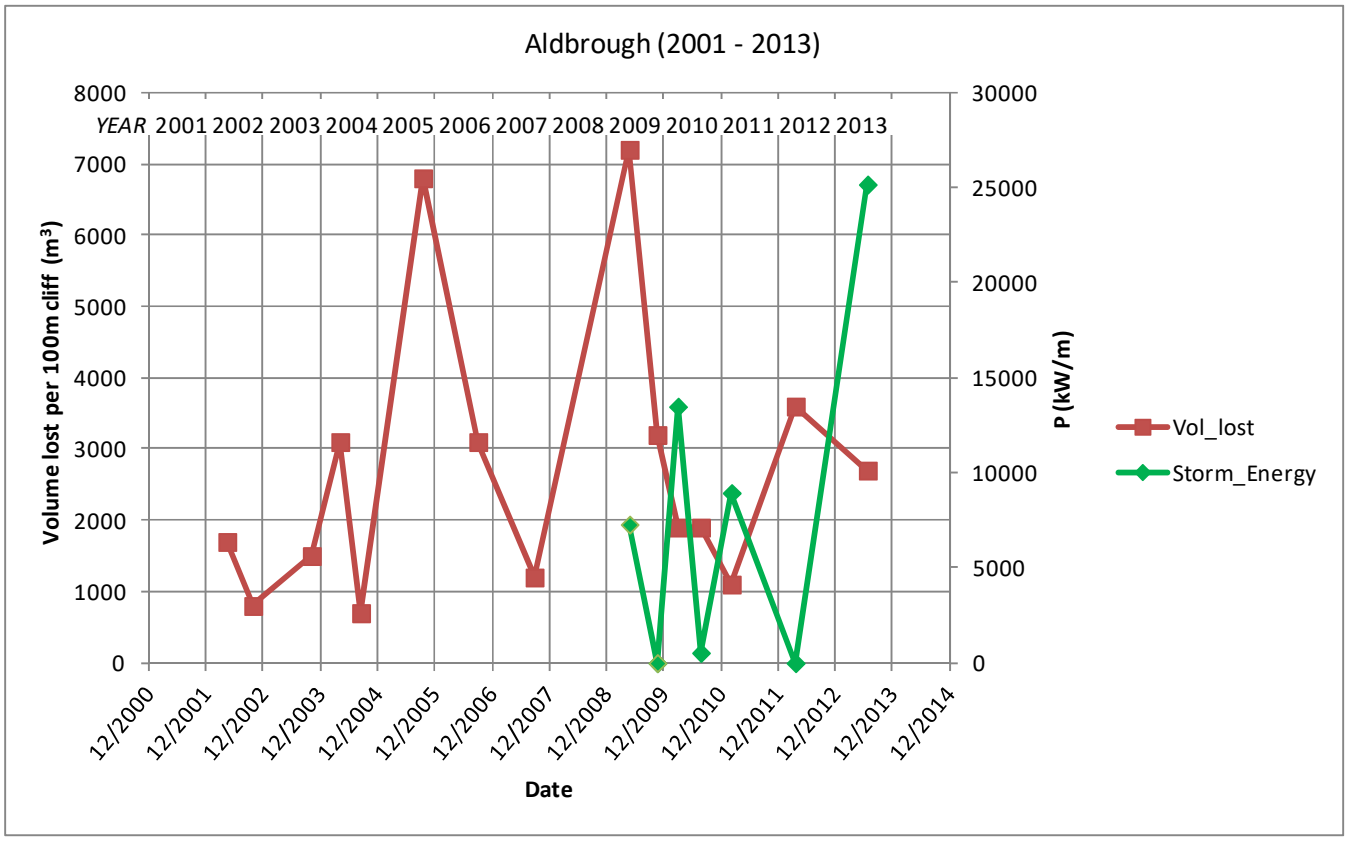

Figure 119 Plot of total 'storm' energy, P and volume lost from the cliff (100m width) for selected TLS surveys at Aldbrough

14.2.1 Data availability

Since April 2012 wind data have been available continuously from the BGS weather station at Aldbrough. Prior to this no wind data have been obtained. Wave data have been available from the CCO Waverider buoy, 'Hornsea', situated 9 km north-east of Aldbrough, starting 10th June 2008. These data have been interpreted here mainly in terms of 'storm' events defined (CCO, 2013) as $H_S > 3$ m, where H_S is the 'significant wave height'. Data from other wave buoys in the WaveNet network, are considered too distant (>40 km) to be applicable to Aldbrough.

14.2.2 Correlations

Results from the wind data recorded by the 'Aldbrough BGS' weather station are shown in Figure 90 and Figure 91 and in Appendix 1. The wind direction diagram (Figure 90) shows a bi-modal disposition with the dominance of wind from the west and south-west and to a lesser extent from the north-north-east, east and south-east. The south-westerlies would be expected to be significant in terms of rainfall, with north-easterlies having less significance. However, this is not borne out by the data which suggest that there is no correlation between rainfall and wind direction, at least for the limited period monitored. Wave height, and consequently enhanced coastal erosion, would be expected to be associated with wind from onshore, in particular from north to north-east, i.e. the source direction having the greatest fetch. Monthly wind direction diagrams for the 'Aldbrough BGS' weather station are shown in Appendix 1. These do not appear to indicate any particular seasonal trends, at least for the limited period monitored to date.

The relationship between average wind speed and 'proportion of which onshore' (taken as the sector N340° to N140° at Aldbrough) is shown in Figure 91. Combinations of high wind speed with high

percentage of onshore wind were seen in April and May 2012 and March 2013. Wave data have been provided by the Channel Coastal Observatory (CCO) and those for the Waverider buoy off Hornsea are summarised in Table 18 and in Appendix 2. The exceedance statistics are shown in Figure 93 and the individual instances in Figure 94. In addition, full wave height datasets divided annually are shown in Figures 105 to 110. No storm events were recorded in 2011. This compares with many storms during the previous two years and in 2013, these mainly occurring in autumn and winter. Principal source direction for storm (and other) waves is from the NNE and NE. The relationship between volumetric losses per 100 m cliff width, derived from the TLS surveys, and storm wave energy summed over the same periods is shown in Figure 119 (*wave data only available from October, 2008*). The 'wave-climate' energy, P was calculated as follows (Dexawave, 2014):

$$P = 0.57 \times (H_S)^2 \times T_P$$

Where: P is wave energy (kW/m)
H_S is significant wave height (m)
T_P is time period between each wave crest (s)

The plot (Figure 119) shows little correlation between the volume loss from the cliff and the storm wave energy. This is almost certainly due to the delay between removal of material from the beach and cliff toe and the renewal of landslide activity. It is not clear to what extent storm waves remove landslide debris directly from the cliff face. Field evidence (e.g. Figure 27) indicates that this factor is observable but probably plays a minor role overall given the incidence of recorded storms.

Wave directions (*direction from whence*) are remarkably consistent over the measurement period, coming principally (annually between 35% and 46%) from the NNE sector. Annual data give an average incidence angle of 42.5° to the coastline at Aldbrough. Onshore waves (wave directions N340° to N140°) comprise between 84 % and 92 % of all waves recorded between 2008 and 2013 (Table 20). Individual 'storm' events have been calculated using the criterion that H_S > 3m, where H_S is significant wave height. These have also been ranked according to duration Table 19.

The contribution of storm surges and tides to coastal erosion, whilst recognised, has not been investigated to date as part of this project. A storm surge, described by the EA as the most serious for 60 years, hit the east coast of England on 5th Dec 2013 causing severe coastal flooding and erosion, most notably in East Anglia. During this event the high tides levels (predicted) at Bridlington and Spurn Point were 6.15 m at 17.54 hrs and 7.25 m at 18.53 hrs, respectively. Wave height recorded by the CCO's 'Hornsea' buoy peaked in the early hours of the 6th Dec with waves in excess of 6 m, accompanied by a peak wind speed of 20.8 m/s (Force 8/9) recorded at the weather station. However, in terms of wave energy alone, higher peaks were recorded on 24th March and 10th October; a maximum wave height of 7.4 m having been recorded on 23rd March. Barometric pressure (average) for 5th Dec at BGS's 'Aldbrough' station was 1023 bar.

14.3 NON-MARINE DEGRADATION OF CLIFF FACE

Within the 'onshore' cliff environment cycles of saturation and desiccation of clay-rich deposits on the cliff slope occur as a result of precipitation and exposure to the sun, respectively. This results in swell/shrink behaviour which enhances degradation of landslipped and, to a lesser extent, in-situ material. This may also have a tendency to cause small reductions in pore pressures near surface, and hence increase effective strength. Tidal cycles of wetting and drying in the 'offshore' environment, i.e. over the lower parts of the cliff, result in near-surface degradation and pre-disposition to mechanical erosion and shallow mudflows. Abundant joints within the tills of the Bridlington Member allow deep penetration of sea water and debris, thus enhancing the overall process of erosion.

The north-easterly aspect of the cliff diminishes the influence of the sun, particularly where the cliff is in the steepest part of its landslide cycle. Shrinkage data for the tills at Aldbrough are summarised in Section 9 and in full in Hobbs et al. (2015b). Shrinkage limit test results for the sampled formations (undisturbed)

at Aldbrough lie in the range 9 to 16 % and volume changes for the same tests in the range 6 to 11 %. Liquid limits lie in the range 30 to 37 % and plasticity indices 13 to 20 %. These results indicate 'low' to 'intermediate' plasticity and low susceptibility to swell/shrink. This would suggest low susceptibility to those erosive factors related to drying & wetting. However, the presence of near-cliff and probably pervasive and closely-spaced discontinuities, mainly in the form of vertical and sub-vertical joints, is likely to have a major influence on the erodibility of cliff-forming materials and their pre-disposition to landsliding. It is unfortunate that this aspect of the geology has not been investigated in detail as part of this project. However, this would probably form the basis of a study in its own right. Such discontinuities are not well exposed in the borehole core and are covered for the most part on the cliff by landslides. It is likely that there is a stress-relief component to their occurrence, though this is difficult to demonstrate. Whilst the dominant fissure trend is perpendicular or sub-perpendicular to the cliff line, some fissures parallel or sub-parallel have been observed; it being likely that the former appear more numerous because they are more exposed. It is anticipated that locally elevated pore pressures could result from waves 'entering' fissures of this type.

15 Conclusions

This report describes the results of a major study of coastal erosion and landsliding on a test section of the Holderness coast at Aldbrough; the results for the period 2001 to 2013 are reported here (the monitoring work is ongoing). The test site forms part of the BGS's 'Slope Dynamics' task, within the 'Landslides' project, and has recently been developed to become a BGS 'coastal landslide field laboratory' to coincide with the introduction in 2012 of four instrumented boreholes landward of the cliff at (initial) distances of 10 and 20 m from the cliff-top (central embayment), and a further two boreholes in 2015, to enable pore pressures and borehole displacement to be measured. The drilling, sampling, instrumentation and geotechnical testing of the boreholes and borehole core are described fully in Hobbs et al. (2015a) and Hobbs et al. (2015b).

It is anticipated that continuing cliff recession will interact progressively with the borehole installations until ultimately slope failure occurs at each location; the process having been continuously or incrementally logged. The intention is for these installations to focus on precursors to slope failure and landslide initiation both on the cliff and landward of it, and to investigate the possibility of geotechnical variations related to stress relief. In these regards the work described here follows that of Butcher (1991). To date, the piezometer and inclinometer data have shown small responses to cliff recession, though these do appear to be correctly oriented, and suggest that resolution of pore pressures and displacement will be good, in preparation for an anticipated major phase of landslide activity (central embayment) in 2015 / 2016.

This study has used predominantly terrestrial LiDAR (TLS or 'laser scanning') methods to model the cliff and platform, and monitor any changes taking place between surveys (typically at intervals of 6 months). The resulting 3D models were used to calculate the amount of material removed by the natural processes of landsliding and erosion by the sea, to construct 'change' models, slope profiles for slope stability analysis and to gain insight into the processes of mass movement on the cliff, and hence quantify cliff recession in 3D. **The results showed that over the 11.75 year period from September 2001 to Jan 2014 (inclusive) a volume of 42,200 m^3 was lost from a selected 100 m run of cliff centred on the test site. This was estimated to have represented 87,900 tonnes of material. Peak amounts were lost during 2004 to 2005 and during 2009 to 2010.** These losses translate to averages of 31 m^3 per metre run per year and 65 tonnes per metre run per year and represent an average increase of 35% in volume loss compared with reported historic values.

It was not possible to separate the contribution of direct mechanical erosion by the sea to cliff recession, as landslide movement was semi-continuous, at least on the monitoring interval time scale of (typically) 6 months. Clearly, erosion by the sea does contribute significantly to cliff recession at Aldbrough by

removing landslide debris from the toe of the cliff, by removing un-slipped and slipped material directly from the lower cliff, both on a daily basis, and ultimately by creating the conditions for continued landsliding. Wave action during high tides at the foot of the cliff creates notches and in some cases small caves which themselves lead to collapse, small falls and rotational landslides; this being partly influenced by beach levels. Whilst the TLS survey encompassed parts of the beach/platform, and their levels could be determined, beach thickness could not due to the fact that platform levels could be reduced by erosion at times when the beach was absent and no survey had been made. However, methods are available to do this (Gunn et al., 2006). Due to the slope angle of the cliff (minimum recorded, 28°), and openness to direct rainfall, erosion due to surface water run-off also would appear to have a contributory, albeit minor, role where this angle is low.

The study has revealed that slope instability of the cliff at the Aldbrough test site has predominantly been by 'rotational' landsliding with subordinate 'toppling' and 'earthflow' failure modes. The rotational failures in some cases develop laterally to form elongate embayments typically 5 – 10 m landward from their flanking promontories. The largest rotational failures typically extend from the cliff-top to a few metres above platform level and usually at or close to the upper boundary of the Bridlington Member. These tend to develop minor multiple regressive rotations within the slipped mass and backscarp, with occasional earthflows in the lower part. The toppling failures are small and closely controlled by jointing and occur within the upper and mid-cliff usually involving blocks of Withernsea Till Member around 2 - 3 m^3 in size, but also within the Bridlington Member and the lower part of the Skipsea Till Member where larger topples and falls occur, particularly at the promontories. Earthflows were infrequent but observed on shallow cliff slopes following periods of heavy or prolonged precipitation. The debris from landsliding was found to be rapidly removed from the cliff toe and lowermost cliff slopes by wave action with a proportion remaining on the beach for a few weeks partly in the form of 'armoured mud-balls' but only after significant mass movements had occurred. Over the monitoring period original landslide embayments and intervening promontories have persisted throughout the monitoring period.

Most forms of mass movement have been influenced by discontinuities within the tills forming the cliffs. These are in most cases pre-existing, but have been affected by localised stress relief resulting from marine erosion, and may also be affected by larger scale stress-relief induced by deep-seated landslides. It has not been possible to determine the extent to which discontinuities (primarily vertical and sub-vertical joints) observed in the cliff face may be projected landward within the body of the deposit.

The hypothesis put forward by Pethick (1996) that landslide embayments at Holderness do not represent large individual landslides and that embayments 'migrate' southward has been shown not to apply at the Aldbrough test site over the monitoring period. Rather, embayments have been shown here to be the result of large individual failures which subsequently break up, the slipped masses gradually reducing in size and vacating the embayment. It has also been shown here at the Aldbrough test site that embayments do not migrate southward but remain in their E-W orientation, at least for the 13 year period of monitoring reported. The reason for this is unclear.

A positive relationship was recorded between rainfall and landslide activity or cliff recession. However, the remoteness of the weather station (23 km) and the infrequency of monitoring surveys did not enable a precise relationship to be developed for most of the project duration (this was finally addressed by the installation of an automatic weather station close to the test site in March 2012). The presence of a sandy beach affected the amount of direct mechanical erosion by wave action, and also may have provided passive resistance to more deeply-seated rotational landsliding, though the latter was not directly observed at any time during monitoring. The movement of 'ords' was observed to be a factor in beach development at the Aldbrough test site, though monitoring frequency was inadequate to characterise their location or track their movement. For the most part the beach was assumed to be up to 2 m deep with parts of the platform sometimes exposed at low tides and occasionally showing a wave-cut step about 0.25 m deep. Results showed that beach elevation, and possibly cliff toe elevation, increased during the monitoring period.

The occurrence of storms appears to be random, though with few in the summer. No relationship was found between storm energy (calculated from summed significant wave heights, $H_S > 3$ m, and wave

periods) and landslide activity or cliff recession. However, wave data from the 'Hornsea' buoy have only been available from 2008. Average onshore wave incidence (all waves) was found to be 42.5° to the coastline with annual averages >84 % of waves 'onshore'. The year 2011 was notably devoid of storms offshore from Aldbrough.

General observations of the Holderness cliffs, at sites other than Aldbrough, indicate that the processes and mechanisms at the Aldbrough test site are typical of the coastline as a whole, albeit with some variation due to cliff height and local lithostratigraphy. The cliff height (16 to 17 m at the Aldbrough test site) determines whether or not a rotational failure mode is predominant. Cliff heights in excess of about 10 m appear to allow rotational failure to dominate at least for lithostratigraphy corresponding to that at Aldbrough. However, a critical (cliff-top) elevation of 15 m OD was suggested by Quinn *et al*. (2010) for "mass failures" to develop at Holderness. The location within the cliff of the weak Dimlington Bed (formerly Laminated Silts), within the Skipsea Till Member, is significant, as this layer preferentially hosts the seaward sectors of rotational slip surfaces in most cases. The 'Laminated Clay' stratum within the Skipsea Till Member may also act as a weak layer susceptible to mass movement. The presence or otherwise of such weak layers at or near the toe of the cliff was also accounted for in the numerical model of Quinn *et al*. (2010). Due to the undulating nature of the stratigraphic boundaries along the Holderness coast, the elevation of landslide toes daylighting in the cliff varies by up to 2 m at the test site.

Cliff slope angles vary widely with both position and time, even within the Aldbrough test site. This suggests that the stability of the cliff at any moment is partly a function of temporary state conditions, possibly related to soil suction resulting from stress relief within the tills and/or local variations of the phreatic surface or minor variations in lithology. The possible contribution of soil suction to enhanced effective strength is being investigated as part of the new (2012 onward) borehole monitoring programme (Hobbs et al., 2015a). The cliff slope stability analysis models, based on the TLS derived profiles, but using assumed phreatic surfaces, produced factors of safety (F) mainly in the range 0.5 to 0.8. The finite element models all produced deep-seated, steep-angled single or multiple rotations with steep backscarps extending either to full cliff height or confined to the upper half of the cliff. These resulted in modelled cliff-top recessions of between 2 and 10 m. In general, there was a good agreement between the observed mode and dimensions of rotational landsliding and the output from the 'FLACslope' stability analyses. Using these as a basis for the 'GALENA' stability analyses produced a range of unstable scenarios that again responded in a manner commensurate with observations, with the notable exception that they predicted instability when the slope was clearly stable, at least in the short term. As has already been discussed this anomaly is believed to be due, either mainly or entirely, to undrained unloading due to suctions in the clay-rich strata within the cliff and lower than predicted phreatic or piezometric levels (refer to Butcher, 1991 and Dixon and Bromhead, 2002). It is intended to test this as part of the ongoing monitoring programme.

The timing of surveys can induce a bias to the calculation of incremental and average values, and the construction of co-relationships; for example where a six-monthly TLS survey either precedes or follows a major storm event. The importance of long-term monitoring in this regard becomes clear. This applies to almost any type of episodic survey, *and even more so to the use of historical maps for calculation of coastal recession* (Brown, 2008). Storm or rainfall events can, after April 2012, be tracked using the weather station. Prior to April 2012 this was not possible at a local scale.

It has not been possible to comprehensively quantify the errors involved in the TLS surveys or the models produced from them. Whilst the repeatability and accuracy of the laser range-finding component of the surveys is very good (repeatability typically 1 mm at 100 m range) many other factors are brought into play during a survey (Buckley *et al*., 2008), in particular the accuracy of positioning and levelling. The resolution of the method overall appears to lie between 0.1 m (favourable conditions) and 2.0 m (adverse conditions) depending on environmental factors (equipment, wind, visibility etc.), data density (laser scans), tripod stability and the quality of dGPS / GNSS positioning data on the day. Importantly, this also varies considerably across the model. Several techniques have been applied to the datasets in an attempt to eliminate known errors the most important of which was to *attach* them to a 'fixed' hinterland datum (road, buildings etc.) where this has been available; this being the only non-dynamic element of the

surveys at the site and the most likely to be of constant elevation and position. Regarding the technical aspects of the surveying, it is concluded that the methodology is of sufficient resolution and accuracy for the geomorphological purpose to which it has been applied in this study.

A brief review of the project to date is given, in terms of benefits and uncertainties, as follows:

Benefits:

- The TLS method of surveying and 3D modelling has been developed and proved suitable for calculating volumetric cliff recession. Continuing improvements have been made in terms of accuracy and efficiency. Surveys are now carried out about twice as fast as in 2001.
- The TLS method of surveying and 3D modelling has been developed and proved suitable for characterising landslide morphology.
- To date, 23 TLS surveys have been carried out over a 12 year period (2001 to 2013), of which 15 were used for the volume calculations described in this report.
- The quality of TLS surveys has improved over the period with steadily improving hardware and software. TLS surveys now contain 10's of millions of data points rather than thousands.
- 3D 'change' models derived from TLS surveys have been successful in showing gross geomorphological variations from one monitoring epoch to the next.
- Continuous annual cliff recession volumes (from TLS) have been calculated (except for 2008).
- Slope stability analyses have reproduced observed landslide behaviour and safety factors indicate that negative pore pressures are operating in the cliff slope to enhance effective strength.
- Wide varieties of landslide types have been observed first hand and modelled using the TLS survey data and slope stability packages. Cycles of landslide behaviour have been investigated and 4 and 11-year cycles postulated.
- A good relationship has been shown between rainfall and volumetric loss from the cliff, though detailed correlations were not possible given the widely spaced monitoring intervals and the remoteness of pre-2012 weather stations.
- The development of landslide embayments has been examined and found to differ, at least locally and for the monitoring period, from one published model for Holderness.
- The dominant landslide mechanism at Aldbrough, deep-seated rotational, has been shown to be influenced by the presence of weak layers, in particular the Dimlington Beds ('Laminated Silts'), as well as the junction of the two major till formations present; these having different geotechnical properties.
- The borehole instrumentation and weather station, installed in 2012, are continuously monitored (with the exception of the inclinometers) and have proved cost-effective and reliable. These have opened new opportunities for fundamental research at the site. The results are reported in Hobbs et al (2015a).
- Early indications are that the borehole instrumentation is responding in a consistent and expected manner and will continue to do so as the cliff recedes towards the boreholes. A major phase of landslide activity is anticipated within the period 2016 / 2017.
- A deterministic approach has produced plausible models for cliff recession, confirmed by observation, and quantitative data for volumes of material displaced. Such detailed data have not been recorded elsewhere in Great Britain over such an extended period.
- Photogrammetry deployed from a small drone (SUAV) has recently been demonstrated as both a viable alternative and a complement to TLS and has been used since 2013.

Uncertainties:

- To date surveys have been too infrequent to capture details of all landslide activity. Thus individual events and sequences of events could not be resolved.
- Surveys have been of variable quality, partly as a result of continuing technical improvements throughout the period and partly due to a poor dGPS (RTK) environment.
- The closest weather station with (discontinuous) pre-2012 data was 15 km from the test site.
- Wave data relevant to the Aldbrough test site have only been available since 2008.

- It has not been possible to install permanent TLS stations, CCTV or time-lapse cameras to capture individual landslide events and sequences of events.
- It was not possible as part of Phase 1 drilling to obtain a fully-cored 'control' borehole at the site. *This was completed in January 2015 as part of Phase 2, though core recovery was poor.*
- Errors in the TLS surveys are difficult to quantify, due to the large number of variables and environmental conditions on the day.
- A comprehensive and detailed 3D geological model (stratigraphic / structural) for the test site has been impossible to define due to widespread obscuration by landslide deposits and incomplete borehole core recovery.
- A limited range of laboratory geotechnical tests was carried out for input to slope stability analyses. *This has been expanded in the Phase 2 programme.*

The contribution of landsliding to 'soft' cliff recession on the Holderness coast has been measured and reported for a 12 year period starting in 2001, though the task is ongoing. The development of 3D to 3.5D models using TLS to calculate recession with unprecedented accuracy has allowed considerable improvements to previous methods for determination of cliff stability, sediment yield and coastal modelling in general; these having been confined previously to 2D measurements and interpretation of historic maps. Actual quantities of cliff material lost to the sea have been calculated over an extended period which has encompassed recognisable cycles of landslide evolution. The continuing technical progress of TLS, and the recent introduction and greater affordability of UAV 'cloud' photogrammetry, point to the possibility of greater coverage and rapidity for surveying and monitoring in the future.

The Shoreline Management Plan (SMP) covering Holderness (SMP, 2010) highlighted "uncertainties in coastal processes understanding" and stated in its summary that "monitoring of cliff recession and beach profiles along the Holderness coast should continue". Additionally, the Eurosion Project (EUROSION, 2004) has pointed to the need for "quantitative assessment of coastal erosion". The work covered by the 'Slope Dynamics' task at Aldbrough, reported here, has addressed many of the factors referred to; at least in terms of principle if not of coverage. Work continues providing a rich 4D dataset, now further augmented by new sensors and technological improvements to existing surveying and modelling methods.

The results of the Aldbrough drilling programme, sampling, sensor installations and geotechnical analyses are given in Hobbs et al. (2015a). Results from the Aldbrough geotechnical laboratory testing programme are given in Hobbs et al. (2015b).

16 Recommendations

As far as the 'Slope Dynamics' task is concerned it is recommended that:

- The TLS monitoring programme is continued at a minimum of 6-monthly intervals, and preferably at 3 monthly intervals.
- The borehole instrumentation and weather station are maintained and developed.
- Newly developed UAV photogrammetry methods for creating 3D change models are further employed as a complement to TLS.
- A means of installing a permanent remote 'camera / CCTV' or TLS station is sought.
- Efforts are continued to streamline data processing and improve accuracy and efficiency of surveys, particularly with regard to software.

The borehole installations from March 2012 and January 2015 should interact significantly with ongoing cliff recession by 2016 or 2017, assuming that observed slope processes continue. Results to date show that interaction with regard to the inclinometer and piezometer data has already begun, albeit to a limited extent. Introduction of the 'PRIME' resistivity arrays (downhole and surface) in January 2015 will add further capability.

17 References

Balson, P. S., Tragheim, D., Newsham, R. (1998) Determination and prediction of sediment yields from recession of the Holderness coast, Eastern England. *Proceedings of the 33rd MAFF Conference of River and Coastal Engineers*; London, Ministry of Agriculture, Fisheries and Food 1998, pp4.5.1-4.6.2.

Bell, F.G. and Forster, A. (1991) The geotechnical characteristics of the Till deposits of Holderness. *In:* Quaternary Engineering Geology. *Geological Society, Engineering Geology Special Publications,* No. 7. Forster, A., Culshaw, M.G., Cripps, J.C. Little, J.A. and Moon, C.F. (eds.). pp 111-118. London.

Bell, F.G. (2002) The geotechnical properties of some till deposits occurring along the coastal areas of Eastern England. *Engineering Geology*, 63 (2002), pp49-68.

Benn, D.I. and Evans, D.J.A. (1996) The interpretation and classification of glacially deformed materials. *Quaternary Science Reviews*, Vol. 15, pp23-52.

Bird, E. (2008) Coastal geomorphology, an introduction. 2nd ed. *Wiley*.

Bisat, W.S. (1939) The relationship of the 'Basement Clays' of Dimlington, Bridlington, and Filey Bay. *The Naturalist*, 133-135, pp161-168.

Bray, M. J. and Hooke, J.M. (1997) Prediction of soft-cliff retreat with accelerating sea-level rise. *Journal of Coastal Research*, 13, pp453-467.

British History (2014) http://www.british-history.ac.uk/report.aspx?compid=16125#s2

Brooks, S.M. and Spencer, T. (2012) Shoreline retreat and sediment release in response to accelerating sea level rise: Measuring and modelling cliffline dynamics on the Suffolk coast, UK. *Global & Planetary Change*, 80-81 (2012), pp165-179.

Brown, S. (2008) Soft cliff retreat adjacent to coastal defences, with particular reference to Holderness and Christchurch Bay, UK. *University of Southampton, School of Civil Engineering & the Environment*, Doctoral Thesis, 333p.

Brunsden, D. and Lee, M. (2004) Behaviour of Coastal Landslide Systems: an Inter-disciplinary View. VI , *Zeitschrift für Geomorphologie, Supplementbände, Band 134.*

Bruun, P. (1962) Sea-level rise as a cause of shore erosion. *Journal of Waterways & Harbours Division ASCE*. 88, 117-130.

BS1377 British Standards Institution (1990) BS1377:1990 Method of test for soils for civil engineering purposes. *British Standards Institution*, London.

BS5930 British Standards Institution (2015) BS5930:2015 Code of practice for ground investigations. *British Standards Institution,* London.

Buckley, S.J., Mills, J.P., Clarke, P.J., Edwards, S.J., Pethick, J. and Mitchell, H.L. (2002) Synergy of dGPS, photogrammetry and INSAR for coastal zone monitoring. Symp. On Geospatial Theory, Processes and Applications, Ottawa, 2002.

Buckley, S.J.,Howell, J.A., Enge, H.D. and Kurz, T.H. (2008) Terrestrial laser scanning in geology: data acquisition, processing and accuracy considerations. *Journal of the Geological Society, London*, Vol. 165, 2008, pp625-638.

Butcher, A.P. (1986) In situ measurements of horizontal earth pressures in a glacial till cliff. M.Sc. Dissertation, University of Surrey, UK, 1986.

Butcher, A.P. (1991) The observation and analysis of a failure in a cliff of glacial clay till at Cowden, Holderness. *In:* Slope Stability Engineering. *Thomas Telford, London,* pp271-276.

Cambers, G. (1976) Temporal scales in coastal erosion systems. Transactions, Institute of British Geographers. 1 (2), pp 246-256.

Catt, J.A. (1991) Quaternary history and glacial deposits of East Yorkshire. *In:* Ehlers, J., Gibbard, P.L., and Rose, J. (eds.) Glacial deposits in Great Britain and Ireland. *Balkema*, Rotterdam, pp185-192.

Clark, C.D., Gibbard, P.L., and Rose, J. (2003) Pleistocene glacial limits in England, Scotland, and Wales. *In:* (Ehlers, J. and Gibbard, P.L. eds.) Quaternary Glaciations – Extent and chronology, Part 1: Europe. *Elsevier, Amsterdam*, pp47-82.

CCO(2013)
http://www.channelcoast.org/data_management/real_time_data/charts/?chart=72andtab=statsanddisp_option=anddata_type=tableandyear=2012, *Channel Coastal Observatory (CCO)*

Dexawave (2014) http://www.dexawave.com

Dickson, M., Walkden, M.; Hall, J., Pearson, S. Rees, J. (2006a) Numerical modelling of potential climate-change impacts on rates of soft-cliff recession, northeast Norfolk, UK. *In:* Sanchez-Arcilla, A., (ed.) *Coastal Dynamics 2005 [proceedings]*. Virginia, USA, American Society of Civil Engineers, 14pp.

Dickson, M., Walkden, M. and Hall, J. (2006b) Modelling the impacts of climate change on an eroding coast over the 21st Century. Tyndall Centre for Climate Change Research Centre, Working Paper 103.

Dixon, N. and Bromhead, E.N. (1991) The mechanics of first-time slides in the London Clay cliff at the Isle of Sheppey, England. *Proc. Int. Conf. on Slope Stability Engineering: Developments and Applications*, Isle of Wight, UK, April 15-18, pp277-282.

Dixon, N. and Bromhead, E.N. (2002) Landsliding in London Clay coastal cliffs. *Quarterly Journal of Engineering Geology& Hydrogeology,* V. 35, pp327-343.

East Riding of Yorkshire Council (2009):
http://www.eastriding.gov.uk/padocs/JUNE2012/33599233F7F511E1977E4437E6597885.pdf

East Riding of Yorkshire Council (2013):
http://www.eastriding.gov.uk/coastalexplorer/pdf/Cliff_erosion_data_table_March2012.pdf

http://www.eastriding.gov.uk/coastalexplorer/pdf/Cliff_Erosion_loss_table_Oct2013.pdf

EUROSION (2004) "Living with coastal erosion in Europe – Sediment and space for sustainability" European Commission, 40p, ISBN 92-894-7496-3, www.eurosion.org

Evans, D.J.A. and Thomson, S.A. (2010) Glacial sediments and landforms of Holderness, eastern England: A glacial depositional model for the North Sea lobe of the British – Irish Ice Sheet. *Earth Science Reviews*, v101, n 3-4 (201008), pp147-189.

Flory, R., Nash, D., Lee, M., Hall, J., Walkden, M. and Hrachowitz, M. (2002) The application of landslide modelling techniques for the prediction of soft coastal cliff recession. *In:* Instability – Planning and Management, *Thomas Telford*, London, 2002, pp249-256.

Foster, C. Diaz Doce, D. (2010) Geosure Version 6 Methodology: Landslides (Slope Instability) *IR/10/091. British Geological Survey, Nottingham*, 34p.

Forster, A., Harrison, M., Cooper, A. H., Jones, L. D., Wildman, G., Newsham, R., Farrant, A. (2004). The National Assessment of the Geological Hazards – Landslide, Running Sand, Compressible Soils, Collapsible Soils, Dissolution and Shrinkable Clay Soils. GeoSure Version 2. *Unpublished BGS Internal Document*.

Gilroy, S.T. (1980) The engineering properties of weathered Devensian tills of Holderness. *Unpubl. M.Sc. Thesis. Univ. of Newcastle-upon-Tyne*.

Gunn, D.A.., Pearson, S.G., Chambers, J.E., Nelder, L.M., Lee, J.R., Beamish, D., Busby, J.P., Tinsley, R.D. & Tinsley, W.H. (2006) An evaluation of combined geophysical and geotechnical methods to characterize beach thickness. *Quarterly Journal of Engineering Geology & Hydrogeology, 39, pp339-355.*

Hackney, C., Darby, S.E and Leyland, J. (2013) Modelling the response of soft cliffs to climate change: a statistical process-response model using accumulated excess energy. *Geomorphology*, 187, pp108-121.

Hampton, M.A. and Griggs, G.B (2004) Formation, evolution and stability of coastal cliffs: status and trends. USGS Professional Paper 1693. *US Department of Interior/US Geological Survey. Diane Publ. Co.*

Hanson, S.; Nicholls, R.J.; Balson, P.S.; Brown, I.; French, J.R.; Spencer, T.; Sutherland, W.J. (2010) Capturing coastal geomorphological change within regional integrated assessment: an outcome-driven fuzzy logic approach. *Journal of Coastal Research*, 26 (5). pp831-842.

Hiatt, M.E., 2002, Sensor Integration Aids Mapping at Ground Zero: Photogrammetric Engineering and Remote Sensing, v. 68 (9), p. 877-879.

Hobbs, P.R.N., Humphreys, B., Rees, J.G., Tragheim, D.G., Jones, L.D., Gibson, A., Rowlands, K., Hunter, G., and Airey, R. (2002) Monitoring the role of landslides in 'soft cliff' coastal recession. *In:* Instability: Planning and Management. Eds. R.G. McInnes and J. Jakeways. *Thomas Telford*, London.

Hobbs, P.R.N., Pennington, C.V.L., Pearson, S.G., Jones, L.D., Foster, C., Lee, J.R., Gibson, A. (2008) Slope Dynamics Project Report: the Norfolk Coast (2000-2006). *British Geological Survey, Open Report* No. OR/08/018.

Hobbs, P.R.N., Jones, L.D., Kirkham, M.P., Roberts, P., Haslam, E.P. and Gunn, D.A. (2014) A new apparatus for determining the shrinkage limit of clay soils. *Géotechnique*, 64, No.3, pp195-203.

Hobbs, P.R.N., Jones, L.D., & Kirkham, M.P. (2015a) Slope Dynamics project report: Holderness Coast – Aldbrough: Drilling & Instrumentation. *British Geological Survey, Internal Report* No IR/15/001.

Hobbs, P.R.N., Kirkham, M.P. & Morgan, D.J.R. (2015b) Geotechnical laboratory testing of glacial deposits from Aldbrough, Phase 2 boreholes. *British Geological Survey, Internal Report* No OR/15/056

Hoek, E. P. 2000. Practical Rock Engineering. *Taylor & Francis, London.*
Hulme, M. and Jenkins, G.J., (1998) *"Climate change scenarios for the UK." In:* UKCIP Technical Report No. 1, 80pp *Climatic Research Unit, Norwich*.

Hulme, M. and Jenkins, G.J. (1998) Climate Change Scenarios for the United Kingdom UKCIP Technical Report No.1, Climatic Research Unit, Norwich, UK, 80pp.

Hunter, G., Pinkerton, H., Airey, R., and Calvari, S., 2003, The application of a long-range laser scanner for monitoring volcanic activity on Mount Etna: Journal of Volcanology and Geothermal Research, v. 123 203-210.

Hutchinson, J. N. (1967) The free degradation of London Clay cliffs. *Proc. Geotech. Conf*., Oslo 1, pp 113-118.

Jeong, U., Park, S.J., Lee, C.W., Lee, J-T., Yoon, W.S., Choi, J.W., Hong, H. and Kwan, K.J. (2007) Construction of a landslide susceptibility map using SINMAPP technique and its validation: a case study. *Proc. 1st Canada-US Rock Mech. Symp*, Vancouver, Canada, 27th-31st May 2007, pp975-978, *Taylor & Francis, London.*

Joyce, M.D. (1969) A geological study of the boulder clay cliffs of Holderness, East Yorkshire. M.Sc. Thesis (unpubl.) University of Leeds.

Kent, G.H.R. (Editor), Allison, K.J., Baggs, A.P., Cooper, T.N., Davidson-Cragoe, C., Walker, J. (2002) A history of the County of York East Riding: Volume 7: Holderness Wapentake, Middle and North Divisions, Middle Division: Aldbrough, *www.british–history.ac.uk*, pp5-27.

Leatherman, S.P. (1990) "Modelling shore response to sea level rise on sedimentary coasts". *Progress in Physical Geography*, 14, pp447-464.

Lee, E.M. (1998) Prediction of cliff recession rates. *In:* Coastal defence and earth science conservation. Ed: J. Hooke. *Geological Society*.

Lee, E.M. (2008) Coastal cliff behaviour: Observations on the relationship between beach levels and recession rates. *Geomorphology*, 101 (2008), pp558-571.
Lee, E.M. (2011) Reflections on the decadal-scale response of coastal cliffs to sea-level rise. Technical Note, *Quarterly Journal of Engineering Geology & Hydrogeology*, 44, pp481-489.

Lee, E.M. and Clark, A.R. (2002) Investigation and management of soft rock cliffs. *Department for Environment, Food, and Rural Affairs. Thomas Telford.*

Lee, E.M., Hall, J.W. and Meadowcroft, I.C. (2002) Coastal cliff recession: the use of probabilistic prediction methods. *Geomorphology*. 40, 3-4 (2001), pp253-269.

Lewis, S.G. (1999) Eastern England. *In:* A revised correlation of Quaternary deposits in the British Isles. D.Q. Bowen (ed.) *Geological Society Special Report* No. 23.

Lott, G K and Knox, R W O'B. (1994) Post Triassic of the Southern North Sea. *In:* Knox, R W O'B and Cordey, W G (editors) Lithostratigraphic nomenclature of the UK North Sea. (*Keyworth, Nottingham: British Geological Survey*.)

McGown, A. and Derbyshire, E. (1977) Genetic influences on the properties of tills. *Quarterly Journal of Engineering Geology*, Vol. 10, pp389-410.

Marsland, A. and Powell, J.J.M. (1985) Field and laboratory investigations of the clay tills at the Building Research Establishment test site at Cowden, Holderness. *Proc. Int. Conf. on Construction in Glacial Tills and Boulder Clay*, Edinburgh, pp147-168.

McMillan, A.A., Hamblin, R.J.O. and Merritt, J.W. (2011) A lithological framework for onshore Quaternary and Neogene (Tertiary) superficial deposits of Great Britain and the Isle of Man. *British Geological Survey*, Research Report RR/10/03.

Miller, P.E., Mills, J.P., Edwards, S.J., Bryan, P.G., Marsh, S.H., Hobbs, P. and Mitchell, H. (2007) A robust surface matching technique for integrated monitoring of coastal geohazards. *Marine Geology*, 30 (2007), pp109-123. *Taylor & Francis*.

Miller, P.E., Mills, J. P., Edwards, S. J., Bryan, P. G., Marsh, S. H., Mitchell, H., and Hobbs, P. (2008) A robust surface matching technique for coastal geohazard assessment and management. *ISPRS Journal of Photogrammetry and Remote Sensing*. Vol.63, iss.5, pp529-542. *Elsevier.*

Moore, A.B., Morris, K.P., Blackwell, G.K., Jones, A.R. and Sims, P.C. (2003) Using geomorphological rules to classify photogrammetrically-derived digital elevation models. *Int. J. Remote Sensing*, 24, No. 13 (2003), pp2613-2626. *Taylor & Francis.*

Pack, R.T. (1995) Statistically-based terrain stability mapping methodology for the Kamloops Forest Region, British Columbia. *In:* Proceedings of the 48th Canadian Geotechnical Conference, *Canadian Geotechnical Society*, Vancouver, B.C., p.617-624.

Paul, M.A. and Little, J.A. (1991) Geotechnical properties of glacial deposits in lowland Britain. *In:* Ehlers, J., Gibbard, P.L. and Rose, J. (eds.) Glacial Deposits in Great Britain and Ireland. *Balkema*, pp389-403.

Paul, F., and Iwan, P. (2001) Data Collection at Major Incident Scenes using Three Dimensional Laser Scanning Techniques, The Institute of Traffic Accident Investigators: 5th International Conference held at York: New York.

Pethick, J. (1996) Coastal slope development: temporal and spatial periodicity in the Holderness cliff recession *In:* Anderson, M.G. and Brooks, S.M. (eds.) Advances in Hillslope Processes., 2. *Wiley, Chichester*, pp897-917.

Pethick, J. and Leggett, D. (1993) "The morphology of the Anglian coast" *In:* 'Coastlines of the Southern North Sea' (ed. R. Hillen and H.J. Verhagen). New York: *American Soc. Civ. Eng*., pp52-64.

Prandle, D., Ballard, G., Banaszek, A., Bell, P., Flatt, D., Hardcastle, P., Harrison, A., Humphery, J., Holdaway, G., Lane, A., Player, R., Williams, J. and Wolf, J. (1996) The Holderness Coastal Experiment, '93-'96. *Proudman Oceanographic Laboratory*. Report No. 44, 1996.

Pringle, A.W. (1985) Holderness coastal erosion and the significance of ords. *Earth Surface Processes and Landforms.* 10:107-124

Pye, K. and Blott, S.J. (2010) Geomorphological assessment of impact of proposed cliff protection works on adjoining areas. (2010) *Kenneth Pye Associates*. External Report No. EX1214, October, 2010.

Quinn, J.D., Philip, L.K. and Murphy, W. (2009) Understanding the recession of the Holderness Coast, East Yorkshire, UK: a new presentation of temporal and spatial patterns. *Quarterly Journal of Engineering Geology & Hydrogeology*, 42, pp165-178.

Quinn, J.D., Rosser, N.J., Murphy, W. and Lawrence, J.A. (2010) Identifying the behavioural characteristics of clay cliffs using intensive monitoring and geotechnical numerical modelling. *Geomorphology*, v120, n 3-4, (20100815), pp107-122, Elsevier B.V.

Rowlands, K., Jones, L., and Whitworth, M. (2003) Photographic Feature: Landslide Laser scanning: a new look at an old problem: Quarterly Journal of Engineering Geology, v. 36 (2), p. 155-158

SINMAP (http://hydrology.usu.edu/sinmap/)

Sladen, J.A. and Wrigley, W. (1983) Geotechnical properties of lodgement till – a review. *In:* Eyles, N. (ed.) Glacial geology: an introduction for engineers and earth scientists. *Pergamon*, pp184-212.

SMP (2010) Flamborough Head to Gibraltar Point Shoreline Management Plan. *Humber Estuary Coastal Authorities Group*. Interim Plan, Dec 2010.

Stive, M.J.F. (2004) How important is global warming for coastal erosion? *Climatic Change*.64, 27-39.

Sumbler, M G. (1999). The stratigraphy of the Chalk Group of Yorkshire, and Lincolnshire. *British Geological Survey Technical Report,* WA/99/02.

Sunamura, T. (1983) Processes of sea-cliff and platform erosion. *In:* Komar, P.D. (ed.) CRC Handbook of Coastal Processes and Erosion*. CRC Press, Boca Raton, FL*, pp233-265.

Trenhaile, A.S. (2009) Modelling the erosion of cohesive clay coasts. *Coastal Engineering*, 56, 1 (2009), pp59-72.

Valentin,H. (1971) Land Loss at Holderness. pp 116-137 in: Steers, J. A. ed. *Applied Coastal Geomorphology*. MacMillan.

Walkden, M.J.A., Hall, J.W and Lee, E.M (2002) "A modelling tool for predicting coastal cliff recession and analysing cliff management options" *In:* 'Instability – Planning and Management', *Thomas Telford, London*, pp415-422.

Walkden, M.J.A. and Hall, J.W. (2005) A predictive mesoscale model of the erosion and profile development of soft rock shores. *Coastal Engineering*, 52(6), pp535-563.

Walkden, M.J.A. and Dickson, M. (2008) Equilibrium erosion of soft rock shores with a shallow or absent beach under increased sea level rise. *Marine Geology*, 251, (1-2), pp75-84.

Walkden, M.J.A., Pearson, S., Mokrech, M., Spencer, T., Nicholls, R.J., Hall, J., Koukoulas, S., Rees, J., Poulton, C. and Dickson, M.E. (2005) "Towards an integrated coastal sediment dynamics and shoreline response simulator" *Tyndall Centre Technical Report* No. 38.

Wildman, G. and Hobbs, P.R.N. (2005) "Scoping study for coastal instability hazard susceptibility – Filey Bay, Beachy Head and Lyme Bay". *British Geological Survey*, Internal Report No. IR/05/018.

Wolf, J. (1998) "Waves at Holderness: Results from in-situ measurements" *Proc. Conf. Oceanology International 98*, 'The Global Ocean', Vol. 3, pp387-398.

Wunderground (2014) http://www.wunderground.com/

Zaitchik, B.F. and van Es, H.M. (2003) Applying a GIS slope-stability model to site-specific landslide prevention in Honduras. *J. Soil & Water Conserv*. Vol. 58, pp45-53

BGS boreholes:

TA23NEBJ4

TA24SWBJ2

Appendix 1: Wind direction data **(BGS Aldbrough weather station)**

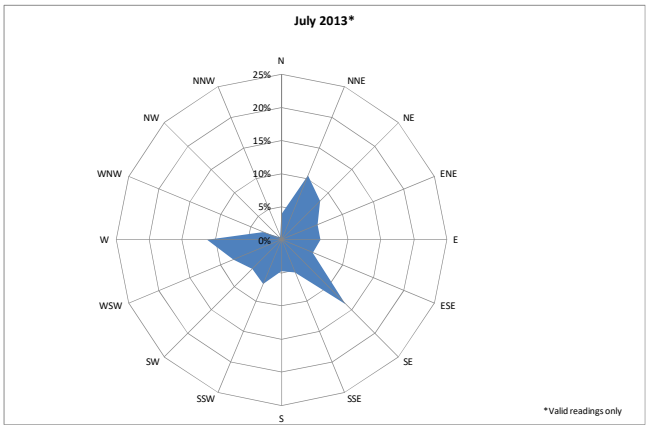

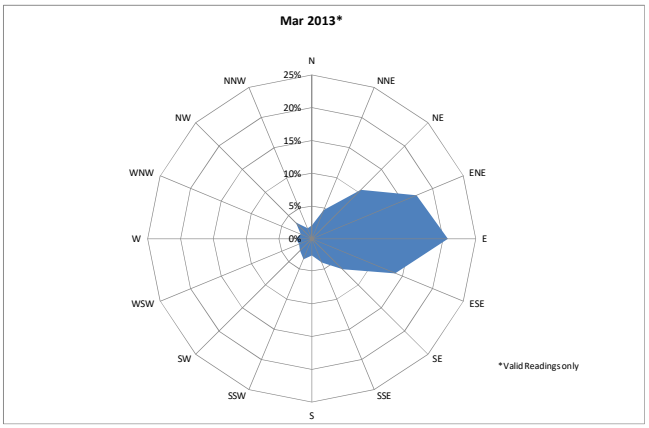

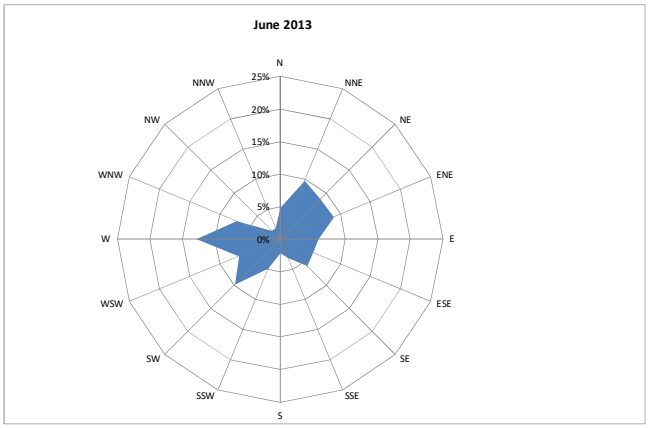

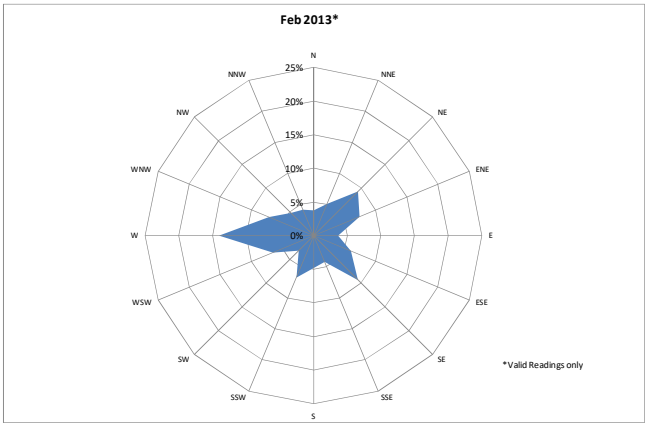

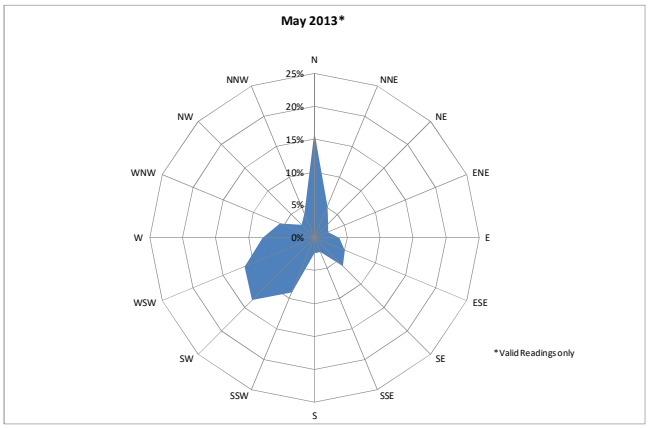

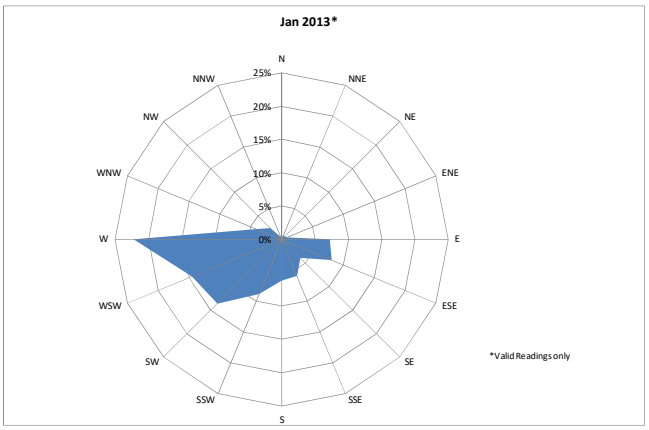

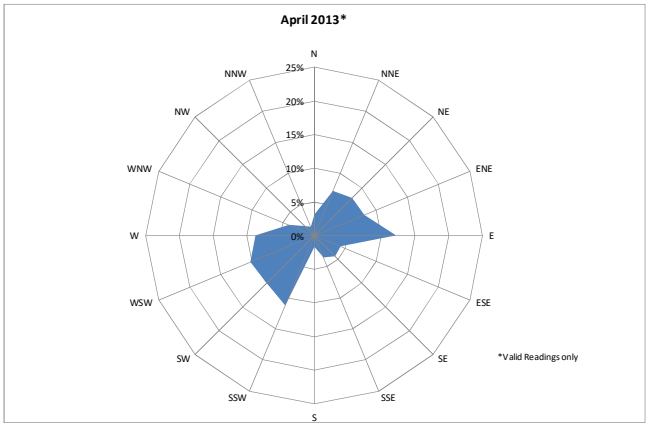

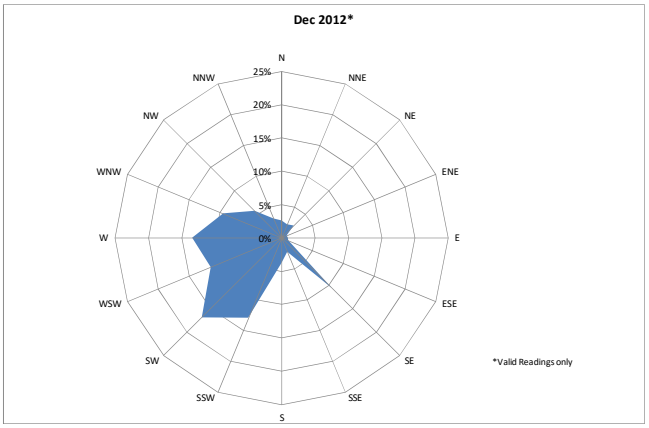

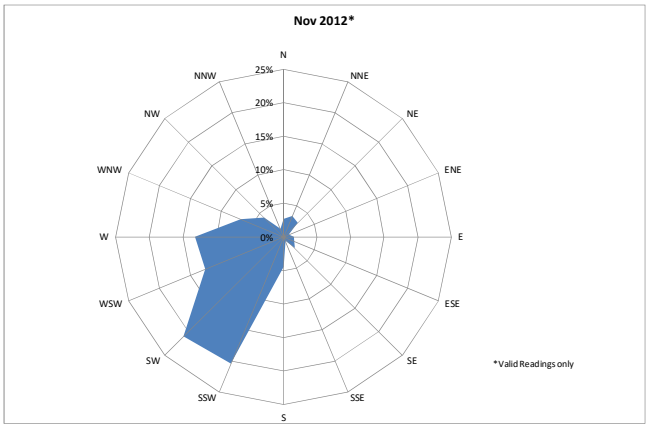
Nov 2012*
N
NNE
NE
ENE
E
ESE
SE
SSE
S
SSW
SW
WSW
W
WNW
NW
NNW
25%
20%
15%
10%
5%
0%
*Valid Readings only

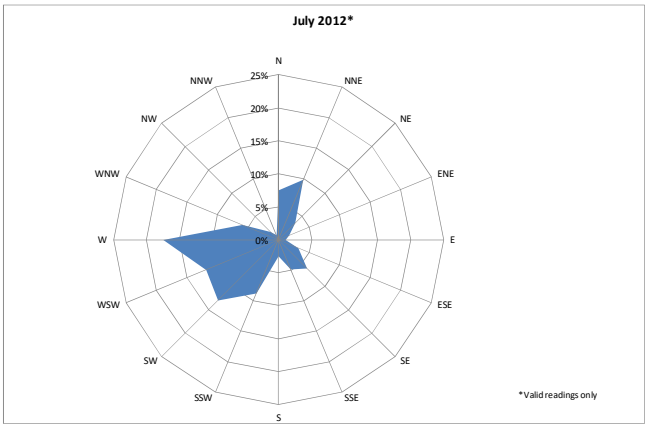
July 2012*
N
NNE
NE
ENE
E
ESE
SE
SSE
S
SSW
SW
WSW
W
WNW
NW
NNW
25%
20%
15%
10%
5%
0%
*Valid readings only

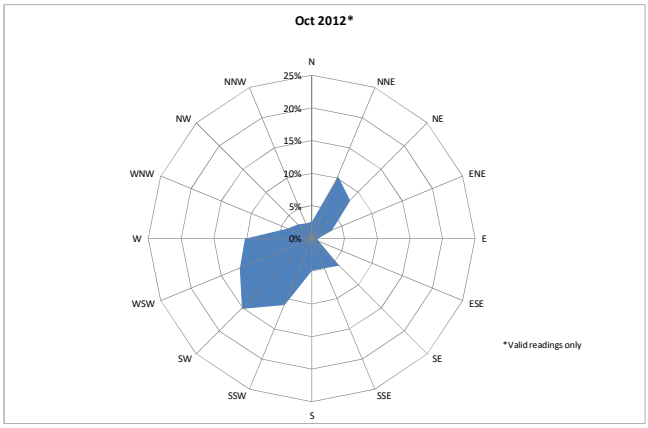
Oct 2012*
N
NNE
NE
ENE
E
ESE
SE
SSE
S
SSW
SW
WSW
W
WNW
NW
NNW
25%
20%
15%
10%
5%
0%
*Valid readings only

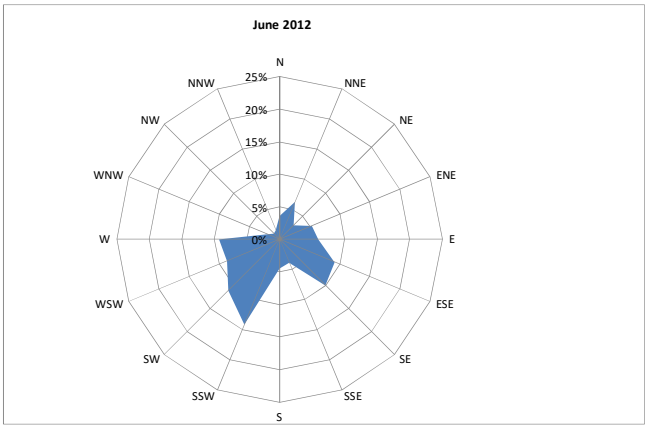
June 2012
N
NNE
NE
ENE
E
ESE
SE
SSE
S
SSW
SW
WSW
W
WNW
NW
NNW
25%
20%
15%
10%
5%
0%

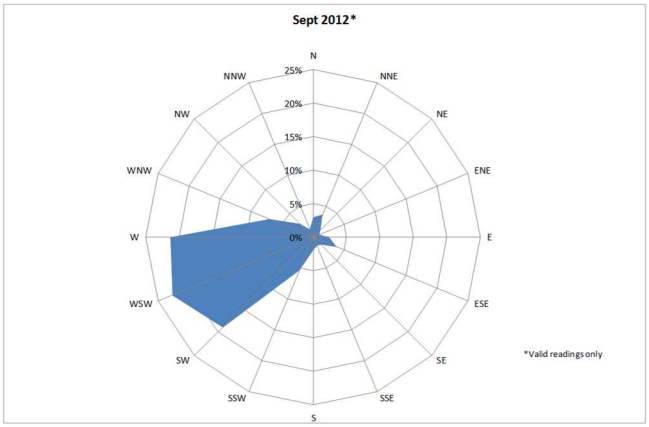
Sept 2012*
N
NNE
NE
ENE
E
ESE
SE
SSE
S
SSW
SW
WSW
W
WNW
NW
NNW
25%
20%
15%
10%
5%
0%
*Valid readings only

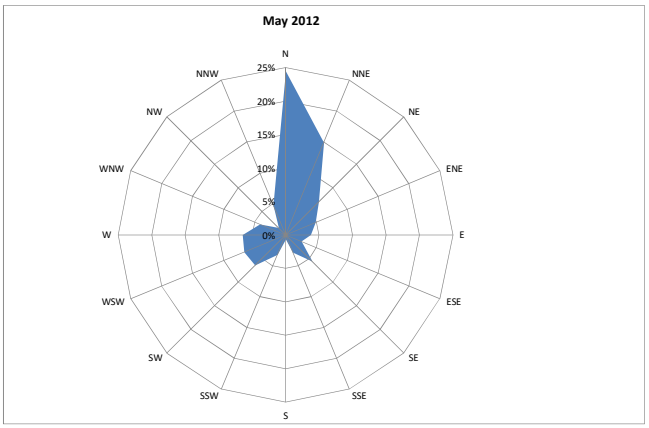
May 2012
N
NNE
NE
ENE
E
ESE
SE
SSE
S
SSW
SW
WSW
W
WNW
NW
NNW
25%
20%
15%
10%
5%
0%

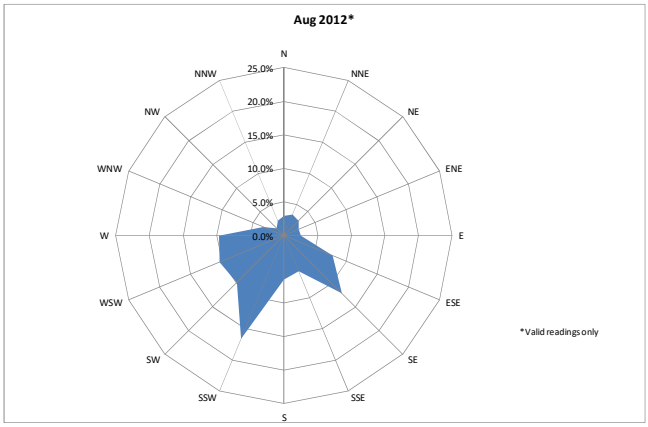
Aug 2012*
N
NNE
NE
ENE
E
ESE
SE
SSE
S
SSW
SW
WSW
W
WNW
NW
NNW
25.0%
20.0%
15.0%
10.0%
5.0%
0.0%
*Valid readings only

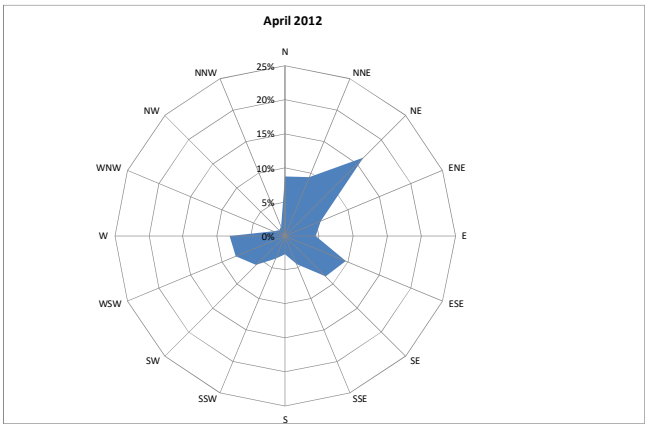
April 2012
N
NNE
NE
ENE
E
ESE
SE
SSE
S
SSW
SW
WSW
W
WNW
NW
NNW
25%
20%
15%
10%
5%
0%

Appendix 2a: Wave direction data (CCO, 'Hornsea' Waverider III buoy)

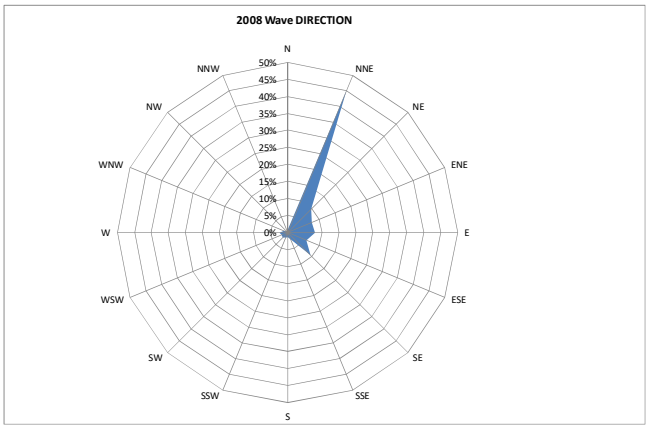

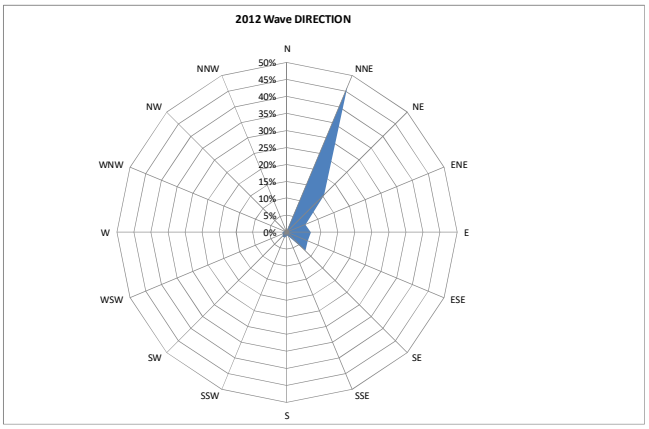

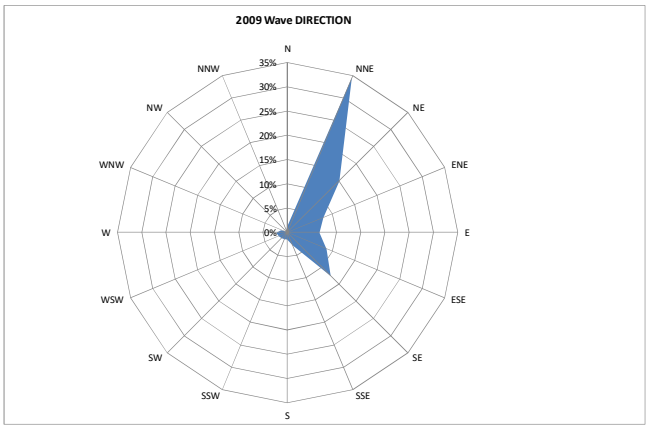

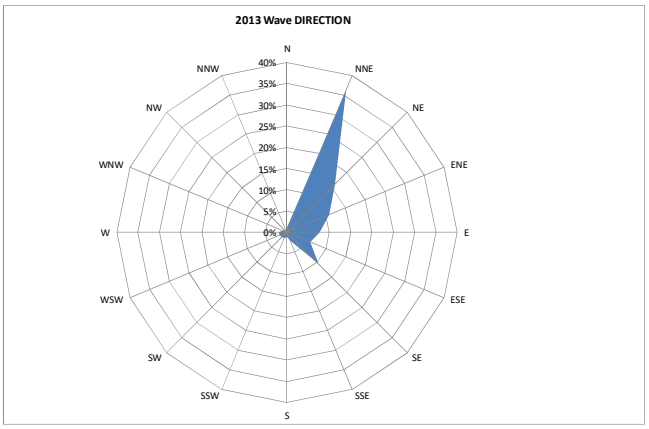

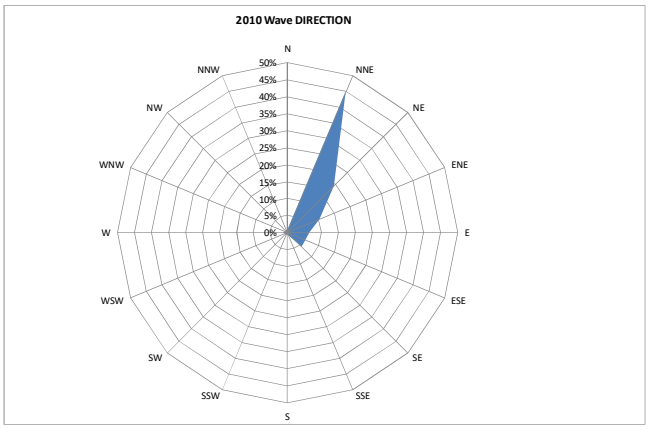

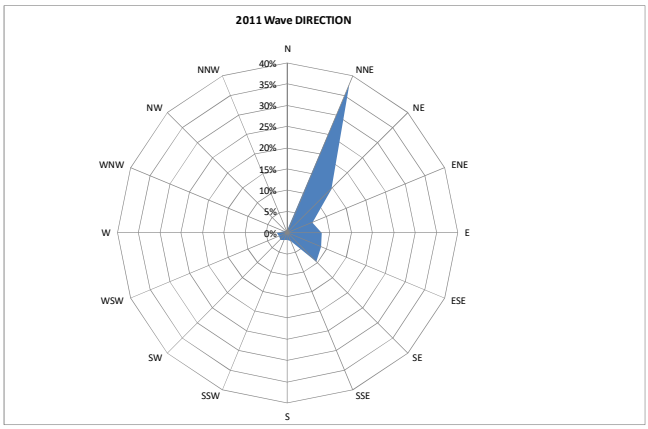

Appendix 2b: Wave data

Hornsea (WaveRider Mk.III buoy)
527071E, 448459N
Water depth = 12 m CD
Spring tide range = 5 m
Data: Channel Coastal Observatory (CCO, 2013)
H_S = Significant wave height (m)
H_{MAX} = Maximum wave height (m)
T_{PEAK} = Dominant wave period (s)
T_Z = Zero up-crossing wave period (s)
Dirp = Wave direction azimuth (°)
T_{SEA} = Sea temperature (°C)

Monthly Averages for 2008

	Hs	Tp	Tz	Dirp	T_{SEA}
	(m)	(s)	(s)	(°)	(°)
June	0.72	6.5	4	98	12.7
July	0.68	6	3.9	87	14
August	0.56	6.2	3.6	90	14.8
September	0.7	7.2	4	72	14
October	0.86	9.2	4.1	70	12.2
November	1.25	8.9	4.6	61	9.8
December	0.94	7.9	4.4	76	7.4

Monthly Averages for 2009

	Hs	Tp	Tz	Dirp	T_{SEA}
	(m)	(s)	(s)	(°)	(°)
January	0.97	7.7	4.3	88	6.1
February	0.98	9.5	4.9	40	4.8
March	0.66	7.7	4	95	6.1
April	0.66	6.3	4	84	7.8
May	0.63	5.4	3.4	119	9.9
June	0.7	6.2	4	69	12.5
July	0.64	6.7	3.8	78	14.5
August	0.46	5.2	3.2	107	15.4
September	0.62	7	3.6	87	14.3
October	1	7.7	4.6	67	13
November	0.91	6.2	3.9	110	11.3
December	1.15	8.3	4.4	62	8.1

Monthly Averages for 2010

	Hs	Tp	Tz	Dirp	T_{SEA}
	(m)	(s)	(s)	(°)	(°)
January	1.52	8.2	5.3	64	5.3
February	1.26	7.7	5	62	4.8
March	0.81	8.6	4.5	52	5.7
April	0.65	8.3	4.3	52	7.4
May	0.77	7.3	4.4	53	9.6
June	0.7	7	4.3	48	12.3
July	0.48	5.4	3.4	99	14.5
August	0.75	6.9	4	65	14.9
September	1.07	7.2	4.5	75	14.5
October	1.02	7.7	4.3	73	12.9
November	1.34	8.5	4.6	62	10.2
December	1.19	8.5	5	50	6.2

Monthly Averages for 2011

	Hs	Tp	Tz	Dirp	T_{SEA}
	(m)	(s)	(s)	(°)	(°)
January	0.9	8.9	4.4	52	5.3
February	0.96	7.8	4.1	83	5.7
March	0.71	9.6	4.9	56	6.2
April	0.58	7.6	3.8	78	8.2
May	0.63	5.5	3.4	125	10.4
June	0.54	6.7	3.8	72	12.7
July	0.91	7.6	4.5	48	14.1
August	0.62	6	3.8	81	14.9
September	0.54	5.3	3.3	125	14.5
October	0.85	7.6	3.9	100	13.2
November	0.88	6.3	3.8	99	11.6
December	0.99	9.3	4.4	76	8.4

Monthly Averages for 2012

	Hs	Tp	Tz	Dirp	T_{SEA}
	(m)	(s)	(s)	(°)	(°)
January	0.89	8	4.1	85	6.9
February	0.86	8.1	4.2	72	5.9
March	0.56	9.8	4.6	49	6.7
April	1.15	8.3	5.1	51	7.9
May	0.93	7.5	4.4	50	9.6
June	0.79	6.7	4.1	74	11.9
July	0.59	6.4	3.8	78	13.7
August	0.55	5.7	3.6	84	14.6
September	0.65	7	3.6	90	13.5
October	0.9	7.3	4.2	74	11.8
November	0.84	8.9	4.1	62	9.5
December	1.14	7.6	4.3	77	7.4

Monthly Averages for 2013

	Hs	Tp	Tz	Dirp	T_{SEA}
	(m)	(s)	(s)	(°)	(°)
January	0.96	7.6	4	83	6.1
February	1.15	7.4	4.5	65	4.9
March	1.7	8.4	5.2	60	4.6
April	0.86	7.4	4	85	5.5
May	0.78	6.9	3.9	71	8
June	0.57	5.6	3.9	75	11.1
July	0.39	5.6	3.5	78	13.5
August	0.45	5.5	3.4	102	14.5
September	0.52	6.3	3.7	89	14.8

Appendix 3: Cliff-top photos

May 1999 (Northward), Northern embayment

May 1999 (Southward), Central embayment

September 2001 (Southward), Central embayment

September 2003 (Northward), Central embayment

May 2004 (Northward), Central embayment (north end)

May 2004 (Southward), Central embayment (southern end)

Sep 2004 (Northward), Central embayment

Nov 2005 (Northward), Central embayment

Nov 2005 (Southward), Central embayment


Sep 2006 (Northward), South & Central embayments

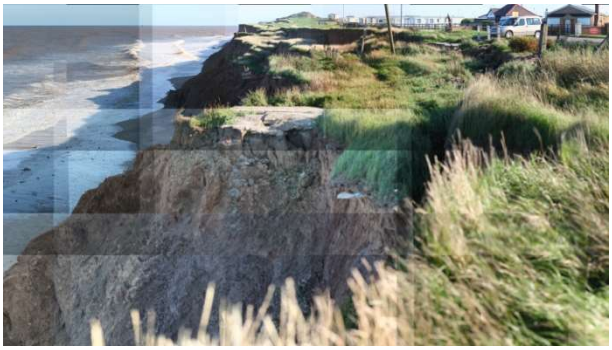
Sep 2006 (Southward), North & Central embayments


Aug 2007 (Northward), South embayment


Aug 2007 (Southward), Central embayment


Oct 2009 (Northward), Central embayment


Oct 2009 (Southward), South embayment

Mar 2010 (Northward), South embayment

Mar 2010 (Southward), Central embayment

Feb 2011 (Northward), Central embayment

Nov 2010 (Northward), Central embayment

Sep 2011 (Northward), Central embayment

Sep 2011 (Southward), Central embayment


Apr2012 (Northward), Central embayment


Apr2012 (Southward), Central embayment


Jul 2012 (Northward), Central embayment


Jul 2012 (Southward), Central embayment


Oct 2012 (Northward), Central embayment


Oct 2012 (Southward), Central embayment

Jun 2013 (Northward), Central embayment

Jun 2013 (Southward), Central embayment

Sep 2013 (Northward), Central embayment

Sep 2013 (Southward), Central embayment

Jan 2014 (Northward), Central embayment

Jan 2014 (Southward), Central embayment

Appendix 4: Field notes (observational extracts)

1999 May
Major recent landslide activity in central embayment (northern part) & northern embayment. Large backscarp (1.5m deep?)
2001 Sep
Central embayment largely bare of slip masses.
2003 Sep
Minor rock fall (topple?) in Withernsea Till (central embayment)
2004 Apr
Large arcuate rotational displacement has occurred (between 10th Oct 2003 & 3rd Feb, 2004) centred approximately on Seaside Road (0.5m backscarp). Landslide toe is slightly above beach level. Considerable movements in northern & southern embayments. Concrete cistern has foundered and lies mid-slope. Other smaller rotations plus topples and mudflows. Beach wholly sand covered, (no visible platform). Open & distorted joints in lower cliff.
2004 May
Landslide initiating on Seaside Road with 1m backscarp and fresh cracks 2m to rear.
2004 Aug
Large re-activation of rotation centred on road. Backscarp 1m high. Toe of main rotation daylighting 2-3 m above beach level. Two incipient arcuate cracks (2 cm drop) at southern end of central embayment. Block falls at toe. Sandy beach with thin shingle boundary between beach and visible platform. Several small mudflows spread across beach at N end of site. Tank now tilted on mid part of lower cliff. Cliff toe highly eroded
2004 Sep
Pre-cursor cracks initiating (central embayment)
2005 Sep
Subsidence (landslide) of promontory between north & central embayments. Incipient rotational landslides in central embayment. Major movement of previously slumped mass in southern embayment. Much erosion at cliff toe.
2005 Nov
Major rotational landslides in northern end of central embayment
2006 Sep
Bungalow No. 361 (Seaside Road) gone. Fresh landslides on incipient surfaces noted in 2005 survey (central & southern embayments). Sections of fresh slip surface visible. Also fresh incipient landslide scarps were noted on the cliff-top with a trend of southward development. Low wall at entrance to caravan park now affected by landslide slumping. Much erosion at cliff toe. Small patch of platform visible at low tide.
2007 Aug
Destruction of curved wall & metal railings at caravan park entrance. Re-activation of existing rotations partic in mid-cliff in central & southern embayments. Only minor fresh incipient cracks at cliff top. High beach levels & offshore bar.
2009 Oct
Major rotational landslide in southern embayment.
2010 Mar
Major multi-rotational landslide continues in central & southern embayments. Fresh incipient landslide scarps noted at cliff-top with a southward trend. Low wall now almost completely destroyed. Signage foundered. Concrete blocks on Seaside Road have been moved back. Much erosion at cliff toe (3m notch).
2011 Feb
Major rotational landslide initiated in central embayment.
2011 Sep
Continuing subsidence & break-up of rotated blcks in central embayment (2m backscarp)
2012 Apr
Bungalow Nos 359 & 357 (Seaside Road) gone
2012 Jul
Minor continuing rotation of landslipped blocks. Further movement of existing (multi-rotational) slipped masses was observed (central embayment – southern end). Sections of fresh slip surface visible. Concrete campsite road (Caravan Road) almost disappeared.
Much erosion at cliff toe (3m notch)
2013 Jun
Bungalow No. 355 (Seaside Road) gone. Small changes compared with the previous survey - further degradation of slumped masses. Access to the beach was good & conditions dry. Concrete road slab now precariously undercut. No fresh fissures or subsidence on cliff-top. Local Authority to move concrete blocks & signs back within next 3 weeks.
2013 Sep
Small changes compared with the previous survey, continuing movement and degradation of slumped masses. Erosion of slipped masses at cliff toe. Access to the beach was good & conditions dry. Full sandy beach, gravel & cobbles at low water. Concrete Caravan Road slab at junction with Seaside Road remains precariously undercut. No fresh fissures or subsidence observed. Local Authority has moved concrete blocks & road signs back about 10m. *Bungalow No. 353 intact and inhabited.*

Appendix 5: Glossary

Argillaceous	Containing clay. Typically applied to fine-grained sedimentary rocks composed of clay and silt-sized particles.
Atterberg Limits	Consistency criteria for defining key water contents of a clay soil. They are: liquid limit, plastic limit and shrinkage limit.
Backshore	The upper part of the active beach above high water and extending to the toe of the beach head, affected by storm waves especially during high tides.
Beach head	The cliff, dune or seawall forming the landward limit of the active beach.
Bedding	The arrangement of sedimentary rocks in beds or layers of varying thickness or character.
Bedrock.	Unweathered rock beneath a cover of soil or superficial deposits.
Berm	A horizontal ledge in an embankment or cutting to ensure the stability of a steep slope.
BGS	British Geological Survey
Bund	An embanked waterfront or quay
Calcareous	Carbonate-rich.
Calcite.	The crystalline form of calcium carbonate, $CaCO_3$.
CCO	Channel Coastal Observatory (Southampton)
Clay	A naturally occurring material which is a plastic material at natural water content and hardens when dried to form a brittle material. It is the only type of soil/rock susceptible to significant shrinkage and swelling. It is made up mainly, but not exclusively, of clay minerals. It is defined by its particle-size range (< 0.002 mm). Clay does not have to be the dominant component of a soil in order to impart clay-like properties to it.
Clay Minerals	A group of minerals with a layer lattice structure which occur as minute platy or fibrous crystals. These tend to have a very large surface area compared with other minerals, thus giving clays their plastic nature and the ability to support large suction forces. They have the ability to take up and retain water and to undergo base exchange.
Cohesion	Attractive force between soil particles (clay) involving a complex association of solid and water. Specifically, the shear strength of a soil at zero normal stress.
Cohesive Soil.	A soil in which particles adhere after wetting and subsequent drying and significant force is required to crumble the soil.
Consolidation.	The process in which pore water drains from a material under an applied load with a consequent reduction in volume of the material (see subsidence).
Density	The mass of a unit volume of a material; often used (incorrectly) as synonym for **Unit weight**. Usually qualified by condition of sample (e.g. saturated, dry).
dGPS	Differential Global Positioning System
Diamict / Diamicton	Sediment (usually glacial) containing wide range of particle types and sizes.
Dirp	Direction from whence waves with highest energy arrive at buoy (0 – 360 degrees)
Discontinuity	Any break in the continuum of a rock mass (e.g. faults, joints).
Drift	Archaic synonym for 'superficial' geological deposits; i.e. those overlying bedrock.
Effective rainfall	Rainfall minus potential evapotranspiration (**ETo**).

Effective Stress The total stress minus pore pressure; i.e. the stress transferred across the solid matter within a rock or soil.

ETo Potential evapotranspiration: the amount of water (mm) lost from the soil due to evaporation and plant transpiration.

Exposure A visible part of an outcrop that is unobscured by soil or other materials.

Faults Planes in the rock mass on which adjacent blocks of rock have moved relative to each other. The relative vertical displacement is termed 'throw'. The faults may be discrete single planes but commonly consist of zones, perhaps up to several tens of metres wide, containing several fractures which have each accommodated some of the total movement. The portrayal of such faults as a single line on the geological map is therefore a generalization.

Ferruginous. Iron-rich. Applied to rocks or soils having a detectable iron content.

Fissility The ability of a rock (e.g. Mudstone) to be broken along closely spaced parallel planes (e.g. Shale).

FLACslope **'**Fast Lagrangian Analysis of Continua' applied to slope stability analysis. A module of the FLAC finite element software suite produced by Itasca Corp.

Foreshore. The intertidal area of the shore below highest tide level and above lowest tide level.

Fluvial/Fluviatile Of, or pertaining to, rivers.

Formation The basic unit of subdivision of geological strata, and comprises strata with common, distinctive, mappable geological characteristics.

GALENA 2D **'**Limit equilibrium' type of slope stability analysis software produced by Clover Technologies.

Glacial Of, or relating to, the presence of ice or glaciers; formed as a result of glaciation.

GLONASS Globalnaya navigatsionnaya sputnikovaya sistema

GNSS Global Navigation and Satellite Systems

GPS Global Positioning System. A system which uses satellite network to locate operator's xyz position on earth's surface. See also **dGPS, GNSS**.

Grading A synonym (engineering) for particle-size analysis (see also **Sorting**).

Groundwater Water contained in saturated soil or rock below the water-table.

Group A stratigraphical unit usually comprising one or more formations with similar or linking characteristics.

Groynes Coastal defence / beach retaining structures consisting of equally spaced (wooden) barriers perpendicular to the coastline.

Gypsum Mineral consisting of hydrous calcium sulphate ($CaSO_4.2H_20$), common in weathered mudstone where it is formed by the breakdown of sulphide minerals in the presence of lime-rich groundwater.

Head A deposit comprising material derived, transported and deposited by solifluction in periglacial regions. May include material derived also by hillwash, creep and other non-glacial slope processes. Composition is very variable and dependent on source material. Thickness is also very variable.

Holocene The most recent subdivision of geologic time (RECENT) which represents the last 10,000 years.

Hs Significant Wave Height (m): average of the highest third of incident waves.

Inclinometer Instrument (usually down a borehole) for measuring changes in inclination, for example due to landsliding.

Index Tests Simple geotechnical laboratory tests which characterise the properties of soil (usually) in a remoulded, homogeneous form, as distinct from 'mechanical properties' which are specific to the conditions applied.

Ironpan Hard layer formed by re-precipitation of iron compounds leached from overlying deposits.

Joint	A surface of fracture or parting in a rock, without displacement; commonly planar and part of a set.
Landslide	A down slope displacement of bedrock or superficial deposits subject to gravity, over one or more shear failure surfaces. Landslides have many types and scales. Landslides may be considered both as 'events' and as geological deposits. Synonym of 'landslip'.
Landslip	See **Landslide.**
Laser Scanner	A high-precision survey instrument, incorporating a laser rangefinder, for measuring distance and orientation of remote objects. The results are used to produce accurate 3D terrain models. Varieties of laser-scanner are mounted in aircraft, road vehicles, or on conventional surveyor's tripods (see **TLS**).
LiDAR	**Li**ght **D**etection **A**nd **R**anging. A terrestrial or aerial based system using laser scanning to produce surface model of ground (see **TLS**)
Lignite	Soft, brown-black earthy type of coal.
Lithology	The characteristics of a rock such as colour, grain size and mineralogy. The material constituting a rock.
Lithostratigraphic Unit	A rock unit defined in terms of lithology and age and not fossil content (Biostratigraphic unit).
Liquid Limit	The moisture content at the point between the liquid and the plastic state of a clay. An Atterberg limit.
Littoral	Of or pertaining to the shore, especially the sea.
Marl	A calcareous mudstone, sensu-strictu having >30% carbonate content.
Massive	Applied to a rock mass containing no visible internal structure.
Mean Low Water	The average height of all low waters measured over a time period.
Median	The 50th percentile of a distribution; that is, the value above and below which 50 % of the distribution lies.
Member	A distinctive, defined unit of strata within a formation characterised by relatively few and distinctive rock types and associations (for example, sandstones, marls, coal seams).
Micaceous	Containing mica, a sheet silica mineral.
Mineral	A naturally occurring chemical compound (or element) with a crystalline structure and a composition which may be defined as a single ratio of elements or a ratio which varies within defined end members.
Moisture Content	See **Water content**.
Morphology	River/estuary/lake/seabed form and its change with time.
mRAD	Milliradians. A measure of angle (one radian = 57.29 degrees)
Mudrock	A term used by engineers, synonymous with mudstone.
Mudstone	A fine-grained, non-fissile, sedimentary rock composed of predominately clay and silt-sized particles.
Natural Water Content	The water content of a geological or engineering material in its natural or 'as found' state.
Ord	A section of beach where elevation is low, exposing underlying platform.
Oriented	Referring to the process of transforming a point cloud (qv.) or surface model (qv.) to an established co-ordinate system.
Outcrop	The area over which a particular rock unit occurs at the surface.
Over-Consolidated (OC)	Deposit such as clay, which in previous geological times was loaded more heavily than now and consequently has a tendency to expand if it has access to water and is subject to progressive shear failure. The moisture content is less than that for an equivalent material which has been normally consolidated.
Panda	A brand of portable, hand-operated ultra-lightweight cone penetrometer manufactured by Sol Solutions.

Palisade	Coastal protective structure remote from the cliff (usually wood).
Particle-Size Analysis (PSA)	The measurement of the range of sizes of particles in a dis-aggregated soil sample. The tests follow standard procedures with sieves being used for coarser sizes and various sedimentation, laser or X-ray methods for the finer sizes usually contained within a suspension.
Particle-Size Distribution (PSD)	The result of a particle-size analysis. It is shown as a 'grading' curve, usually in terms of % by weight passing particular sizes. The terms 'clay', 'silt', 'sand' and 'gravel' are defined by their particle sizes.
Perched Ground Water	Unconfined groundwater separated from an underlying main body of groundwater by an unsaturated zone.
Periglacial	An environment beyond the periphery of an ice sheet influenced by severe cold, where permafrost and freeze-thaw conditions are widespread. Fossil periglacial features may persist to the present day or may have been removed by subsequent glaciation or erosion.
Permeability	The property or capacity of a rock, sediment or soil for transmitting a fluid; frequently used as a synonym for 'hydraulic conductivity' (engineering). The property may be measured in the field or in the laboratory using various direct or indirect methods.
Permafrost	Permanently frozen ground, may be continuous (never thaws), discontinuous (with unfrozen patches, especially in summer) or sporadic (unfrozen areas exceed frozen areas). The surface layer subject to seasonal thaw is the 'active layer'.
pH	Measure of acidity/alkalinity on a scale of 1 to 14 (<7 is acid, >7 is alkaline).
Phreatic surface	See **Water table**
Piezometer	Device (usually down a borehole) to measure **pore pressure**.
Plasticity Index	The difference between the liquid and plastic limits. It shows the range of water contents for which the clay can be said to behave plastically. It is often used as a guide to swell/shrink behaviour, compressibility, strength and other geotechnical properties.
Plastic Limit	The water content at the lower limit of the plastic state of a clay. It is the minimum water content at which a soil can be rolled into a thread 3mm in diameter without crumbling. The plastic limit is an Atterberg limit.
Platform	The bedrock component of the foreshore.
Pleistocene	The first epoch of the Quaternary Period prior to the Holocene from about 2 million years to 10.000 years ago.
Point Cloud	The raw data produced by laser scanning. Each point has a discrete xyz location which is initially related to the co-ordinate system of the scanner.
Pore pressure	The pressure of water contained in the pores of a soil or rock.
Pyrite	The most widespread sulphide mineral, FeS_2 (iron pyrites).
Shear Box	A laboratory apparatus for measuring the shear strength (qv.) of a rectangular shaped soil sample
Quartz	The most common silica mineral (SiO_2) on Earth.
Quaternary	A sub-era that covers the time from the end of the Tertiary to the present, approximately the last 2.0 Ma, and includes the Pleistocene and Holocene.
Residual Shear Strength	The strength along a shear surface which has previously failed or has undergone significant displacement. Generally the minimum shear strength. Tends to be constant for a given soil.
Revetment	Coastal protective structure covering the cliff base (usually stone or concrete).
Rockhead	The upper surface of bedrock at surface (or its position) or below a cover of superficial deposits.

RTK Real-time kinetic: dGPS updated live by phone or radio link from network.

Running Sand Fluidisation of sand and flow into an excavation below the water table or into a perched water table, under the influence of water flow into an excavation.

Sand A soil with a particle-size range 0.06 to 2.0 mm. Commonly consists of quartz particles in a loose state.

Sandstone Sandstones are clastic rocks of mainly sand-sized particles (0.06 - 2.0 mm diameter), generally with quartz being the dominant component. Sandstones exhibit some form of cementation.

Saturation The extent to which the pores within a soil or rock are filled with water (or other liquid).

Sedimentary Rocks Rocks which formed from sediments deposited under the action of gravity through a fluid medium and were subsequently lithified. Commonly: mudstone, siltstone, sandstone and conglomerate.

Sediment Budget The balance between sediment added to and removed from the coastal system. To calculate the sediment budget for a coastal segment, one must identify all the sediment sources and sinks, and estimate how much sediment is being added to or taken from the system.

Shale A fissile mudstone.

Shear Planes/Surfaces A series of closely spaced, parallel surfaces along which differential movement has taken place. Usually associated with landslides or stress-relief. May be polished/striated (slickensides).

Shear Strength The maximum stress that a soil or rock can withstand before failing catastrophically or being subject to large unrecoverable deformations.

Shore Platform A surface of erosion that slopes gently seaward from the beach head.

Shrinkage limit The water content below which significant volume change of a clayey soil does not occur.

Siderite Carbonate mineral of iron ($FeCO_3$).

Significant Wave Height, H_S Mean wave height of the highest third of waves.

Silt A soil with a particle-size range 0.002 to 0.06 mm (between clay and sand).

Siltstone A sedimentary rock intermediate in grain size between sandstone and mudstone.

Slickensides See shear planes.

Solid A term used in geology to indicate mappable bedrock (see also Superficial).

Solifluction The slow, viscous, down slope flow of waterlogged surface material, especially over frozen ground.

Sorting A descriptive term to express the range and distribution of particle sizes in a sediment or sedimentary rock, which has implications regarding the environment of deposition. Well-sorted (=poorly graded of engineering geology terminology) indicates a small range of particle sizes, poorly sorted (=well-graded) indicates a larger range.

Standard Penetration Test (SPT) A long-established in-situ test for soil where the number of blows (N) with a standard weight falling through a standard distance to drive a standard cone or sample tube a set distance is counted. Used as an indication of lithology and bearing capacity of a soil.

T_P Time period between each wave crest (seconds).

Stiffness The ability of a material to resist deformation.

Strain A measure of deformation resulting from application of stress.

Stratigraphy The study of the sequence of deposition of rock units through time and space.

Stress The force per unit area to which it is applied. Frequently used as synonym for pressure.

Subcrop	The area over which a particular rock unit or deposit occurs immediately beneath another deposit, e.g. the Solid unit lying below Superficial Deposits (i.e. at rockhead).
Superficial Deposits	A general term for usually unlithified deposits of Quaternary age overlying bedrock; formerly called 'drift'.
Terrestrial LiDAR	LiDAR operated from the ground, as opposed to the air (see **LiDAR, TLS**)
Till	An unsorted mixture which may contain any combination of clay, sand, silt, gravel, cobbles and boulders (diamict) deposited by glacial action without subsequent reworking by melt water.
TLS	Terrestrial LiDAR survey
Triaxial Test	A laboratory test designed to measure the stress required to deform a sample until it fails, or until a constant rate of deformation is obtained.
Undrained	Condition applied to strength tests where pore fluid is prevented from escaping under an applied load. This does not enable an effective stress condition to develop.
Uniaxial Compressive Strength (UCS)	The strength of a rock sample (usually a cylinder) subjected to an axial stress causing failure (usually in an undrained condition) in the laboratory.
Unit Weight	The weight of a unit volume of a material. Often used (incorrectly) as synonym for Density. Usually qualified by condition of sample (e.g. saturated, dry)
VW Piezo	Vibrating wire **piezometer** (sensor for measuring water pressure in the ground).
Water Content	In a geotechnical context: the mass of water in a soil/rock as a % of the dry mass (usually dried at 105ºC). Synonymous with moisture content.
Water Table	The level in the rocks at which the pore water pressure is at atmospheric, and below which all voids are water filled; it generally follows the surface topography, but with less relief, and meets the ground surface at lakes and most rivers. Water can occur above a water table.
Wave direction	Compass direction from whence wave comes (degrees from North)
Weathering	The physical and chemical processes leading to the breakdown of rock materials (e.g. due to water, wind, temperature).
Wind direction	Compass direction from whence wind comes (degrees from North)

.